THE MINOR PLANET BULLETIN

BULLETIN OF THE MINOR PLANETS SECTION OF THE ASSOCIATION OF LUNAR AND PLANETARY OBSERVERS

VOLUME 48, NUMBER 1, A.D. 2021 JANUARY-MARCH 1.

ROTATION PERIOD DETERMINATION FOR ASTEROID 2409 CHAPMAN

Alessandro Marchini
Astronomical Observatory, DSFTA - University of Siena (K54)
Via Roma 56, 53100 - Siena, ITALY
marchini@unisi.it

Riccardo Papini
Wild Boar Remote Observatory (K49)
San Casciano in Val di Pesa (FI), ITALY

Marc Deldem
Observatoire Les Barres (K22)
Lamanon, FRANCE

Raoul Behrend
Observatoire de Genève
CH1290 Sauverny, SWITZERLAND

(Received: 2020 October 15 Revised: 2020 November 6)

Photometric observations of the main-belt asteroid 2409 Chapman were conducted in order to determine its rotation period. We found P = 3.1534 ± 0.0006 h, A = 0.14 ± 0.01 mag as the synodic period and lightcurve amplitude for this asteroid.

CCD photometric observations of the main-belt asteroid 2409 Chapman were carried out in 2020 October 7-10. At the Astronomical Observatory of the University of Siena (K54), a facility inside the Department of Physical Sciences, Earth and Environment (DSFTA, 2020), were used a 0.30-m *f*/5.6 Maksutov-Cassegrain telescope, a SBIG STL-6303E NABG CCD camera with clear filter; the pixel scale was 2.30 arcsec when binned at 2×2 pixels. At the Wild Boar Remote Observatory (K49) data were obtained with a 0.235-m *f*/10 (SCT) telescope, a SBIG ST8-XME NABG CCD camera unfiltered; the pixel scale was 1.60 arcsec in binning 2×2. At the Observatoire Les Barres (K22) data were obtained with a 0.20-m *f*/10 (SCT) telescope reduced at f/8.1, a SBIG ST8-XME NABG CCD camera unfiltered; the pixel scale was 1.12 arcsec in binning 1×1.

Data processing and analysis were done with *MPO Canopus* (Warner, 2018). All images were calibrated with dark and flat-field frames and the instrumental magnitudes converted to R magnitudes using solar-colored field stars from a version of the CMC-15 catalogue distributed with *MPO Canopus*. Table I shows the observing circumstances and results.

This target was observed within the Photometric Survey for Asynchronous Binary Asteroids under the leadership of Petr Pravec from Ondřejov Observatory, Czech Republic (Pravec *et al.*, 2006; Pravec, 2020web). A search through the asteroid lightcurve database (LCDB; Warner *et al.*, 2009) indicates that our results may be the first reported lightcurve observations and results for this asteroid.

2409 Chapman (1979 UG) was discovered on 1979 Oct. 17 by E. Bowell at the Anderson Mesa station of the Lowell Observatory and named in honor of Clark R. Chapman, planetary astronomer at the Planetary Science Institute in Tucson. He has made outstanding contributions to our understanding of asteroid compositions and physical processes, particularly surface mineralogical identification, taxonomy and collisional evolution. [Ref: Minor Planet Circ. 6209]. It is a main-belt asteroid with a semi-major axis of 2.266 AU, eccentricity 0.191, inclination 3.513 deg, and an orbital period of 3.41 years. Its absolute magnitude is H = 12.7 (JPL, 2020) while its spectral class is S (Bus and Binzel, 2002; Xu et al., 1995). The WISE/NEOWISE satellite infrared radiometry survey (Masiero et al., 2012) found a diameter D = 8.70 ± 0.14 km using an absolute magnitude H =12.6.

Observations were conducted over four nights and collected 361 data points. The period analysis shows a solution for the rotational period of P = 3.1534 ± 0.0006 h with an amplitude A = 0.14 ± 0.01 mag, suggested by the strongest peak in the period spectrum. Petr Pravec and Peter Kušnirák performed an independent analysis on our data and found P = 3.1531 ± 0.0005 h, A = 0.139 ± 0.006 mag, which matches perfectly with our result (private communication).

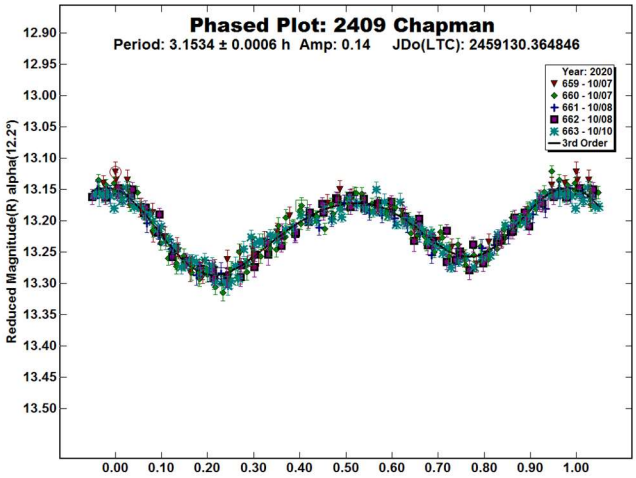

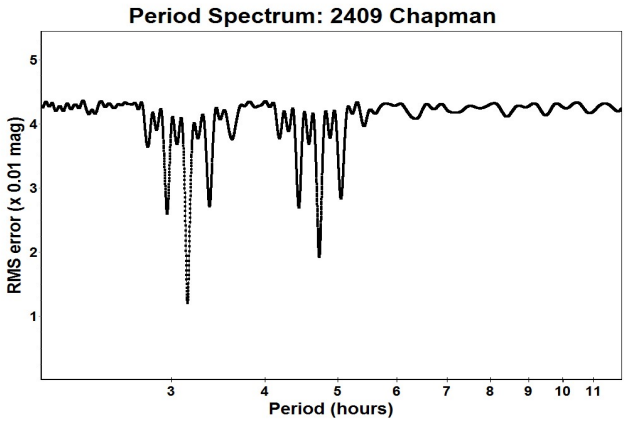

Acknowledgements

The authors desire to thank Petr Pravec and Peter Kušnirák for their independent analysis and the kind collaboration on this target proposed within the Photometric Survey for Asynchronous Binary Asteroids collaboration. Minor Planet Circulars (MPCs) are published by the International Astronomical Union's Minor Planet Center.
https://www.minorplanetcenter.net/iau/ECS/MPCArchive/MPCArchive_TBL.html

References

Bus, S.J.; Binzel R.P. (2002). "Phase II of the small main-belt asteroid spectroscopic survey: A feature-based taxonomy." *Icarus* **158**, 146-177.

DSFTA (2020). Dipartimento di Scienze Fisiche, della Terra e dell'Ambiente – Astronomical Observatory.
https://www.dsfta.unisi.it/en/research/labs/astronomical-observatory

Harris, A.W.; Young, J.W.; Scaltriti, F.; Zappala, V. (1984). "Lightcurves and phase relations of the asteroids 82 Alkmene and 444 Gyptis." *Icarus* **57**, 251-258.

JPL (2020). Small-Body Database Browser.
http://ssd.jpl.nasa.gov/sbdb.cgi#top

Masiero, J.R.; Mainzer, A.K.; Grav, T.; Bauer, J.M.; Cutri, R.M.; Nugent, C.; Cabrera, M.S. (2012). "Preliminary Analysis of WISE/NEOWISE 3-Band Cryogenic and Post-cryogenic Observations of Main Belt Asteroids." *Astrophys. J. Letters* **759**, L8.

Pravec, P.; Scheirich, P.; Kušnirák, P.; Šarounová, L.; Mottola, S.; Hahn, G.; Brown, P.; Esquerdo, G.; Kaiser, N.; Krzeminski, Z.; Pray, D.P.; Warner, B.D.; Harris, A.W.; Nolan, M.C.; Howell, E.S.; Benner, L.A.M.; Margot, J.-L.; Galád, A.; Holliday, W.; Hicks, M.D. Krugly, Yu.N.; Tholen, D.; Whiteley, R.; Marchis, F.; DeGraff, D.R.; Grauer, A.; Larson, S.; Velichko, F.P.; Cooney, W.R.; Stephens, R.; Zhu, J.; Kirsch, K.; Dyvig, R.; Snyder, L.; Reddy, V.; Moore, S.; Gajdoš, Š.; Világi, J.; Masi, G.; Higgins, D.; Funkhouser, G.; Knight, B.; Slivan, S.; Behrend, R.; Grenon, M.; Burki, G.; Roy, R.; Demeautis, C.; Matter, D.; Waelchli, N.; Revaz, Y.; Klotz, A.; Rieugné, M.; Thierry, P.; Cotrez, V.; Brunetto, L.; Kober, G. (2006). "Photometric survey of binary near-Earth asteroids." *Icarus* **181**, 63-93.

Pravec, P. (2020web). Photometric Survey for Asynchronous Binary Asteroids web site.
http://www.asu.cas.cz/~asteroid/binastphotsurvey.htm

Warner, B.D.; Harris, A.W.; Pravec, P. (2009). "The Asteroid Lightcurve Database." *Icarus* **202**, 134-146. Updated 2020 Aug. *http://www.minorplanet.info/lightcurvedatabase.html*

Warner, B.D. (2018). MPO Software, MPO Canopus v10.7.7.0. Bdw Publishing. *http://minorplanetobserver.com*

Xu, S.; Binzel, R.P.; Burbine T.H.; Bus S.J. (1995). "Small main-belt asteroid spectroscopic survey: Initial Results." *Icarus* **115**, 1-35.

Number	Name	2020/mm/dd	Phase	L_{PAB}	B_{PAB}	Period(h)	P.E.	Amp	A.E.	Grp
2409	Chapman	10/07-10/10	12.2,10.9	32	-5	3.1534	0.0006	0.14	0.01	MB

Table I. Observing circumstances and results. The phase angle is given for the first and last date. If preceded by an asterisk, the phase angle reached an extrema during the period. L_{PAB} and B_{PAB} are the approximate phase angle bisector longitude/latitude at mid-date range (see Harris *et al.*, 1984). Grp is the asteroid family/group (Warner *et al.*, 2009).

DETERMINING THE ROTATIONAL PERIOD AND LIGHTCURVE OF MAIN-BELT ASTEROID 5433 KAIREN

Roberto Bonamico
BSA Osservatorio (K76)
Strada Collarelle 53
12038 Savigliano, Cuneo, ITALY
info@osservatorioastronomicobsa.it
website: http://www.osservatorioastronomicobsa.it

(Received: 2020 October 14)

CCD photometric observations were made of the main-belt asteroid 5433 Kairen. The results of lightcurve analysis gave P = 10.7624 ± 0.0031 h, A = 0.34 mag.

During 2020 September, the BSA astronomical observatory studied the rotation period of the asteroid 5433 Kiren in the main belt. This asteroid was chosen from the CALL website (*http://minorplanet.info /call.html)*.

Observations were made with a Marcon 0.30-m *f*/5 Newtonian telescope with an Atik 314L+ CCD camera (Sony ICX285AL, 1360×1024×6.5µ). The observatory used *Maxim DL* (Diffraction Limited, 200) for camera control, *The Sky 6 Pro* (Bisque, 2020) for mount control, and *Voyager* (2020) to automate the entire observatory.

All photometric reductions were done with *MPO Canopus* v10.7.12.9 (*http://bdwpublishing.com*). Precise night-to-night zero-point calibration was obtained using the Comparison Star Selector utility in *MPO Canopus*. Whenever possible, the observatory uses five solar-colored comparison stars from the MPOSC3 catalog supplied with *MPO Canopus*.

5433 Kairen. The asteroid was discovered on 1988 August 10 by Takuo Kojima. The orbit has a semi-major axis of 2.45 AU and eccentricity of 0.22. The five observational evenings allowed establishing a period of rotation of 10.7624 h and an amplitude of 0.34 mag.

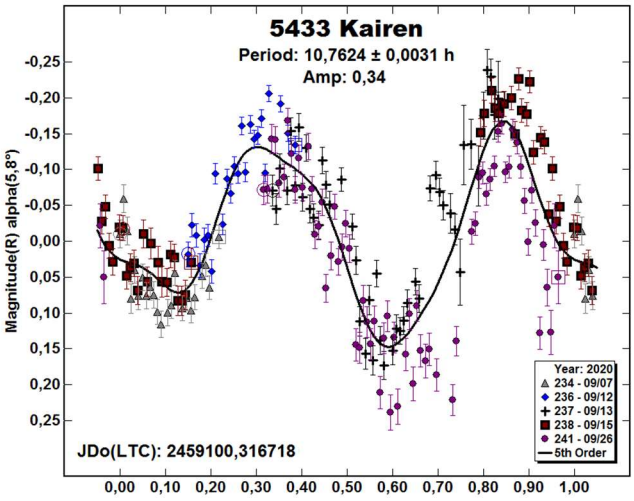

References

Bisque (2020). *The Sky 6 Pro*. Software Bisque. *http://www.bisque.com*

Diffraction Limited (2020). *Maxim DL* software. *http://diffractionlimited.com/product/maxim-dl/*

Harris, A.W.; Young, J.W.; Scaltriti, F.; Zappala, V. (1984). "Lightcurves and phase relations of the asteroids 82 Alkmene and 444 Gyptis." *Icarus* **57**, 251-258.

Voyager (2020). *Voyager* software. *http://software.starkeeper.it*

Warner, B.D.; Harris, A.W.; Pravec, P. (2009). "The Asteroid Lightcurve Database." *Icarus* **202**, 134-146. Updated 2020 April. *http://www.minorplanet.info/lightcurvedatabase.html*

Number	Name	yyyy mm/dd	Phase	L_{PAB}	B_{PAB}	Period(h)	P.E.	Amp	A.E.	Grp
5433	Kairen	2020 09/07-09/26	5.6,12.4	341	10	10.7624	0.0031	0.34	0.05	MB

Table I. Observing circumstances and results. The phase angle is given for the first and last date. If preceded by an asterisk, the phase angle reached an extremum during the period. L_{PAB} and B_{PAB} are the approximate phase angle bisector longitude/latitude at mid-date range (see Harris et al., 1984). Grp is the asteroid family/group (Warner et al., 2009).

LIGHTCURVE AND ROTATION PERIOD OF 426 HIPPO

Frederick Pilcher
Organ Mesa Observatory (G50)
4438 Organ Mesa Loop
Las Cruces, NM 88011 USA
fpilcher35@gmail.com

Vladimir Benishek
Belgrade Astronomical Observatory
Volgina 7, 11060 Belgrade 38 SERBIA

Roberto Bonamico
BSA Osservatorio (K76)
Strata Collarelle 53
12038 Savigliano, Cuneo, ITALY

Andrea Ferrero
Bigmuskie Observatory (B88)
via Italo Aresca 12
14047 Mombercelli, Asti, ITALY

Jonathan Kemp
Middlebury College
Mittelman Observatory
Middlebury, VT 05753 USA

Caroline E. Odden
Phillips Academy Observatory
180 Main Street
Andover, MA 01810 USA

Riccardo Papini
Wild Boar Remote Observatory (K49)
San Casciano in Valdi Pesi (FI) ITALY

(Received: 2020 Oct 2 Revised: 2020 Nov 9)

Minor Planet 426 Hippo at its year 2020 opposition displayed an unymmetric bimodal lightcurve with synodic rotation period of 67.52 ± 0.01 h, amplitude 0.26 ± 0.02 mag.

Several previously published rotation periods of 426 Hippo are mutually inconsistent: Mohamed (1995), >32 h; Behrend (2005), 8.18 h; Pray (2006), 34.3 h; Pal et. al. (2020), 67.5309 h. It was the goal of this investigation to obtain full phase coverage of the longest published period 67.5 hours and obtain a definitive period.

First author Pilcher suffered catastrophic equipment failure after 10 sessions and before full phase coverage was achieved. He thanks all of the collaborating authors for contributing additional lightcurves to obtain full phase coverage to a period of 67.52 hours. The equipment and respective sessions by each author are reported in Table II.

Calibration stars for all sessions are solar colored stars whose g', r', and i' magnitudes were obtained from the APASS catalog or r' magnitudes from the CMC15 catalog, both from the VizieR web site. Sessions from the several individual observers were adjusted vertically for best fit.

The data from all sessions provide full phase coverage and a good fit to a bimodal lightcurve with period 67.52 ± 0.01 h and amplitude 0.26 ± 0.02 mag. The bimodal lightcurve is sufficiently asymmetric to definitively rule out a period near 34 hours. This new result is consistent with Pal et. al. (2020) and rules out all other previously published periods.

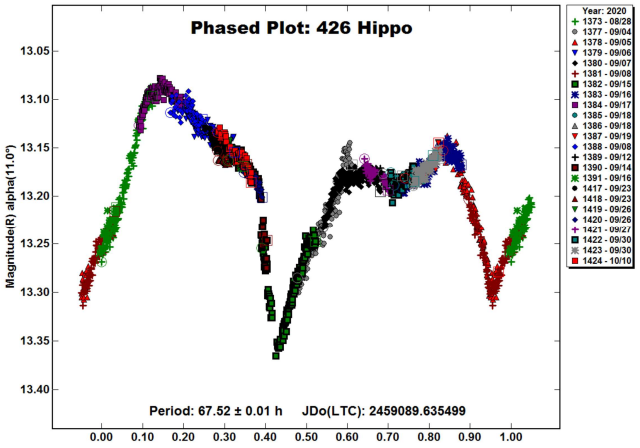

Acknowledgments

This work includes observations obtained with the Mittelman Observatories 0.5-m telescope at New Mexico Skies, Mayhill, New Mexico, USA.

References

Behrend, R. (2005). Observatoire de Geneve web site. *http://obswww.unige.ch/~behrend/page_cou.html.*

Harris, A.W.; Young, J.W.; Scaltriti, F.; Zappala, V. (1984). "Lightcurves and phase relations of the asteroids 82 Alkmene and 444 Gyptis." *Icarus* **57**, 251-258.

Mohamed, R.A.; Krugly, Y.N.; Lupishko, D.F. (1995). "Light curves and rotation periods of asteroids 371 Bohemia, 426 Hippo, 480 Hansa, and 735 Marghanna." *Astron. J.* **109**, 1877-1879.

Pal, A.; Szakáts, R.; Kiss, C.; Bódi, A.; Bognár, Z.; Kalup, C.; Kiss, L.L.; Marton, G.; Molnár, L.; Plachy, E.; Sárneczky, K.; Szabó, G.M.; Szabó, R. (2020). "Solar System Objects Observed with TESS – First Data Release: Bright Main-belt and Trojan Asteroids from the Southern Survey." *Ap. J. Supl. Ser.* **247**, 26-34.

Pray, D.P. (2006). "Lightcurve Analysis of Asteroids 326, 329, 426, 619, 1829, 1967, 10158, and 42267." *Minor Planet Bull.* **33**, 4-5.

VizieR web site. *vizier-u.strasbg.fr/viz-bin/VizieR*

Number	Name	yyyy mm/dd	Phase	L_{PAB}	B_{PAB}	Period(h)	P.E.	Amp	A.E.
426	Hippo	2020 08/28-10/10	*11.0,7.0	2	18	67.52	0.01	0.26	0.02

Table I. Observing circumstances and results. The phase angle is given for the first and last date. L_{PAB} and B_{PAB} are the approximate phase angle bisector longitude/latitude at mid-date range (see Harris et al., 1984).

Observer Observatory (MPC code)	Telescope	CCD	Filter	Sessions
Pilcher Organ Mesa Observatory (G50)	0.35-m SCT f/10.0	SBIG STL-1001E	C	1373-1384
Benishek Sopot Observatory	0.35-m SCT f/6.7	SBIG ST8-XME	C	1385
Bonamico Osservatorio Astronomico BSA (K76)	0.30-m NRT f/5	ATIK 314L+	C	1388, 1391
Ferrero Bigmuskie Observatory (B88)	0.30-m RCT f/8	Moravian G3 01000	C	1389-1390
Kemp Mittleman Observatories at New Mexico Skies Measurer Caroline E. Odden	0.51-m CDK f/6.8	FLI ProLine PL16803	L	1417-1424
Papini Wild Boar Remote Observatory (K49)	0.23 cm SCT f/10.0	SBIG ST8-XME	C	1386-1387

Table II. Observing equipment and sessions. CDK: Corrected Dall-Kirkham, NRT: Newtonian Reflector, RCT: Ritchey-Chretien, SCT: Schmidt-Cassegrain. Filters: C: Clear, L: Luminance

LIGHTCURVES AND ROTATION PERIODS OF 49 PALES, 383 JANINA, AND 764 GEDANIA

Frederick Pilcher
Organ Mesa Observatory (G50)
4438 Organ Mesa Loop
Las Cruces, NM 88011 USA
fpilcher35@gmail.com

(Received: 2020 October 12)

Synodic rotation periods and amplitudes are found for 49 Pales: 20.702 ± 0.001 h, 0.18 ± 0.01 mag, with 4 maxima and minima per cycle; 383 Janina: 6.4298 ± 0.0001 h, 0.17 ± 0.02 mag; 764 Gedania: 24.968 ± 0.003 h, 0.22 ± 0.02 mag.

Observations to obtain the data used in this paper were made at the Organ Mesa Observatory with a 0.35-m Meade LX200 GPS Schmidt-Cassegrain (SCT) and SBIG STL-1001E CCD. exposures were 60 seconds, unguided, with R filter for 49 Pales and clear filter for 383 Janina and 764 Gedania. Photometric measurement and lightcurve construction are with *MPO Canopus* software. To reduce the number of points on the lightcurves and make them easier to read, data points have been binned in sets of 3 with a maximum time difference of 5 minutes.

49 Pales. Two early published rotation periods were by Schober et al. (1979), 10.42 hours; and by Tedesco (1979), 10.3 hours, and for many years the period was believed to be near 10.4 hours. Behrend (2013) published a very sparse lightcurve which suggested a period <10 hours. Pilcher et al. (2016) made a much more comprehensive investigation that found a period 20.704 hours with an unsymmetric quadrimodal lightcurve. Behrend (2016) complemented this study with a period 20.7057 hours. Two subsequent studies confirm both the longer period and the unsymmetric quadrimodal lightcurve: Pilcher (2017), 20.705 hours, and Pilcher (2018), 20.709 hours. New observations on 7 nights 2020 Aug. 11 - 27 provide a fit to a period 20.702 ± 0.001 hours, again with an unsymmetric quadrimodal lightcurve, and amplitude 0.18 ± 0.01 magnitudes. This is consistent with other recent values.

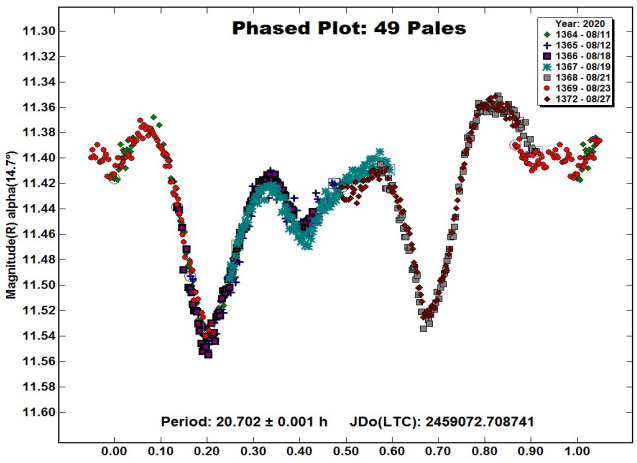

383 Janina. Previously published rotation periods are by Tedesco (1979), 6.4 hours; Clark (2006), 4.636 hours; Erasmus et al. (2020), 6.429 hours. New observations on 5 nights 2020 Sept. 2 - Oct. 11 provide a good fit to a lightcurve with period 6.4298 ± 0.0001 hours, amplitude 0.17 ± 0.02 magnitudes. This is consistent with all previous studies except Clark (2006).

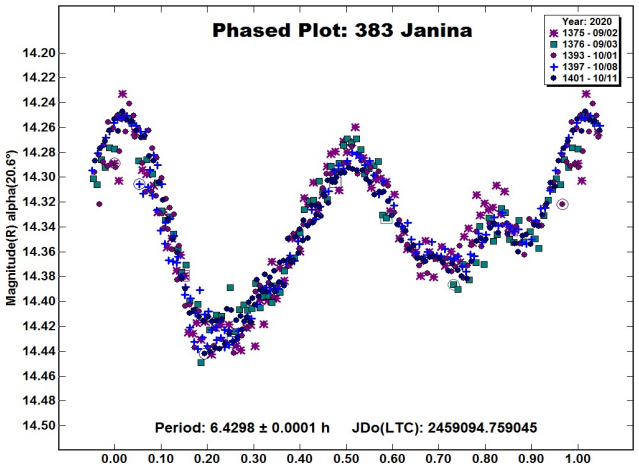

764 Gedania. Previously published rotation periods are by Behrend (2006), 24.9751 hours; Brinsfield (2010), 24.817 hours; Aznar Macias et al. (2016), 19.16 hours; and Pal et al. (2020), 25.1172 hours. New observations on 16 nights 2020 June 17 - July 18 provide a good fit to a lightcurve with period 24.968 ± 0.003 hours, amplitude 0.22 ± 0.02 magnitudes. The new value is consistent with all previously reported periods except Aznar Macias et al.

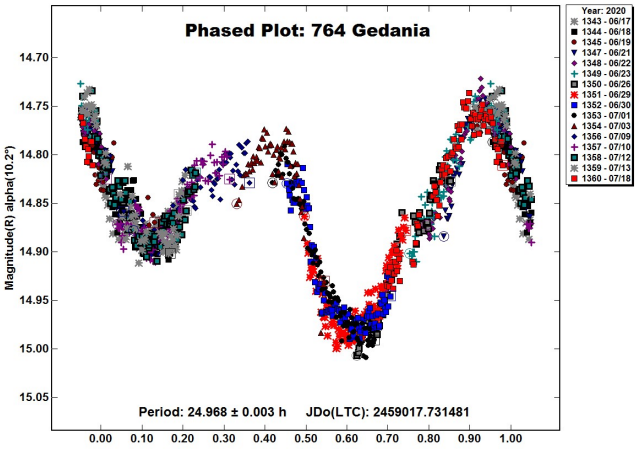

References

Aznar Macias, A.; Garceran, A.C.; Mansego, E.A.; Rodriguez, P.B.; de Haro, J.L.; Fornas Silva, A.; Fornas Silva, G.; Martinez, V.M.; Chiner, O.R. (2016). "Twenty-three asteroids lightcurves at Observadore de Asteroides, 2015 October - December." *Minor Planet Bull.* **43**, 174-181.

Behrend, R. (2006, 2013, 2016). Observatoire de Geneve web site. *http://*obswww.unige.ch/*~behrend/page_cou.html*.

Brinsfield, J.W. (2010). "Asteroid lightcurve analysis at the Via Capote Observatory: 2009 3rd quarter." *Minor Planet Bull.* **37**, 19-20.

Clark, M. (2006). "Lightcurve results for 383 Janina, 899 Jokaste, 1825 Klare, 2525 O'Steen, 5064 Tanchozuru, and (17939) 1999 HH8." *Minor Planet Bull.* **33**, 53-56.

Erasmus, N.; Navarro-Mesa, S.; McNeill, A.; Trilling, D.E.; Sickafoose, A.A.; Denneau, L.; Flewelling, H.; Heinze, A.; Tonry, J.L. (2020). "Investigating taxonomic diversity within asteroid families through ATLAS dual-band photometry." *Astrophys. J. Suppl. Ser.* **247**, id.13.

Harris, A.W.; Young, J.W.; Scaltriti, F.; Zappala, V. (1984). "Lightcurves and phase relations of the asteroids 82 Alkmene and 444 Gyptis." *Icarus* **57**, 251-258.

Pal, A.; Szakats, R.; Kiss, C.; Bodi, A.; Bognar, Z.; Kalup, C.; Kiss, L.; Marton, G.; Plachy, E.; Sarneczky, K.; Szabo, G.; Szabo, R (2020). "Solar system objects observed with TESS - First data release: Bright main-belt and Trojan asteroids from the southern survey." *Astrophys. J. Suppl. Ser.* **247**, id.26.

Pilcher, F.; Benishek, V.; Klinglesmith, D.A. (2016). "Rotation Period, Color Indices, and H-G Parameters for 49 Pales." *Minor Planet Bull.* **43**, 182-183.

Pilcher, F. (2017). "Rotation Period Determinations for 49 Pales, 96 Aegle, 106 Dione, 375 Ursula, and 576 Emanuela." *Minor Planet Bull.* **44**, 249-251.

Pilcher, F. (2018). "New lightcurves of 33 Polyhymnia, 49 Pales, 289 Nenetta, 504 Cora, and 821 Fanny." *Minor Planet Bull.* **45**, 356-359.

Schober, H.J.; Scaltriti, F.; Zappala, V. (1979). "Photoelectric photometry and rotation periods of three large and dark asteroids - 49 Pales, 88 Thisbe, and 92 Undina." *Astron. Astrophys. Suppl. Ser.* **36**, 1-8.

Tedesco, E.F. (1979). PhD Dissertation, New Mexico State University.

Number	Name	2020 mm/dd	Phase	L_{PAB}	B_{PAB}	Period(h)	P.E.	Amp	A.E.
49	Pales	08/11-08/27	14.7, 9.2	353	4	20.702	0.001	0.18	0.01
383	Janina	09/02-10/11	20.6,10.9	40	-3	6.4298	0.0001	0.17	0.02
764	Gedania	06/17-07/18	10.2, 2.7	296	7	24.968	0.003	0.22	0.02

Table I. Observing circumstances and results. The phase angle is given for the first and last date, unless a minimum (second value was reached). L_{PAB} and B_{PAB} are the approximate phase angle bisector longitude/latitude at mid-date range (see Harris et al., 1984).

LIGHTCURVES OF THREE MAIN-BELT ASTEROIDS

Andrea Ferrero
Bigmuskie Observatory (B88)
via Italo Aresca 12
14047 Mombercelli, Asti, ITALY
bigmuskie@outlook.com

(Received: 2020 October 14)

In this paper we present the result of a photometric work on three asteroids:
(18879) 1999 XJ143, P = 33.53 ± 0.01 h, A = 0.50 mag;
(19562) 1999 JM81, P = 9.024 ± 0.001 h, A = 0.78 mag;
(65936) 1998 FJ69, P = 2.800 ± 0.001 h, A = 0.19 mag.

During Northern summer of 2020, Bigmuskie Observatory observed three main-belt asteroids to determinate their rotational periods. All targets were found using the CALL website ephemeris generator (Warner, 2020); none of them had previously reported rotation periods.

All targets were worked with a Marcon 0.30-m *f*/8 Ritchey-Chretien telescope. The camera was a Moravian G3 01000 equipped with a KAF-1001E CCD (1024×1024×24μ). The combination gave a pixel scale of 2 arcsec/pixel and a field-of-view of 36×36 arcmin. Exposures were unguided and taken through a Toptec R filter to reduce light pollution as much as possible. Telescope and camera control were managed by *Maxim DL* (Diffraction Limited, 2020) and *The Sky 6 Pro* (Bisque, 2020). *Voyager* (2020) automated the entire observatory. All photometric reductions were done with *MPO Canopus* v10.7.12.9 (Warner, 2018), which permits obtaining fast results and precise night-to-night zero-point calibration using its Comparison Star Selector.

(18879) 1999 XJ143. With the period close to 1.5 Earth days, it was necessary to observe the target many nights to reach the right result. Our analysis found is P = 33.53 ± 0.01 h and amplitude of A = 0.50 mag.

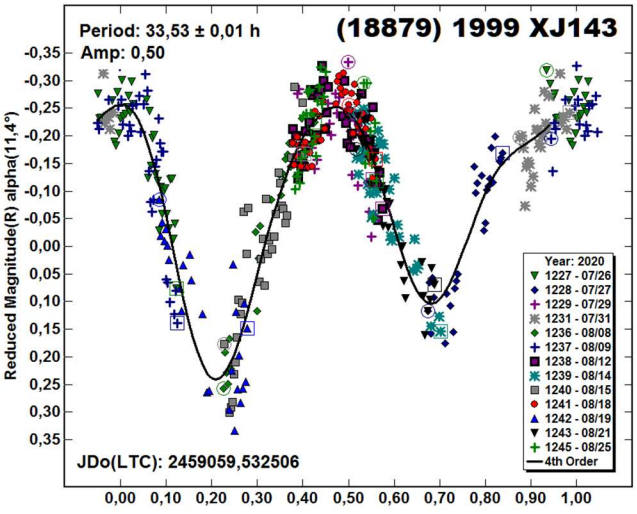

(19562) 1999 JM81. This was a very easy target; the result leaves no room for other solutions: P = 9.024 ± 0.001 h, A = 0.78 mag.

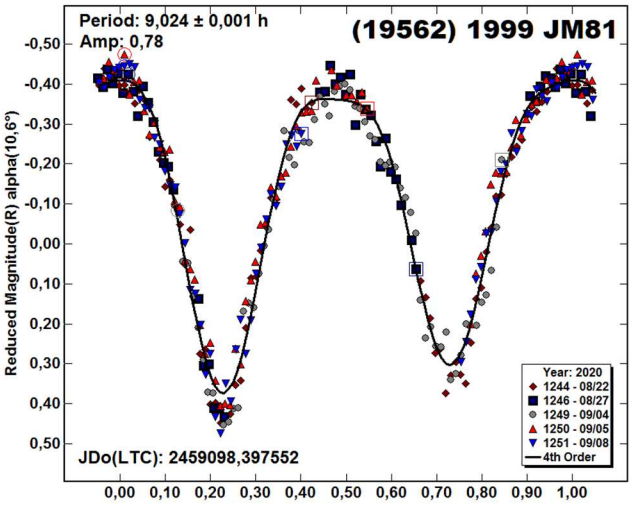

(65936) 1998 FJ69. The very low amplitude, V~16, and interference from field stars produced a somewhat unreliable result, even if it seemed that no other periods were possible. The period is P = 2.800 ± 0.001 h and A = 0.19 mag.

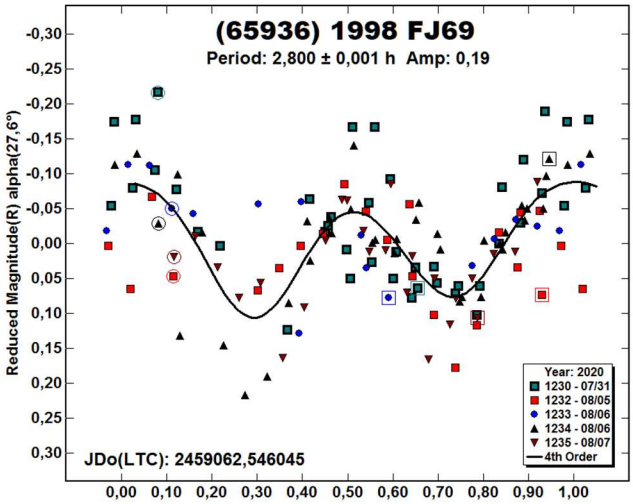

References

Bisque (2020). Software Bisque. *The Sky Pro 6*. *http://www.bisque.com*

Diffraction Limited (2020). *Maxim DL* software. *http://diffractionlimited.com/product/maxim-dl/*

Harris, A.W.; Young, J.W.; Scaltriti, F.; Zappala, V. (1984). "Lightcurves and phase relations of the asteroids 82 Alkmene and 444 Gyptis." *Icarus* **57**, 251-258.

Voyager (2020). Observatory control software. *http://software.starkeeper.it*

Warner, B.D.; Harris, A.W.; Pravec, P. (2009). "The Asteroid Lightcurve Database." *Icarus* **202**, 134-146. Updated 2020 07 20. *http://www.minorplanet.info/lightcurvedatabase.html*

Warner, B.D. (2018). *MPO Canopus* software. *http://bdwpublishing.com*

Warner, B.D. (2020). CALL website ephemeris generator. *http://www.minorplanet.info/PHP/call_OppLCDBQuery.php*

Number	Name	yyyy mm/dd	Phase	L_{PAB}	B_{PAB}	Period(h)	P.E.	Amp	A.E.	Grp
18879	1999 XJ143	2020 07/26-08/25	11.5,15.8	310	17	33.53	0.01	0.50	0.05	MB
19562	1999 JM81	2020 08/22-09/08	10.8,9.9	340	15	9.024	0.001	0.78	0.05	MB
65936	1998 FJ69	2020 07/31-08/07	27.9,26.0	328	34	2.800	0.001	0.19	0.05	MB

Table I. Observing circumstances and results. The phase angle is given for the first and last date. If preceded by an asterisk, the phase angle reached an extremum during the period. L_{PAB} and B_{PAB} are the approximate phase angle bisector longitude/latitude at mid-date range (see Harris et al., 1984). Grp is the asteroid family/group (Warner et al., 2009).

ANALYSIS OF LIGHTCURVES TO FIND THE ROTATION PERIODS OF THREE ASTEROIDS

Ernesto Benitez, Abbi Campanella, Dylan Cowger, Renée Kirk,
Joseph Weller, Lucy Wilkerson, Angela Wroblewski
Department of Astronomy, University of Maryland
Room 1113 PSC Bldg. 415
College Park, MD 20742-2421
ebenite1@terpmail.umd.edu

(Received: 2020 September 20)

We attempted to determine the rotation periods of 2684 Douglas, 4137 Crabtree, and (498066) 2007 RM133. A search of the asteroid lightcurve database (LCDB; Warner et al., 2009) revealed no known periods for these asteroids. Observations were collected using the 443mm reflector iTelescope T17 located in Siding Spring, Australia, over multiple nights in June, July, and August. Aperture photometry was then performed for each night the asteroids were observed. We did not conclusively determine their respective rotation periods; however, we constrained the possible range of plausible rotation periods.

During the months of 2020 June through August, we gathered photometric data on three asteroids using the iTelescope T17 located in Siding Spring Observatory, Australia. The T17 is a 443 mm *f*/6.8 reflector telescope that rests at an altitude of 1122 m. The scientific package includes the FLI ProLine E2V CCD47-10-1-109 CCD with a multitude of filters; our investigation used only the Clear/Luminance filter. The telescope/CCD system FOV is 15.5×15.5 arcmin with a 1024×1024-pixel array. This CCD is sensitive in the near infrared band and has non-antiblooming gates (NABG); this required limited exposure to avoid saturation.

2684 Douglas was discovered on 1981 January 3 at the Anderson Mesa station, southeast of Flagstaff, Arizona (JPL, 2020). This main-belt asteroid has been observed to have an absolute magnitude of 11.6, a diameter of 15.962 ± 0.255 km, and a geometric albedo of 0.159 (Masiero et al., 2011). We observed the asteroid as it crossed the galactic center throughout the nights of June 15, 19, and 28. Of these nights, June 28 yielded the longest period of uninterrupted observing (Figure 1). The resulting data allowed us to visually constrain the rotation period to approximately four hours. This helps eliminating alias periods generated by the Fourier fitting and give a baseline for the general shape of the phased lightcurve.

The nights of June 15 and 19 were characterized by short periods of uninterrupted observing followed by unfavorable weather conditions. Therefore, we focused on fitting these datasets to the baseline set of June 28. The resulting period of 4.007 ± 0.001 h (Figure 2) was expected given the baseline of Figure 1; however, the fit was not uniformly constrained throughout the various features of the lightcurve. Of particular note is the scatter of the first peak in Figure 2. This scattering could be indicative of a binary system and we therefore investigated the possibility using the built-in Dual Period Search function of *MPO Canopus*. The phased lightcurve of the primary period found was less scattered in the first peak than Figure 2 but the lightcurve of the secondary period had variations inconsistent with what is expected for a secondary body. The period reported in Figure 2 is our best fit; however, as seen in the rms vs. period (period spectrum) plot of Figure 3, this is not by a significant margin.

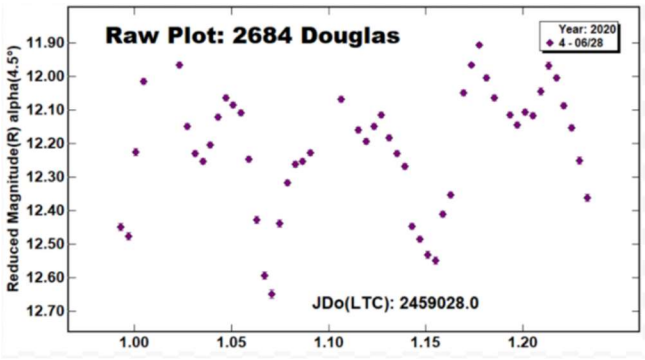

Figure 1. Lightcurve for 2684 Douglas based on data obtained on night of 2020 June 28.

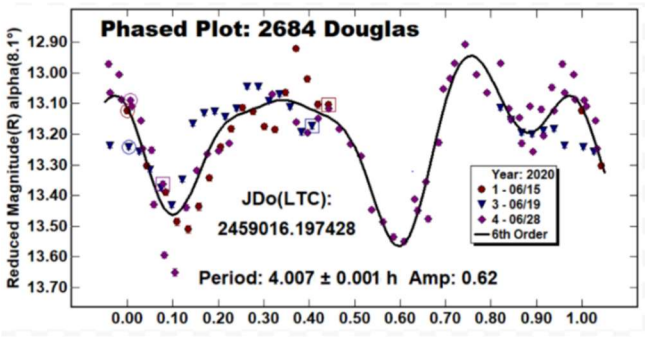

Figure 2. Phased lightcurve for 2684 Douglas.

Number	Name	yyyy mm/dd	Phase	L_{PAB}	B_{PAB}	Period(h)	P.E.	Amp	A.E.	Grp
2684	Douglas	2020 06/15-08/17	*8.2,14.9	282	9	4.007	0.001	0.62	-	MB
4137	Crabtree	2020 06/18-08/16	*12.2,15.7	290	-5	13.6621	0.0103	0.25	-	MB
498066	2007 RM133	2020 06/16-08/17	*16.0,26.3	287	-3	-	-	-	-	NEO

Table I. Observing circumstances and results. The phase angle is given for the first and last date. If preceded by an asterisk, the phase angle reached an extremum during the period. L_{PAB} and B_{PAB} are the approximate phase angle bisector longitude/latitude at mid-date range (see Harris et al., 1984). Grp is the asteroid family/group (Warner et al., 2009).

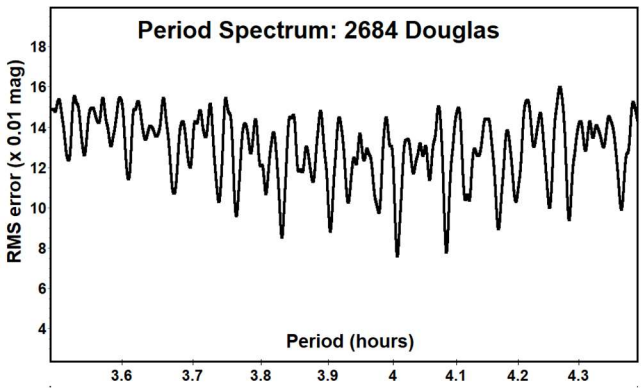

Figure 3. Reported rms vs. period from Fourier fitting of Figure 2.

Additionally, 2684 Douglas crossing the galactic center made the photometry process more challenging due to the crowded field-of-view. Residual light from stars may have contributed to the scattering of points in the phased lightcurve. The reported period of 4.007 ± 0.001 h is preliminary; additional nights of observation would constrain the rotation period.

4137 Crabtree was discovered in 1970 by L. Kohoutek. Crabtree is named for William Crabtree, a cloth merchant who was the second person to knowingly observe a transit of Venus (JPL, 2020). It is a main-belt asteroid with a diameter of about 6.54 km and absolute magnitude of 13.1 (JPL, 2020). We observed the asteroid on the nights of 2020 June 26, July 23, and August 13. Using *MPO Canopus* to analyze the data, a possible rotation period of about 13.7 h was found. We believe that the steady decrease in brightness displayed by the phased plot is only half of the actual period. A rotation period of 13 h falls just outside the average rotation period range of asteroids, which is 2 to 12 h. This result is not final and future observations will be needed. As seen in Figure 5, the period spectrum shows that there are many periods that fit the data almost as well. This can be attributed to the relatively small number of observations made of a long rotation period.

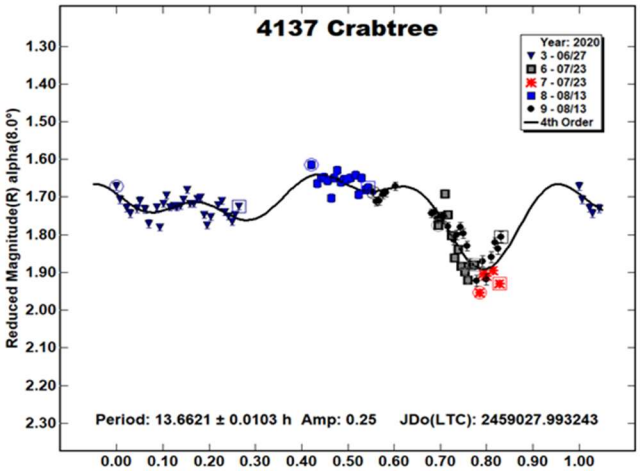

Figure 4. Phased lightcurve for 4137 Crabtree.

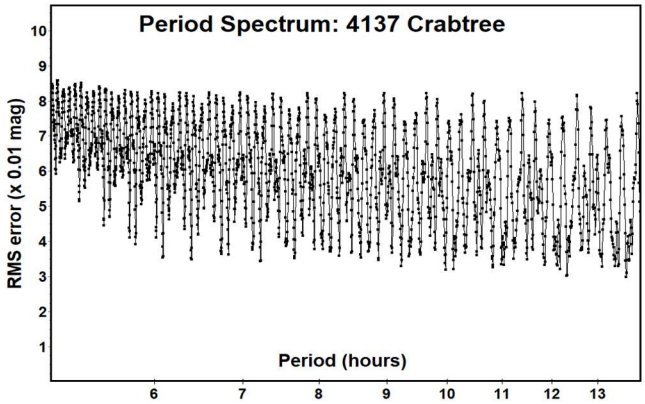

Figure 5. Reported rms vs. period from Fourier fitting of Figure 4.

(498066) 2007 RM133, a near-Earth Amor type asteroid (NEA), was discovered in 2007 by CSS at Catalina (JPL, 2020). It has an absolute magnitude of 18.1, a diameter of 0.589 ± 0.083 km, and a geometric albedo of 0.268 ± 0.077 (Mainzer et al., 2011). Our observations took place on June 16 and July 24, although unfavorable weather conditions greatly limited the total amount of images taken on July 24.

The observations on June 16 yielded a probable trough and peak (Figure 6). We believe that a quarter of the total rotation period was observed, suggesting that the period is approximately 19.2 h. Figure 8 shows the period spectrum when searching the June 16 data set using the Fourier period search tool in *MPO Canopus*. This tool reported a period of 9.1 ± 2.3 h (Figure 7), which we believe to be about half of the true period of (498066) 2007 RM133.

Using the June 16 data (Figure 6) and July 24 data (Figure 9) in the same phased plot did not yield any enlightening conclusions about the rotation period due to the lack of an identifiable lightcurve shape in Figure 9. Future observations are necessary to further constrain the period of (498066) 2007 RM133.

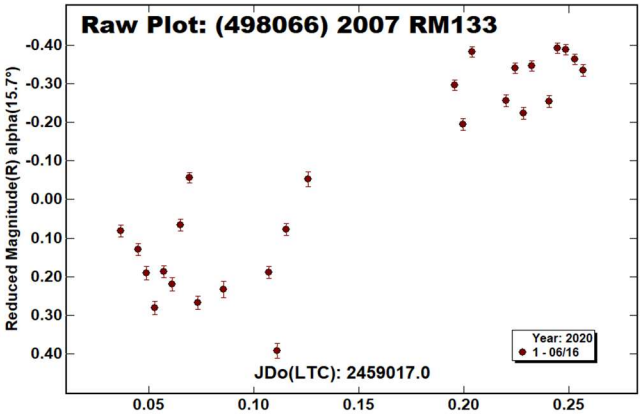

Figure 6. Unphased lightcurve for (498066) 2007 RM133 as observed on June 16.

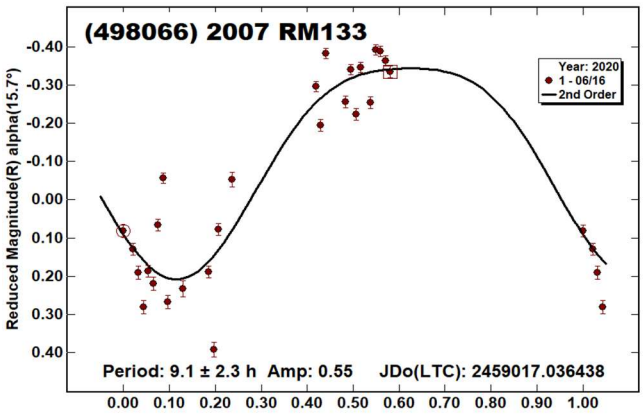

Figure 7. Phased lightcurve for (498066) 2007 RM133 as observed on June 16.

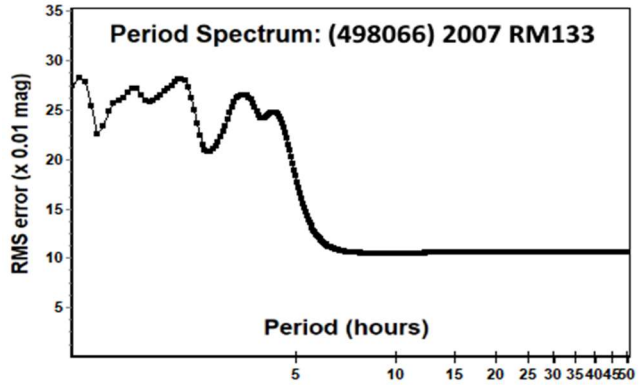

Figure 8. Reported rms vs. period from Fourier fitting of Figure 7.

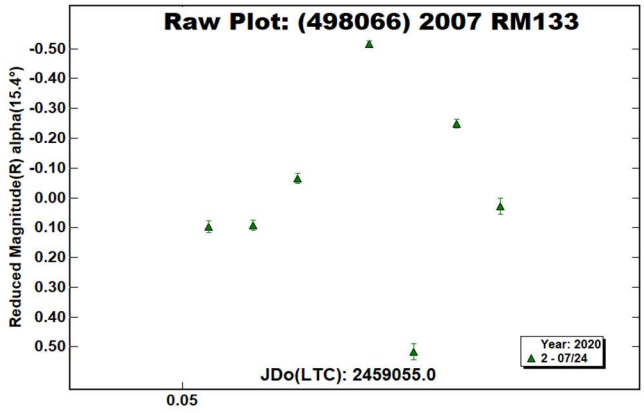

Figure 9. Unphased lightcurve for (498066) 2007 RM133 as observed on July 24th.

Acknowledgements

Funding for this research was generously provided by the University of Maryland Department of Astronomy. Observations were made possible thanks to iTelescope for allowing use of their T17 telescope. Also, thank you Brian Warner for special assistance with *MPO Canopus*.

References

Harris, A.W.; Young, J.W.; Scaltriti, F.; Zappala, V. (1984). "Lightcurves and phase relations of the asteroids 82 Alkmene and 444 Gyptis." *Icarus* **57**, 251-258.

JPL (2020). Small Body Database Search Engine. *http://ssd.jpl.gov/sbdb_query.cgi*

Mainzer, A.; Grav, T.; Bauer, J.; Masiero, J.; McMillan, R.S.; Cutri, R.M.; Walker, R.; Wright, E.; Eisenhardt, P.; Tholen, D.J.; Spahr, T.; Jedicke, R.; Denneau, L.; DeBaun, E.; Elsbury, D.; Gautier, T.; Gomillion, S.; Hand, E.; Mo, W.; Watikins, J.; Wilkins, A.; Bryngelson, G.L.; Del Pino Molia, A.; Desai, S.; Gomez Camus, M.; Hidalgo, S.L.; Konstantopoulos, I.; Larsen, J.A.; Maleszewski, C.; Malkan, M.A.; Mauduit, J.-C.; Mullan, B.L.; Olszewski, E.W.; Pforr, J.; Saro, A.; Scotti, J.V.; Wasserman, L.H. (2011). "NEOWISE observations of near-Earth objects: Preliminary results." *Ap. J.* **743**, A156.

Masiero, J.R.; Mainzer, A.K.; Grav, T.; Bauer, J.M.; Cutri, R.M.; Dailey, J.; Eisenhardt, P.R.M.; McMillan, R.S.; Spahr, T.B.; Skrutskie, M.F.; Tholen, D.; Walker, R.G.; Wright, E.L.; DeBaun, E.; Elsbury, D.; Gautier, T., IV; Gomillion, S.; Wilkins, A. (2011). "Main Belt Asteroids with WISE/NEOWISE. I. Preliminary Albedos and Diameters." *Ap. J.* **741**, A68.

Warner, B.D.; Harris, A.W.; Pravec, P. (2009). "The Asteroid Lightcurve Database." *Icarus* **202**, 134-146. Updated 2020 Sep. *http://www.minorplanet.info/lightcurvedatabase.html*

ROTATIONAL PERIODS AND LIGHTCURVE DETERMINATION OF 6259 MAILLOL, 6792 AKIYAMATAKASHI AND 85275 (1994 LY)

Alfonso Noschese
AstroCampania Associazione, Naples, ITALY
Osservatorio Salvatore Di Giacomo (L07)
Via Salvatore Di Giacomo 7b
Agerola (Na) ITALY
and
Osservatorio Elianto (K68)
via V. Emanuele III, 95, 84098
Pontecagnano (SA) ITALY
a.noschese@astrocampania.it

Antonio Catapano, Maurizio Mollica, Antonio Vecchione
AstroCampania Associazione, Naples, ITALY
Osservatorio Salvatore Di Giacomo (L07)
Via Salvatore Di Giacomo 7b, 80051
Agerola (Na) ITALY

(Received: 2020 October 13)

The lightcurves and rotation period determinations for 6259 Maillol, 6792 Akiyamatakashi, and (85275) 1994 LY are reported in this paper.

The aim of this research was to find the rotational period and lightcurve of an Amor-family asteroid (85275) 1994 LY and of two main belt asteroids, 6259 Maillol and 6792 Akiyamatakashi.

CCD photometric observations of 6259 Maillol were mainly carried out at the Elianto Observatory located in southern Italy (Pontecagnano) using a 0.3-m Newtonian telescope operating at *f*/4 equipped with a Moravian KAF1603 ME CCD camera (1536×1024 array of 9-micron pixels) with a clear filter.

Six sessions of measurements were performed at Salvatore Di Giacomo Observatory (L07) located at Agerola (Naples), Italy. The observations were made using a 0.50-m *f*/8 Ritchey-Chretien, FLI-PL4240 CCD camera (2048×2048array of 13.5-micron pixels), and clear filter. One session was performed using a 0.25-m *f*/8 Ritchey-Chretien telescope located in southern Italy (Pontecagnano) equipped with a SBIG STT-8300 CCD camera (3326×2504 array of 5.4-micron pixels), and clear filter.

Some photometric observations were also acquired at Siding Spring Observatory, Australia (Q62), by means of remote telescopes iTelescope-T17 (2020); iTelescope-T30 (2020). The iTelescope-T17 is 0.43-m *f*/6.8 Planewave CDK equipped with a FLI ProLine PL4710 CCD camera and clear filter. The iTelescope-T30 is a 0.50-m *f*/6.8 CDK equipped with a FLI-PL6303E CCD camera and clear filter.

Two of the CCD photometric observations of 6792 Akiyamatakashi were carried out at the Osservatorio Salvatore di Giacomo, Agerola (MPC code L07), with the same equipment described above. An observing session was obtained by of Elianto observatory, also with the same equipment described above.

In the case of (85275) 1994 LY, all the CCD photometric observations were obtained from the Osservatorio Salvatore di Giacomo, Agerola, with the same equipment as above, except that an R filter was used.

All images were astrometrically aligned, and dark and flat-field corrected using *Maxim DL* software. *MPO Canopus* (Warner, 2017) was used to measure the magnitudes, perform Fourier analysis, and produce the final lightcurves. In particular, data were reduced in *MPO Canopus* using differential photometry. Night-to-night zero-point calibration was accomplished by selecting up to five comparison stars with near-solar colors using the "comp star selector" feature. To analyze the data points, the ATLAS star catalog (Tonry et al., 2018) was used for determining the comparison star magnitudes. The "StarBGone" routine within *MPO Canopus* was used to subtract stars that occasionally merged with the asteroid during the observations. *MPO Canopus* was also used for rotation period analysis. The software employs a FALC Fourier analysis algorithm developed by Harris (Harris et al., 1989).

6259 Maillol was discovered at Palomar on 1973 September 30 by C.J. van Houten, I. van Houten-Groeneveld, and T. Gehrels. It is a main-belt asteroid with a semi-major axis of 2.277 au, orbital period of 3.4 y, eccentricity of 0.136, and inclination of 6.702 deg. This asteroid has a diameter of about 4.7 kilometer, an absolute magnitude of 13.8 and a geometric albedo of 0.24 (JPL, 2020). There were no previous lightcurve entries in the LCDB (Warner et al., 2009) for this member of the Flora family/group. CCD photometric observations were performed between 2020 April 1 and May 27. Twenty-five observing sessions, with exposures between 180 s and 420 s, produced a data set of 1014 points for lightcurve analysis. Our observations led to a period of 2.3582 h with an amplitude of 0.08 mag.

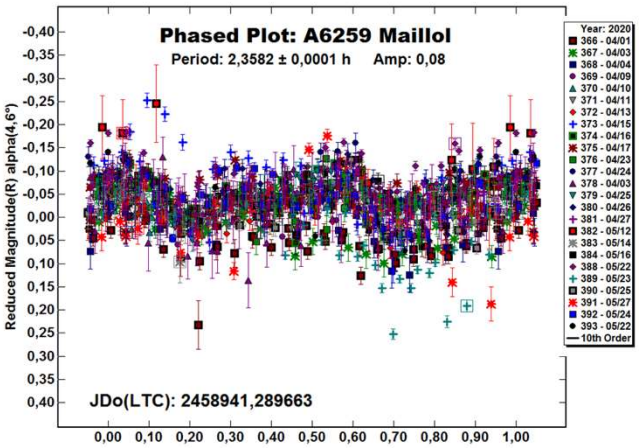

Number	Name	20yy mm/dd	Phase	L_{PAB}	B_{PAB}	Period(h)	P.E.	Amp	A.E.	Grp
6259	Maillol	04/01-05/27	4.57-24.28	200	2	2.3582	0.0001	0.08	0.02	MB
6792	Akiyamatakashi	09/18-10/09	5.67-11.09	2	-6	7.5316	0.0002	0.29	0.02	MB
85275	1994 LY	07/08-08/20	37.56-53.36	287	22	2.6952	0.0001	0.09	0.02	AMOR

Table I. Observing circumstances and results. The phase angle is given for the first and last date. LPAB and BPAB are the approximate phase angle bisector longitude and latitude at mid-date range (Harris et al., 1984). Grp is the asteroid family/group (Warner et al., 2009).

6792 Akiyamatakashi was discovered on 1991 November 30 by M. Akiyama and T. Furuta at Susono. It is a main-belt asteroid with a semi-major axis of 2.376 au, orbital period of 3.67 y, eccentricity of 0.244, and inclination of 3.69 deg. This object has a diameter of about 8.2 kilometer, an absolute magnitude of 13.1 and a geometric albedo of 0.24 (JPL, 2020). There were no previous lightcurve entries in the LCDB for this object. CCD photometric observations were performed between 2020 September 18 and October 9. Three observing sessions, with exposures between 90 s and 360 s, produced a data set of 442 data points for lightcurve analysis. The resulting bimodal solution gives a period of 7.5316 h with an amplitude of 0.29 mag.

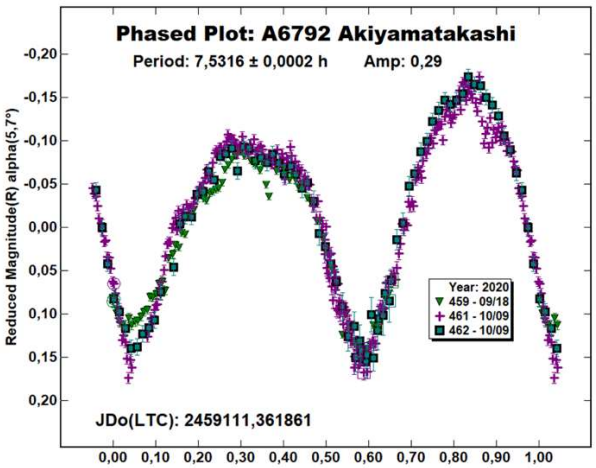

(85275) 1994 LY was discovered at Palomar on 1994 June 11 by E.F. Helin. It is a mid-sized Amor class asteroid whose orbit approaches the orbit of Earth but does not cross it. This asteroid has a semi-major axis of 1.890 au, orbital period of 2.6 y, eccentricity of 0.442 and inclination of 17.718 deg. Its diameter is about 2.5 km, absolute magnitude H = 16.1, and geometric albedo of p_V = 0.09 (JPL, 2020). Pravec et al. (2007) reported a period of 2.6962 h and a suspected secondary period 48.5 h. Brinsfield (2008) reported a period of 2.7 h, which was subsequently refined by Apostolovska et al. (2009) to 2.6960 h. None of them indicated seeing mutual events or attenuations. Very recently, Warner et al. (2020) have shown the binary nature of this asteroid. From their results, the rotational period of the primary is 2.6960 h (confirming the previous findings) while the satellite's lightcurve is characterized by a period of 16.6238 h.

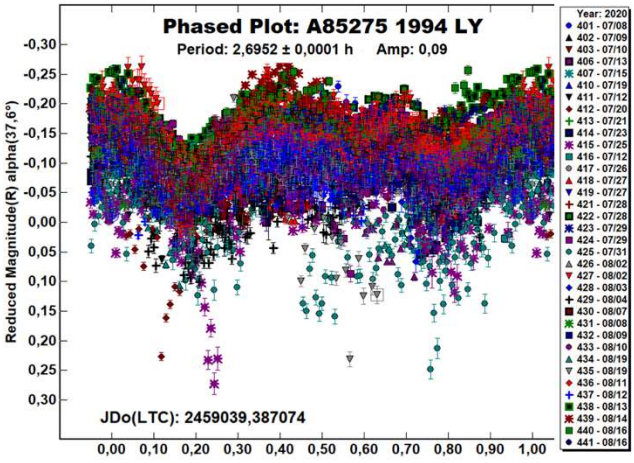

We performed CCD photometric observations between 2020 July 8 and August 20. Thirty-six observing sessions, with exposures of 30 s to 180 s, a data set of 6310 points for lightcurve analysis. This led to a period of 2.6952 h and amplitude of 0.09 mag, which is in good agreement with the reported results by the abovementioned groups. We also tried to search for the satellite's period but we didn't find a satisfactory solution, most likely because the noisy data prevented us from finding a signature of the satellite.

References

Apostolovska, G.; Ivanova, V.; Kostov, A. (2009) "CCD Photometry of 967 Helionape, 3415 Danby, (85275) 1994 LY, 2007 DT103, and 2007 TU24." *Minor Planet Bull*. **36**, 27-28.

Brinsfield, J.W. (2008). "The Rotation Periods of 1465 Autonoma, 1656 Suomi, 4483 Petofi, 4853 Marielukac, and (85275) 1994 LY." *Minor Planet Bull*. **35**, 23-24.

Harris, A.W.; Young, J.W.; Scaltriti, F.; Zappala, V. (1984). "Lightcurves and phase relations of the asteroids 82 Alkmene and 444 Gyptis." *Icarus* **57**, 251-258.

Harris, A.W.; Young, J.W.; Bowell, E.; Martin, L.J.; Millis, R.L.; Poutanen, M.; Scaltriti, F.; Zappala, V.; Schober, H.J.; Debehogne, H.; Zeigler, K.W. (1989). "Photoelectric Observations of Asteroids 3, 24, 60, 261, and 863." *Icarus* **77**, 171-186.

JPL (2020). Small-Body Database Browser. *https://ssd.jpl.nasa.gov/sbdb.cgi*

Pravec, P.; Wolf, M.; Sarounova, L. (2007). *http://www.asu.cas.cz/~ppravec/neo.htm*

Tonry, J.L.; Denneau, L.; Flewelling, H.; Heinze, A.N.; Onken, C.A.; Smartt, S.J.; Stalder, B.; Weiland, H.J.; Wolf, C. (2018). "The ATLAS All-Sky Stellar Reference Catalog." *Astrophys. J.* **867**, A105.

Warner, B.D.; Harris, A.W.; Pravec, P. (2009). "The Asteroid Lightcurve Database." *Icarus* **202**, 134-146. Updated 2020 Aug. *http://www.minorplanet.info/lightcurvedatabase.html*

Warner, B.D. (2017). MPO Software, *MPO Canopus* version 10.7.11.1. *http://bdwpublishing.com*

Warner, B.D.; Stephens, R.D.; Harris, A.W. (2020). "Binary Asteroids at the Center for Solar System Studies." *Minor Planet Bull*. **47**, 305-308.

LIGHTCURVE ANALYSIS OF L4 TROJAN ASTERIODS AT THE CENTER FOR SOLAR SYSTEM STUDIES: 2020 JULY TO SEPTEMBER

Robert D. Stephens
Center for Solar System Studies (CS3) / MoreData!
11355 Mount Johnson Ct., Rancho Cucamonga, CA 91737 USA
rstephens@foxandstephens.com

Brian D. Warner
Center for Solar System Studies (CS3) / MoreData!
Eaton, CO

(Received: 2020 October 11)

Lightcurves for three L4 Jovian Trojan asteroids were obtained at the Center for Solar System Studies (CS3) from 2020 July to September.

CCD photometric observations of three Trojan asteroids from the L_4 (Greek) Lagrange point were obtained at the Center for Solar System Studies (CS3, MPC U81). For several years, CS3 has been conducting a study of Jovian Trojan asteroids. This is another in a series of papers reporting data analysis being accumulated for family pole and shape model studies. It is anticipated that for most Jovian Trojans, two to five dense lightcurves per target at oppositions well distributed in ecliptic longitudes will be needed and can be supplemented with reliable sparse data for the brighter Trojan asteroids. For two of these targets we were able to get preliminary pole positions and create shape models from sparse data and the dense lightcurves obtained to date. These preliminary models will be improved as more data are acquired at future oppositions and will be published at a later date.

Table I lists the telescopes and CCD cameras that were used to make the observations. Images were unbinned with no filter and had master flats and darks applied. The exposures depended upon various factors including magnitude of the target, sky motion, and Moon illumination.

Telescope	Camera
0.40-m f/10 Schmidt-Cass	FLI Proline 1001E
0.40-m f/10 Schmidt-Cass	Fli Microline 1001E
0.35-m f/10 Schmidt-Cass	Fli Microline 1001E

Table I. List of telescopes and CCD cameras used at CS3.

Image processing, measurement, and period analysis were done using *MPO Canopus* (Bdw Publishing), which incorporates the Fourier analysis algorithm (FALC) developed by Harris (Harris et al., 1989). The Comp Star Selector feature in *MPO Canopus* was used to limit the comparison stars to near solar color. Night-to-night calibration was done using field stars from the ATLAS catalog (Tonry et al., 2018), which has Sloan *griz* magnitudes that were derived from the GAIA and Pan-STARR catalogs and are the "native" magnitudes of the catalog.

To reduce the resetting nightly zero points, we use the ATLAS r′ (SR) magnitudes. Those adjustments are mostly ≤ 0.03 mag. The occasions where larger corrections were required may have been related in part to using unfiltered observations, poor centroiding of the reference stars, and not correcting for second-order extinction terms.

Unless otherwise indicated, the Y-axis of lightcurves gives ATLAS SR "sky" (catalog) magnitudes. During period analysis, the magnitudes were normalized to the phase angle given in parentheses using G = 0.15. The X-axis rotational phase ranges from –0.05 to 1.05.

The amplitude indicated in the plots (e.g. Amp. 0.23) is the amplitude of the Fourier model curve and not necessarily the adopted amplitude of the lightcurve.

Targets selected for this L_4 observing campaign were mostly based upon the availability of dense lightcurves acquired in previous years. We obtained two to four lightcurves for most of these Trojans at previous oppositions.

For brevity, only some of the previously reported rotational periods may be referenced. A complete list is available at the lightcurve database (LCDB; Warner et al., 2009).

To evaluate the quality of the data obtained and to determine how much more data might be needed, preliminary pole and shape models were created for all of these targets. Sparse data observations were obtained from the Catalina Sky Survey and USNO-Flagstaff survey using the AstDyS-3 site (*http://hamilton.dm.unipi.it/asdys2/*). These sparse data were combined with our dense data as well as any other dense data found in the ALCDEF asteroid photometry database (*http://www.alcdef.org/*) using *MPO LCInvert*, (Bdw Publishing). This Windows-based program incorporates the algorithms developed by Kaasalainen and Torppa (2001) and Kaasalainen et al. (2001) and converted by Josef Ďurech from the original FORTRAN to C. A period search was made over a sufficiently wide range to assure finding a global minimum in χ^2 values.

911 Agamemnon. Reliable rotational rates for this Trojan were obtained four times in the past (Stephens, 2009; Mottola et al., 2011; French et al., 2012; Stephens et al., 2014), each time finding a period near 6.59 h. The 2020 results are in good agreement. Using sparse data from the Asteroids - Dynamic Site, a preliminary shape model with a sidereal rotational period of 6.581801 ± 0.00001 h was created.

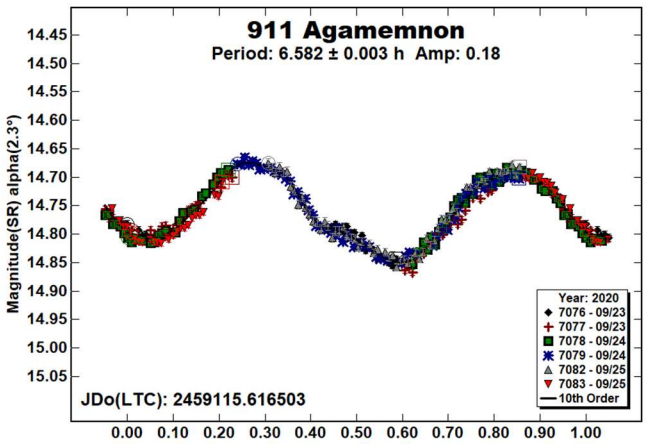

Number	Name	2019 mm/dd	Phase	L_{PAB}	B_{PAB}	Period(h)	P.E.	Amp	A.E.
911	Agamemnon	09/23-09/25	2.3,2.3	2	10	6.582	0.003	0.18	0.01
1143	Odysseus	09/19-09/22	2.3,2.9	345	3	10.099	0.003	0.18	0.01
3548	Eurybates	09/27-09/29	3.5,3.0	19	-4	8.74	0.12	0.12	0.02

Table II. Observing circumstances and results. The phase angle is given for the first and last date. If preceded by an asterisk, the phase angle reached an extrema during the period. L_{PAB} and B_{PAB} are the approximate phase angle bisector longitude/latitude at mid-date range (see Harris et al., 1984).

1143 Odysseus. Odysseus has been observed many times in the past. Molnar et al. (2008), Mottola et al. (2011), Shevchenko et al. (2012), Stephens et al. (2014), Waszczak et al. (2015), Ryan et al., (2017), and Szabó et al. (2017) each found a period near 10.11 h. The data collected this year, when combined with our previous data and available sparse data, were used to create a preliminary shape model with a sidereal rotational period of 10.11479 ± 0.00001 h.

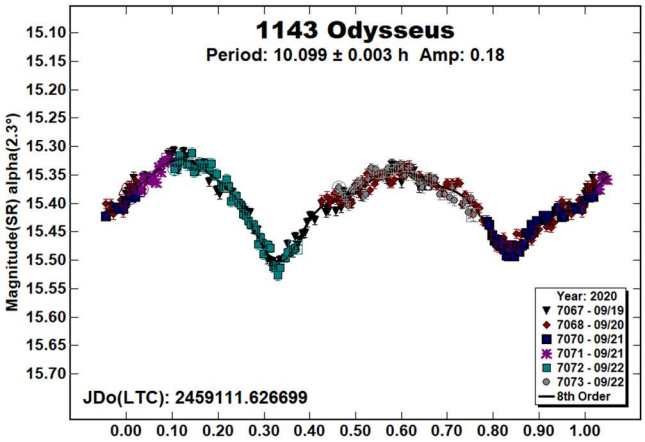

3548 Eurybates. Being a target of the Lucy mission to observe Jovian Trojan asteroids, Eurybates has already been well studied. Stephens (2010), Mottola et al. (2011), and Pál et al. (2020) each found periods near 8.71 h. Mottola et al. (2016) were able to determine a sidereal rotational period of 8.702724 ± 0.000001 h. Observations were made this year in hope of being able to determine a shape model and pole solution. Our period is in good agreement with previous results.

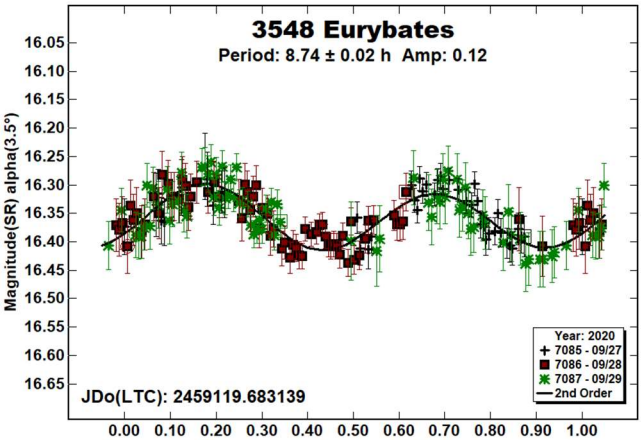

Acknowledgements

Observations at CS3 and continued support of the asteroid lightcurve database (LCDB; Warner et al., 2009) are supported by NASA grant 80NSSC18K0851. This work includes data from the Asteroid Terrestrial-impact Last Alert System (ATLAS) project. ATLAS is primarily funded to search for near earth asteroids through NASA grants NN12AR55G, 80NSSC18K0284, and 80NSSC18K1575; byproducts of the NEO search include images and catalogs from the survey area. The ATLAS science products have been made possible through the contributions of the University of Hawaii Institute for Astronomy, the Queen's University Belfast, the Space Telescope Science Institute, and the South African Astronomical Observatory. The purchase of a FLI-1001E CCD camera was made possible by a 2013 Gene Shoemaker NEO Grants from the Planetary Society.

References

Asteroids - Dynamic Site. *https://newton.spacedys.com/astdys/*

Asteroid Lightcurve Photometry Database (ALCDEF). *http://www.alcdef.org/*

French, L.M.; Stephens, R.D.; Coley, D.R.; Megna, R.; Wasserman, L.H. (2012). "Photometry of 17 Jovian Trojan Asteroids." *Minor Planet Bull.* **39**, 116-120.

Harris, A.W.; Young, J.W.; Scaltriti, F.; Zappala, V. (1984). "Lightcurves and phase relations of the asteroids 82 Alkmene and 444 Gyptis." *Icarus* **57**, 251-258.

Harris, A.W.; Young, J.W.; Bowell, E.; Martin, L.J.; Millis, R.L.; Poutanen, M.; Scaltriti, F.; Zappala, V.; Schober, H.J.; Debehogne, H.; Zeigler, K.W. (1989). "Photoelectric Observations of Asteroids 3, 24, 60, 261, and 863." *Icarus* **77**, 171-186.

Kaasalainen, M.; Torppa J. (2001). "Optimization Methods for Asteroid Lightcurve Inversion. I. Shape Determination." *Icarus* **153**, 24-36.

Kaasalainen, M.; Torppa, J.; Muinonen, K. (2001). "Optimization Methods for Asteroid Lightcurve Inversion. II. The Complete Inverse Problem." *Icarus* **153**, 37-51.

Molnar, L.A.; Jaegert, M.J.; Hoogeboom, K.M. (2008). "Lightcurve Analysis of an Unbiased Sample of Trojan Asteroids." *Minor Planet Bull.* **35**, 82-84.

Mottola, S.; Di Martino, M.; Erikson, A.; Gonano-Beurer, M.; Carbognani, A.; Carsenty, U.; Hahn, G.; Schober, H.; Lahulla, F.; Delbò, M.; Lagerkvist, C. (2011). "Rotational Properties of Jupiter Trojans. I. Light Curves of 80 Objects." *Astron. J.* **141**, A170.

Mottola, S.; Marchi, S.; Buie, M.W.; Hellmich, S.; Di Martino, M.; Proffe, G.; Levison, H.F.; Zangari, A.M. (2016). "Ground-based characterization of Eurybates and Orus, two fly-by targets of the Lucy Discovery mission." *AAS DPS meeting*. **48**, 208.04.

Pál, A.; Szakáts, R; Kiss, C.; Bódi, A.; Bognár, Z.; Kalup, C.; Kiss, L.; Marton, G.; Molnár, L.; Plachy, E.; Sárneczky, K.; Szabó, G.; Szabó, R. (2020). "Solar System Objects Observed with TESS - First Data Release: Bright Main-belt and Trojan Asteroids from the Southern Survey." *Astron. J.* **247**, id 26.

Ryan, E.L.; Sharkey, B.; Woodward, C.E. (2017). "Trojan Asteroids in the Kepler Campaign 6 Field." *Astron. J.* **153**, id 116.

Shevchenko, V.G.; Belskaya, I.N.; Slyusarev, I.G.; Krugly, Yu.N.; Chiorny, V.G.; Gaftonyuk, N.M.; Donchev, Z.; Ivanova, V.; Ibrahimov, M.A.; Ehgamberdiev, Sh.A.; Molotov, I.E. (2012). "Opposition effect of Trojan asteroids." *Icarus* **217**, 202-208.

Stephens, R.D. (2009). "Asteroids Observed from GMARS and Santana Observatories." *Minor Planet Bull.* **36**, 59-62.

Stephens, R.D. (2010). "Trojan Asteroids Observed from GMARS and Santana Observatories: 2009 October - December." *Minor Planet Bull.* **37**, 47-48.

Stephens, R.D.; Coley, D.R.; French, L.M.; (2014). "Trojan Asteroids Observed from CS3: 2014 January-May." *Minor Planet Bull.* **43**, 210-212.

Szabó, Gy.M.; Pál, A.; Kiss, Cs.; Kiss, L.L.; Molnár, L.; Hanyecz, O.; Plachy, E.; Sárneczky, K.; Szabó, R. (2017). "The heart of the swarm: K2 photometry and rotational characteristics of 56 Jovian Trojan asteroids." *Astron. & Astrophys.* **599,** A44.

Tonry, J.L.; Denneau, L.; Flewelling, H.; Heinze, A.N.; Onken, C.A.; Smartt, S.J.; Stalder, B.; Weiland, H.J.; Wolf, C. (2018). "The ATLAS All-Sky Stellar Reference Catalog." *Astrophys. J.* **867**, A105.

Warner, B.D.; Harris, A.W.; Pravec, P. (2009). "The Asteroid Lightcurve Database." *Icarus* **202**, 134-146. Updated 2020 July. *http://www.minorplanet.info/lightcurvedatabase.html*

Waszczak, A.; Chang, C.-K.; Ofek, E.O.; Laher, R.; Masci, F.; Levitan, D.; Surace, J.; Cheng, Y.-C.; Ip, W.-H.; Kinoshita, D.; Helou, G.; Prince, T.A.; Kulkarni, S. (2015). "Asteroid Light Curves from the Palomar Transient Factory Survey: Rotation Periods and Phase Functions from Sparse Photometry." *Astron. J.* **150**, A75.

LIGHTCURVES OF THREE HILDAS

W. Romanishin
1933 Whispering Pines Cir.
Norman, OK 73072 USA
wromanishin@ou.edu

(Received: 2020 Oct 15 Revised: 2020 Nov 1)

I present lightcurves for three Hilda population objects. For 1748 Mauderli, I find a period of 6.003 h, in agreement with some but not all published values. For two other objects, 1439 Vogtia and 2246 Bowell, I find good agreement with previous periods. The observations for these two objects were made in 2013, so they can be useful for providing additional time baselines for shape models.

All CCD images were reduced and measured using custom scripts using the IRAF software package. Reduction steps included subtraction of background images to reduce the effects of contaminating stars and galaxies, and pairwise comparison of seeing and transparency monitoring stars to look for stellar variations during the night.

1748 Maurdeli is a member of the Hilda group discovered on 1966 Sep 7 by P. Wild at Zimmerwald. Period values around 6.00 h have been published by Gonano et al. (1991), Dahlgren et al. (1998) and Romanishin (2020). Warner and Stephens (2018) present a preferred period of 5.320 h and alternate periods of 5.552 and 5.981 h. In Romanishin (2020), I suggest that Mauderli may be a contact or close binary due to sharp V-shaped minima.

I remotely observed Mauderli near its opposition in August 2020 using the 0.6-m telescope (CHI-1) of the Telescope Live system located at El Sauce Observatory in Chile and a 0.5-m telescope (T30) at the iTelescope observatory in Australia. Exposures on both telescopes were 120 s long. Using CHI-1, I obtained observations on three nights through a Sloan r filter. On 2020 Aug 23, I obtained 93 exposures, spanning about 4.6 h, on 2020 Aug 27, 78 exposures spanning 3.5 h and on 2020 Aug 28, 45 exposures spanning 2.0 h. Using T30 and the available red filter, I obtained 87 exposures on 2020 Aug 27, spanning 3.6 h. Due to weather and telescope scheduling constraints, I was unable to obtain a complete lightcurve on any single night. However, as the two telescopes are about 9 hours apart in longitude (~1.5 times the period), I was able to observe the entire lightcurve at low airmass, roughly half from Chile and half from Australia.

For this object, photometric calibration was made with reference to Pan-STARRS catalog r magnitudes of stars in each field. Magnitudes were reduced to absolute Sloan r band system using the Bowell et al. (1989) H,G formalism, with G = 0.15. Small magnitude corrections were required to superimpose the light curves.

Number	Name	yyyy mm/dd	Phase	L_{PAB}	B_{PAB}	Period(h)	P.E.	Amp	A.E.
1439	Vogtia	2013 05/05-05/08	2.4,1.5	233	-1	12.927	0.01	0.34	0.02
1748	Mauderli	2020 08/23-08/28	2.1,3.8	325	-1	6.003	0.005	0.11	0.01
2246	Bowell	2013 05/04-05/04	3.7	233	7	4.985	0.01	0.26	0.02

Table I. Observing circumstances and results. The phase angle is given for the first and last date. If preceded by an asterisk, the phase angle reached an extrema during the period. L_{PAB} and B_{PAB} are the approximate phase angle bisector longitude/latitude at mid-date range (see Harris et al., 1984).

Phased lightcurves for all published period values were calculated and examined, and lightcurves with finer period spacing around the best of these were produced and examined. The best overall fit is for a period of 6.003 h. Periods of 5.32, 5.55 or 5.98 h do not give acceptable phased lightcurves. The magnitude plotted for Mauderli is the reduced magnitude in the Sloan r band.

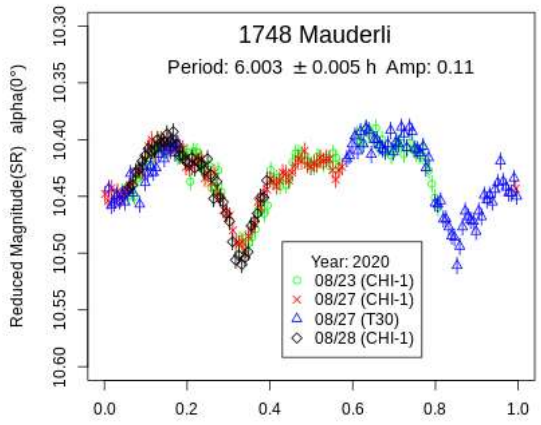

1439 Vogtia is a Hilda group object discovered on 1937 Oct 11 by K. Reinmuth at Heidelberg.

I observed Vogtia with the 0.9-m SMARTS telescope at Cerro Tololo Observatory in Chile on two night in May of 2013, using 150-s long exposures. On 2013 May 5, I obtained 157 exposures spanning 8.3 h, and on 2013 May 8, 162 exposures spanning 8.8 h. I find a period of 12.927 h, in reasonable agreement with the 12.95 h period of Dahlgren et al. (1998) and good agreement with the 12.933 h period of Warner and Stephens (2020).

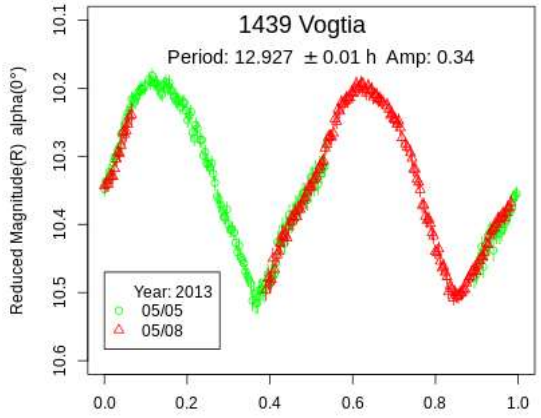

2246 Bowell is a Hilda discovered 1979 Dec 14 by E. Bowell at Lowell Observatory. Using the SMARTS telescope, I obtained 99 exposures, each 150-s, spanning 5.6 h on 2013 May 4. I find a period of 4.985 h, which is in reasonable agreement with the published periods of 4.992 h (Dahlgren et al. 1998) and 4.997 h (Warner and Stephens 2019).

For both Vogtia and Bowell, photometric calibration in the Landolt R magnitude system was made using observations of several Landolt standard fields each night (Clem and Landolt, 2013). The reduced Landolt R band magnitude is plotted for Vogtia and Bowell.

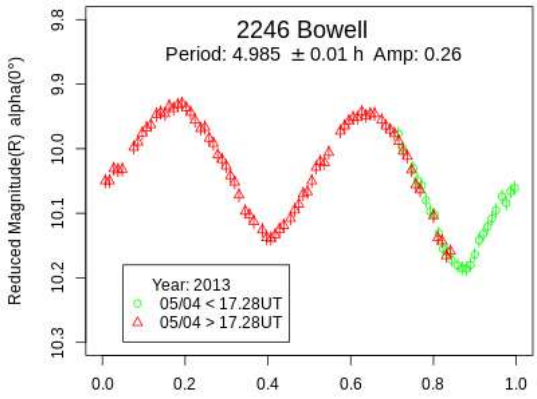

References

Bowell, E.; Hapke, E.B.; Domingue, D.; Lumme, K.; Peltoniemi, J.; Harris, A.W. (1989). "Application of Photometric Models to Asteroids." In *Asteroids II* (R.P. Binzel, R. Gehrels, M.S. Matthews, eds.) pp 524-556. Univ of Arizona Press, Tucson.

Clem, J.L.; Landolt, A.U. (2013). "Faint UBVR Standard Star Fields." *Astronomical Journal*, **146**, A88.

Dahlgren, M.; Lahulla, J.F.; Lagerkvist, C.-I.; Lagerros, J.; Mottola, S.; Erikson, A.; Gonano-Beurer, M. (1998). "A Study of Hilda Asteroids." *Icarus* **133**, 247-285.

Gonano, M.; Di Martino, M.; Mottola, S.; Neukum, G. (1991). "Physical Study of Outer Belt Asteroids." *Adv. Space Res.* **11**, 197-200.

Harris, A.W.; Young, J.W.; Scaltriti, F.; Zappala, V. (1984). "Lightcurves and phase relations of the asteroids 82 Alkmene and 444 Gyptis." *Icarus* **57**, 251-258.

Romanishin, W. (2020). "(1748) Mauderli: A Possible Binary in the Hilda Population." *Res. Notes AAS*, **4**, A44.

Warner, B.D.; Stephens, R.D. (2018). "Lightcurve Analysis of Hilda Asteroids at the Center for Solar System Studies: 2018 April-June." *Minor Planet Bull*. **45**, 390.

Warner, B.D.; Stephens, R.D. (2019). "Lightcurve Analysis of Hilda Asteroids at the Center for Solar System Studies: 2019 January-March." *Minor Planet Bull*. **46**, 294.

Warner, B.D.; Stephens, R.D. (2020). "Lightcurve Analysis of Hilda Asteroids at the Center for Solar System Studies: 2019 December- 2020 April." *Minor Planet Bull*. **47**, 196.

LIGHTCURVE ANALYSIS OF HILDA ASTEROIDS AT THE CENTER FOR SOLAR SYSTEM STUDIES: 2020 AUGUST - SEPTEMBER

Brian D. Warner
Center for Solar System Studies / MoreData!
446 Sycamore Ave.
Eaton, CO 80615 USA
brian@MinorPlanetObserver.com

Robert D. Stephens
Center for Solar System Studies / MoreData!
Rancho Cucamonga, CA

(Received: 2020 October 11)

New CCD photometric observations of four Hilda asteroid members were made from 2020 August through September: 499 Venusia, 1162 Larissa, 2760 Kacha, and (13035) 1989 UA6. One of them, 2760 Kacha, showed weak signs of a secondary period, but its origin may be only a harmonic artifact of Fourier analysis.

CCD photometric observations of Hilda asteroids are made at the Center for Solar System Studies (CS3) as part of an ongoing study of this family/group that is located between the outer main-belt and Jupiter Trojans in a 3:2 orbital resonance with Jupiter. The goal is to determine the spin rate statistics of the Hildas and to find pole and shape models when possible. We also look to examine the degree of influence that the YORP (Yarkovsky–O'Keefe–Radzievskii–Paddack) effect (Rubincam, 2000) has on distant objects and to compare the spin rate distribution against the Jupiter Trojans, which can provide evidence that the Hildas are more "comet-like" than main-belt asteroids.

Table I lists the telescopes and CCD cameras that are combined to make observations. Up to seven telescopes are commonly used for observations. All the cameras use CCD chips from the KAF blue-enhanced family and so have essentially the same response. The pixel scales ranged from 1.24-1.60 arcsec/pixel. All lightcurve observations were unfiltered since a clear filter can result in a 0.1-0.3 magnitude loss. The exposures varied depending on the asteroid's brightness.

Telescopes	Cameras
0.30-m *f*/6.3 Schmidt-Cass	FLI Microline 1001E
0.35-m *f*/9.1 Schmidt-Cass	FLI Proline 1001E
0.35-m *f*/11 Schmidt-Cass	SBIG STL-1001E
0.40-m f/10 Schmidt-Cass	
0.50-m *f*/8.1 Ritchey-Chrétien	

Table I. List of available telescopes and CCD cameras at CS3. The exact combination for each telescope/camera pair can vary due to maintenance or specific needs.

To reduce the number of times and amounts of adjusting nightly zero points, we use the ATLAS catalog r´ (SR) magnitudes (Tonry et al., 2018). Those adjustments are usually ≤ ±0.03 mag. The rare greater corrections may have been related in part to using unfiltered observations, poor centroiding of the reference stars, and not correcting for second-order extinction. Another cause may be selecting what appears to be a single star but is actually an unresolved pair.

The Y-axis values are ATLAS SR "sky" (catalog) magnitudes. During period analysis, the magnitudes were normalized to the comparison stars used in the earliest session and to the phase angle given in parentheses using $G = 0.15$. The X-axis shows rotational phase from –0.05 to 1.05. If the plot includes the amplitude, e.g., "Amp: 0.65", this is the amplitude of the Fourier model curve and *not necessarily the adopted amplitude for the lightcurve*.

Our initial search for previous results started with the asteroid lightcurve database (LCDB; Warner et al., 2009) found on-line at *http://www.minorplanet.info/lightcurvedatabase.html*. Readers are strongly encouraged to obtain, when possible, the original references listed in the LCDB. From here on, we'll use only "LCDB" to reference the paper by Warner et al. (2009).

499 Venusia. Two previous rotational periods listed in the LCDB are from Dahlgren et al. (1998, 13.48h) and Behrend (2006web, 13.486 h). Hanuš et al. (2011) used a combination of dense and sparse data sets to find a sidereal period of 13.4871 h and a pole with J2000 ecliptic coordinates of (λ,β) = (37°, 50°) or (212°, 46°). Our synodic period of 13.53 h is more than one-sigma from the previous results, more than might be expected from the sidereal-synodic difference. A larger data set, one that filled in the entire lightcurve may have moved the result closer to the others.

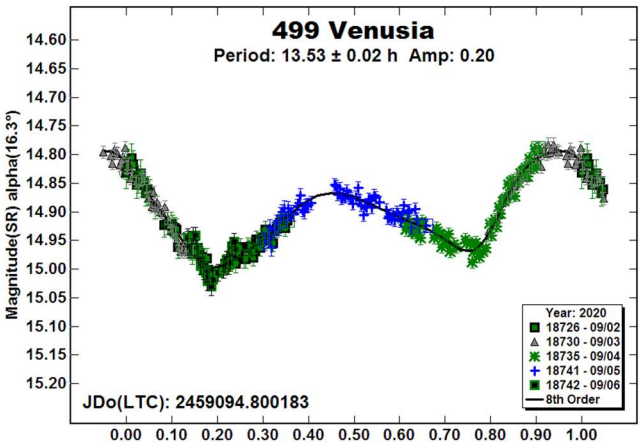

1162 Larissa. Pligge et al. (2011) found a period of 6.520 h for this 44-km Hilda. Warner and Stephens (2017) found a similar result of 6.514 based on 2017 observations. Our results from 2020 are in reasonably good agreement.

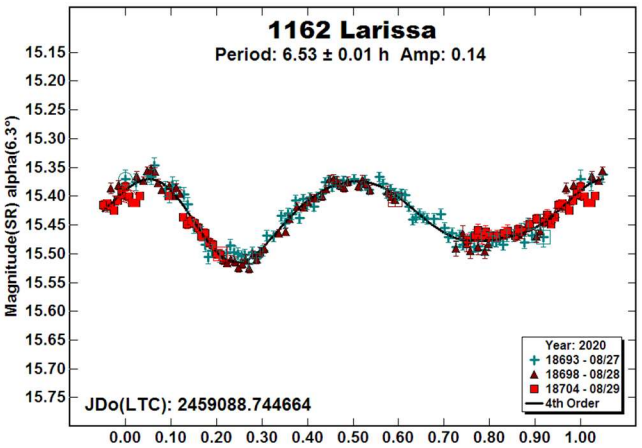

Number	Name	20yy/mm/dd	Phase	L_{PAB}	B_{PAB}	Period(h)	P.E.	Amp	A.E.
499	Venusia	09/02-09/06	16.3,15.8	38	2	13.53	0.02	0.20	0.01
1162	Larissa	08/27-08/29	6.3,5.8	357	-2	6.53	0.01	0.14	0.01
2760	Kacha	08/31-09/22	10.1,5.7	20	6	26.247	0.005	0.27	0.02
						15.63	0.02	0.04	0.01
13035	1989 UA6	08/30-09/09	5.3,2.5	354	-4	10.647	0.003	0.40	0.03

Table II. Observing circumstances. The phase angle (α) is given at the start and end of each date range. L_{PAB} and B_{PAB} are the average phase angle bisector longitude and latitude (see Harris *et al.*, 1984).

2760 Kacha. Dahlgren et al. (1998) reported a period of 13.0 h for the 58-km Larissa. Ďurech et al. (2018b) used lightcurve inversion to find a sidereal period of 53.040 h and pole with J2000 ecliptic coordinates of (λ,β) = (101°, –30°). Our synodic period is almost exactly one-half that found by Durech et al (2018b).

Trying to fit our data to near 53 h produced a very ragged lightcurve. To get it close to a reasonable fit would have required unacceptably large zero-point offsets. Also, given the apparent lightcurve amplitude of 0.27 mag, it was not likely that even an ill-fitting result near 53 h was correct (Harris et al., 2014).

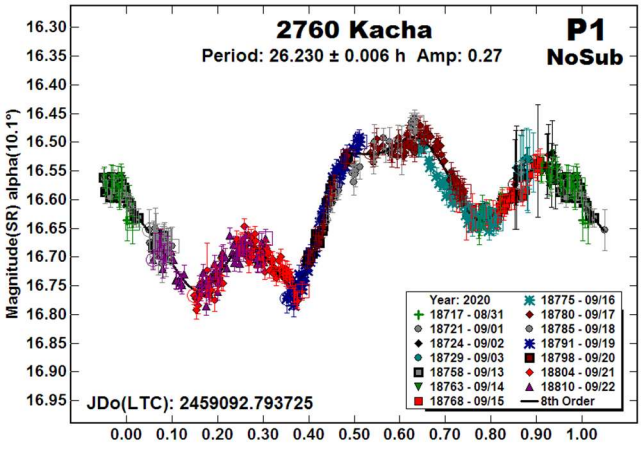

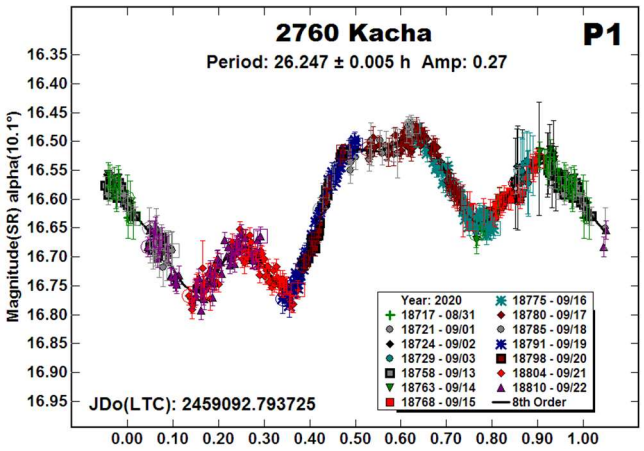

Even after getting a close fit to 26.230 h, parts of the lightcurve did not quite line-up. We used the dual-period search feature of *MPO Canopus* to see if a second period was present.

The period spectrum shows several possible, but relatively weak, possibilities with the lowest RMS at about 15.6 h. Refinement of the two periods led to a final result of P_2 = 15.63 h which, when subtracted from the full data set, produced a cleaner lightcurve for P_1 = 26.230 h. A search for a secondary period that would improve the results for a period of 53 h was unsuccessful.

Tumbling is unlikely given the period and diameter (Pravec et al., 2014), so it's doubtful that the P_2 lightcurve has a physical origin. Given that P_2 is almost an exact 3:2 ratio with an Earth day and is also very close to being a 5:3 ratio with P_1, it's more likely that P_2 is the result of a harmonic artifact from the Fourier analysis and acts as a "noise filter" for the data set.

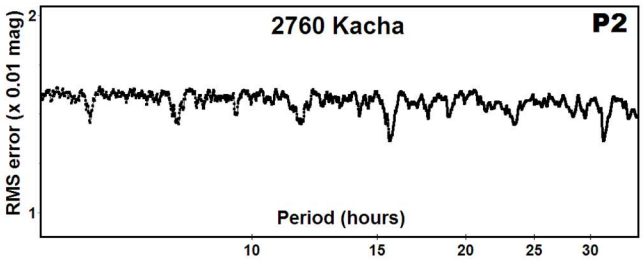

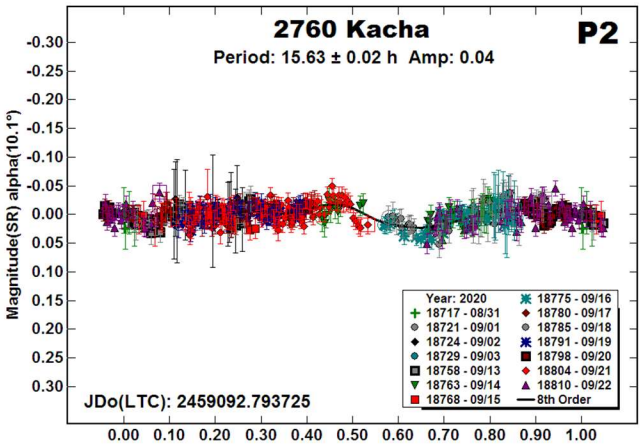

(13035) 1989 UA6. Ďurech et al. (2018a) used lightcurve inversion to find a sidereal period $P_{Sideral}$ = 10.65696 h and a pole with J2000 ecliptic coordinates of (λ, β) = (142°, 46°) or (323°, 37°). We (Warner and Stephens, 2018) observed the 24-km asteroid in 2018 and found a synodic period of 10.639 h. Our result from the 2020 observations is in very good agreement.

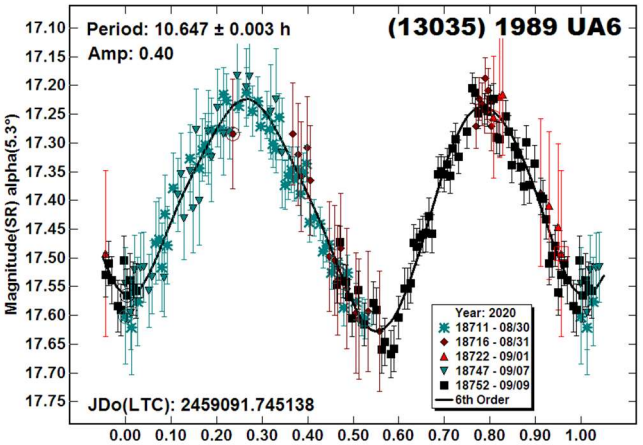

Acknowledgements

Funding for observations at CS3 and work on the asteroid lightcurve database (Warner et al., 2009) and ALCDEF database (*alcdef.org*) are supported by NASA grant 80NSSC18K0851.

This work includes data from the Asteroid Terrestrial-impact Last Alert System (ATLAS) project. ATLAS is primarily funded to search for near earth asteroids through NASA grants NN12AR55G, 80NSSC18K0284, and 80NSSC18K1575; byproducts of the NEO search include images and catalogs from the survey area. The ATLAS science products have been made possible through the contributions of the University of Hawaii Institute for Astronomy, the Queen's University Belfast, the Space Telescope Science Institute, and the South African Astronomical Observatory.

The authors gratefully acknowledge Shoemaker NEO Grants from the Planetary Society (2007, 2013). These were used to purchase some of the telescopes and CCD cameras used in this research.

References

Behrend, R. (2006web). Observatoire de Geneve web site. *http://obswww.unige.ch/~behrend/page_cou.html*

Dahlgren, M.; Lahulla, J.F.; Lagerkvist, C.-I.; Lagerros, J.; Mottola, S.; Erikson, A.; Gonano-Beurer, M.; Di Martino, M. (1998). "A Study of Hilda Asteroids. V. Lightcurves of 47 Hilda Asteroids." *Icarus* **133**, 247-285.

Ďurech, J.; Hanuš, J.; Ali-Lagoa, V. (2018a). "Asteroid models reconstructed from the Lowell Photometric Database and WISE data." *Astron. Astrophys*. **617**, A57.

Ďurech, J.; Hanuš, J. (2018b). "Reconstruction of asteroid spin states from Gaia DR2 photometry." *Astron. Astrophys*. **620**, A91.

Hanuš, J.; Brož, M.; Ďurech, J.; Warner, B.D.; Brinsfield, J.; Durkee, R.; Higgins, D.; Koff, R.A.; Oey, J.; Pilcher, F.; Stephens, R.; Strabla, L.P.; Ulisse, Q.; Girelli, R. (2011). "An anisotropic distribution of spin vectors in asteroid families." *Astron. Astrophys.* **559**, A134.

Harris, A.W.; Young, J.W.; Scaltriti, F.; Zappala, V. (1984). "Lightcurves and phase relations of the asteroids 82 Alkmene and 444 Gyptis." *Icarus* **57**, 251-258.

Harris, A.W.; Pravec, P.; Galad, A.; Skiff, B.A.; Warner, B.D.; Vilagi, J.; Gajdos, S.; Carbognani, A.; Hornoch, K.; Kusnirak, P.; Cooney, W.R.; Gross, J.; Terrell, D.; Higgins, D.; Bowell, E.; Koehn, B.W. (2014). "On the maximum amplitude of harmonics on an asteroid lightcurve." *Icarus* **235**, 55-59.

Pligge, Z.; Monnier, A.; Pharo, J.; Stolze, K.; Yim, A.; Ditteon, R. (2011). "Asteroid Lightcurve Analysis at the Oakley Southern Sky Observatory: 2010 May." *Minor Planet Bull*. **38**, 5-7.

Pravec, P.; Scheirich, P.; Ďurech, J.; Pollock, J.; Kusnirak, P.; Hornoch, K.; Galad, A.; Vokrouhlicky, D.; Harris, A.W.; Jehin, E.; Manfroid, J.; Opitom, C.; Gillon, M.; Colas, F.; Oey, J.; Vrastil, J.; Reichart, D.; Ivarsen, K.; Haislip, J.; LaCluyze, A. (2014). "The tumbling state of (99942) Apophis." *Icarus* **233**, 48-60.

Rubincam, D.P. (2000). "Relative Spin-up and Spin-down of Small Asteroids." *Icarus* **148**, 2-11.

Tonry, J.L.; Denneau, L.; Flewelling, H.; Heinze, A.N.; Onken, C.A.; Smartt, S.J.; Stalder, B.; Weiland, H.J.; Wolf, C. (2018). "The ATLAS All-Sky Stellar Reference Catalog." *Astrophys. J.* **867**, A105.

Warner, B.D.; Stephens, R.D. (2017). "Lightcurve Analysis of Hilda Asteroids at the Center for Solar System Studies: 2016 December thru 2017 April." *Minor Planet Bull*. **44**, 220-222.

Warner, B.D.; Stephens, R.D. (2018). "Lightcurve Analysis of Hilda Asteroids at the Center for Solar System Studies: 2018 April-June." *Minor Planet Bull*. **45**, 390-393.

Warner, B.D.; Harris, A.W.; Pravec, P. (2009). "The Asteroid Lightcurve Database." *Icarus* **202**, 134-146. Updated 2020 June. *http://www.minorplanet.info/lightcurvedatabase.html*

COLLABORATIVE ASTEROID PHOTOMETRY FROM UAI: 2020 JULY-SEPTEMBER

Lorenzo Franco
Balzaretto Observatory (A81), Rome, ITALY
lor_franco@libero.it

Giulio Scarfi
Iota Scorpii Observatory (K78), La Spezia, ITALY

Alessandro Marchini
Astronomical Observatory, DSFTA - University of Siena (K54)
Via Roma 56, 53100 - Siena, ITALY

Pietro Aceti, Massimo Banfi
Seveso Observatory (C24) & Felizzano Observatory
Seveso, ITALY

Riccardo Papini, Fabio Salvaggio
Wild Boar Remote Observatory (K49)
San Casciano in Val di Pesa (FI), ITALY

Ernesto Guido, Antonio Catapano
AstroCampania Associazione - Osservatorio Astronomico
Salvatore di Giacomo (L07), Agerola, ITALY

Adriano Valvasori, Ernesto Guido
ALMO Observatory (G18), Padulle (BO), ITALY

Massimiliano Mannucci, Nico Montigiani
Osservatorio Astronomico Margherita Hack (A57)
Florence, ITALY

Antonio De Pieri, Antonino Brosio
Parco Astronomico Lilio (K96), Savelli (KR), ITALY

Luciano Tinelli
GAV (Gruppo Astrofili Villasanta), Villasanta, ITALY

Alessio Ciarnella
GrAG (Gruppo Astrofili Galileo Galilei), Viterbo, ITALY

Ernesto Guido, Marco Rocchetto
Telescope Live (X02), El Sauce, CHILE

(Received: 2020 October 4)

Photometric observations of six main-belt and one near-Earth asteroids were made in order to acquire lightcurves for shape/spin axis modeling. The synodic period and lightcurve amplitude were found for 375 Ursula: 16.900 ± 0.004 h, 0.09 mag; 444 Gyptis: 6.2136 ± 0.0006 h, 0.09 mag; 737 Arequipa: 7.024 ± 0.001 h, 0.14 mag; 1146 Biarmia: 5.4697 ± 0.0007 h, 0.17 mag; 1346 Gotha: 2.6366 ± 0.0006 h, 0.11 mag; 1656 Suomi: 2.5892 ± 0.0006 h, 0.11 mag; 2020 PL2: 0.3606 ± 0.0001 h, 1.5 mag.

Collaborative asteroid photometry was done inside the Italian Amateur Astronomers Union (UAI; 2020) group. The targets were selected mainly in order to acquire lightcurves for shape/spin axis modeling. Table I shows the observing circumstances and results.

The CCD observations were made in 2020 July-September using the instrumentation described in the Table II. Lightcurve analysis was performed at the Balzaretto Observatory with *MPO Canopus* (Warner, 2019). All the images were calibrated with dark and flat frames and converted to R magnitudes using solar colored field stars from the CMC15 catalogue distributed with *MPO Canopus*.

In the following, we frequently reference the asteroid lightcurve database (LCDB; Warner et al., 2009), which will be cited with only "LCDB" from here on.

375 Ursula is an Xc-type (Bus and Binzel, 2002) outer main-belt asteroid discovered on 1893 September 18 by A. Charlois at Nice. Collaborative observations were made over six nights. The period analysis shows a synodic period of P = 16.900 ± 0.004 h with an amplitude A = 0.09 ± 0.02 mag. The period is close to the previously published results in the LCDB.

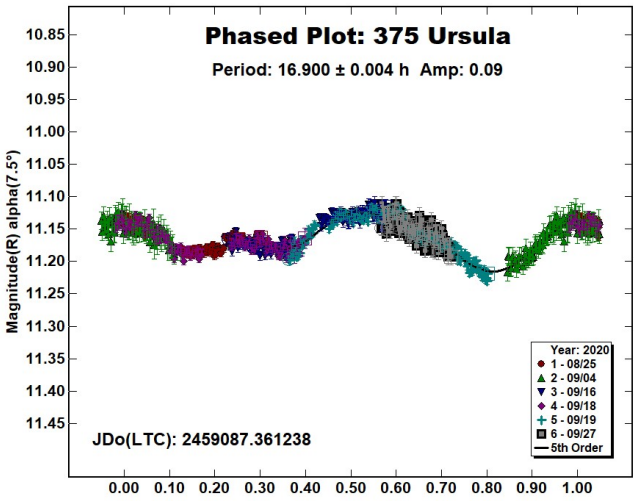

444 Gyptis is a C-type (Bus and Binzel, 2002) middle main-belt asteroid discovered on 1899 March 31 by J. Coggia at Marseille. Collaborative observations were made over six nights. The period analysis shows a synodic period of P = 6.2136 ± 0.0006 h with an amplitude A = 0.09 ± 0.03 mag. The period is close to the previously published results in the LCDB.

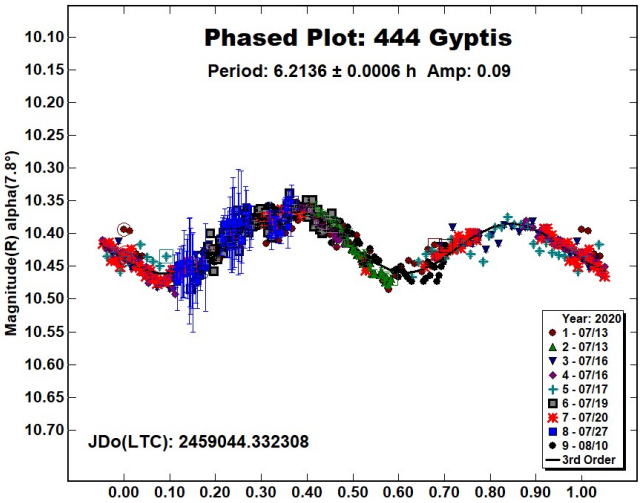

Number	Name	2020 mm/dd	Phase	L_{PAB}	B_{PAB}	Period(h)	P.E.	Amp	A.E.	Grp
375	Ursula	08/25-09/27	*7.5,6.6	350	5	16.900	0.004	0.09	0.02	MB-O
444	Gyptis	07/13-08/10	*7.8,11.7	299	13	6.2136	0.0006	0.09	0.03	MB-M
737	Arequipa	08/22-09/13	15.5,3.6	355	5	7.024	0.001	0.14	0.02	MB-M
1146	Biarmia	07/18-08/06	15.1,11.8	317	23	5.4697	0.0007	0.17	0.02	MB-O
1346	Gotha	07/14-07/19	6.4,7.1	289	15	2.6366	0.0006	0.11	0.04	MB-M
1656	Suomi	08/09-08/19	13.8,12.6	324	21	2.5892	0.0006	0.11	0.05	H
	2020 PL2	08/14-08/15	26.3,30.9	323	15	0.3606	0.0001	1.5	0.2	NEA

Table I. Observing circumstances and results. The first line gives the results for the primary of a binary system. The second line gives the orbital period of the satellite and the maximum attenuation. The phase angle is given for the first and last date. If preceded by an asterisk, the phase angle reached an extremum during the period. L_{PAB} and B_{PAB} are the approximate phase angle bisector longitude/latitude at mid-date range (see Harris et al., 1984). Grp is the asteroid family/group (Warner et al., 2009).

737 Arequipa is an S-type (Bus and Binzel, 2002) middle main-belt asteroid discovered on 1912 December 7 by J.H. Metcalf at Winchester. Collaborative observations were made over six nights. We found a synodic period of P = 7.024 ± 0.001 h with an amplitude A = 0.14 ± 0.02 mag. The period is close to the previously published results in the LCDB.

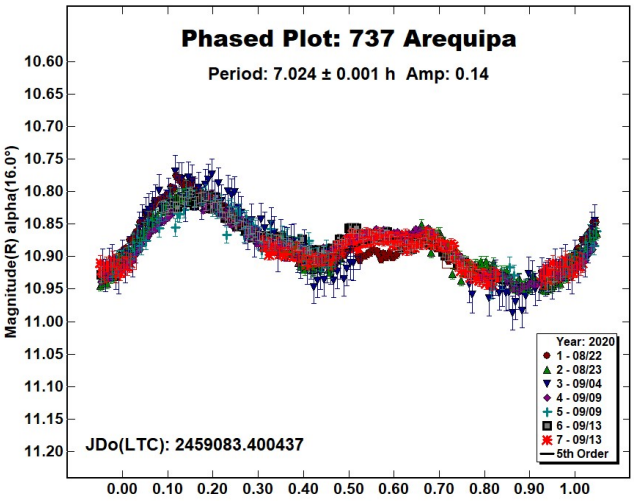

1346 Gotha is a medium-albedo middle main-belt asteroid discovered on 1929 February 5 by K. Reinmuth at Heidelberg. Collaborative observations were made over three nights. We found a synodic period of P = 2.6366 ± 0.0006 h with an amplitude A = 0.11 ± 0.04 mag. The period is close to the previously published results in the LCDB.

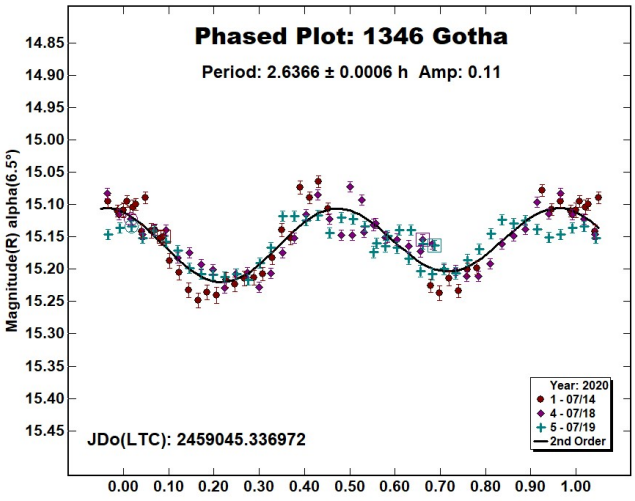

1146 Biarmia is an X-type (Tholen, 1984) outer main-belt asteroid discovered on 1929 May 7 by G. Neujmin at Simeis. Collaborative observations were made over six nights. We found a synodic period of P = 5.4697 ± 0.0007 h with a moderate amplitude A = 0.17 ± 0.02 mag. The period is close to previously published results in the LCDB.

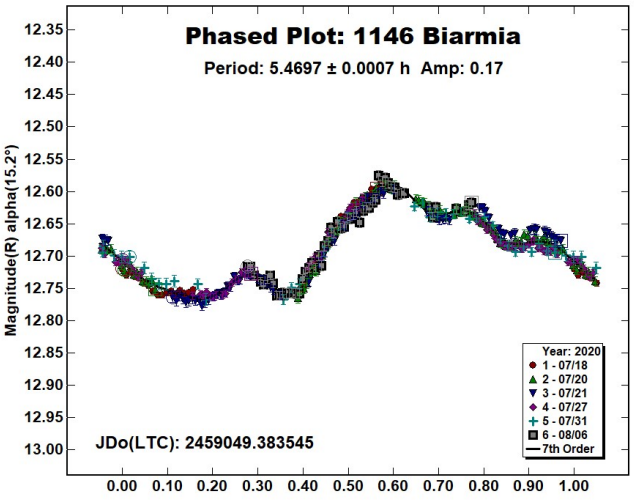

1656 Suomi is a S-type (Sanchez, 2013) member of the Hungaria group; it was discovered on 1942 March 11 by Y. Vaisala at Turku. Collaborative observations were made over five nights. The period analysis shows a synodic period of P = 2.5892 ± 0.0006 h with an amplitude A = 0.11 ± 0.05 mag. The period is close to the previously published results in the LCDB.

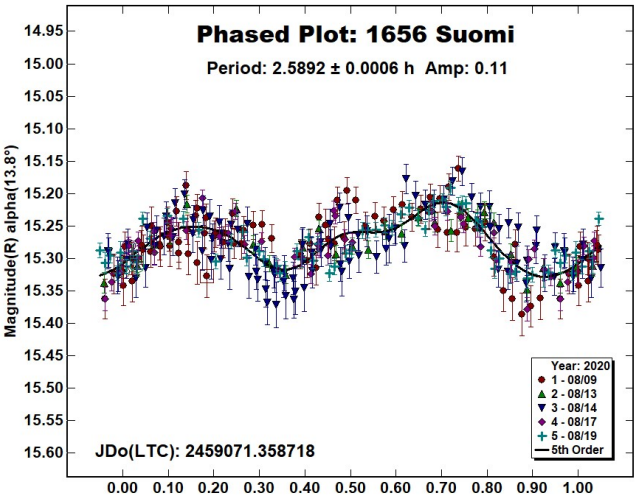

Observatory (MPC code)	Telescope	CCD	Filter	Observed Asteroids (#Sess)
Iota Scorpii(K78)	0.40-m RCT f/8.0	SBIG STXL-6303e(bin 2×2)	Rc	375(3),444(2),737(4), 1146(4),1656(2)
Astronomical Observatory of the University of Siena(K54)	0.30-m MCT f/5.6	SBIG STL-6303e(bin 2×2)	Rc	375(1),444(1),1146(1), 1656(2)
Seveso Observatory (C24)	0.30-m SCT f/6.3	SBIG ST9	Rc	375(2),737(2)
WBRO (K49)	0.235-m SCT f/10	SBIG ST8-XME	C	444(3), 737(1)
Salvatore di Giacomo (L07)	0.50-m RCT f/8.0	FLI PL4240	C	2020 PL2(2)
ALMO Observatory (G18)	0.235-m SCT f/5.1	Atik 4000	Rc	444(1),1146(1)
Osservatorio Astronomico Margherita Hack (A57)	0.35-m SCT f/8.3	SBIG ST10XME (bin 2×2)	Rc	1346(2)
Parco Astronomico Lilio (K96)	0.50-m RCT f/8.0	FLI PL1001	r'	1346(1)
GAV	0.20-m SCT f/6.3	SXV-H9	Rc	444(1)
GrAG	0.25-m NRT f/4.8	SBIG ST8-XME	C	1656(1)
Telescope Live, El Sauce (X02)	0.60-m NRT f/3.8	FLI PL 16803	R	444(1)

Table II. Listing of participating observing stations, equipment, filter, and the asteroids observed. The number in parentheses indicates the

2020 PL2 is an Aten near-Earth asteroid first detected on 2020 August 13 by ATLAS Haleakala. Astrometric and photometric observations were in the following hours by Ernesto Guido and Antonio Catapano at the Salvatore di Giacomo Observatory (L07).

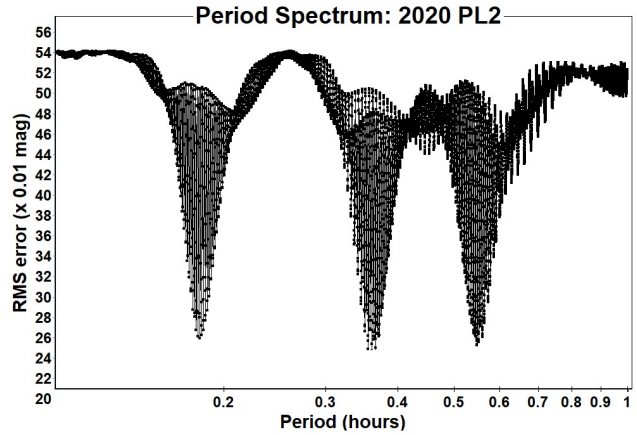

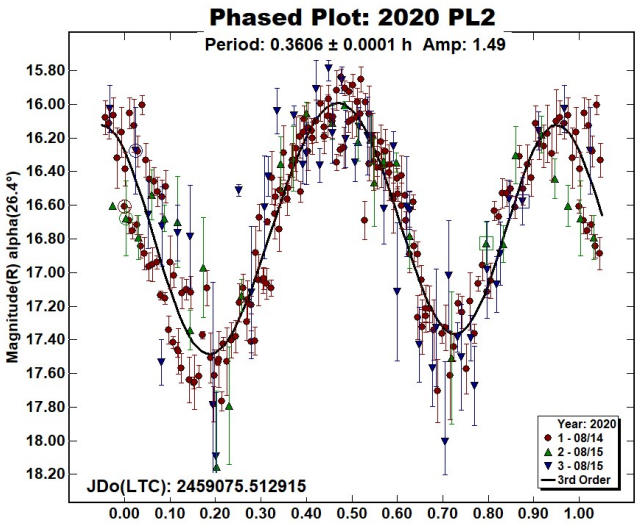

The period spectrum shows many possible solutions. We prefer the one featuring bimodal lightcurve, synodic period P = 0.3606 ± 0.0001 h (~ 21.6 min), and amplitude A = 1.5 ± 0.2 mag. Given the rotation period and large amplitude, this is likely a strength-bound, elongated asteroid.

References

Bus, S.J.; Binzel, R.P. (2002). "Phase II of the Small Main-Belt Asteroid Spectroscopic Survey - A Feature-Based Taxonomy." *Icarus* **158**, 146-177.

DSFTA (2020), Dipartimento di Scienze Fisiche, della Terra e dell'Ambiente – Astronomical Observatory, University of Siena. *https://www.dsfta.unisi.it/en/research/labs-eng/astronomicalobservatory*

Harris, A.W.; Young, J.W.; Scaltriti, F.; Zappala, V. (1984). "Lightcurves and phase relations of the asteroids 82 Alkmene and 444 Gyptis." *Icarus* **57**, 251-258.

Sanchez, J.A.; Michelsen, R.; Reddy, V.; Nathues, A. (2013). "Surface composition and taxonomic classification of a group of near-Earth and Mars-crossing asteroids." *Icarus* **225**, 131-140.

Tholen, D.J. (1984). "Asteroid taxonomy from cluster analysis of Photometry." Doctoral Thesis. University Arizona, Tucson.

UAI (2020). "Unione Astrofili Italiani" web site. *https://www.uai.it*

Warner, B.D. (2019). MPO Software, *MPO Canopus* v10.8.1.1. Bdw Publishing. *http://bdwpublishing.com*

Warner, B.D.; Harris, A.W.; Pravec, P. (2009). "The asteroid lightcurve database." *Icarus* **202**, 134-146. Updated 2020 Aug 28. *http://www.minorplanet.info/lightcurvedatabase.html*

PHOTOMETRIC OBSERVATIONS OF SEVEN MINOR PLANETS

Tom Polakis
Command Module Observatory
121 W. Alameda Dr.
Tempe, AZ 85282 USA
tpolakis@cox.net

(Received: 2020 Oct 11 Revised: 2020 Nov 8)

Phased lightcurves and synodic rotation periods for seven main-belt asteroids are presented, based on CCD observations made from 2020 September through 2020 October. All the data have been submitted to the ALCDEF database.

CCD photometric observations of seven main-belt asteroids were performed at Command Module Observatory (MPC V02) in Tempe, AZ. Images were taken using a 0.32-m f/6.7 Modified Dall-Kirkham telescope, SBIG STXL-6303 CCD camera, and a 'clear' glass filter. Exposure time for all the images was 2 minutes. The image scale after 2×2 binning was 1.76 arcsec/pixel. Table I shows the observing circumstances and results. All of the images for these seven asteroids were obtained between 2020 September and 2020 October.

Images were calibrated using a dozen bias, dark, and flat frames. Flat-field images were made using an electroluminescent panel. Image calibration and alignment was performed using MaxIm DL software.

The data reduction and period analysis were done using *MPO Canopus* (Warner, 2020). The 45′×30′ field of the CCD typically enables the use of the same field center for three consecutive nights. In these fields, the asteroid and three to five comparison stars were measured. Comparison stars were selected with colors within the range of 0.5 < B-V < 0.95 to correspond with color ranges of asteroids. In order to reduce the internal scatter in the data, the brightest stars of appropriate color that had peak ADU counts below the range where chip response becomes nonlinear were selected. MPO Canopus plots instrumental vs. catalog magnitudes for solar-colored stars, which is useful for selecting comp stars of suitable color and brightness.

Since the sensitivity of the KAF-6303 chip peaks in the red, the clear-filtered images were reduced to Sloan r′ to minimize error with respect to a color term. Comparison star magnitudes were obtained from the ATLAS catalog (Tonry et al., 2018), which is incorporated directly into MPO Canopus. The ATLAS catalog derives Sloan griz magnitudes using a number of available catalogs. The consistency of the ATLAS comp star magnitudes and color-indices allowed the separate nightly runs to be linked often with no zero-point offset required or shifts of only a few hundredths of a magnitude in a series.

A 9-pixel (16-arcsec) diameter measuring aperture was used for asteroids and comp stars. It was typically necessary to employ star subtraction to remove contamination by field stars. For the asteroids described here, I note the RMS scatter on the phased lightcurves, which gives an indication of the overall data quality including errors from the calibration of the frames, measurement of the comp stars, the asteroid itself, and the period-fit. Period determination was done using the MPO Canopus Fourier-type FALC fitting method (cf. Harris et al., 1989). Phased lightcurves show the maximum at phase zero. Magnitudes in these plots are apparent and scaled by MPO Canopus to the first night.

Most asteroids were selected from the CALL website (Warner, 2011) using the criteria of magnitude greater than 15.5 and quality of results, U, less than 2+. In this set of observations, 1 of the 7 asteroids had no previous period analysis, 1 had U = 1, and 3 had U = 2. The Asteroid Lightcurve Database (LCDB; Warner et al., 2009) was consulted to locate previously published results. All the new data for these asteroids can be found in the ALCDEF database.

426 Hippo. Auguste Charlois discovered this asteroid in a highly eccentric orbit from Nice in 1897. Pray (2006) published a synodic period of 34.3 ± 0.2 h. More recent period analyses claim double that value: Durech (2018) computed 67.504 ± 0.002 h and Pal (2020) shows 67.5309 ± 0.0005 h. During nine nights, 715 images were gathered, resulting in a period of 66.78 ± 0.09 h, agreeing with the more recent values. The amplitude is 0.14 mag, with an RMS error of 0.014 mag.

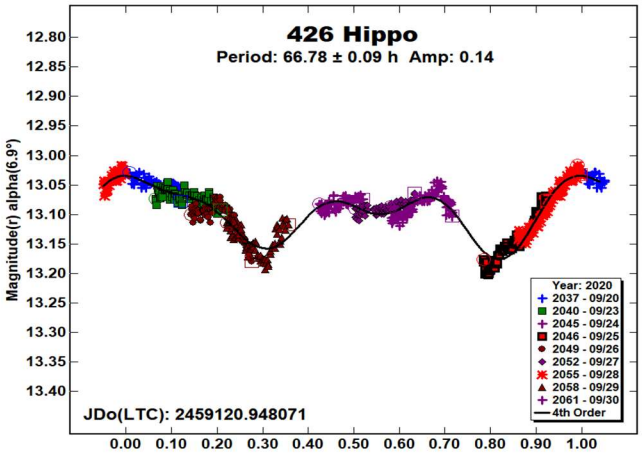

716 Berkeley. This outer main-belt asteroid was discovered at Vienna in 1911 by Johann Palisa. Garlitz (2011) shows a period of 15.55 ± 0.04 h, and Behrend (2018) obtained 34.3 ± 0.06 h. A total of 233 data points gathered over four nights were used to compute a period of 15.46 ± 0.04 h, agreeing with Garlitz's value. The lightcurve has an amplitude of 0.20 mag, and an RMS error of 0.029 mag.

Number	Name	2020/mm/dd	Phase	L_{PAB}	B_{PAB}	Period(h)	P.E.	Amp	A.E.	Grp
426	Hippo	09/20-09/30	6.9,7.1	2	19	66.78	0.09	0.14	0.01	MB-O
716	Berkeley	10/03-10/06	3.1,3.7	7	-7	15.46	0.04	0.21	0.03	MB-O
805	Hormuthia	10/01-10/06	9.9,11.6	345	-1	35.64	0.12	0.05	0.02	MB-O
1537	Transylvania	09/23-09/30	3.4,6.4	357	4	144.2	0.2	0.78	0.03	MB-O
1576	Fabiola	10/06-10/07	3.5,3.9	5	0	6.891	0.007	0.24	0.02	THM
2299	Hanko	09/23-09/30	4.3,1.4	6	-2	87.60	0.12	0.43	0.03	MB-I
3970	Herran	10/03-10/05	3.3,3.8	7	-5	8.053	0.005	0.59	0.04	EUN

Table I. Observing circumstances and results. The phase angle is given for the first and last date. If preceded by an asterisk, the phase angle reached an extrema during the period. L_{PAB} and B_{PAB} are the approximate phase angle bisector longitude/latitude at mid-date range (see Harris et al., 1984). Grp is the asteroid family/group (Warner et al., 2009).

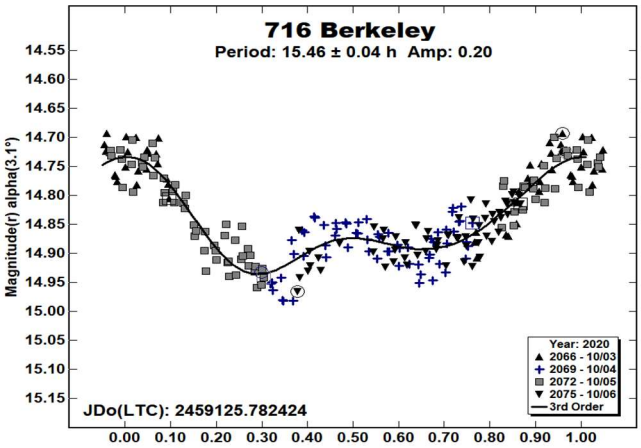

805 Hormuthia is a Max Wolf discovery, made in 1915 at Heidelberg. Two periods appear in the LCDB, both made difficult by the minor planet's small amplitude. Pilcher and Benishek (2009) computed 9.510 ± 0.001 h, and Behrend (2019) produced a period of 23.76 ± 0.05 h. A total of 576 data images obtained during six nights were used to calculate a trimodal solution of 35.64 ± 0.12 h, disagreeing with prior assessments. The data did not respond well to force-fitting either of the two published periods. The RMS error on the fit of 0.020 mag is significant relative to the amplitude of 0.050 mag.

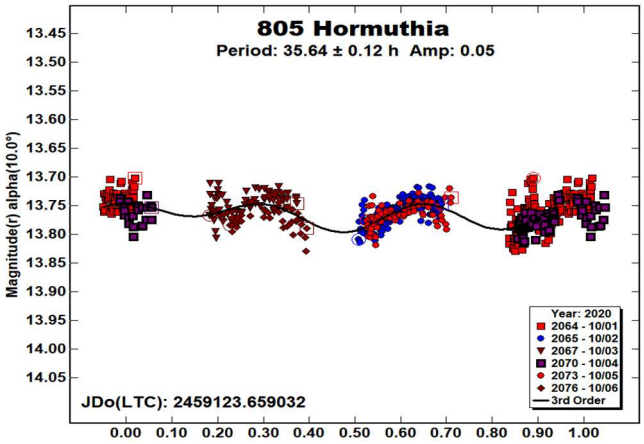

1537 Transylvania. Gyula Strommer discovered this minor planet in 1950 from Budapest. No precise periods appear in the LCDB. The slow rotation rate required eight nights and 543 data points to obtain a good period solution of 144.2 ± 0.2 h. The amplitude is a generous 0.78 mag, with an RMS error on the fit of 0.029 mag. Note that the 2020 opposition was very favorable for this eccentric orbit, and the asteroid will be significantly fainter until the 2025 opposition.

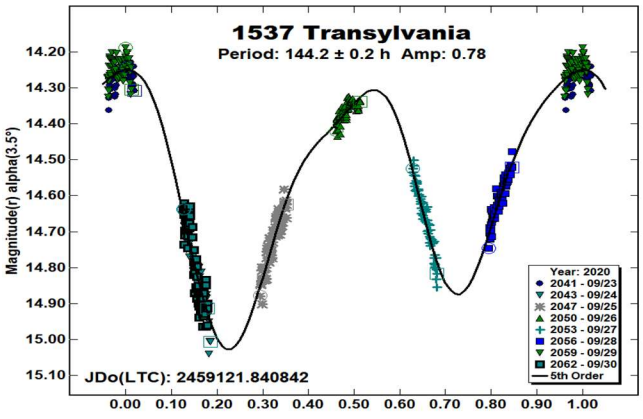

1576 Fabiola is a Themis-family asteroid, discovered by Sylvain Arend at Uccle in 1948. Despite its short period, only two solutions appear in the LCDB. Lagerqvist (1987) used photographs to obtain a period of 6.7 h, and Benishek (2018) used modern methods to refine it to 6.8890 ± 0.0003 h. Only two nights and 268 images were sufficient to compute a period of 6.891 ± 0.007 h, in agreement with published values. The amplitude is 0.24 ± 0.023 mag.

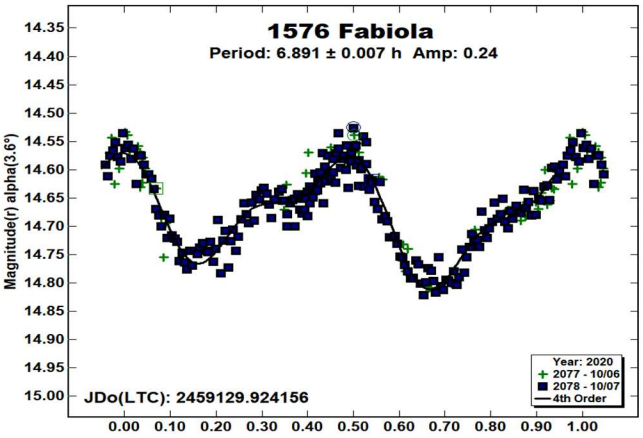

2299 Hanko is an inner main-belt minor planet in a highly eccentric orbit. Yrjö Vaisala discovered it in 1941 at Turku. It has no published periods. During eight nights near the very favorable 2020 opposition, 489 images were gathered, producing a new solution of 87.60 ± 0.12 h. The amplitude is 0.43 ± 0.029 mag.

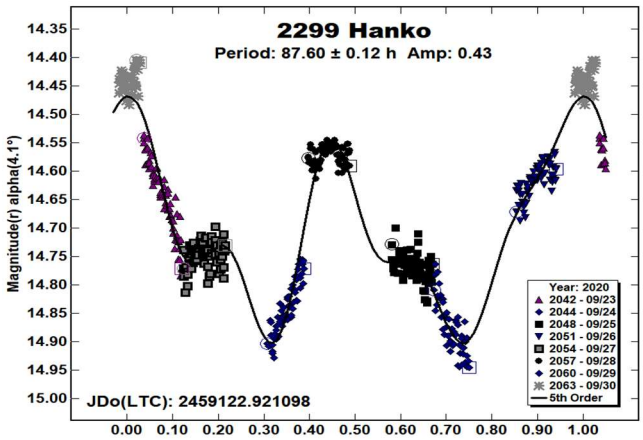

3970 Herran is a member of the Eunomia family, discovered by Carlos Torres in 1979 at Cerro El Roble. Two agreeing period solutions are published: Kim (2014) shows 8.09 ± 0.05 h, and Pal (2020) calculated 8.04608 ± 0.0619 h. During three nights, 168 images were taken, and the resulting period solution is 8.053 ± 0.005 h, in agreement with prior estimates.

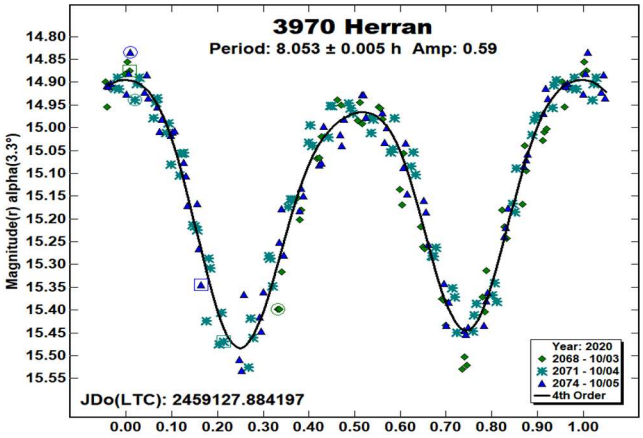

Acknowledgements

The author would like to express his gratitude to Brian Skiff for his indispensable mentoring in data acquisition and reduction. Thanks also go out to Brian Warner for support of his MPO Canopus software package.

References

Behrend, R. (2018, 2019). Observatoire de Geneve web site. *http://obswww.unige.ch/~behrend/page_cou.html*

Benishek, V. (2018). "Lightcurve and Rotation Period Determinations for 29 Asteroids." *Minor Planet Bull.* **45**, 82-91.

Durech, J.; Hanus, J.; Ali-Lagoa, V. (2018). "Asteroid models reconstructed from the Lowell Photometric Database and WISE data." *Astron. Astrophys*. **617**, A57.

Garlitz, J. (2011). Personal web site. *http://eoni.com/~garlitzj/Period.htm*

Harris, A.W.; Young, J.W.; Scaltriti, F.; Zappala, V. (1984). "Lightcurves and phase relations of the asteroids 82 Alkmene and 444 Gyptis." *Icarus* **57**, 251-258.

Harris, A.W.; Young, J.W.; Bowell, E.; Martin, L.J.; Millis, R.L.; Poutanen, M.; Scaltriti, F.; Zappala, V.; Schober, H.J.; Debehogne, H.; Zeigler, K.W. (1989). "Photoelectric Observations of Asteroids 3, 24, 60, 261, and 863." *Icarus* **77**, 171-186.

Kim, M.-J.; Choi, Y.-J.; Moon, H.-K.; Byun, Y.-I.; et al. (2014). "Rotational Properties of the Maria Asteroid Family." *Astron. J.* **147**, A56.

Lagerqvist, C. (1987). "Photographic photometry of 110 main-belt asteroids." *Astron. Astrophys. Suppl.* **31**, 361-381.

Pal, A.; Szakáts, R.; Kiss, C.; Bódi, A.; Bognár, Z.; Kalup, C.; Kiss, L.L.; Marton, G.; Molnár, L.; Plachy, E.; Sárneczky, K.; Szabó, G.M.; Szabó, R. (2020). "Solar System Objects Observed with TESS – First Data Release: Bright Main-belt and Trojan Asteroids from the Southern Survey." *Ap. J. Supl. Ser*. **247**, 26-34.

Pilcher, F.; Benishek, V. (2009). "Period Determinations for 634 Ute and 805 Hormuthia." *Minor Planet Bull.* **36**, 29-30.

Pray, D.P. (2006). "Lightcurve analysis of asteroids 326, 329, 426, 619, 1829, 1967, 2453, 10518 and 42267." *Minor Planet Bull*. **33**, 4-5.

Tonry, J.L.; Denneau, L.; Flewelling, H.; Heinze, A.N.; and five additional co-authors. (2018). "The ATLAS all-sky stellar reference catalog." *Astrophys. J.* **867**, 105.

Warner, B.D.; Harris, A.W.; Pravec, P. (2009). "The Asteroid Lightcurve Database." *Icarus* **202**, 134-146. Updated 2020 Aug. *http://www.minorplanet.info/lightcurvedatabase.html*

Warner, B.D. (2011). Collaborative Asteroid Lightcurve Link website. *http://www.minorplanet.info/call.html*

Warner. B.D. (2020). *MPO Canopus* software. *http://bdwpublishing.com*

LIGHTCURVE ANALYSIS FOR FOUR NEAR-EARTH ASTEROIDS

Peter Birtwhistle
Great Shefford Observatory
Phlox Cottage, Wantage Road
Great Shefford, Berkshire, RG17 7DA
United Kingdom
peter@birtwhistle.org.uk

(Received: 2020 Aug 30 Revised: 2020 Nov 8)

Lightcurves for four near-Earth asteroids observed from Great Shefford Observatory during close approaches in 2018 and 2020 are reported: 2018 CB, 2018 GE3, 2020 KK7 and 2020 SW. All are small (H > 23) fast or super-fast rotators.

Photometric observations of near-Earth asteroids during close approaches to Earth in 2018 and 2020 were made at Great Shefford Observatory using a 0.40-m Schmidt-Cassegrain and Apogee Alta U47+ CCD camera. All observations were made unfiltered and with the telescope operating with a focal reducer at f/6. The 1K×1K, 13-micron CCD was binned 2×2 resulting in an image scale of 2.16 arcsec/pixel. *Astrometrica* (Raab, 2018) was used to measure photometry using APASS Johnson V band data from the UCAC4 catalogue and *MPO Canopus* (Warner, 2018; 2020), incorporating the Fourier algorithm developed by Harris (Harris et al., 1989) was used for lightcurve analysis.

2018 CB. This small Apollo object was discovered on 2018 Feb 4 (Fuls et al., 2018), 5 days before making a very close approach to Earth, at ~70,000 km, or 0.18 Lunar Distances on 2018 Feb 9 22:28 UT. It was tracked from Great Shefford for 3.5 hours, from 18:01 UT to within an hour of closest approach and its proximity posed some challenges. The apparent rate of motion increased from 400 to over 1,200 arcsec/min, so exposures were limited initially to 1.0 s, reducing down to 0.4 s by the end. The phase angle increased from 68° to 114° and this caused the amplitude of light variations to increase very rapidly, especially at the end of the observing period. 2018 CB moved across 48° of sky and this necessitated the telescope being repositioned 116 times. A total of 1,841 images were measured and imported into Canopus as 116 separate sessions, but due to the increasing lightcurve amplitude only the first 38 (covering 90 minutes) have been used here to derive a lightcurve. The apparent mag was +12 - +13 throughout. A search of the Asteroid Lightcurve Database (LCDB; Warner et al., 2009) and wider searches did not find any previously reported results for 2018 CB.

The period spectrum favours an asymmetric bimodal solution with period 0.089241 h but a quadrimodal solution also appears to be a possibility, with relatively small amplitude (0.24) at high phase angle (67° - 80°). But a split-halves diagram using double the bimodal period shows the two halves to be essentially the same so the bimodal solution is assumed correct in this analysis.

Small adjustments to the zero-points of the sessions were made to minimize the overall RMS fit of the lightcurve, the largest adjustment being 0.07 mag and the RMS for all adjustments was 0.03 mag.

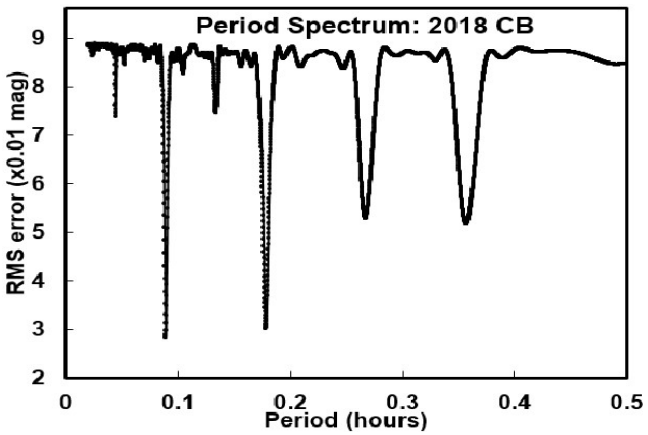

The remaining 78 sessions show a similar period when analysed with Canopus, but with lightcurve features rapidly increasing in size. The coefficients from the 4th order Fourier solution generated for the phased lightcurve plot were used to model the lightcurve for all available data points. Phased plots of relative magnitude for four separate periods, to illustrate the amplitude changes are given, together with a plot of the Amplitude vs Phase Angle relationship, horizontal bars indicating the range of phase angles included in each amplitude determination.

It is not possible to determine what contributions phase angle or changing 'pole-on' geometry contributed, but an empirical formula approximating the observed non-linear Amplitude / Phase Angle relationship in the range 68° < α < 106° is:

$$\text{Amplitude} \approx 0.0104\, e^{\,0.0413\,\alpha}$$

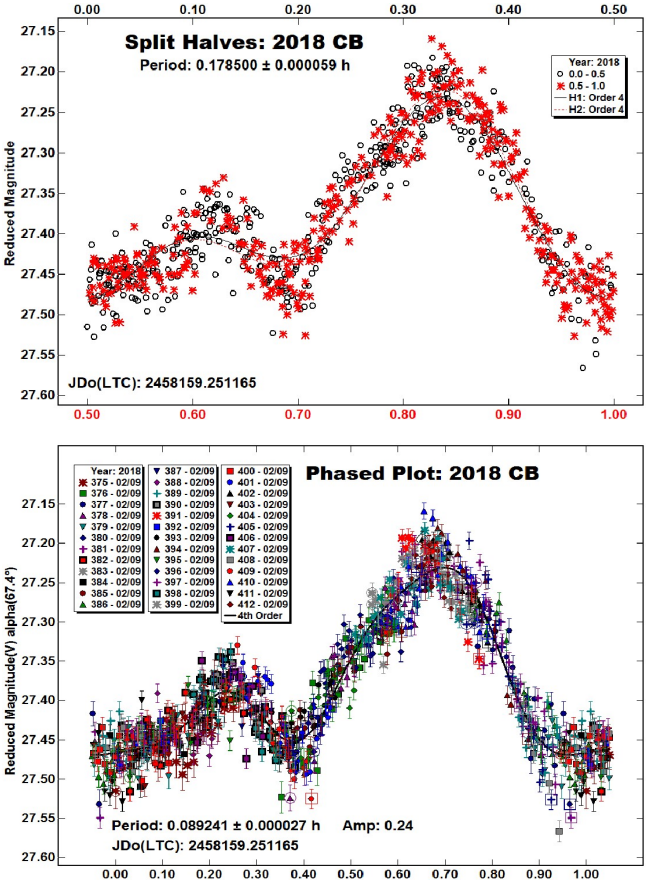

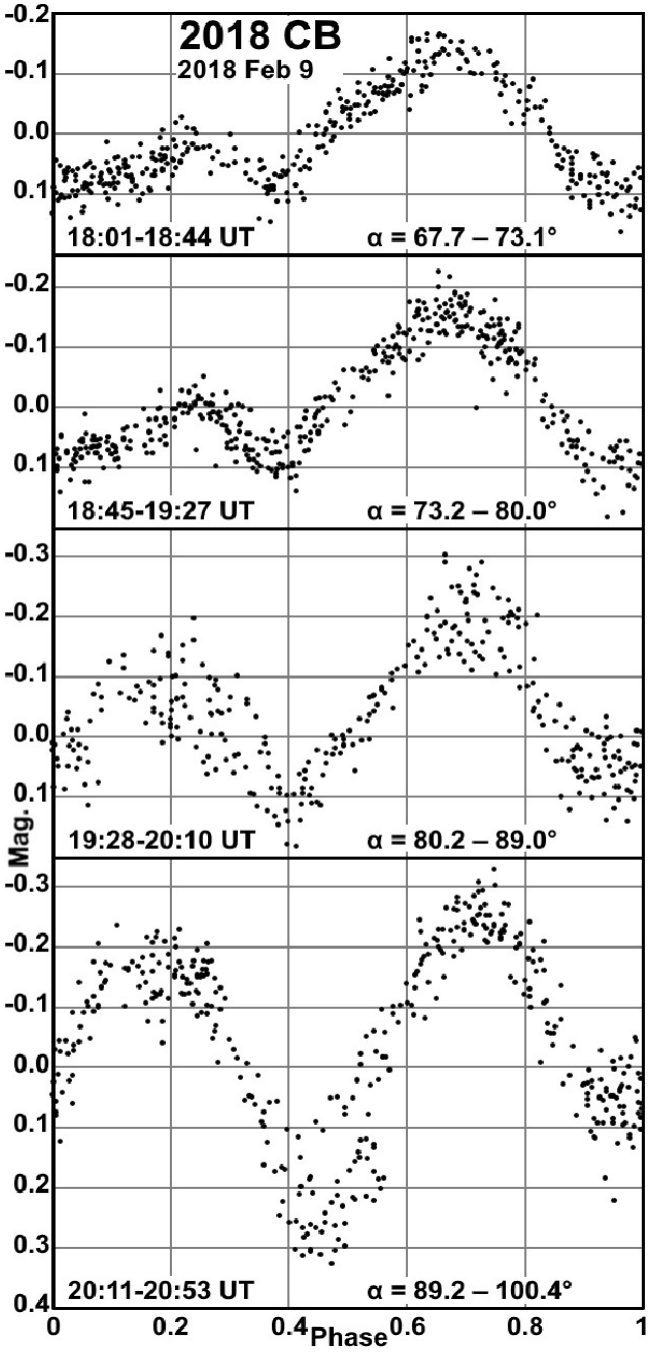

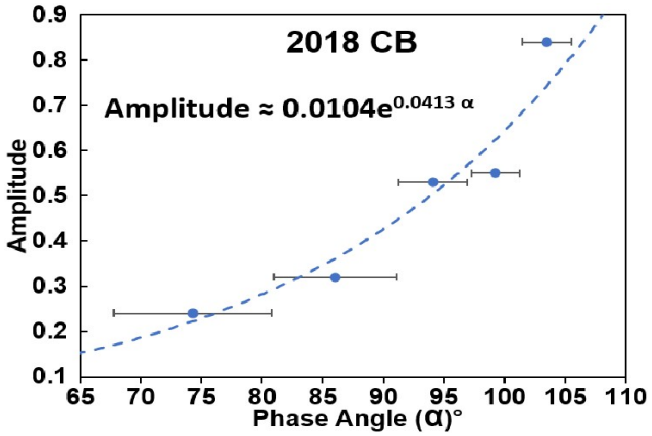

2018 GE3. An Apollo object discovered on 2018 April 11 (Tichy et al., 2018) and making a close approach to Earth on 2018 April 15.28 UT was followed from 21:57-01:16 UT on the night of 2018 April 14/15 as it brightened to apparent mag ≥+13. Distance from Earth decreased from 940,000 to 602,000 km during that period and because of the large apparent rate of motion (77, increasing to 187 arcsec/min) exposures were reduced from 5 s down to 2 s to ensure the trail was always enclosed in a 3-pixel radius annulus in Astrometrica. The telescope was repositioned 22 times and 1274 images were obtained. Measurements made in Astrometrica were imported into 22 sessions within Canopus and small adjustments to the zero-points of the sessions were made to minimize the overall RMS fit of the lightcurve, the largest adjustment being 0.13 mag and the RMS for all adjustments was 0.06 mag. A bimodal solution of 0.304097 ± 0.000042 h with amplitude of 0.92 mag indicates that 10.9 revolutions of 2018 GE3 occurred during the 3 h 19 min it was under observation.

A search of the LCDB provides one previously reported lightcurve (Gornea et al., 2018), from observations covering 2018 April 14 22:44–23:43 UT, entirely within the period observed from Great Shefford and with P = 0.304 h and A = 0.93 mag agrees very well with the solution determined here.

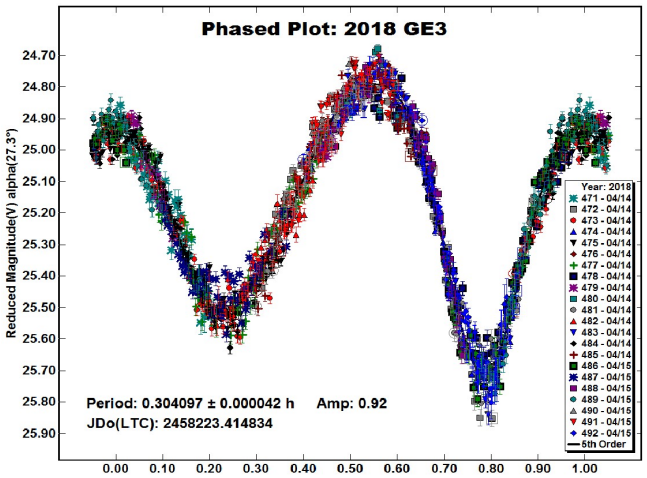

2020 KK7. This Apollo object was discovered on 2020 May 25 (Bulger et al., 2020a) and was only brighter than18 mag on 2 nights before passing Earth at 1.3 Lunar Distances on 2020 June 2.4 UTC. A search of the LCDB and wider searches do not reveal any previously reported lightcurve results. 2020 KK7 was observed from Great Shefford on 2020 May 31 at the start and end of the night for astrometry purposes (runs 1 & 2 in Table 1), then again on 2020 June 01 at start and end of the night for astrometry (runs 3 & 5) and also during a 43-min period in between, specifically for photometry (run 4).

Run	2020 May/June dd hh:mm	-dd hh:mm	Fields/ Points	Phase range	Exp
1	31 22:36	-31 22:58	2/69	23.6-23.7	10,8
2	01 00:47	-01 00:57	1/58	24.3	6
3	01 21:50	-01 22:07	4/202	42.8-43.4	1
4	02 01:34	-02 02:17	8/368	52.5-54.9	3.8,2.4
5	02 02:19	-02 02:27	2/118	55.0-55.5	1

Table I. Summary of observing runs. The start and end times of images used is given. Fields/Points gives the number of times the telescope was repositioned to different fields during the run together with the number of data points used in the analysis. Phase range gives the phase at start and end of each run. Exp is the exposure times in seconds used during the runs.

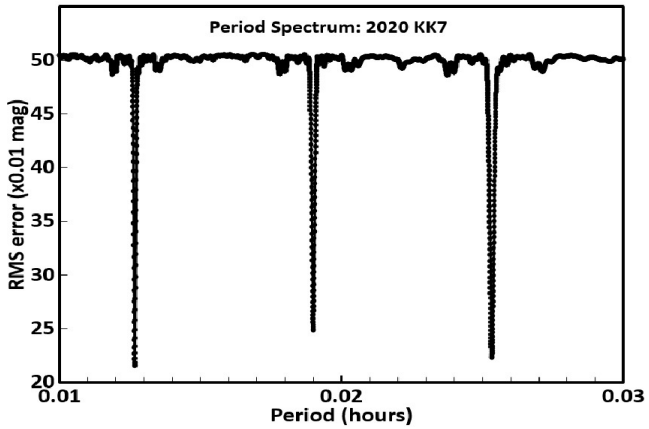

2020 KK7 was 18th mag on the first night and 16th mag on the second but on both nights large variations in magnitude were evident between consecutive exposures. On the first night the object was too faint to see on individual exposures at minimum, but on the second night it was visible throughout its light variations. As the object approached the Earth on the second night the apparent speed exceeded 200 arcsec/min and exposures were limited to less than 4 seconds to keep the trails short enough to measure with a 3-pixel radius annulus in Astrometrica. The 368 measures obtained during run 4 involved the telescope being repositioned 8 times due to the fast motion of the object and these measures were imported into Canopus. The resulting period spectrum indicates a bimodal solution is marginally preferable but is also suggested from the large amplitude (Harris et al., 2014), though the large phase angle will have enhanced the observed amplitude and made this inference somewhat less conclusive.

Small adjustments to the zero-points of the 8 sessions were made to minimize the overall RMS fit of the lightcurve, the largest adjustment was 0.1 mag and the RMS for all adjustments was 0.06 mag. With a period of 45.6 s, 2020 KK7 completed 57 revolutions during the 43 minutes of run 4.

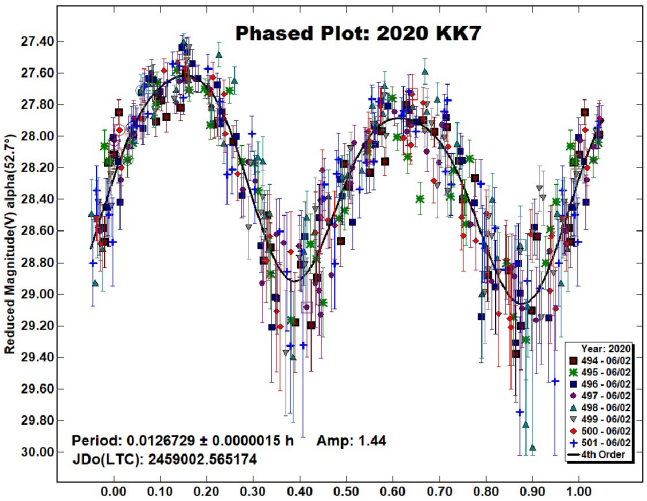

Measurements obtained from the start of run 3 and the end of run 5 were affected by twilight and have not been used in the analysis but runs 1, 2 and the latter half of run 3 were measured and the peak brightness values selected and combined with the peak brightness from the lightcurve produced from run 4 to plot an H-G diagram which gives H_V = 25.35 ± 0.31, G = 0.01 ± 0.12. Assuming a value of G = 0.15 results in H_V = 25.65.

The JPL Small-Body Database Browser (JPL, 2020) gives H = 26.328 ± 0.293 assuming G = 0.15 and as this is calculated from photometry submitted with astrometry to the Minor Planet Center taken with a variety of exposure lengths it can be regarded as being derived from the average brightness of the lightcurve, especially due to the short 46-s rotation period. The value of H_V with assumed G=0.15 determined here for the peak magnitude can be adjusted by half the amplitude to give an average brightness figure, i.e.

$$H_V \text{ (average mag)} = 25.65 + 0.72 = 26.37$$

and this is in good agreement with the JPL value.

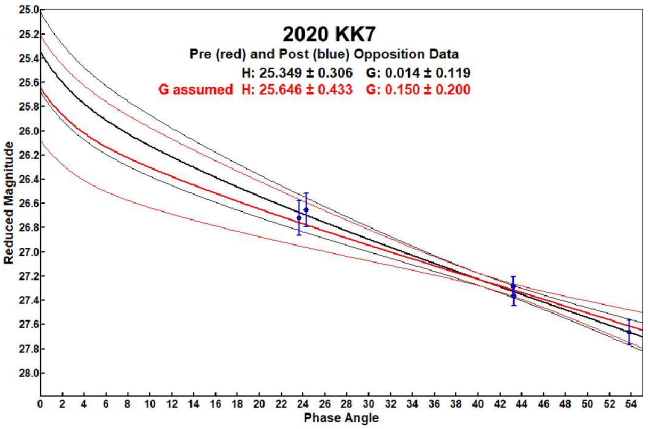

2020 SW. Notable for a very close approach to 21,700 km from the Earth's surface on 2020 Sep 24.47 UT, this small Apollo object was discovered by Kacper Wierzchoś (Bulger et al., 2020b) and for such a small object with the unusually long lead-time of nearly 7 days before its passage. It was observed at Great Shefford to within 10 hours of close approach when it was well within the orbit of the Moon, though its sky motion was not excessive (50 arcsec/min) as it headed almost directly toward Earth. The apparent mag was ≥16 throughout the period of observation and exposures as long as 15 s were possible without excessive trailing, but as large brightness variations were obvious between trial exposures taken 6 s apart the decision was made to limit exposures to 4 s or less to capture any superfast rotation present. Exposures of 4, 2 and 1 seconds were taken, but the 1 second exposures were not used in this analysis due to the larger noise in measurements. The longer, 4 s exposure length, at 0.14 * Period (*P*) is below the 0.185*P* threshold where a reduction in strength of the lightcurve's 2nd harmonic and smoothing of the lightcurve would become problematic, due to the derived very short 28.5 second rotation period (Pravec et al., 2000). As with the other analyses here, small zero-point adjustments to the six sessions were made to minimise the overall RMS fit of the lightcurve, the largest adjustment was 0.05 mag and the RMS for all adjustments was 0.03 mag. 2020 SW completed 362 revolutions during the 2 h 51 min elapsed time used to produce the lightcurve.

Number	Name	Intg. time	Intg. / Period	Min a/b
	2018 CB	1.0	0.003	1.1
	2018 GE3	4.9	0.004	1.6
	2020 KK7	3.8	0.083	1.7
	2020 SW	4.0	0.14	1.6

Table II. Ancillary information, listing the longest integration time used (seconds), the fraction of the period represented by the integration time (see Pravec et al., 2000) and the calculated minimum elongation of the asteroid (Kwiatkowski et al., 2010).

A search of the ADS (2020) and the LCDB did not find any previously reported results but a preliminary result published on Twitter (Wells and Bamberger, 2020) of P = 0.00790 ± 0.00001 h, Amp = 0.72 agrees well with this analysis.

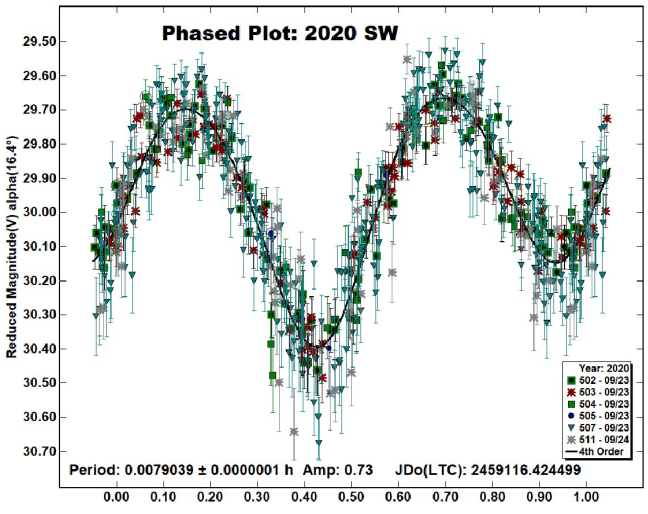

References

ADS (2020). Astrophysics Data System *https://ui.adsabs.harvard.edu/*

Bulger, J.; Chambers, K.; Lowe, T.; Schultz, A.; Willman, M.; Chastel, S.; Huber, M.; Ramanjooloo, Y.; Wainscoat, R.; Weryk, R.; Dukes, T.; Rankin, D.; Christensen, E.J.; Farneth, G.A.; and 21 colleagues. (2020a) "2020 KK7." MPEC 2020-L01. *https://www.minorplanetcenter.net/mpec/K20/K20L01.html*

Bulger, J.; Chambers, K.; Lowe, T.; Schultz, A.; Willman, M.; Chastel, S.; Huber, M.; Ramanjooloo, Y.; Wainscoat, R.; Weryk, R.; Wierzchos, K.W.; Christensen, E.J.; Farneth, G.A.; Fuls, D.C.; and 11 colleagues. (2020b) "2020 SW." MPEC 2020-S83. *https://www.minorplanetcenter.net/mpec/K20/K20S83.html*

Fuls, D.C.; Christensen, E.J.; Gibbs, A.R.; Grauer, A.D.; Johnson, J.A.; Kowalski, R.A.; Larson, S.M.; Leonard, G.J.; Matheny, R.G.; Seaman, R.L.; Shelly, F.C.; Adamovsky, M.; Nishiyama, K.; Fujiwara, T. (2018) "2018 CB." MPEC 2018-C12. *https://www.minorplanetcenter.net/mpec/K18/K18C12.html*

Gornea, A.I.; Sonka, A.B.; Birlan, M.; Anghel, S. (2018). "Photometric Observations of Near-Earth Asteroid 2018 GE3." *Minor Planet Bull.* **45**, 315-316.

Harris, A.W.; Young, J.W.; Scaltriti, F.; Zappala, V. (1984). "Lightcurves and phase relations of the asteroids 82 Alkmene and 444 Gyptis." *Icarus* **57**, 251-258.

Harris, A.W.; Young, J.W.; Bowell, E.; Martin, L.J.; Millis, R.L.; Poutanen, M.; Scaltriti, F.; Zappala, V.; Schober, H.J.; Debehogne, H.; Zeigler, K. (1989). "Photoelectric Observations of Asteroids 3, 24, 60, 261, and 863." *Icarus* **77**, 171-186.

Harris, A.W.; Pravec, P.; Galad, A.; Skiff, B.A.; Warner, B.D.; Vilagi, J.; Gajdos, S.; Carbognani, A.; Hornoch, K.; Kusnirak, P.; Cooney, W.R.; Gross, J.; Terrell, D.; Higgins, D.; Bowell, E.; Koehn, B.W. (2014). "On the maximum amplitude of harmonics of an asteroid lightcurve." *Icarus* **235**, 55-59.

JPL (2020). Small-Body Database Browser. *https://ssd.jpl.nasa.gov/sbdb.cgi*

Kwiatkowski, T.; Buckley, D.A.H.; O'Donoghue, D.; Crause, L.; Crawford, S.; Hashimoto, Y.; Kniazev, A.; Loaring, N.; Romero Colmenero, E.; Sefako, R.; Still, M.; Vaisanen, P. (2010). "Photometric survey of the very small near-Earth asteroids with the SALT telescope - I. Lightcurves and periods for 14 objects." *Astronomy & Astrophysics* **509**, A94.

Pravec, P.; Hergenrother, C.; Whiteley, R.; Sarounova, L.; Kusnirak, P.; Wolf, M. (2000). "Fast Rotating Asteroids 1999 TY2, 1999 SF10, and 1998 WB2." *Icarus* **147**, 477-486.

Raab, H. (2018). Astrometrica software, version 4.12.0.448. *http://www.astrometrica.at/*

Tichy, M.; Ticha, J.; Fumagalli, A.; Sicoli, P.; Testa, A.; Montanar, U.; Pettarin, E.; Gibbs, A.R.; Africano, B.M.; Christensen, E.J.; Fuls, D.C.; Grauer, A.D.; Johnson, J.A.; Kowalski, R.A.; and 12 colleagues. (2018) "2018 GE3." MPEC 2018-G94. *https://www.minorplanetcenter.net/mpec/K18/K18G94.html*

Warner, B.D. (2018). MPO Software Canopus, version 10.7.12.9. Bdw Publishing, Colorado Springs, CO.

Warner, B.D. (2020). MPO Software Canopus, version 10.8.2.8. Bdw Publishing, Colorado Springs, CO.

Warner, B.D.; Harris, A.W.; Pravec, P. (2009). "The Asteroid Lightcurve Database." *Icarus* **202**, 134-146. Updated 2020 Sep. *http://www.MinorPlanet.info/lightcurvedatabase.html*

Wells, G.; Bamberger, D. (2020). "Last night, we observed the small asteroid 2020 SW." *https://twitter.com/NBObservatories/status/1309147647178166272*

Number	Name	yyyy mm/ dd	Phase	L_{PAB}	B_{PAB}	Period(h)	P.E.	Amp	A.E	Grp	H
	2018 CB	2018 02/09-02/09	67.7,103.5	107	17	0.089241	0.000027	0.24	0.05	NEA	25.9
	2018 GE3	2018 04/14-04/14	27.4,33.9	217	9	0.304097	0.000042	0.92	0.05	NEA	23.8
	2020 KK7	2020 05/31-06/02	23.6,55.5	248	19	0.0126729	0.0000015	1.44	0.10	NEA	26.3
	2020 SW	2020 09/23-09/24	16.4,14.8	5	7	0.0079039	0.0000001	0.73	0.07	NEA	29.1

Table III. Observing circumstances and results. The phase angle is given for the first and last date. If preceded by an asterisk, the phase angle reached an extrema during the period. L_{PAB} and B_{PAB} are the approximate phase angle bisector longitude/latitude at mid-date range (see Harris et al., 1984). Grp is the asteroid family/group (Warner et al., 2009) and H is the absolute magnitude at 1 au from Sun and Earth taken from the SBDB (JPL, 2020).

NEAR-EARTH ASTEROID LIGHTCURVE ANALYSIS AT THE CENTER FOR SOLAR SYSTEM STUDIES: 2020 JULY-SEPTEMBER

Brian D. Warner
Center for Solar System Studies / MoreData!
446 Sycamore Ave.
Eaton, CO 80615 USA
brian@MinorPlanetObserver.com

Robert D. Stephens
Center for Solar System Studies / MoreData!
Rancho Cucamonga, CA 91730

(Received: 2020 October 13)

Lightcurves for 25 near-Earth asteroids (NEAs) obtained at the Center for Solar System Studies (CS3) from 2020 July to September were analyzed for rotation period, peak-to-peak amplitude, and signs of satellites or tumbling.

CCD photometric observations of 25 near-Earth asteroids (NEAs) were made at the Center for Solar System Studies (CS3) from 2020 July-September. Table I lists the telescopes and CCD cameras that are combined to make observations.

Up to nine telescopes can be used for the campaign, although seven is more common. All the cameras use CCD chips from the KAF blue-enhanced family and so have essentially the same response. The pixel scales ranged from 1.24-1.60 arcsec/pixel.

Telescopes	Cameras
0.30-m *f*/6.3 Schmidt-Cass	FLI Microline 1001E
0.35-m *f*/9.1 Schmidt-Cass	FLI Proline 1001E
0.40-m *f*/10 Schmidt-Cass	SBIG STL-1001E
0.40-m *f*/10 Schmidt-Cass	
0.50-m *f*/8.1 Ritchey-Chrétien	

Table I. List of available telescopes and CCD cameras at CS3. The exact combination for each telescope/camera pair can vary due to maintenance or specific needs.

All lightcurve observations were unfiltered since a clear filter can cause a 0.1-0.3 mag loss. The exposure duration varied depending on the asteroid's brightness and sky motion. Guiding on a field star sometimes resulted in a trailed image for the asteroid.

Measurements were made using *MPO Canopus*. The Comp Star Selector utility in *MPO Canopus* found up to five comparison stars of near solar-color for differential photometry. Comp star magnitudes were taken from the ATLAS star catalog (Tonry et al., 2018), which has Sloan *griz* magnitudes that were derived from the GAIA and Pan-STARR catalogs, among others, and are the "native" magnitudes of the catalog.

To reduce the number and amount of nightly zero-point adjustments, we use the ATLAS r′ (SR) magnitudes. Those adjustments are mostly ≤ 0.03 mag. The occasions where larger corrections were required may have been related in part to using unfiltered observations, poor centroiding of the reference stars, and not correcting for second-order extinction terms.

Unless otherwise indicated, the Y-axis of lightcurves is ATLAS SR "sky" (catalog) magnitudes. During period analysis, the magnitudes were normalized to the comparison stars used in the earliest session and to the phase angle given in parentheses using G = 0.15, unless another value is given. The X-axis shows rotational phase from –0.05 to 1.05. If the plot includes the amplitude, e.g., "Amp: 0.65", this is the amplitude of the Fourier model curve and *not necessarily the adopted amplitude for the lightcurve*.

Our initial search for previous results started with the asteroid lightcurve database (LCDB; Warner et al., 2009) found on-line at *http://www.minorplanet.info/lightcurvedatabase.html*. Readers are strongly encouraged to obtain, when possible, the original references listed in the LCDB. From here on, we'll use only "LCDB" to reference the paper by Warner et al. (2009).

4055 Magellan. Pravec et al. (2000web) reported a period of 7.475 h. It's been observed at CS3 during three previous apparitions: Warner (2014b; 6.384 h), Warner (2015; 7.496 h), and Warner (2017b; 7.52 h). Our 2020 results are in good agreement with all of those, except Warner (2014b).

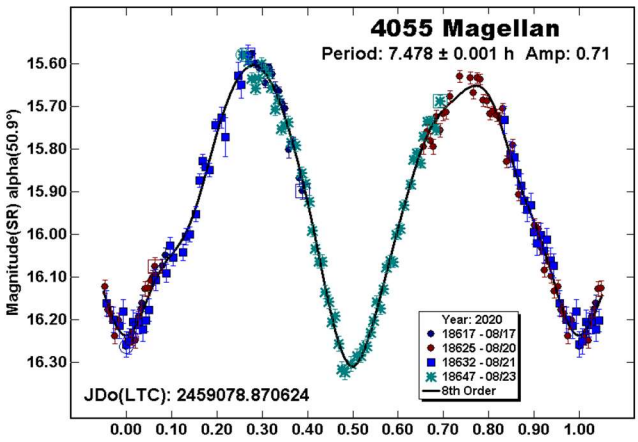

We re-visited the 2014 images. They were not ideal given poor seeing and very crowded star fields. It was apparent that simply resetting the comp star magnitudes from APASS V (Henden et al., 2009) to ATLAS SR would not be enough and so the images were re-measured with *MPO Canopus* making judicious use of the StarBGone (SBG) star subtraction feature.

This meant reviewing and measuring the images one-at-a-time, relying on SBG only when the asteroid and a field star had similar magnitudes. For brighter stars, SBG was used only to reduce their effect on sky background corrections; an image was bypassed when the asteroid and brighter star were judged to be too close, i.e., the star was in or near the sky background annulus.

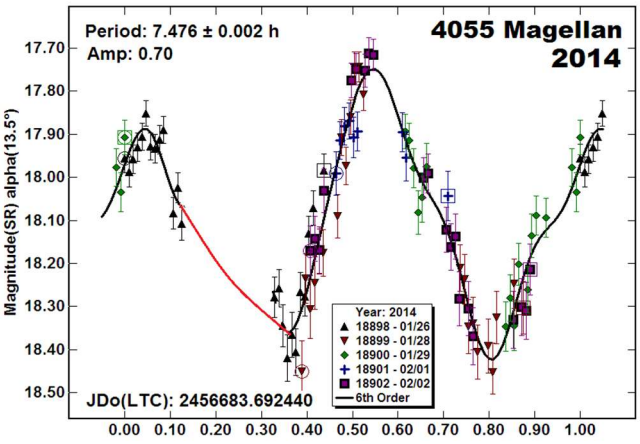

The resulting period spectrum showed a strong preference for P = 7.476 h, which is in near perfect agreement with the previous results. The revised lightcurve was not fully-covered. Using higher orders improved the RMS fit but the Fourier curve amplitude was much larger than the data showed. The red line is arbitrary and used to complete the Fourier curve using the 6th-order fit.

9162 Kwiila. The period spectrum showed several nearly-likely solutions, each nearly commensurate with an Earth day. We adopted P = 15.13 h since the amplitude virtually assured that the lightcurve would be bimodal, despite the somewhat large phase angle (Harris et al, 2014). The LCDB had no previous results.

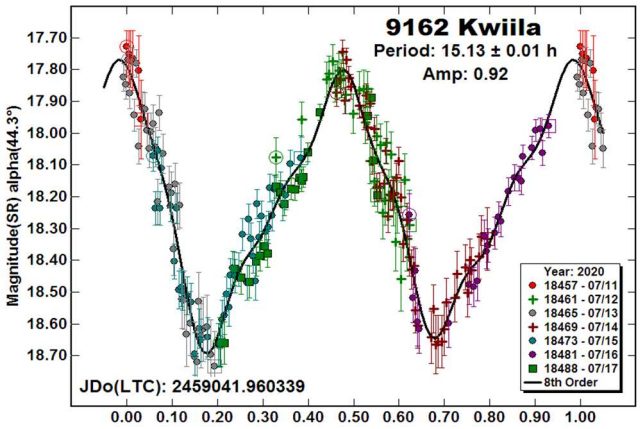

(19764) 2000 NF5. Pravec et al. (2000web) reported a period of 59.3 h but no signs of tumbling. However, the period and diameter of 1.9 km favor 2000 NF5 being a tumbler (Pravec et al., 2005).

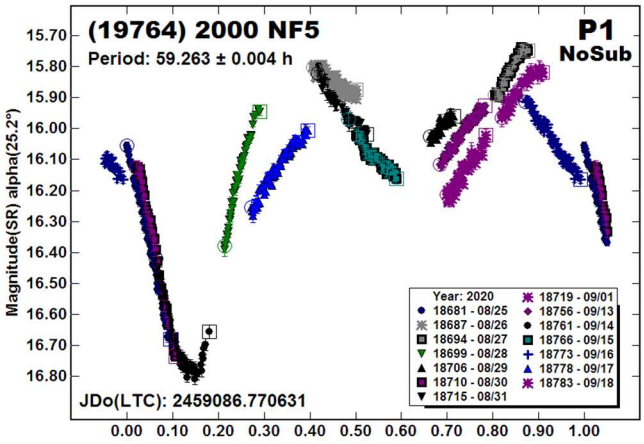

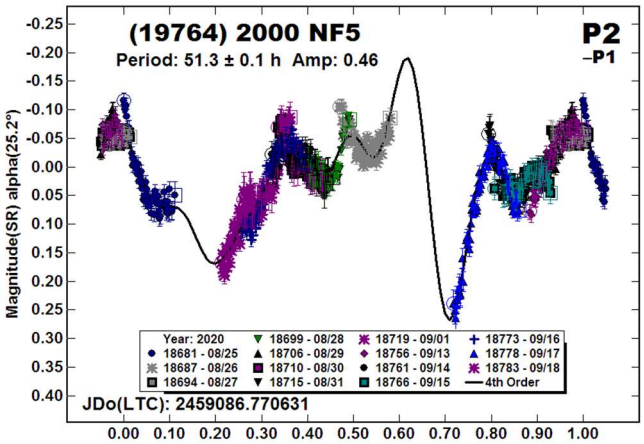

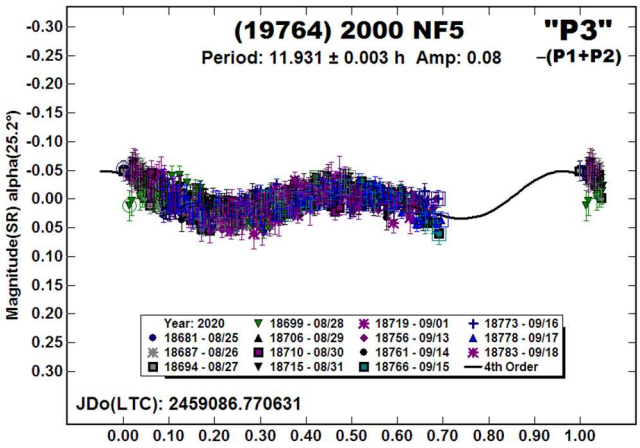

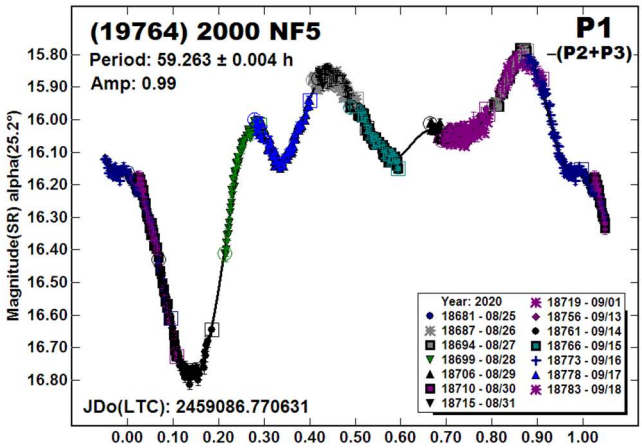

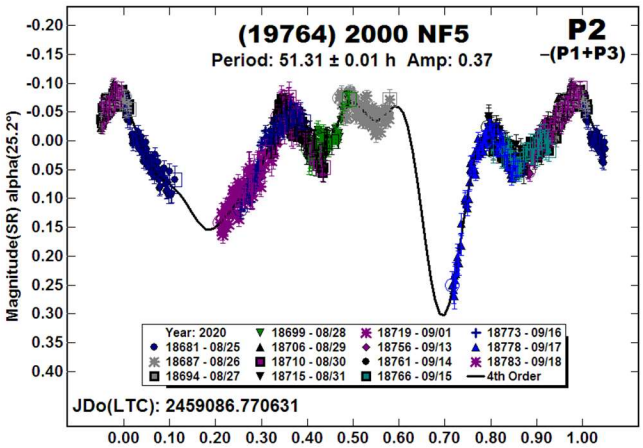

After a few observing sessions, it seemed almost certain that the asteroid was in a tumbling state, e.g., points in the lightcurve with coverage from more than one session didn't fit a single-period solution ("P1 – NoSub").

MPO Canopus is not fully capable of handling tumbling asteroids since the two periods are the sum of integral multiples of the two frequencies (see Pravec et al., 2005). On occasion, however, two periods can be extracted, though they may not be the true periods of precession and rotation.

The first step was to see if we could find a secondary period subtracting the Fourier curve for P_1 = 59.263 h. This led to P_2 = 51.3 h but the fit of the lightcurves for each solution still showed large deviations, e.g., the "P2 – P1" plot.

Sometimes it's possible to improve the results after finding a third period, even though it has no physical origin. Instead, it is a harmonic artifact of the Fourier analysis. In this case, a third solution was found by subtracting the P_1 and P_2 Fourier curves: a bimodal lightcurve with amplitude of 0.08 mag and P_3 = 11.931 h ("P3" plot). This is almost exactly one-half of an Earth day and, more important, has a 5:1 integral ratio with P_1 and so reinforces the idea of P_3 being a harmonic artifact of the Fourier analysis.

Subtracting P_3 from the data produced greatly improved, but still not perfect, fits for the P_1 ("P1–(P2+P3)") and P_2 ("P2 – (P1+P3)") lightcurves. We again note that these may not be the true periods of precession and rotation but can serve as a guide to future observations. Unfortunately, the asteroid remains V > 18 until 2030 September, when it again reaches V ~ 15.6.

(53435) 1999 VM40. Pravec et al. (2000web) reported a period of about 5.19 h. Carbognani (2014) found a shorter period of 5.09h. Two apparitions were observed from CS3: Warner (2014a, 5.186 h), Warner (2014b, 5.172 h). Our 2020 data set was somewhat sparse and covered a span of only four days. From it, we found a period of 5.193 h, which agrees with Pravec et al. (2000web).

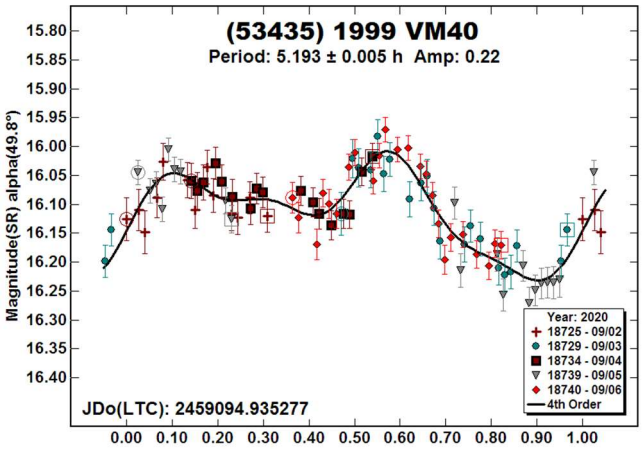

(87684) 2000 SY2. Higgins (2005) first reported a period of 8.80 h for this 1.8-km NEA. Later, Warner (2017a) found a period of 2.5712 h and lightcurve amplitude of 0.09 mag. Our initial analysis of the 2020 observations, despite the low amplitude, showed variations that seem to exceed the error bars.

Based on this, we used the dual-period search feature of *MPO Canopus* and found several possibilities for a secondary period that corresponded to 7, 8, and 9 rotations over 24 h. After several iterations, we found the principal period of P_1 = 2.571 h and secondary period of P_2 = 2.676 h.

These periods have an almost integral ratio of 25:24 and so one is likely a harmonic of the other, or of the true period, found by the Fourier analysis. Based on the tumbling damping times given by Pravec et al. (2005; 2014) for the asteroid's size and period, it's highly unlikely that the asteroid is tumbling. Instead, the periods are just two of several nearly-commensurate possibilities and so the true period remains uncertain.

Since either period makes this a good candidate for being a binary, we did search out to 30 hours for a secondary period. Anything beyond 5 h produced a lightcurve with large gaps, reaching up to 90% when the period was near 24 h.

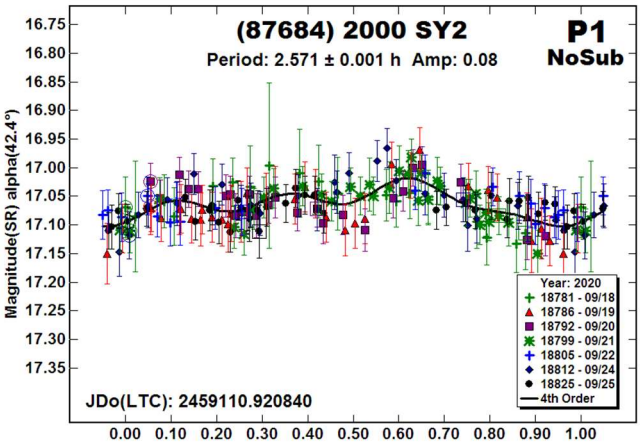

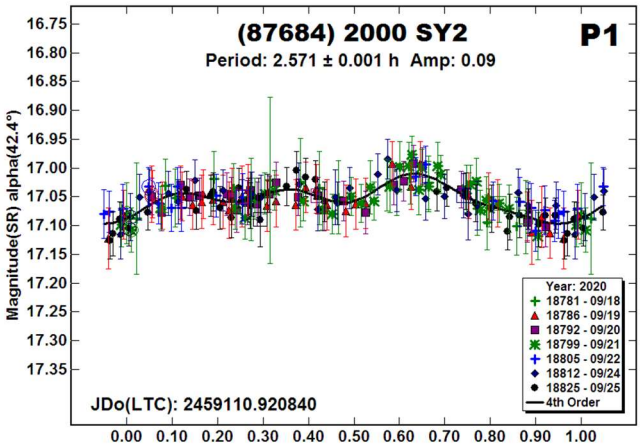

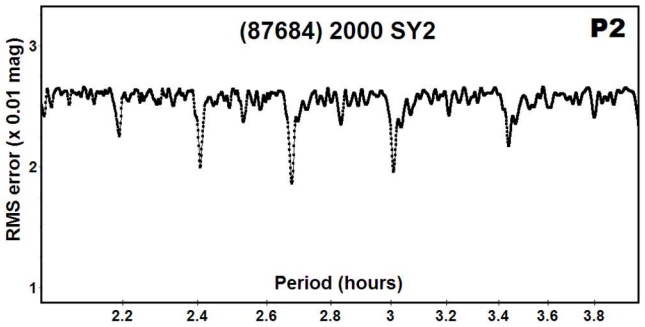

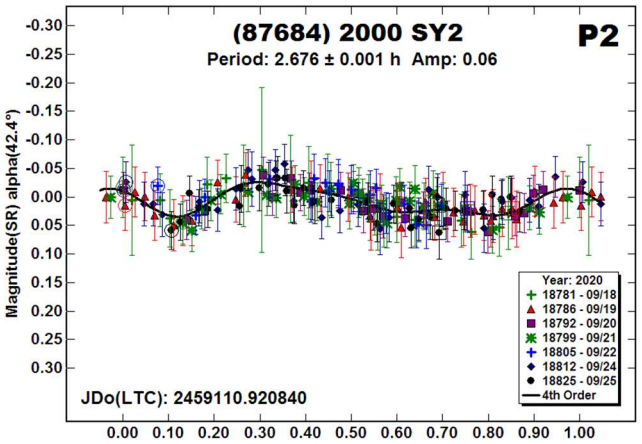

(136900) 1998 HL49, (137108) 1999 AN10, (145656) 4788 P-L. There were no previous rotation periods given in the LCDB for these three NEAs. The estimated diameter for 1998 HL49 is 1.1 km, assuming an albedo of 0.20 (Warner et al., 2009). That assumption is supported by Lin et al. (2018), who classified it as a taxonomic type S. However, Carry et al. (2016) found it to be a type V asteroid. Using the average albedo of $p_V \sim 0.4$ for this class from Warner et al. (2009), the diameter would shrink to about 700 m.

The estimated diameter for 1999 AN10 is about 780 m when using $H = 17.9$ and assuming type S and $p_V = 0.2$. For 4788 P-L, the estimated diameter is 1.6 km, also when assuming $p_V = 0.2$.

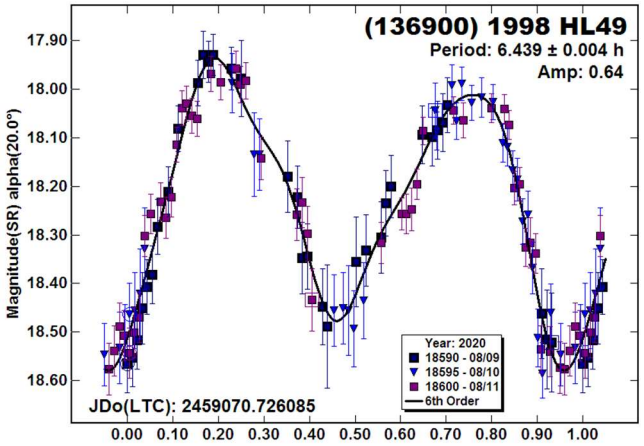

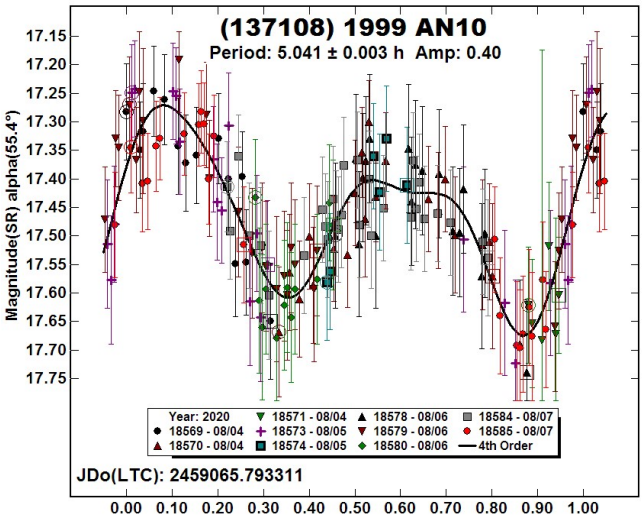

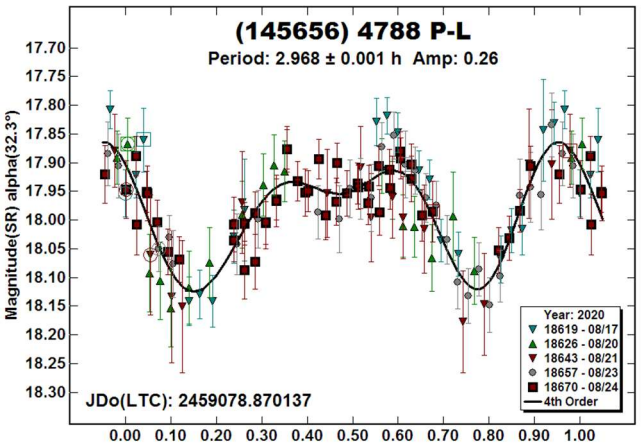

162173 Ryugu was the target of the Hayabusa-2 encounter and return mission. The in-situ observations allowed finding a precise rotation period of 7.63262 h and equatorial size of 1004 m and polar size of 872 m (Watanabe et al., 2019). Despite what appeared to be a good data set, it could not be fit to the 7.63 h found by Watanabe et al. Instead, it produced a strong RMS minimum at 7.40 h. All attempts to fit the data to the longer period were to no avail. Needless to say, we defer to the period found by Watanabe et al.

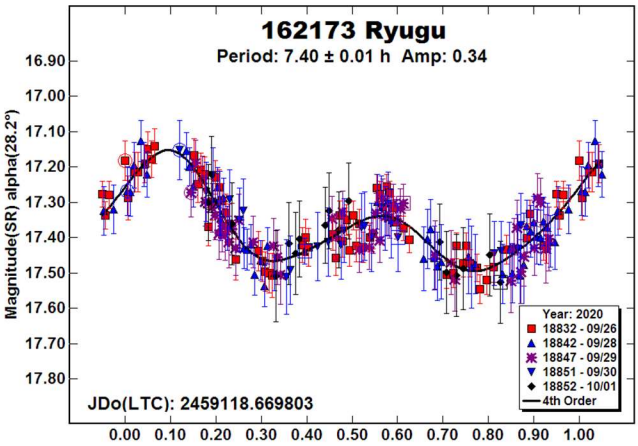

(285990) 2001 SK9, (380128) 1997 WB21, (411165) 2010 DF1. There were no rotation periods found in the LCDB for these three asteroids. The estimated diameter for 2001 SK9 is 800 m. For 1997 WB21, Mainzer et al. (2016) used data from the WISE mission to find $D = 3.13 \pm 0.07$ km and $p_V = 0.104 \pm 0.17$ when using $H = 15.6$. The MPCOrb file gives $H = 16.2$. Using Harris and Harris (1997), gives corrected values of $D = 3.10$, $p_V = 0.061$.

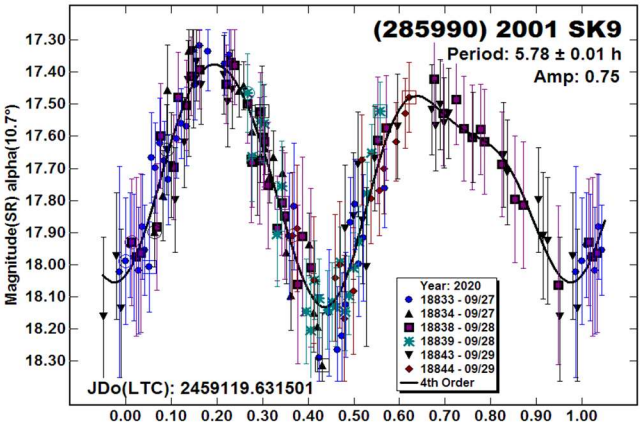

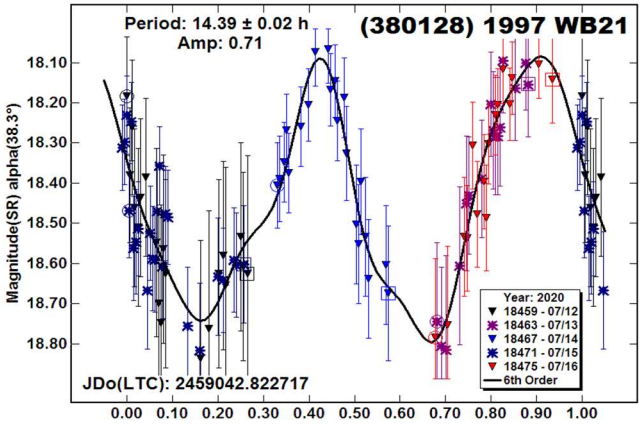

The period for 2010 DF1 was nearly commensurate with an Earth day and so the incomplete data set produced several nearly equal and commensurate solutions. Being guided by Harris et al. (2014), we adopted P = 45.8 h since it comes closest to producing a symmetrical bimodal lightcurve with amplitude of 0.60 mag.

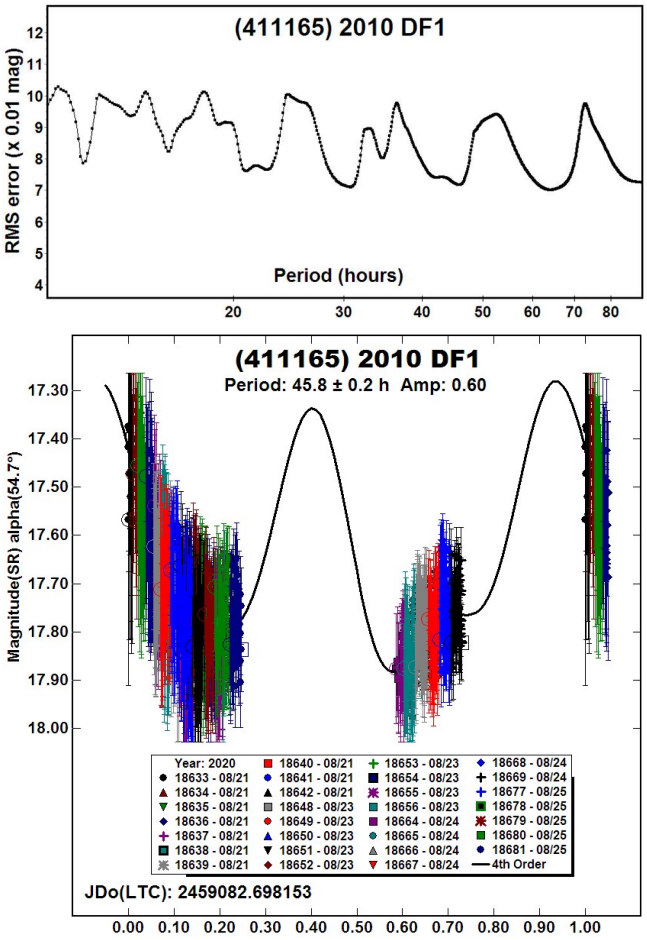

(450648) 2006 UC63. This 310-m NEA was observed from CS3 in 2018. At that time, we reported a period of 10.13 h (Warner, 2018). This turned out to be entirely wrong.

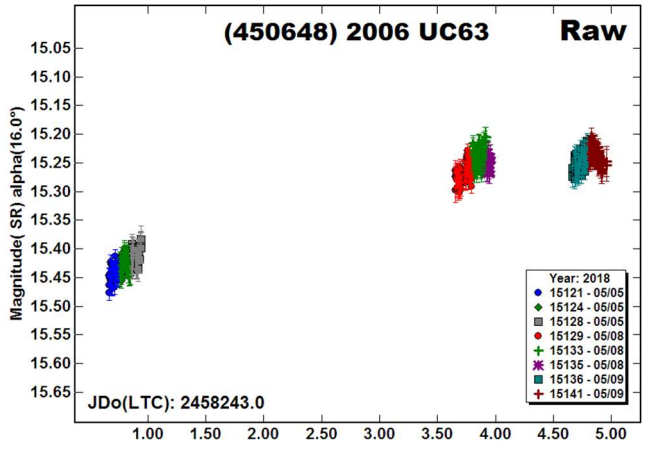

After Pravec et al. (2019web) produced a lightcurve with a period of 740 h, we re-visited our data and, as many times before, converted the comp star magnitudes from V to ATLAS SR. A raw plot of the revised data set shows a clear long-period trend on the order of 400 h, if assuming that the first and last sessions are, respectively, close to the minimum and maximum of the lightcurve. Even so, the period spectrum was still favoring well less than 100 hours.

There is a conundrum when working a long-period object or one that has a period nearly, but not exactly, commensurate with an Earth day. For example, assume a period of just more than 48 hours and observations are made every 24 hours. If circumstances are just right, each night's data catches *almost* the same part of lightcurve but, all other considerations notwithstanding, is just a bit higher or lower in the curve. When a raw plot (magnitude vs. JD) is made, the data set can take on the appearance of having a very long-period. This may help explain why the period spectrum was led astray.

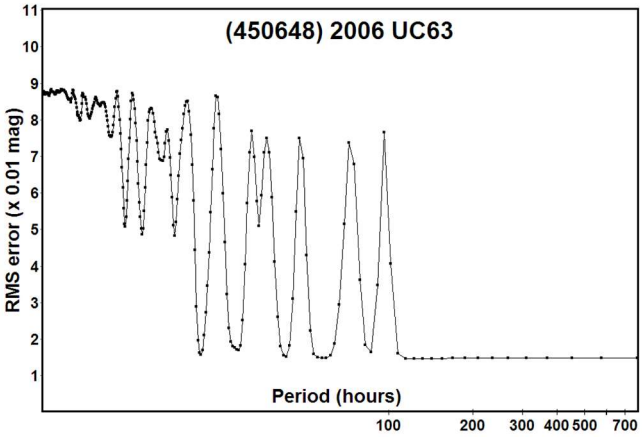

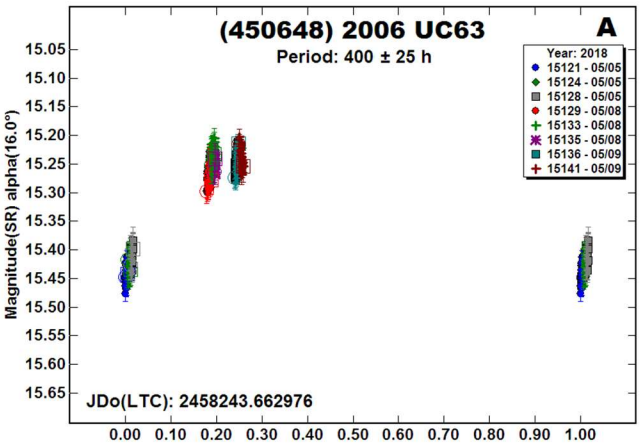

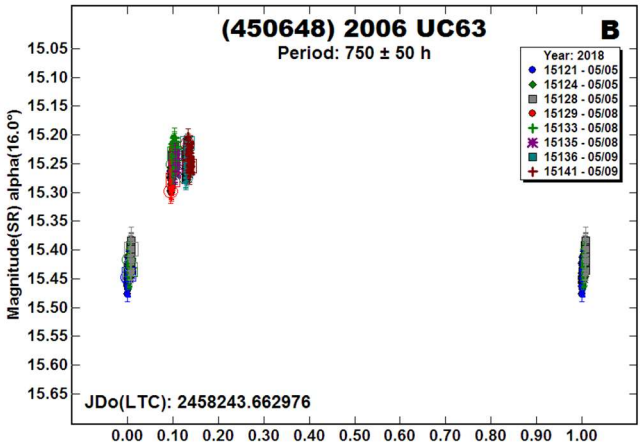

Taking the Pravec et al. (2019web) result as a guide, we found half-period solutions and doubled those to try to match their result. Two possibilities emerged. The first solution at 400 h ("A") is premised on the assumption that the first and last sessions were at an extrema of the true lightcurve and that lightcurve was bimodal. Given the apparent amplitude and relatively low phase angle, this seemed to be a safe assumption (Harris et al., 2014).

The second solution at 750 h ("B") was forced close to that from Pravec et al. (2019web). In this case, the assumption was that the last two sessions were near a maximum and that the first session is between it and the preceding minimum.

Unfortunately, we relied on the erroneous 10-h solution and so gave up on the asteroid much too soon. If nothing else, this shows the importance of using catalogs such as ATLAS, GAIA, and Pan-STARRS, all of which have very low systematic errors across their sky coverage. It's also important to use native magnitudes, i.e., those that were measured directly or corrected with well-defined transforms that have < 0.01-0.02 errors. For most common uses, these would be the SG, SR, and SI magnitudes from ATLAS and Pan-STARRS.

(480936) 2003 QH5. There were no rotation periods given in the LCDB for 2003 OH5. Mainzer et al. (2016) used WISE data to find $D = 0.537 \pm 0.088$ km and $p_V = 0.056 \pm 0.030$. This albedo is a bit on the dark side for NEAs, but there is a known but relatively small number of type C and other dark asteroids in the NEA orbital space.

The period spectrum favored 6.74 h, which we adopted because of the somewhat large amplitude. However, the phase angle was large and so the true lightcurve may have been altered by deep shadowing effects. Other solutions strayed from a nearly symmetrical bimodal solution but, because of the large phase angle, that may not be a completely safe assumption.

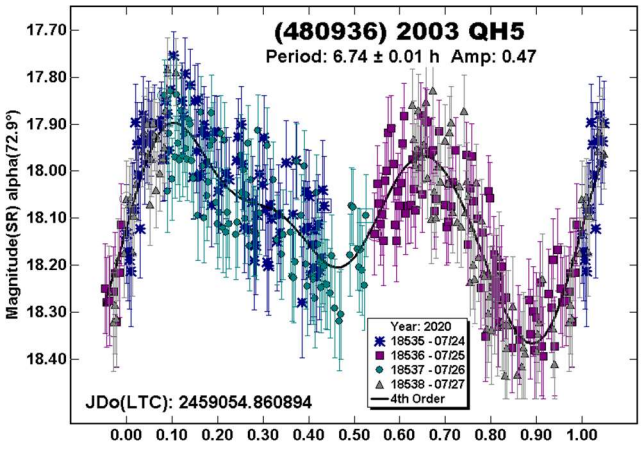

2003 BK47. This appears to be the first reported rotation period for 2003 QH5, which has an estimated diameter of 820 m. We could not obtain an extensive data set and so the period spectrum showed a few solutions that were nearly commensurate with an Earth day.

As in previous cases, we adopted a bimodal solution based on the 0.41 mag amplitude (Harris et al., 2014). Also, a consideration was that slopes of the Fourier curve were consistent with the adopted period.

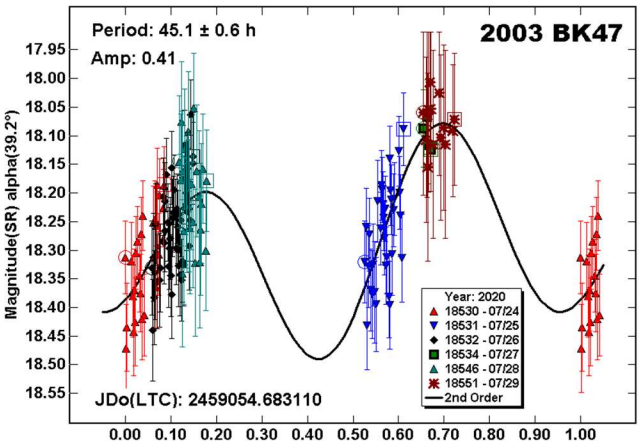

2005 QS10. The period spectrum, having tens of nearly equal RMS minimums, was of little use in finding a definitive period for 2005 QS10, which has an estimated diameter of 540 m.

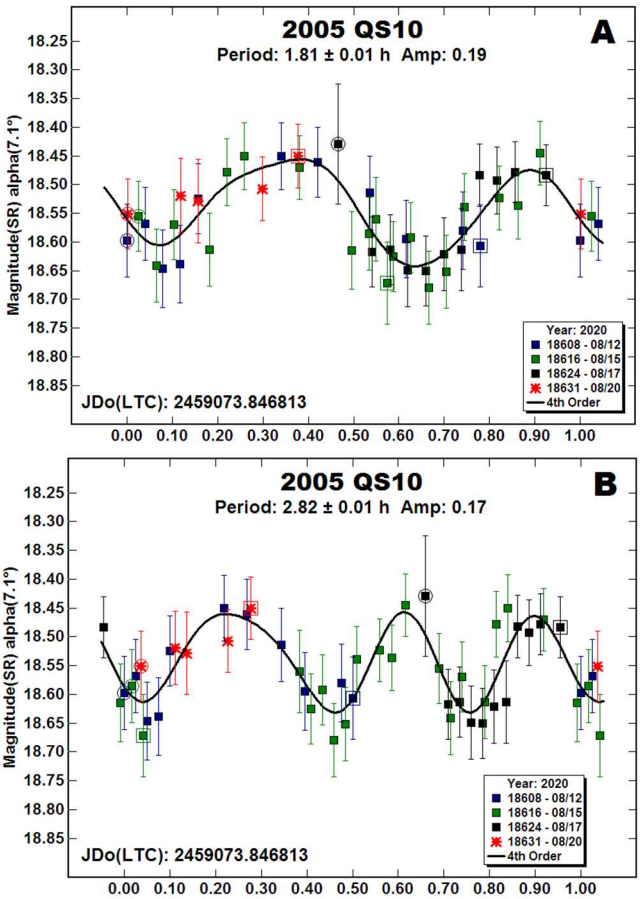

We have adopted a period of 1.81 h because the lightcurve is bimodal and completely covered. The alternate solution was a trimodal fit at 2.82 h but it could easily be the result of a *fit by exclusion*, which is where the Fourier analysis finds a local RMS minimum by reducing the number of overlapping data points.

Any period < 2.2 h, the approximate location of the spin barrier on the frequency-diameter (F-D) plot from the LCDB, calls for a check that the combination of the diameter and period do not make the asteroid particularly unusual.

As seen in the F-D plot, even with the shorter period, the asteroid lies barely above the spin barrier, adding to our confidence in that shorter period.

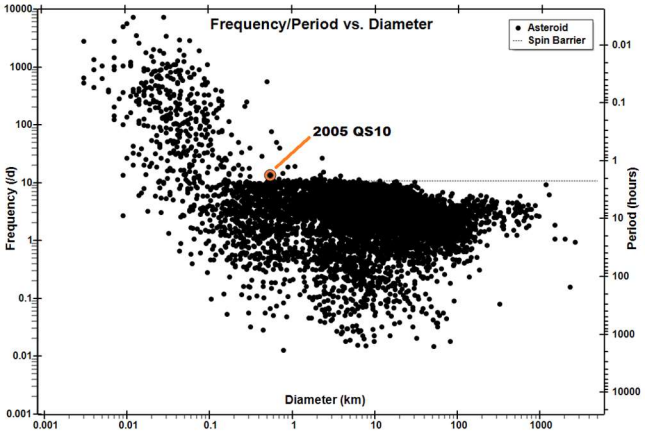

2006 HB. The LCDB listed no rotation period. The solution is not definitive. Given the period and 480-m diameter, tumbling is not out of the question (Pravec et al., 2005; 2014).

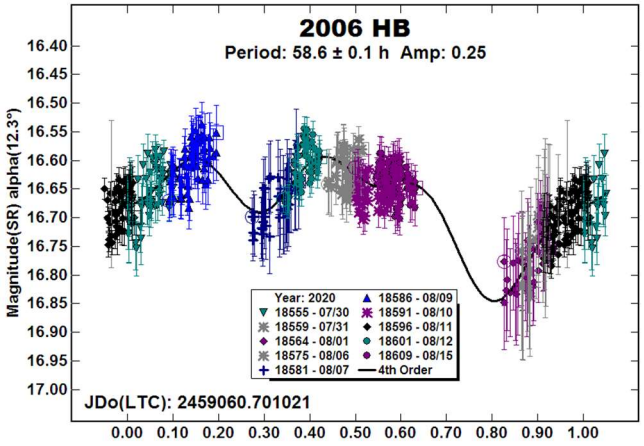

2006 NL. The LCDB listed no previous rotation period results for this 480-m NEA. The viewing aspect (phase/phase angle bisector) was changing rapidly at the time. For example, the phase angle decreased by nearly 9° from July 9 to July 10.

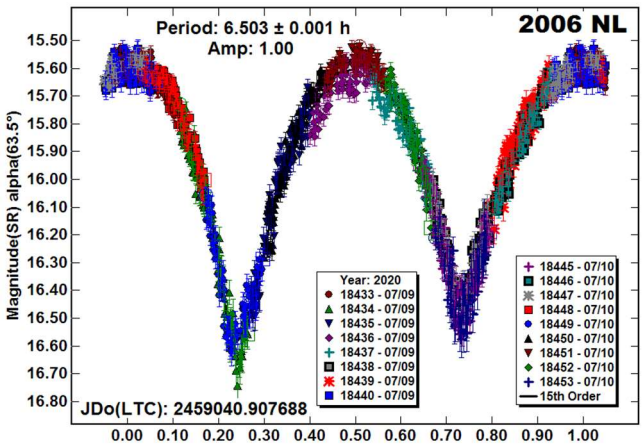

Changes in the lightcurve can be seen as ill-fitting sections in the plot of the combined data set. When isolating the nights, the curves have better fits but very different shapes and synodic periods. The increasing synodic period with decreasing phase angle indicates the asteroid is in retrograde rotation.

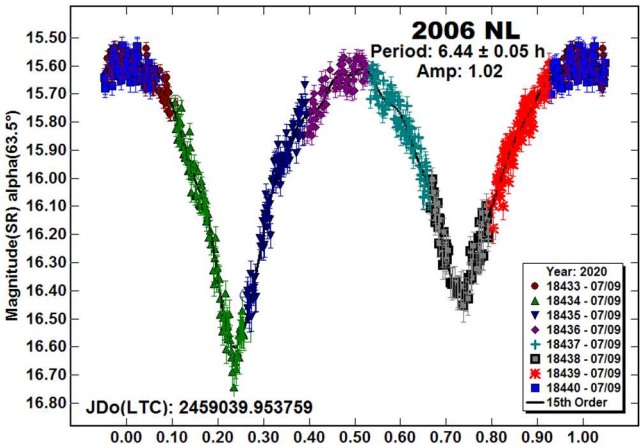

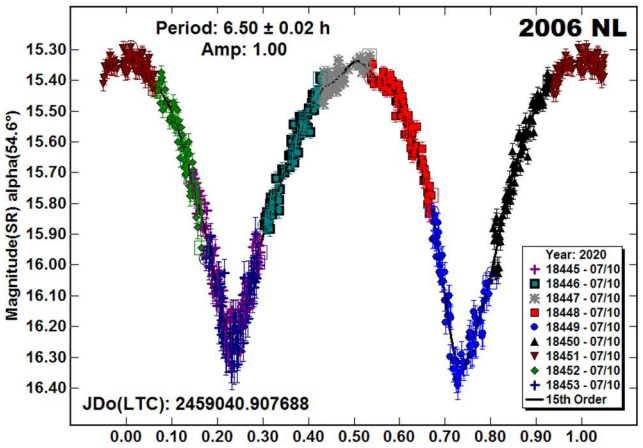

2006 UD63. Our data set covered some parts of the lightcurve more than once and so we have good confidence in the period of 83.97 h. The amplitude and phase angle also support the result being somewhat close to the true period.

Based on Pravec et al. (2005; 2014), this is a good candidate for tumbling. However, what parts of the lightcurve that were covered twice agreed well and the slopes of the individual sessions have the correct slope in relation to the Fourier curve. This would seem to preclude tumbling, at least within the noise of the data set.

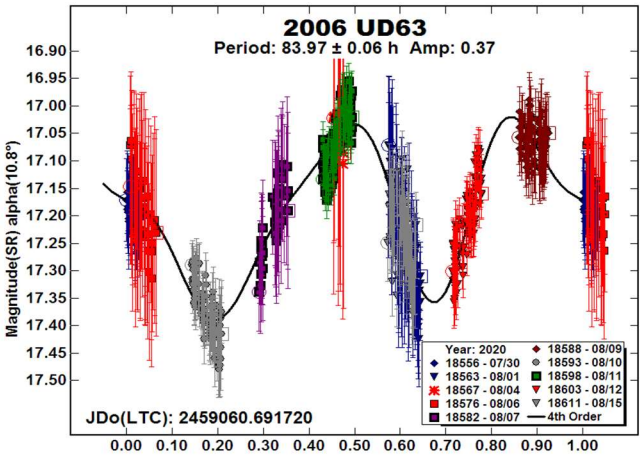

2007 VX137, 2014 LW21, 2016 PN, 2016 NV38, 2018 LM4. These five NEAs had no rotation period entries in the LCDB. The estimated diameter for 2007 VX137 is 600 m. For 2014 LW21, the diameter is 540 m.

The lightcurve shape for 2016 PN is asymmetrical, but this could be due to the phase angle of 44°. Attempts to fit to other periods were fruitless. The estimated diameter is 260 m. Despite a noisy data set, we were able to find a nearly secure period of 18.85 h for 2016 NV38, which has an estimated diameter of 570 m.

The data set for the 520-m 2018 LM4 was noisy given that it was V > 17.5 during the time of the observations. The period spectrum was very ambiguous. We adopted a 2nd-order lightcurve with a period of 40.6 h, but it's hardly definitive.

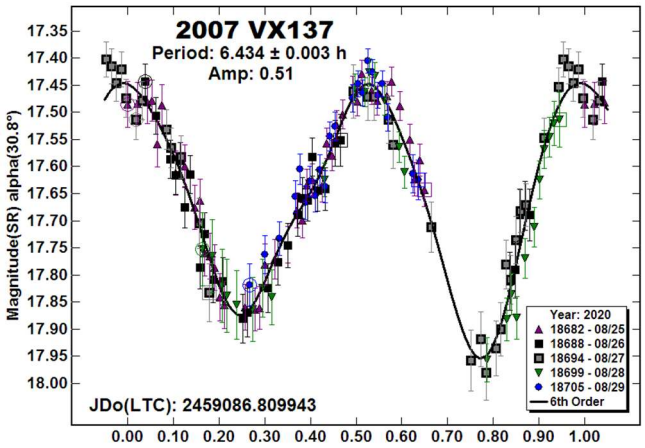

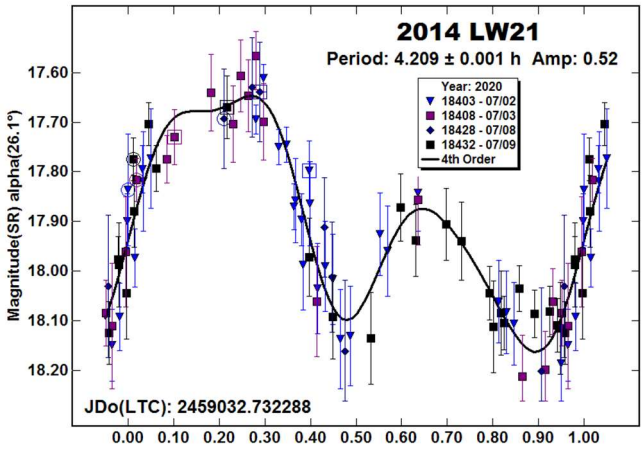

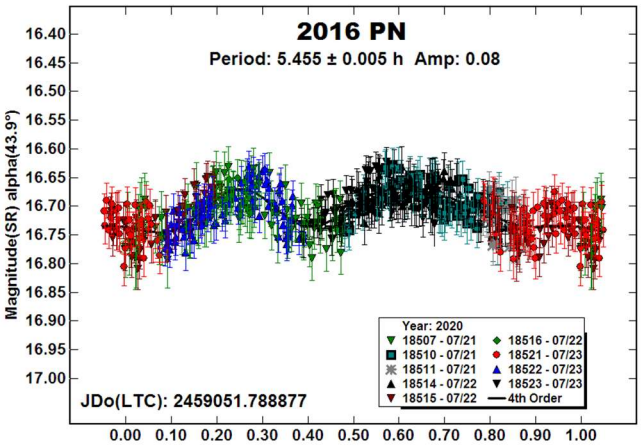

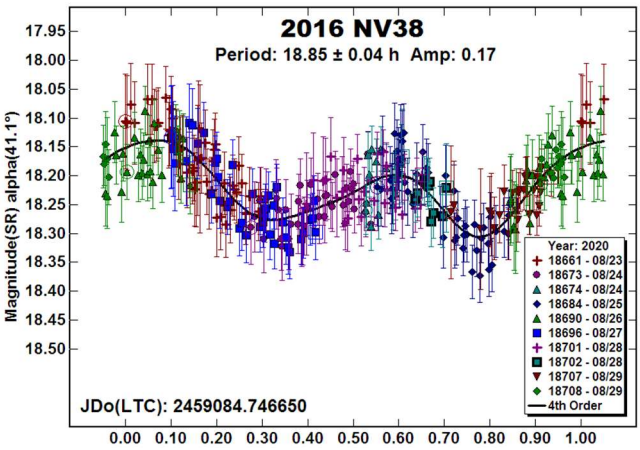

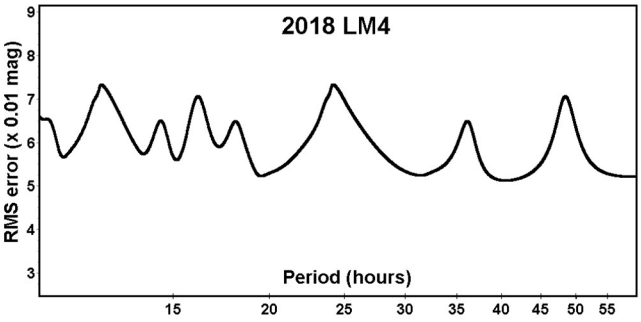

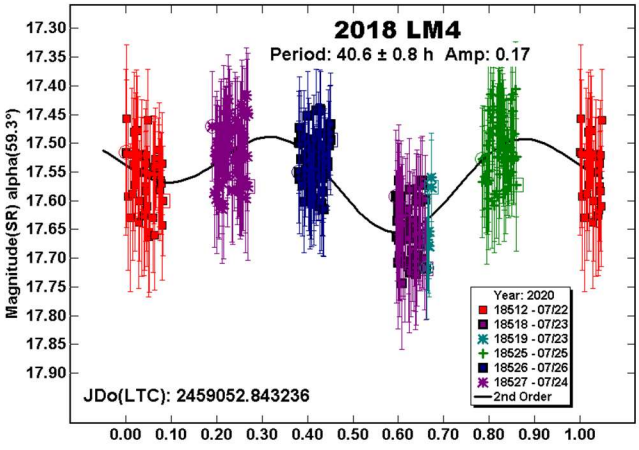

2020 SN. The estimated diameter for this NEA is only 30 m. Given that, the likelihood was that the period was $P << 2$ h and so requiring short exposures. The combination of being V ~ 17.5 and moving rapidly across the sky led to a noisy data set that, fortunately, still allowed finding a period.

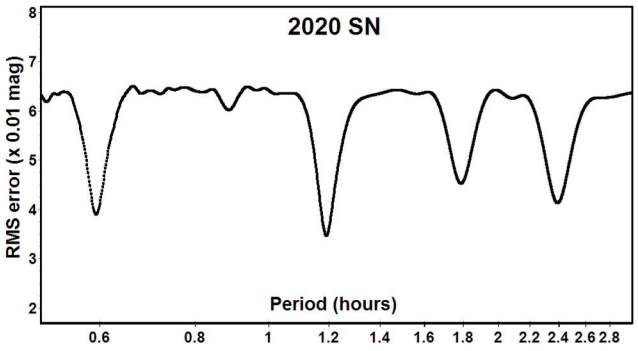

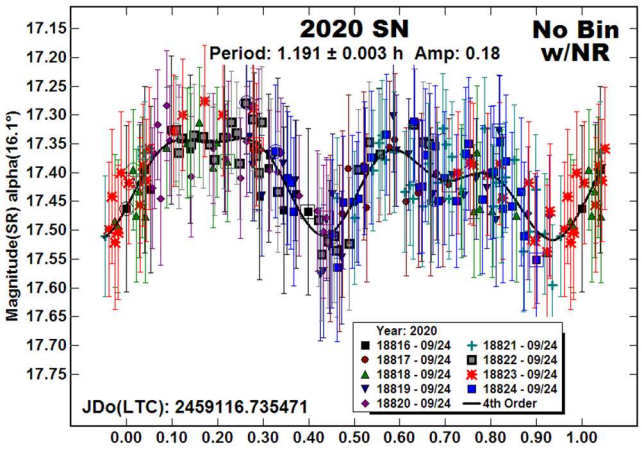

To improve the fit we did a dual-period search using *MPO Canopus* but not with the intent of finding a secondary period with a physical origin. Instead, the 4th-order secondary period was used as a "noise filter" to help decrease the scatter. The resulting plot shows the net result. We also tried binning the data points 2×1, meaning 2 points per bin that were no more than 1 minute apart. This did not change or improve the result.

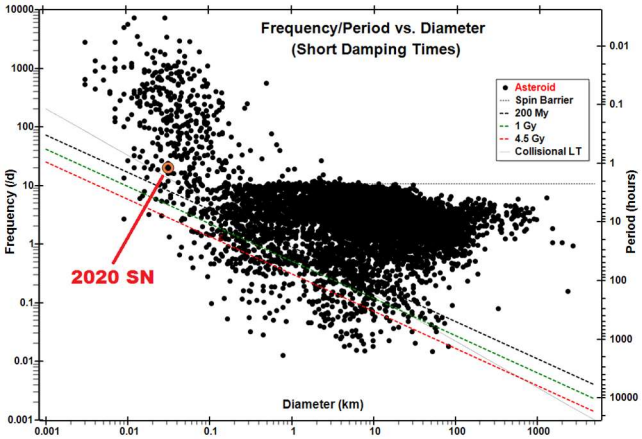

As shown in the frequency-diameter plot from the LCDB, the small diameter and short period of 2020 SN make it fit nicely among similar objects.

Acknowledgements

Funding for observations at CS3 and work on the asteroid lightcurve database (Warner et al., 2009) and ALCDEF database (*alcdef.org*) are supported by NASA grant 80NSSC18K0851.

The authors gratefully acknowledge Shoemaker NEO Grants from the Planetary Society (2007, 2013). These were used to purchase some of the telescopes and CCD cameras used in this research.

This work includes data from the Asteroid Terrestrial-impact Last Alert System (ATLAS) project. ATLAS is primarily funded to search for near earth asteroids through NASA grants NN12AR55G, 80NSSC18K0284, and 80NSSC18K1575; byproducts of the NEO search include images and catalogs from the survey area. The ATLAS science products have been made possible through the contributions of the University of Hawaii Institute for Astronomy, the Queen's University Belfast, the Space Telescope Science Institute, and the South African Astronomical Observatory.

References

References from web sites should be considered transitory, unless from an agency with a long lifetime expectancy. Sites run by private individuals, even if on an institutional web site, do not necessarily fall into this category.

Carbognani, A. (2014). "Asteroids Lightcurves at OAVdA: 2013 December - 2014 June." *Minor Planet Bull*. **41**, 265-270.

Carry, B.; Solano, E.; Eggl, S.; DeMeo, F.E. (2016). "Spectral properties of near-Earth and Mars-crossing asteroids using Sloan photometry." *Icarus* **268**, 340-354.

Harris, A.W.; Harris, A.W. (1997). "On the Revision of Radiometric Albedos and Diameters of Asteroids." *Icarus* **126**, 450-454.

Harris, A.W.; Young, J.W.; Scaltriti, F.; Zappala, V. (1984). "Lightcurves and phase relations of the asteroids 82 Alkmene and 444 Gyptis." *Icarus* **57**, 251-258.

Harris, A.W.; Pravec, P.; Galad, A.; Skiff, B.A.; Warner, B.D.; Vilagi, J.; Gajdos, S.; Carbognani, A.; Hornoch, K.; Kusnirak, P.; Cooney, W.R.; Gross, J.; Terrell, D.; Higgins, D.; Bowell, E.; Koehn, B.W. (2014). "On the maximum amplitude of harmonics on an asteroid lightcurve." *Icarus* **235**, 55-59.

Henden, A.A.; Terrell, D.; Levine, S.E.; Templeton, M.; Smith, T.C.; Welch, D.L. (2009). *http://www.aavso.org/apass*

Higgins, D.J. (2005). "Lightcurve and period determination for 479 Caprera, 2351 O'Higgins, (36378) 2000 OL19, (52750) 1998 KK17, (87684) 2000 SY2." *Minor Planet Bull*. **32**, 36-38.

Lin, C.-H.; Ip, W.-H.; Lin, Z.-Y.; Cheng, Yu.-C.; Lin, H.-W.; Chang, C.K. (2018). "Photometric survey and taxonomic identifications of 92 near-Earth asteroids." *Planet. Space Sci.* **152**, 116-135.

Mainzer, A.K.; Bauer, J.M.; Cutri, R.M.; Grav, T.; Kramer, E.A.; Masiero, J.R.; Nugent, C.R.; Sonnett, S.M.; Stevenson, R.A.; Wright, E.L. (2016). "NEOWISE Diameters and Albedos V1.0." NASA Planetary Data System. EAR-A-COMPIL-5-NEOWISEDIAM-V1.0.

Pravec, P.; Wolf, M.; Sarounova, L. (2000web, 2019web) *http://www.asu.cas.cz/~ppravec/neo.htm*

Pravec, P.; Harris, A.W.; Scheirich, P.; Kušnirák, P.; Šarounová, L.; Hergenrother, C.W.; Mottola, S.; Hicks, M.D.; Masi, G.; Krugly, Yu.N.; Shevchenko, V.G.; Nolan, M.C.; Howell, E.S.; Kaasalainen, M.; Galád, A.; Brown, P.; Degraff, D.R.; Lambert, J.V.; Cooney, W.R.; Foglia, S. (2005). "Tumbling asteroids." *Icarus* **173**, 108-131.

Pravec, P.; Scheirich, P.; Durech, J.; Pollock, J.; Kusnirak, P.; Hornoch, K.; Galad, A.; Vokrouhlicky, D.; Harris, A.W.; Jehin, E.; Manfroid, J.; Opitom, C.; Gillon, M.; Colas, F.; Oey, J.; Vrastil, J.; Reichart, D.; Ivarsen, K.; Haislip, J.; LaCluyze, A. (2014). "The tumbling state of (99942) Apophis." *Icarus* **233**, 48-60.

Tonry, J.L.; Denneau, L.; Flewelling, H.; Heinze, A.N.; Onken, C.A.; Smartt, S.J.; Stalder, B.; Weiland, H.J.; Wolf, C. (2018). "The ATLAS All-Sky Stellar Reference Catalog." *Ap. J.* **867**, A105.

Warner, B.D. (2014a). "Near-Earth Asteroid Lightcurve Analysis at CS3-Palmer Divide Station: 2013 September-December." *Minor Planet Bull*. **41**, 113-124.

Warner, B.D. (2014b). "Near-Earth Asteroid Lightcurve Analysis at CS3-Palmer Divide Station: 2014 January-March." *Minor Planet Bull*. **41**, 157-168.

Warner, B.D. (2015). "Near-Earth Asteroid Lightcurve Analysis at CS3-Palmer Divide Station: 2015 March-June." *Minor Planet Bull*. **42**, 256-266.

Warner, B.D. (2017a). "Near-Earth Asteroid Lightcurve Analysis at CS3-Palmer Divide Station: 2016 July-September." *Minor Planet Bull*. **44**, 22-36.

Warner, B.D. (2017b). "Near-Earth Asteroid Lightcurve Analysis at CS3-Palmer Divide Station: 2016 December thru 2017 April." *Minor Planet Bull*. **44**, 223-237.

Warner, B.D. (2018). "Near-Earth Asteroid Lightcurve Analysis at CS3-Palmer Divide Station: 2018 April-June." *Minor Planet Bull.* **45**, 366-379.

Warner, B.D.; Harris, A.W.; Pravec, P. (2009). "The Asteroid Lightcurve Database." *Icarus* **202**, 134-146. Updated 2020 June. *http://www.minorplanet.info/lightcurvedatabase.html*

Watanabe, S.; Hirabayashi, M.; Hirata, N.; and 85 co-authors. (2019). "Hayabusa2 arrives at the carbonaceous asteroid 162173 Ruygu – A spinning top rubble pile." *Science* **364**, 268-272.

Number	Name	2020 mm/dd	Phase	L_{PAB}	B_{PAB}	Period(h)	P.E.	Amp	A.E.
4055	Magellan	08/17-08/23	50.9,49.2	19	-7	7.478	0.001	0.71	0.03
		2014/01/26-02/02	13.5,14.9	113	-23	7.476	0.002	0.7	0.05
9162	Kwiila	07/11-07/17	44.2,48.4	326	18	15.13	0.01	0.92	0.05
19764	2000 NF5	08/26-09/18	24.5,5.7	192	2	[T]59.263	0.004	0.99	0.02
						51.31	0.01	0.37	0.03
53435	1999 VM40	09/02-09/06	49.8,50.5	33	-18	5.193	0.005	0.22	0.03
87684	2000 SY2	09/18-09/25	42.5,38.2	36	-21	[A]2.571	0.001	0.09	0.01
						2.676	0.001	0.06	0.01
136900	1998 HL49	08/09-08/11	20.0,19.7	330	18	6.439	0.004	0.64	0.03
137108	1999 AN10	08/04-08/07	55.4,51.0	348	23	5.041	0.003	0.40	0.05
145656	4788 P-L	08/17-08/24	32.4,27.8	5	1	2.968	0.001	0.26	0.03
162173	Ryugu	09/26-10/01	28.2,28.7	9	19	7.40	0.01	0.34	0.03
285990	2001 SK9	09/27-09/29	10.6,9.5	6	10	5.78	0.01	0.75	0.06
380128	1997 WB21	07/12-07/16	38.2,40.0	318	4	14.39	0.02	0.71	0.05
411165	2010 DF1	08/21-08/25	53.5,23.8	347	10	45.8	0.2	0.60	0.05
450648	2006 UC63	2018/05/05-05/09	16.2,23.5	219	10	[A]750	50	0.25	0.05
						400	25	0.25	0.10
480936	2003 QH5	07/24-07/27	73.0,69.8	341	19	6.74	0.01	0.47	0.05
	2003 BK47	07/24-07/29	39.2,44.2	272	22	45.1	0.6	0.41	0.05
	2005 QS10	08/12-08/20	7.2,2.6	326	4	[A]1.81	0.01	0.19	0.03
						2.82	0.01	0.17	0.02
	2006 HB	07/30-08/15	12.3,7.8	315	7	58.6	0.1	0.25	0.03
	2006 NL	07/09-07/10	62.3,53.4	288	32	6.503	0.001	1.01	0.04
	2006 UD63	07/30-08/15	*10.8,7.6	313	5	83.97	0.06	0.37	0.04
	2007 VX137	08/25-08/29	30.9,28.9	357	-7	6.434	0.003	0.48	0.03
	2014 LW21	07/02-07/09	26.1,23.4	296	16	4.209	0.001	0.56	0.05
	2016 NV38	08/23-08/29	41.1,40.6	205	18	18.85	0.04	0.17	0.03
	2016 PN	07/21-07/23	43.9,35.5	321	9	5.455	0.005	0.08	0.02
	2018 LM4	07/22-07/26	59.3,60.1	341	1	40.6	0.8	0.17	0.03
	2020 SN	09/24-09/24	17.2	9	6	1.193	0.003	0.19	0.04

Table II. Observing circumstances. [A]Ambiguous period. [T]Dominant period of a tumbling asteroid. The second line gives the secondary period. The phase angle (α) is given at the start and end of each date range. If there is an asterisk before the first phase value, the phase angle reached a maximum or minimum during the period. L_{PAB} and B_{PAB} are, respectively the average phase angle bisector longitude and latitude (see Harris et al.,1984).

ON CONFIRMED AND SUSPECTED BINARY ASTEROIDS OBSERVED AT THE CENTER FOR SOLAR SYSTEM STUDIES

Brian D. Warner
Center for Solar System Studies / MoreData!
446 Sycamore Ave.
Eaton, CO 80615 USA
brian@MinorPlanetObserver.com

Robert D. Stephens
Center for Solar System Studies / MoreData!
Rancho Cucamonga, CA 91730

Alan W. Harris
MoreData!
La Cañada, CA 91011

(Received: 2020 October 10)

The analysis of observations made at the Center for Solar System Studies from 2020 July through September, led to the discovery or confirmation of two binary asteroids: the Vestoid 4030 Archenhold and NEA (85275) 1994 LY. The latter had been reported as a suspected binary by Pravec et al. (2007web). An additional nine asteroids were found to have a secondary period but without confirming mutual events (occultations/eclipses) due to a satellite: the known Hungaria binary 2577 Litva, 5928 Pindarus (Hilda), 7174 Semois (Hilda), (16970) 1998 VV2 (Hilda), (39282) 2001 BM36 (Hilda), (119356) 2001 SF235 (inner main-belt), (159402) 1999 AP10 (NEA), (420302) 2011 XZ1 (NEA), and 2019 AN5 (NEA). We discuss the likelihood of eight of those objects actually being binary.

CCD photometric observations at the Center for Solar System Studies in 2020 July through September led to discovery or confirmation of two binary asteroids and an additional nine suspected binaries based on the presence of a secondary period. Those nine did not display the required mutual events (occultations/eclipses) to confirm a satellite and so the origin of the secondary period cannot be confirmed. Table I lists the telescopes and CCD cameras that were combined to make the observations.

All the cameras use CCD chips from the KAF blue-enhanced family and so have essentially the same response. The pixel scales ranged from 1.24-1.60 arcsec/pixel.

Telescopes	Cameras
0.30-m *f*/6.3 Schmidt-Cass	FLI Microline 1001E
0.35-m *f*/9.1 Schmidt-Cass	FLI Proline 1001E
0.40-m *f*/10 Schmidt-Cass	SBIG STL-1001E
0.40-m *f*/10 Schmidt-Cass	
0.50-m *f*/8.1 Ritchey-Chrétien	

Table I. List of available telescopes and CCD cameras at CS3. The exact combination for each telescope/camera pair can vary due to maintenance or specific needs.

All lightcurve observations were unfiltered since a clear filter can cause a 0.1-0.3 mag loss. The exposure duration varied depending on the asteroid's brightness and sky motion. Guiding on a field star sometimes resulted in a trailed image for the asteroid.

Measurements were made using *MPO Canopus*. The Comp Star Selector utility in *MPO Canopus* found up to five comparison stars of near solar-color for differential photometry. Comp star magnitudes were taken from ATLAS catalog (Tonry et al., 2018), which has Sloan *griz* magnitudes that were derived from the GAIA and Pan-STARR catalogs, among others, and are the "native" magnitudes of the catalog.

To reduce the number of times and amount of resetting nightly zero points, we use the ATLAS r´ (SR) magnitudes. Those adjustments are mostly ≤ 0.03 mag. The occasions where larger corrections were required may have been related in part to using unfiltered observations, poor centroiding of the reference stars, and not correcting for second-order extinction terms.

The Y-axis of the primary lightcurves gives ATLAS SR "sky" (catalog) magnitudes. The values on the Y-axis of the secondary lightcurves are usually differential magnitudes with 0.0 corresponding to the average magnitude of the primary curve.

During period analysis, the magnitudes were normalized to the comparison stars used in the earliest session and to the phase angle given in parentheses using $G = 0.15$. The X-axis shows rotational phase from –0.05 to 1.05. If the plot includes the amplitude, e.g., "Amp: 0.65", this is the amplitude of the Fourier model curve and *not necessarily the adopted amplitude for the lightcurve*.

Our initial search for previous results started with the asteroid lightcurve database (LCDB; Warner et al., 2009a) found on-line at *http://www.minorplanet.info/lightcurvedatabase.html*. Readers are strongly encouraged to obtain, when possible, the original references listed in the LCDB. From here on, we'll use only "LCDB" to reference the paper by Warner et al. (2009a).

2577 Litva. This Hungaria member was found to be a binary by Warner et al. (2009b). The satellite orbital period was 35.78 h and the estimated effective diameter secondary-to-primary ratio was ≥0.35. In addition, a third period of 5.7 h was reported; conjecture was that this was due to a third body. This was found to be the case when Merline et al. (2013) reported a second satellite for the system with an estimated orbital period of 214 days! That second satellite is too small to be detected with lightcurves alone.

Our observations in 2020 found a primary period compatible with earlier results. It appears that the viewing geometry didn't favor seeing mutual events (occultations/eclipses) due to the first satellite. The P_{ORB} lightcurve was forced to match the period from Warner (2011).

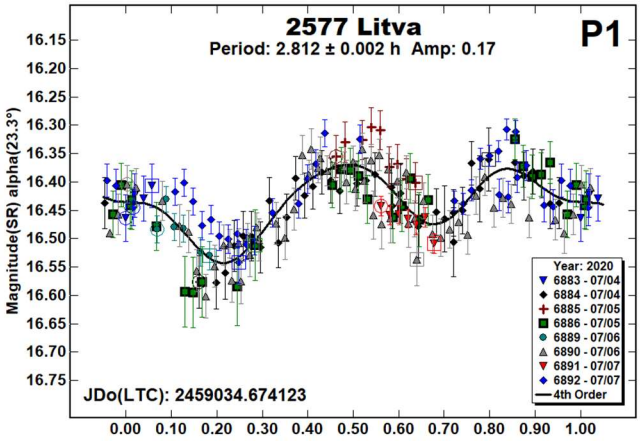

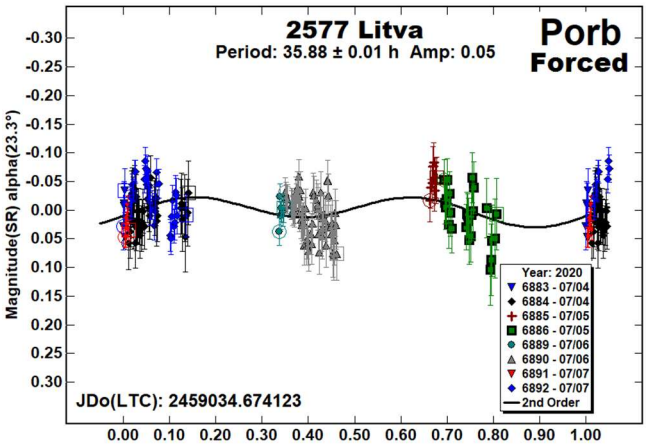

4030 Archenhold. Initial observations of this 7 km Vestoid clearly showed deviations from the general lightcurve. Follow-up observations and analysis confirmed a new binary discovery.

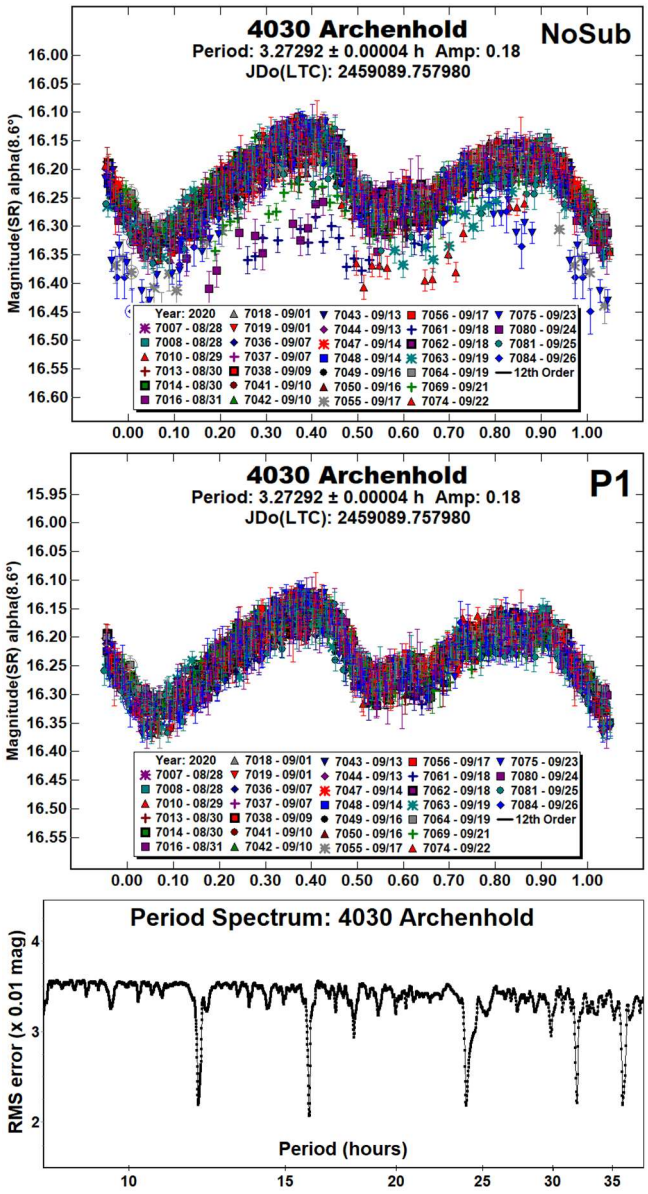

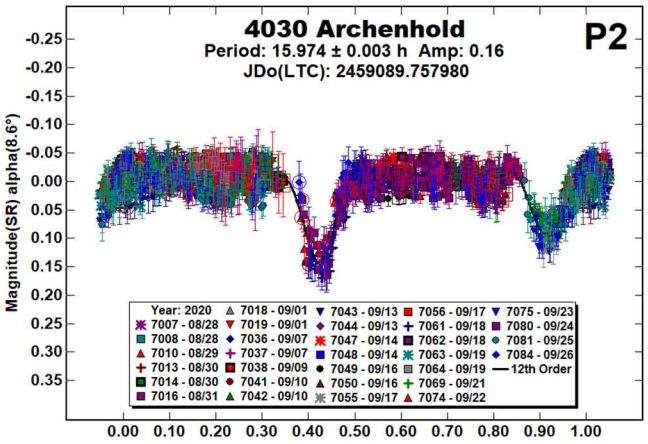

The P2 plot shows the mutual events due to the satellite. Pravec (private communications) suggested that an orbital period of 48 h was almost as likely. Were the two mutual events the same depth, this would seem more probable. However, with the events ranging from 0.10 to 0.15 mag, thus avoiding confusion about where in the P2 plot that a given event occurred, we believe our period of 15.974 h is the more likely.

5928 Pindarus. Analysis of data obtained in 2020 clearly indicated a very long period for this 26 km Hilda member. This contradicted the period of 6.01 h reported by Warner and Stephens (2018).

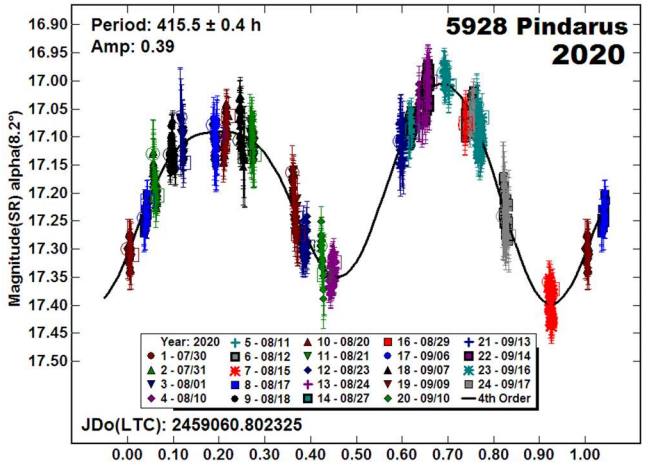

The data from 2018 were re-visited by first converting V magnitudes derived from the ATLAS star catalog (Tonry et al., 2018) to the native Sloan SR (r′) magnitudes to avoid the inherent 0.03-0.05 mag errors in the SR/SG to V transformations.

While the initial search found a period near 58 hours, at least one of the sessions had the wrong slope compared to the Fourier curve. When forcing the data to a period of 415 h, the result is something close to what's expected for a large amplitude lightcurve with data just covering one extreme (maximum in this case) and approaching the following extreme (minimum), i.e., the fall from maximum to minimum was about 0.25 rotation period.

A 4th-order Fourier fit was forced to the 415-h period, which had an extremely large amplitude as the algorithm tried to fill in the missing parts of the curve. This fit was applied in a dual-period search to see if there were signs of a secondary period. If so, this would make the object a candidate for the subclass of very wide binaries (see Warner, 2016; Jacobson et al., 2014).

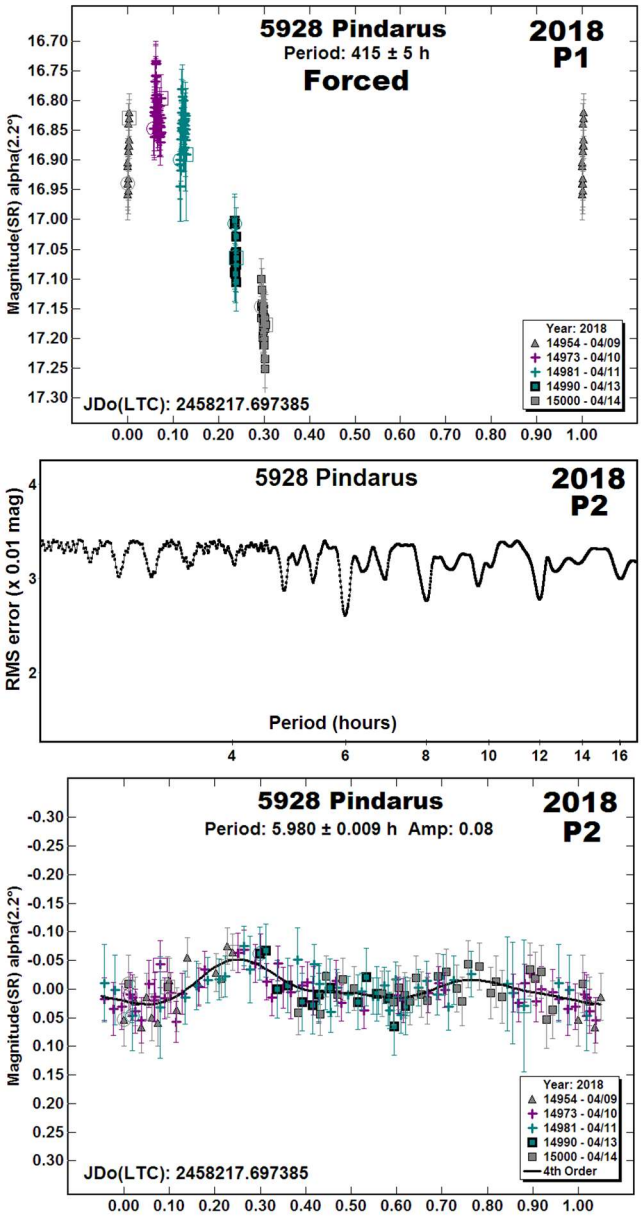

The result was a small amplitude bimodal lightcurve with a period of 5.980 h. The two periods are compatible with previous very wide binary candidates. In addition, based on the period and amplitude of the dominant period, the secondary period is too short for one associated with tumbling. On the other hand, based on Pravec et al. (2014, and references therein), the 415-h period and diameter make Pindarus a good candidate for tumbling.

7174 Semois. This Hilda has an estimated diameter of 25 km. Given the size and being in the outer reaches of the main-belt, this would not be considered a good candidate for a binary created by spin-up due to YORP (Yarkovsky–O'Keefe–Radzievskii–Paddack; Rubincam, 2000). If actually binary, then a different model would have to be found for its formation.

Previous observations by Warner and Stephens (2017) led to a reported period of 7.456 h. Pál et al. (2020) used TESS data to find a period of 34.6676 h. The two periods don't have a simple integral ratio and, as it turns out, both may be right.

The raw observations of the asteroid at CS3 in 2020 August-September showed a confused data set that appeared that it might defy analysis. We first tried to find a period near 7.45 h and, surprisingly, the period spectrum showed a strong minimum for about that period. The resulting lightcurve was still unsatisfactory and so a dual-period search was done using *MPO Canopus*. The result was surprising.

After several iterations of finding one period, subtracting it to find another, and then using that result to find the first period again, there were two periods, both closely matching a previous result. The "primary" period is 7.490 h, close to Warner and Stephens (2017). The lightcurve is intriguing since it seems to resemble one seen for an elongated satellite that is tidally-locked with its orbital period. However, the period is too short for that to be likely.

The secondary period was 34.57 h, which is about 0.1 h shorter than that from Pál et al. (2020). Its lightcurve is a bit asymmetrical, which casts some doubt on the solution but no other period, or combination of P1/P2, produced anything with nearly as good of fit for both.

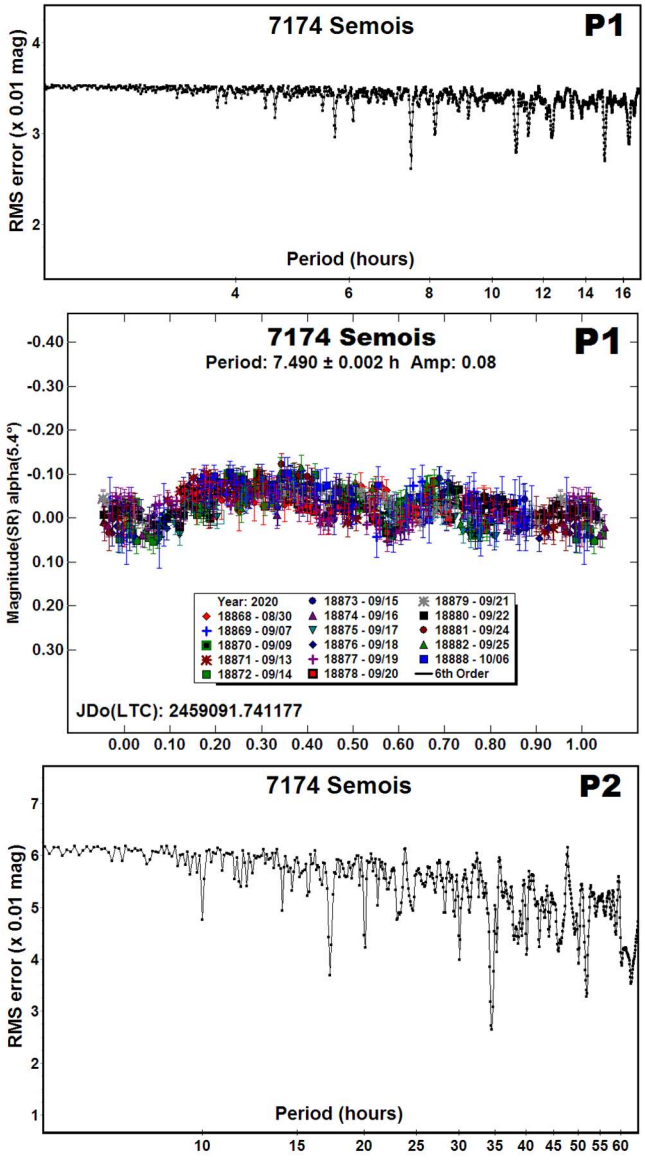

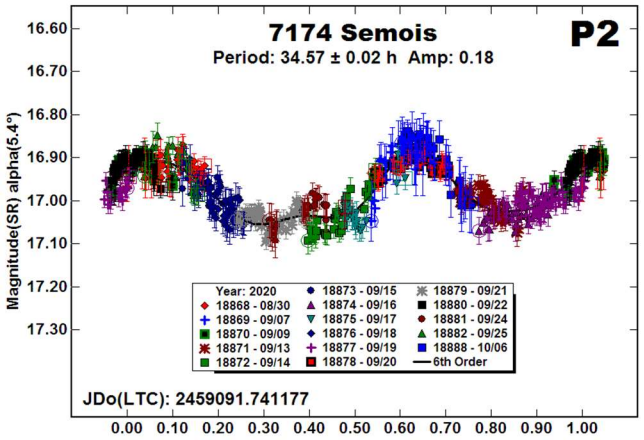

The size and even the longest period are far below the requirements for tumbling (Pravec et al., 2014 and references therein). We cannot provide a definitive answer regarding nature of the system and the origins of the two periods. Looking ahead, the asteroid remains V > 18 until late 2024, reaching V ~ 17.6 in 2025 March. Follow-up observations might resolve the mystery.

(16970) 1998 VV2. This is another Hilda (24 km) where binary formation is highly unlikely to be due to the YORP thermal effect. Given the noisy data set, the solution for P2 is not secure. Assuming its validity, the two 0.10 mag events at 0.12 and 0.62 orbital phase indicate Ds/Dp ≥ 0.31 for the secondary-to-primary effective diameter ratio.

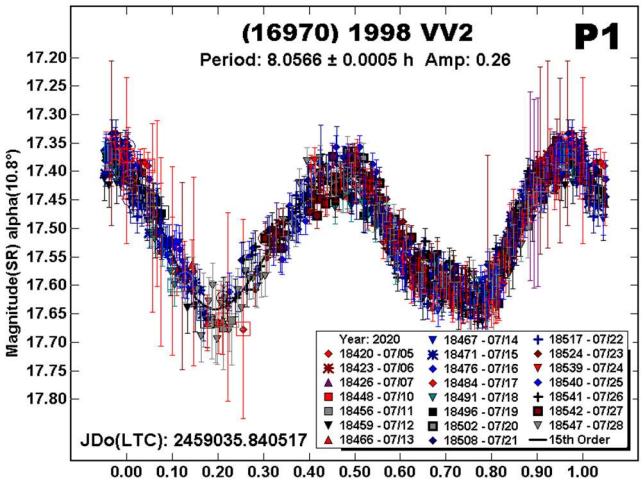

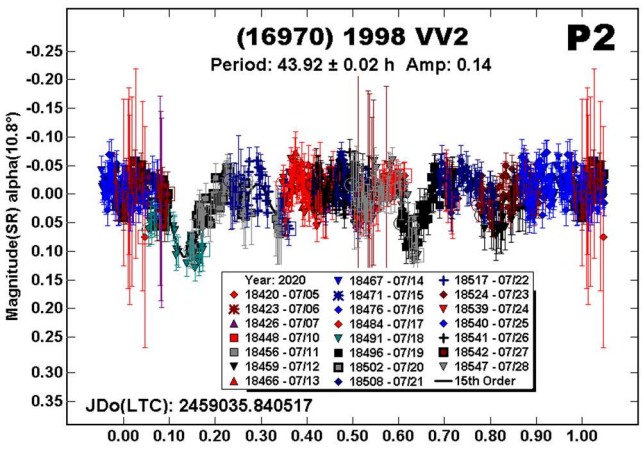

(39282) 2001 BM36. This 20-km Hilda is one of the better candidates for being a very wide binary. The raw data showed a clear long-period trend and so it took almost a month before most of the 620-h lightcurve could be covered. The result is almost a *fit by exclusion*, which is due to a local minimum in the period spectrum where the number of overlapping data points is kept to a minimum. However, a search for the half-period near 300 h and the amplitude gives us good confidence in the P_1 result.

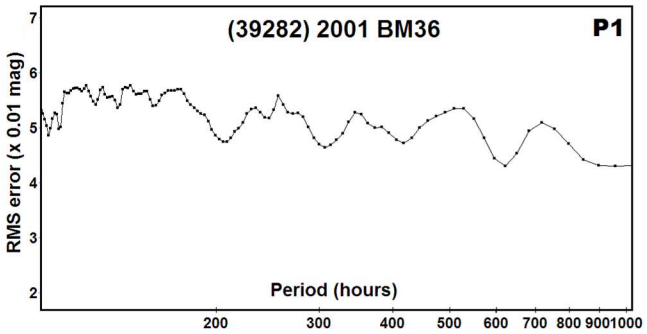

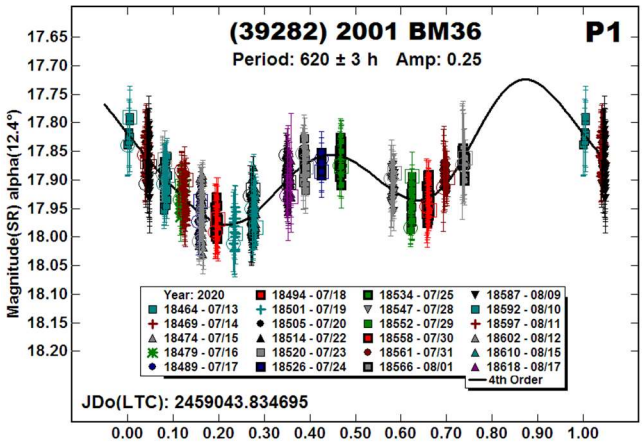

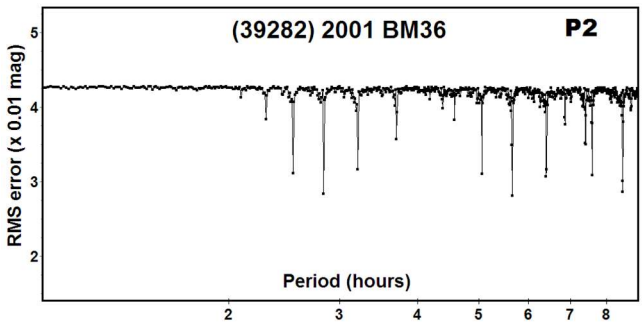

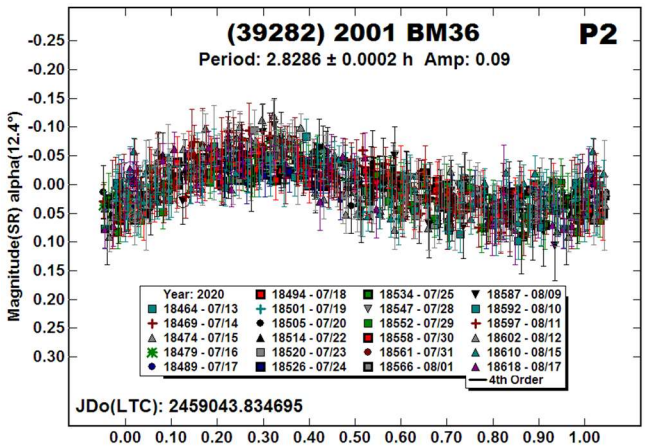

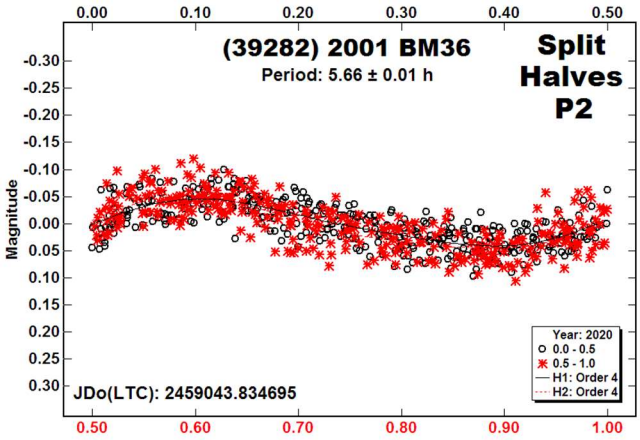

In the dual-period analysis with *MPO Canopus*, a strong secondary period appeared at 2.8286 h but with a monomodal lightcurve. This is entirely plausible given the low amplitude and phase angle (Harris et al., 2014). A split-halves plot (see Harris et al., 2014) showed a high degree of symmetry for the two halves of a bimodal solution near 5.66 h. With such symmetry, the half-period can be just as correct. We adopted the shorter period because it's more in line with other candidates where the small satellite has a period similar to that of the primary in an "ordinary" small binary asteroid.

(85275) 1994 LY. Pravec et al. (2007web) found a period of 2.6962 h for the NEA and suspected a satellite with a period of 48.5 h. Our initial data showed the tell-tale signs of a satellite: deviations from the general lightcurve (NoSub).

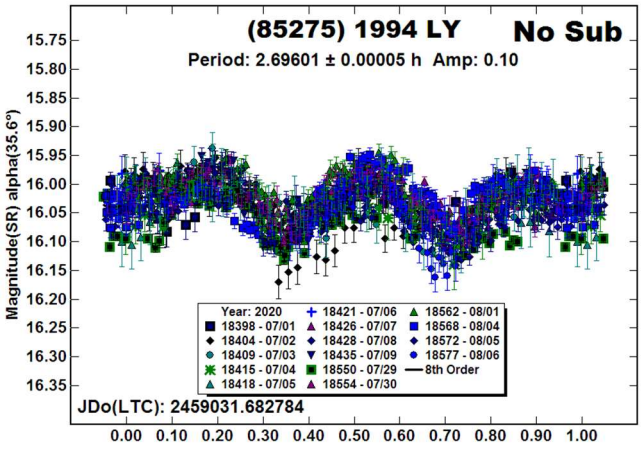

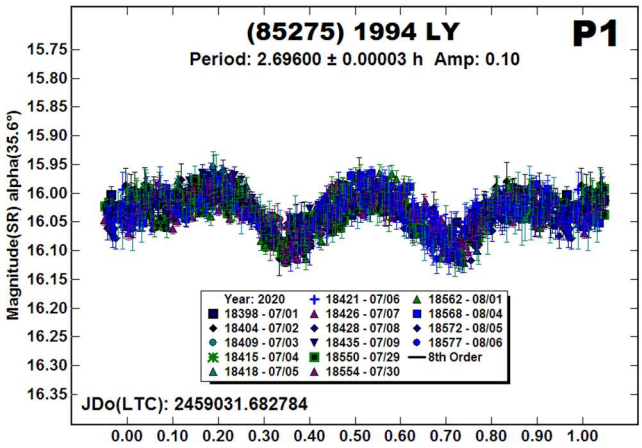

We did a dual-period search with *MPO Canopus* and found a strong solution at 2.69600 h, which is similar to that found without the search. The iterative process of finding one period, then the other, re-finding the first period, and so on continued until a final solution of 16.6238 h was found for the secondary period (P2). The period spectrum does show a potential solution near the 48 h found by Pravec et al. (2007web), but the lightcurve featured 8 minimum/maximum pairs.

The lightcurve for the satellite shows what appears to be two events properly spaced about one-half period apart. From those events, we estimate the effective secondary-to-primary diameter ratio to be ≥ 0.26.

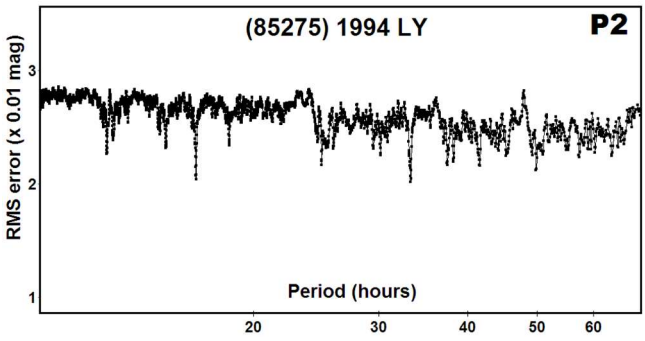

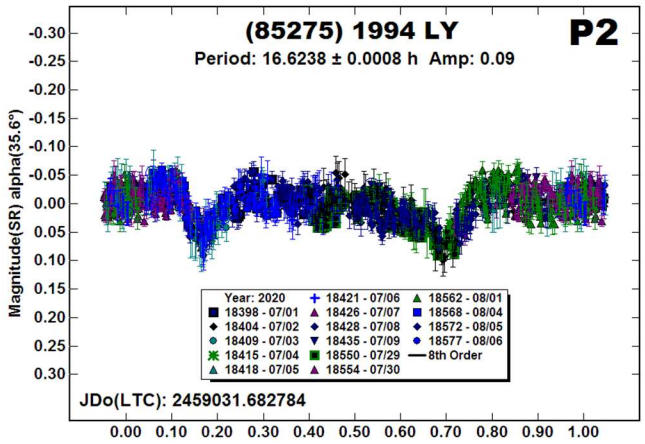

(119356) 2001 SF235. There were no previous entries of any kind in the LCDB for this 1.5 km inner main-belt asteroid. The raw plot for each night indicated a long period with moderate amplitude. Because of the sparse data set, a 2nd-order fit was used since higher order Fourier curves were physically impossible.

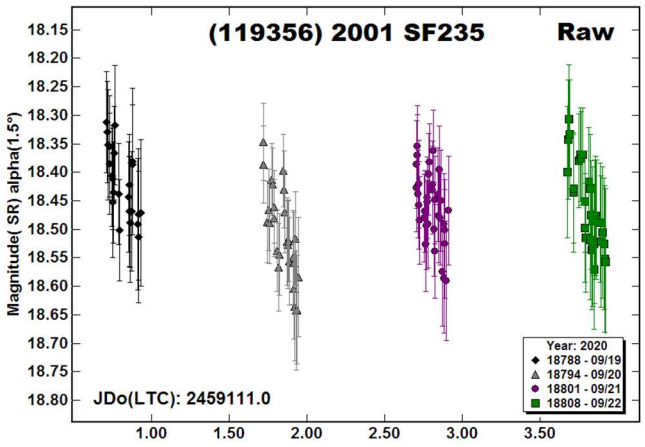

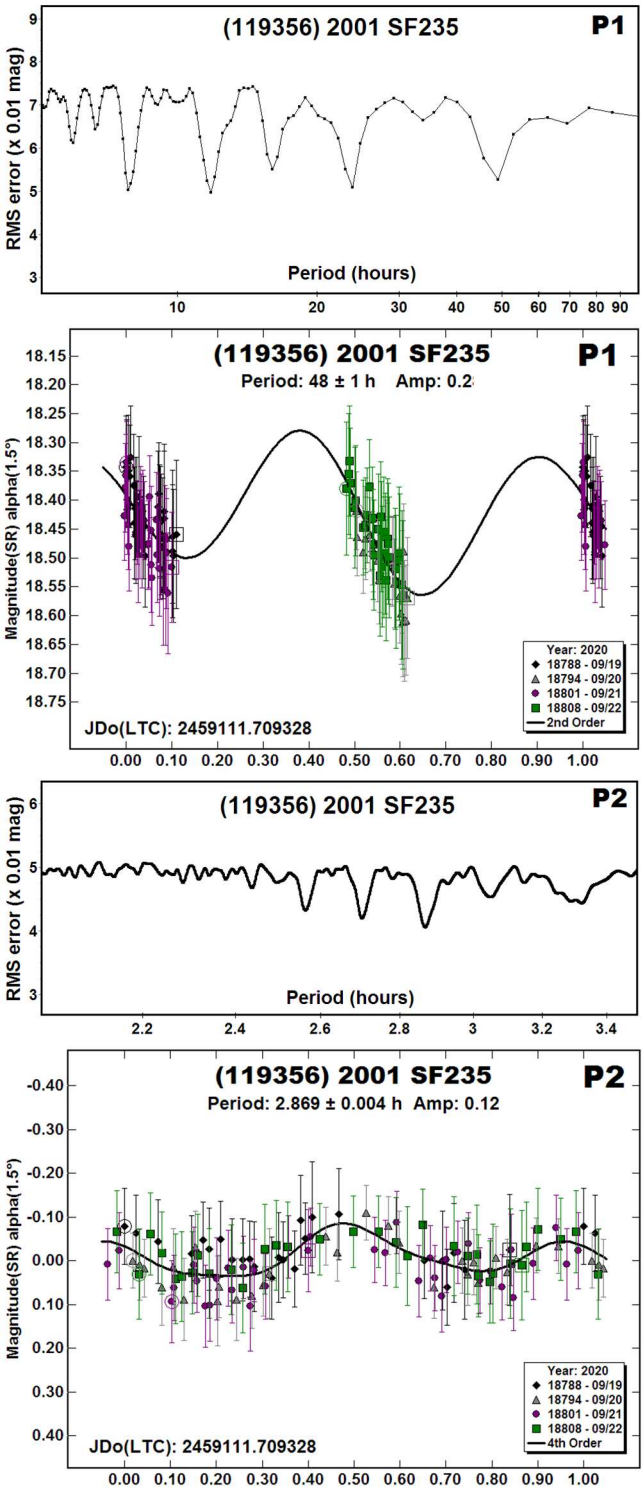

The period spectrum, as expected, showed several solutions that were nearly commensurate with an Earth day. We adopted 48 h because the bimodal lightcurve had reasonable slopes and amplitude. A 24-h solution produced a monomodal lightcurve. With an amplitude of only 0.20 mag for both solutions, the shorter period cannot be formally excluded (Harris et al., 2014).

We again did a dual period search using *MPO Canopus*, subtracting the 48-h solution from the data, and found a secondary lightcurve with a period of 2.869 h. The two periods are compatible with this being a very wide binary candidate but, again, the absence of mutual events leaves open the true nature of this asteroid.

(159402) 1999 AP10. Franco et al. (2010) observed this 1.8-km NEA in 2009 and found a period of 7.908 h. Hasegawa et al. (2018) reported the same synodic period of 7.911 h based on separate lightcurves from 2009 September, October, and December.

Analysis of our data in obtained in 2020 July found a comparable period of 7.9219 h. However, a single-period solution did not provide a good fit to the data so we tried a dual-period search using *MPO Canopus*. That search found a strong solution near 28 h, which was further refined to 28.461 h. The two periods don't have a simple integral ratio, which helps eliminate the possibility of the Fourier analysis latching onto higher-order harmonics of the dominant period.

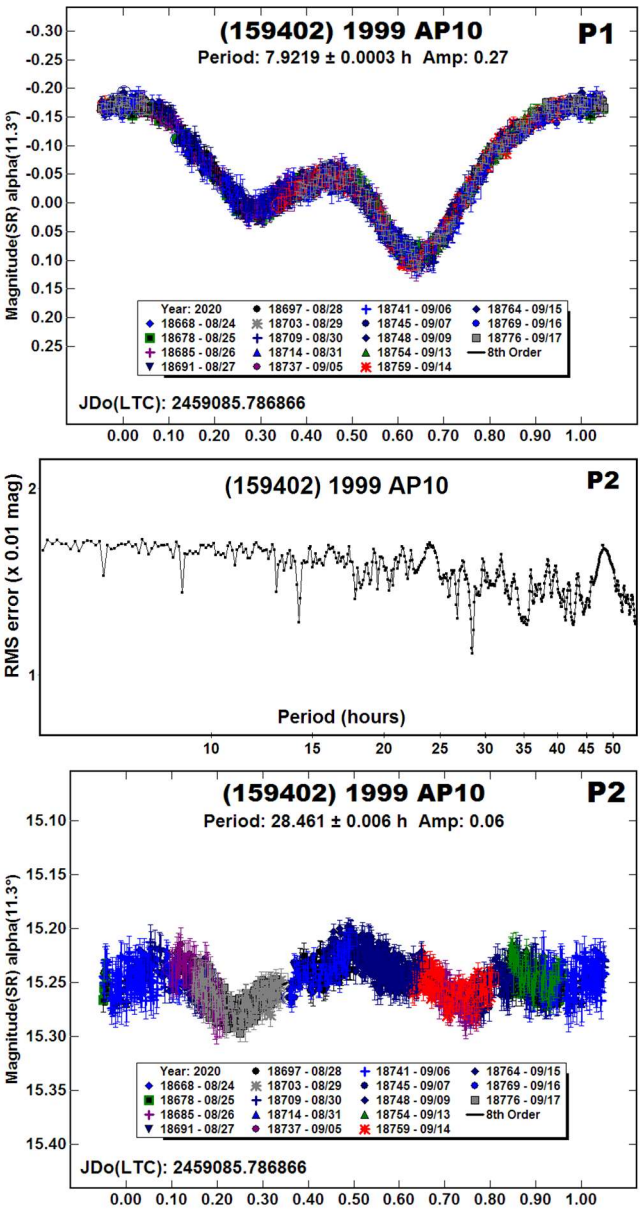

The shape of the P_2 lightcurve is interesting. It doesn't show obvious signs of mutual events, but may indicate a highly-elongated body that is tidally-locked to its orbital period.

As part of an on-going campaign to support radar observations, we observed 1999 AP10 about two weeks later, starting in early October. Once again, the single-period solution didn't provide a good fit and we did a dual-period search using *MPO Canopus*.

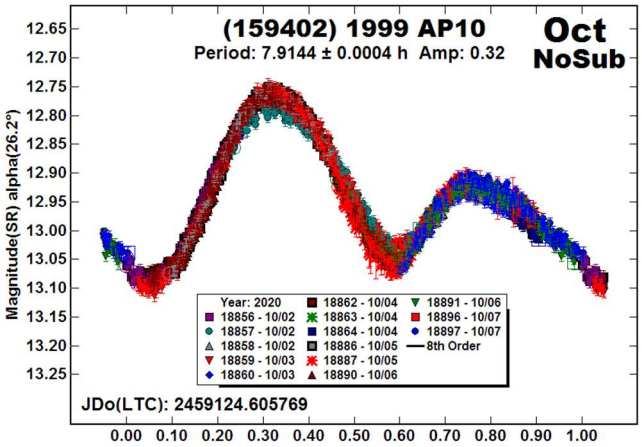

As might be expected with the large change in phase angle and viewing aspect, the amplitude of the lightcurve increased, by about 0.05 mag. The synodic period also changed, being slightly shorter. This would indicate that the asteroid's rotation is retrograde.

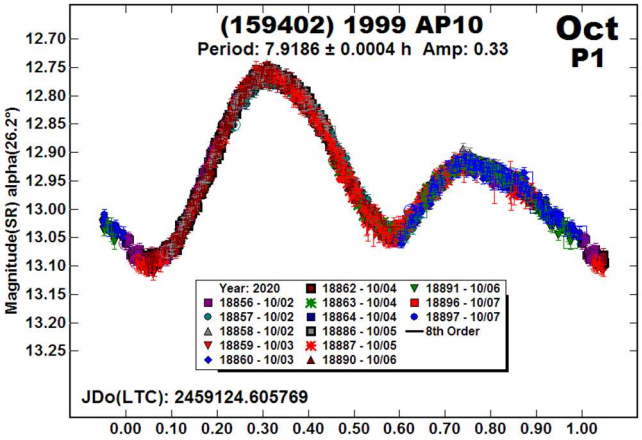

The dual-period search initially favored a secondary period of 20.9 h, which is far too large a change despite the changes in viewing aspect. We forced P_2 to a range of 28-30 h and made minute adjustments to the zero-points (≤ 0.10) mag to get the lowest RMS value. Eventually, we found P_2 = 29.30 ± 0.02. This is still substantially different from the July result, but this might be attributed to the significant change in the P_2 lightcurve, which decreased in amplitude and took on a shape that appeared to show mutual events. Comparing with radar observations will be interesting.

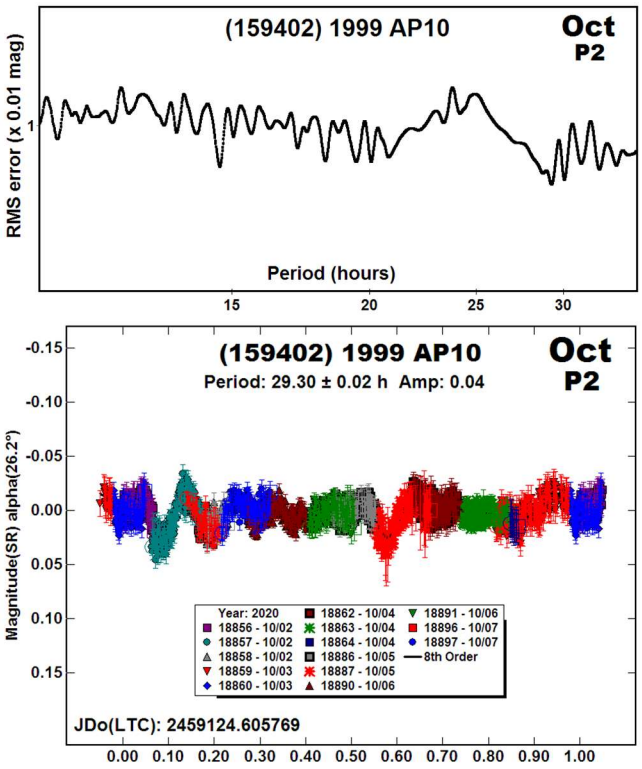

(420302) 2011 XZ1. When we worked this 940-m NEA in 2020 July, we found an ambiguous solution of either 13.427 h or 13.4118 h. There were no signs of a second period in the data set. The period spectrum actually favored the shorter period but, after observing the asteroid more than two months later and analyzing those data, we adopted the longer period for the July observations.

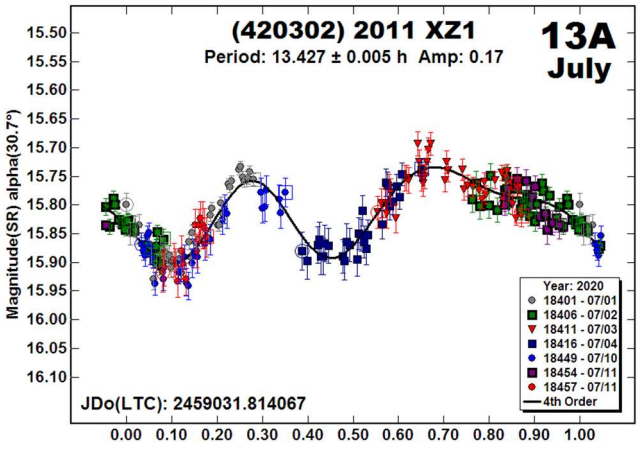

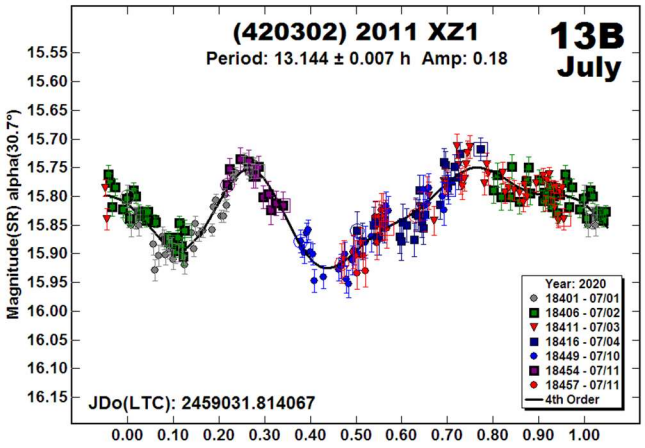

The period search based on the 2020 September/October data showed a strong solution at about 13.4 h. Despite the noisy data (obtained near full moon), a single period fit was off more than was liked. The dual-period feature of *MPO Canopus* was used once again to see what might be found. The result was P_2 = 32.42 h. The other possibilities in the period spectrum produced poor fits and/or strange lightcurve shapes.

The two periods have a 2.4:1 ratio, this is close to an integer ratio of 5:2, which raises concern that one of the two periods is just a harmonic artifact of the other found during Fourier analysis.

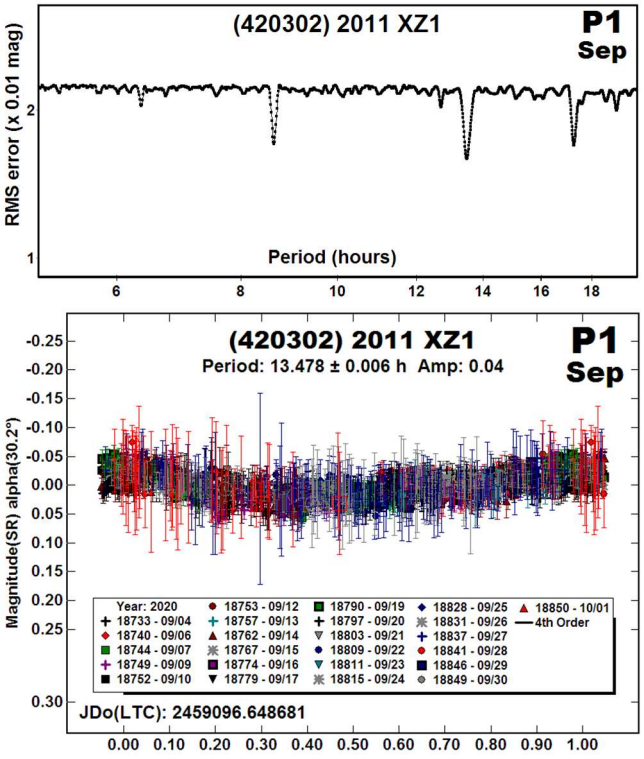

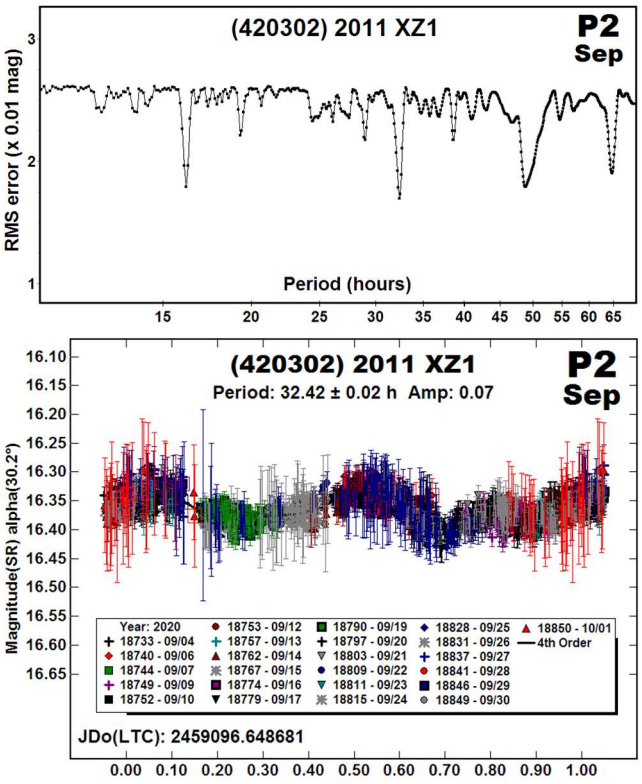

Follow up observations may be a long time coming. This was a very favorable apparition for the asteroid, which will stay at V > 18 mag until 2045 July when it reaches V ~ 14.8.

2019 AN5. There were no previous results of any kind in the LCDB for this 180-m NEA. Given the size, it was possible that this would be a super-fast rotator (P < 2 h). It proved to be quite the opposite.

A plot of the raw data seemed to indicate a long period and so we started with that premise to find a period. This led to a period of 51.16 h with lightcurve amplitude of about 0.44 mag.

Dual-period searches are almost always made with longer period asteroids to check of the possibility of the asteroid being a very wide binary. With the noisy data set, we didn't have much hope of finding a secondary period should the amplitude be small.

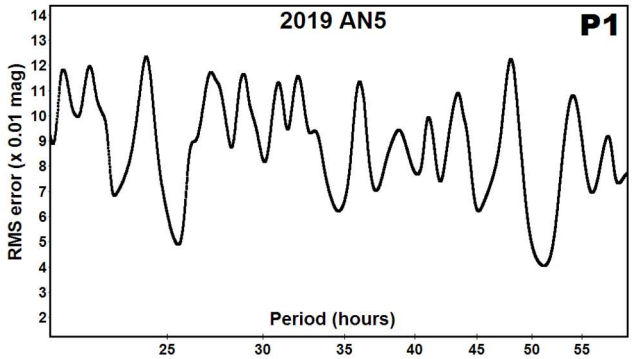

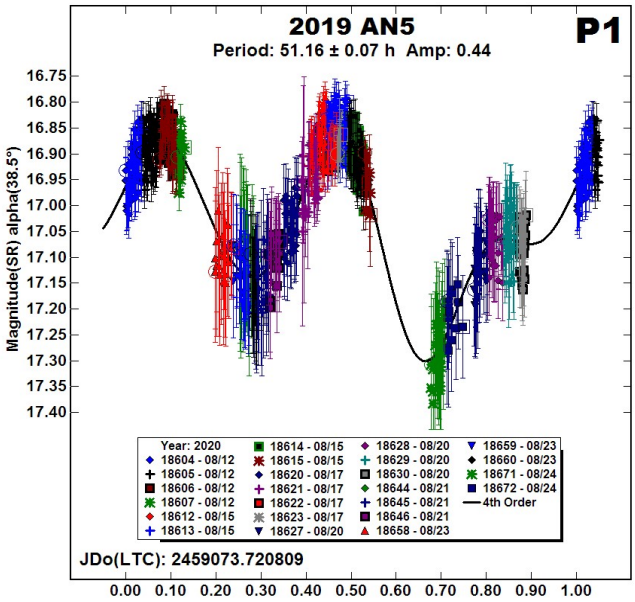

The period spectrum for a second period showed a likely solution near 13 h. After several iterations, we found P_2 = 13.25 h with A_2 = 0.12 mag. The noise nearly dominates the lightcurve, so while being optimistic, we acknowledge that the solution may not be valid.

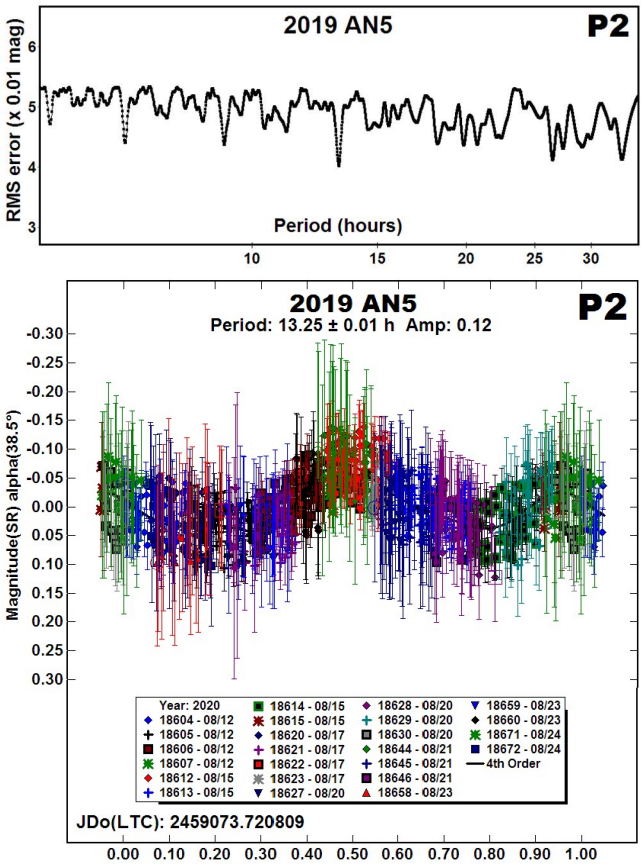

The two periods don't have a simple integral ratio, which raises the confidence in the results, if only a little. If the two periods are valid, it would make 2019 AN5 another very wide binary candidate.

Acknowledgements

Funding for observations at CS3 and work on the asteroid lightcurve database (Warner et al., 2009a) and ALCDEF database (*alcdef.org*) are supported by NASA grant 80NSSC18K0851. The authors gratefully acknowledge Shoemaker NEO Grants from the Planetary Society (2007, 2013). These were used to purchase some of the telescopes and CCD cameras used in this research. This work includes data from the Asteroid Terrestrial-impact Last Alert System (ATLAS) project. ATLAS is primarily funded to search for near earth asteroids through NASA grants NN12AR55G, 80NSSC18K0284, and 80NSSC18K1575; byproducts of the NEO search include images and catalogs from the survey area. The ATLAS science products have been made possible through the contributions of the University of Hawaii Institute for Astronomy, the Queen's University Belfast, the Space Telescope Science Institute, and the South African Astronomical Observatory.

References

References from web sites should be considered transitory, unless from an agency with a long lifetime expectancy. Sites run by private individuals, even if on an institutional web site, do not necessarily fall into this category.

Franco, L.; Carbognani, A.; Wiggins, P.; Koehn, B.W.; Schmidt, R. (2010). "Collaborative Lightcurve Photometry of Near-Earth Asteroid (159402) 1999 AP10." *Minor Planet Bull*. **37**, 83-85.

Harris, A.W.; Young, J.W.; Scaltriti, F.; Zappala, V. (1984). "Lightcurves and phase relations of the asteroids 82 Alkmene and 444 Gyptis." *Icarus* **57**, 251-258.

Harris, A.W.; Pravec, P.; Galad, A.; Skiff, B.A.; Warner, B.D.; Vilagi, J.; Gajdos, S.; Carbognani, A.; Hornoch, K.; Kusnirak, P.; Cooney, W.R.; Gross, J.; Terrell, D.; Higgins, D.; Bowell, E.; Koehn, B.W. (2014). "On the maximum amplitude of harmonics on an asteroid lightcurve." *Icarus* **235**, 55-59.

Hasegawa, S.; Kuroda, D.; Kitazato, K.; Kasuga, T.; Sekiguchi, T.; Takato, N.; Aoki, K.; Arai, A.; and 36 co-authors. (2018). "Physical properties of near-Earth asteroids with a low delta-v: Survey of target candidates for the Hayabusa2 mission." *Pub. Astron. Soc. Japan* **70**, A114.

Jacobson, S.A.; Scheeres, D.J.; McMahon, J. (2014). "Formation of the Wide Asynchronous Binary Asteroid Population." *Ap. J.* **780,** A60.

Merline, W.J.; Tamblyn, P.M.; Warner, B.D.; Pravec, P.; Tamblyn, J.P.; Neyman, C.; Conrad, A.R.; Owen, W.M.; Carry, B.; Drummond, J.D.; Chapman, C.R.; Enke, B.L.; Grundy, W.M.; Veillet, C.; Porter, S.B.; Arcidiacono, C.; Christou, J.C.; Durda, D.D.; Harris, A.W.; Weaver, H.A.; Dumas, C.; Terrell, D.; Maley, P. (2013). "S/2012 (2577) 1." *IAUC* **9267**.

Pál, A.; Szakáts, R.; Kiss, C.; Bódi, A.; Bognár, Z.; Kalup, C.; Kiss, L.L.; Marton, G.; Molnár, L.; Plachy, E.; Sárneczky, K.; Szabó, G.M.; Szabó, R. (2020). "Solar System Objects Observed with TESS - First Data Release: Bright Main-belt and Trojan Asteroids from the Southern Survey." *Ap. J. Supl. Ser.* **247**, id.26.

Pravec, P.; Wolf, M.; Sarounova, L. (2007web). *http://www.asu.cas.cz/~ppravec/neo.htm*

Pravec, P.; Scheirich, P.; Durech, J.; Pollock, J.; Kusnirak, P.; Hornoch, K.; Galad, A.; Vokrouhlicky, D.; Harris, A.W.; Jehin, E.; Manfroid, J.; Opitom, C.; Gillon, M.; Colas, F.; Oey, J.; Vrastil, J.; Reichart, D.; Ivarsen, K.; Haislip, J.; LaCluyze, A. (2014). "The tumbling state of (99942) Apophis." *Icarus* **233**, 48-60.

Rubincam, D.P. (2000). "Radiative Spin-up and Spin-down of Small Asteroids." *Icarus* **148**, 2-11.

Tonry, J.L.; Denneau, L.; Flewelling, H.; Heinze, A.N.; Onken, C.A.; Smartt, S.J.; Stalder, B.; Weiland, H.J.; Wolf, C. (2018). "The ATLAS All-Sky Stellar Reference Catalog." *Ap. J.* **867**, A105.

Warner, B.D. (2011). "A Quartet of Known and Suspected Hungaria Binary Asteroids." *Minor Planet Bull*. **38**, 33-36.

Warner, B.D. (2016). "Three Additional Candidates for the Group of Very Wide Binaries." *Minor Planet Bul.* **43**, 306-309.

Warner, B.D.; Stephens, R.D. (2017). "Lightcurve Analysis of Hilda Asteroids at the Center for Solar System Studies: 2017 April thru July." *Minor Planet Bull.* **44**, 331-334.

Warner, B.D.; Stephens, R.D. (2018). "Lightcurve Analysis of Hilda Asteroids at the Center for Solar System Studies: 2018 April-June." *Minor Planet Bull.* **45**, 390-393.

Warner, B.D.; Harris, A.W.; Pravec, P. (2009a). "The Asteroid Lightcurve Database." *Icarus* **202**, 134-146. Updated 2020 Aug. *http://www.minorplanet.info/lightcurvedatabase.html*

Warner, B.D.; Pravec, P.; Harris, A.W.; Higgins, D.; Bembrick, C.; Brinsfield, J. (2009b). "(2577) Litva." *CBET* **1715**.

Number	Name	2020 mm/dd	Phase	L_{PAB}	B_{PAB}	Period(h)	P.E.	Amp	A.E.	Grp/Dr
2577	Litva	07/04-07/07	23.3,23.8	248	29	2.812	0.002	0.17	0.03	H
						[F]35.88	0.01	0.05	0.02	
4030	Archenhold	08/28-09/26	*8.6,6.3	351	1	3.27292	0.00004	0.18	0.01	V
						15.974	0.003	0.16	0.01	0.31
5928	Pindarus	07/30-09/17	*8.2,6.2	326	2	415.5	0.4	0.39	0.03	HIL
5928	Pindarus	18/04/09-04/14	*2.2,2.2	202	7	[F]415	5	0.38	0.06	HIL
						5.980	0.009	0.08	0.01	
7174	Semois	08/30-10/06	*5.4,6.0	354	0	7.490	0.001	0.08	0.01	HIL
						34.57	0.02	0.18	0.02	
16970	1998 VV2	07/05-07/28	10.8,5.4	319	10	8.0566	0.0005	0.26	0.03	HIL
						43.92	0.02	0.14	0.02	0.31
39282	2001 BM36	07/05-08/17	14.0,3.4	332	6	620	3	0.25	0.02	HIL
						2.8286	0.0002	0.09	0.01	
85275	1994 LY	07/01-08/06	35.6,46.2	283	26	2.69600	0.00003	0.10	0.01	NEA
						16.6238	0.0008	0.09	0.01	0.26
119356	2001 SF235	09/19-09/22	1.5,3.2	354	0	48	1	0.25	0.03	MB-I
						2.869	0.004	0.12	0.2	
159402	1999 AP10	08/24-09/17	*11.3,12.4	341	-5	7.9219	0.0003	0.27	0.02	NEA
						28.461	0.006	0.06	0.01	
159402	1999 AP10	10/02-10/07	26.3,32.9	356	9	7.9186	0.0004	0.33	0.02	NEA
						29.30	0.01	0.04	0.01	
420302	2011 XZ1	07/10-07/11	33.7,34.1	310	9	[A]13.427	0.005	0.17	0.02	NEA
						13.144	0.007	0.18	0.02	
420302	2011 XZ1	09/03-10/01	30.6,18.5	160	18	13.478	0.006	0.04	0.01	NEA
						32.42	0.02	0.07	0.01	
	2019 AN5	08/12-08/24	38.8,85.5	152	17	51.16	0.07	0.44	0.04	NEA
						13.25	0.01	0.12	0.03	

Table II. Observing circumstances. [F]Period forced to stated value. [A]Ambiguous period. The first line gives the primary (adopted) period for the system. The second line gives the secondary period. If the Grp/Dr column has a value on the second line, the object is considered a confirmed binary and the value is the estimated effective diameter ratio of the secondary to primary (Ds/Dp).

The phase angle (α) is given at the start and end of each date range. If there is an asterisk before the first phase value, the phase angle reached a maximum or minimum during the period. L_{PAB} and B_{PAB} are, respectively the average phase angle bisector longitude and latitude (see Harris et al.,1984). For the Grp/Dr column, the first line gives the group/family based on Warner et al. (2009a). H: Hungaria, HIL: Hilda, V: Vestoid, MB-I, inner main-belt, NEA: Near-Earth asteroid.

ASTEROID PHOTOMETRY AND LIGHTCURVE ANALYSIS AT GORA OBSERVATORIES

Milagros Colazo
Instituto de Astronomía Teórica y Experimental (IATE-CONICET), ARGENTINA
Facultad de Matemática, Astronomía y Física, Universidad Nacional de Córdoba, ARGENTINA
Grupo de Observadores de Rotaciones de Asteroides (GORA), ARGENTINA
https://aoacm.com.ar/gora/index.php
milirita.colazovinovo@gmail.com

Ariel Stechina, César Fornari, Marcos Santucho, Aldo Mottino, Eduardo Pulver, Raúl Melia, Néstor Suárez, Damián Scotta, Andrés Chapman, Julian Oey, Erick Meza, Ezequiel Bellocchio, Mario Morales, Tiago Speranza, Fabricio Romero, Matías Suligoy, Patricio Tourne Passarino, Mateo Borello, Rafael Farfán, Fernando Limón, Jesús Delgado, Ramón Naves, Carlos Colazo.
Grupo de Observadores de Rotaciones de Asteroides (GORA) ARGENTINA

Grupo de Observación de Asteroides (GOAS), ESPAÑA

Comisión Nacional de Investigación y Desarrollo Aeroespacial del Perú (CONIDA), PERÚ

Grupo de Astrometría y Fotometría (GAF), ARGENTINA

Estación Astrofísica Bosque Alegre (MPC 821)
Bosque Alegre (Córdoba- ARGENTINA)

Observatorio Astronómico El Gato Gris (MPC I19)
Tanti (Córdoba-Argentina)

Observatorio Cruz del Sur (MPC I39)
San Justo (Buenos Aires- ARGENTINA)

Observatorio Orbis Tertius (MPC X14)
Córdoba (Córdoba- ARGENTINA)

Observatorio de Sencelles (MPC K14)
Sencelles (Mallorca-Islas Baleares-ESPAÑA)

Observatorio Galileo Galilei (MPC X31)
Oro Verde (Entre Ríos- ARGENTINA)

Observatorio Antares (MPC X39)
Pilar (Buenos Aires- ARGENTINA)

Observatorio AstroPilar (GORA APB)
Pilar (Buenos Aires- ARGENTINA)

Observatorio de Aldo Mottino (GORA OAM)
Rosario (Santa Fe- ARGENTINA)

Observatorio Astro Pulver (GORA OAP)
Rosario (Santa Fe- ARGENTINA)

Observatorio de Ariel Stechina 1 (GORA OAS)
Reconquista (Santa Fe- ARGENTINA)

Observatorio de Ariel Stechina 2 (GORA OA2)
Reconquista (Santa Fe- ARGENTINA)

Observatorio de Damián Scotta (GORA ODS)
San Carlos Centro (Santa Fe-ARGENTINA)

Observatorio Astronómico de Moquegua 1 (GORA OMP)
(MPC W73), Cambrune (Moquegua- PERÚ)

Observatorio Municipal de Reconquista (GORA OMR)
Reconquista (Santa Fe- ARGENTINA)

Observatorio de Raúl Melia (GORA RMG)
Gálvez (Santa Fe-ARGENTINA)

Observatorio Uraniborg (MPC Z55)
Écija (Sevilla- ESPAÑA)

Observatorio Mazariegos (MPC Z50)
Mazariegos (Palencia- ESPAÑA)

Observatorio Nuevos Horizontes (MPC Z73)
Camas (Sevilla- ESPAÑA)

Observatorio Montcabrer (MPC 213)
Cabrils (Barcelona- ESPAÑA)

Blue Mountains Observatory (MPC Q68)
Leura NSW (Blue Mountains-AUSTRALIA)

(Received: 2020 October 4)

Synodic rotation periods and amplitudes are reported for 57 Mnemosyne, 188 Menippe, 191 Kolga, 236 Honoria, 261 Prymno, 270 Anahita, 469 Argentina, 530 Turandot, 584 Semiramis, 921 Jovita, 936 Kunigunde, 994 Otthild, 1157 Arabia, 1180 Rita, 1269 Rollandia, 1594 Danjon, 3519 Ambiorix, and (52768) 1998 OR2.

In this work, we present periods and amplitudes of lightcurves for 57 Mnemosyne, 188 Menippe, 191 Kolga, 236 Honoria, 261 Prymno, 270 Anahita, 469 Argentina, 530 Turandot, 584 Semiramis, 921 Jovita, 936 Kunigunde, 994 Otthild, 1157 Arabia, 1180 Rita, 1269 Rollandia, 1594 Danjon, 3519 Ambiorix, and (52768) 1998 OR2.

These results are the product of a collaborative work by GORA (Grupo de Observadores de Rotaciones de Asteroides) group. In previous publications (Colazo et. al 2020a; Colazo et al. 2020b) we limited ourselves to the use of differential photometry for the analysis of our observations. However, on this occasion, we applied relative photometry assigning V magnitudes to the calibration stars, especially when observing more challenging asteroids.

Image acquisition was performed without filters and with exposure times of a few minutes. All images were corrected using dark frames and, in some cases, bias and flat-field frames were also used. Photometry measurements were performed using *FotoDif* software and for the analysis we employed *Periodos* software (Mazzone, 2012).

Below, we present the results for each asteroid. The lightcurve figures contain the estimated period and period error and the estimated amplitude and amplitude error. In the reference boxes, the columns represent, respectively, the marker, observatory MPC code or - failing that - the GORA internal code, session date, session off-set, and number of data points.

Targets were selected based on 1) those asteroids with magnitudes accessible to the equipment of all participants, 2) those with favorable observation conditions from Argentina i.e. with negative declinations, and 3) objects with few periods reported in the literature and/or with a quality code U < 3 in the Asteroid Lightcurve Database (LCDB; Warner et al., 2009).

57 Mnemosyne. We found two reports of periods in the literature for this asteroid: P = 12.463 ± 0.007 h with an amplitude of 0.12 mag (Harris et al., 1992) and P = 12.66 ± 0.03 h with A = 0.14 ± 0.01 mag (Ditteon and Hawkins, 2007). In this paper we propose a new period corresponding to P = 26.12 ± 0.01 h and lightcurve amplitude of A = 0.24±0.01 mag.

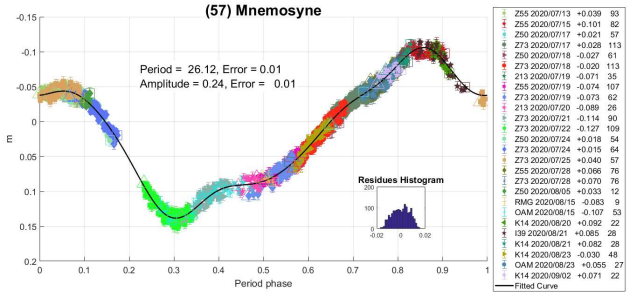

188 Mennipe. This main-belt asteroid was discovered in 1878 by Christian Heinrich Friedrich (C.H.F.) Peters, is of taxonomic type S, and has an estimated diameter of 35.75 km. The last reported periods are 11.98 ± 0.02 h (Warner and Higgins, 2010) and 11.9765 ± 0.0005 h, A = 0.28 ± 0.02 mag (Hanuš et al., 2011). This object was one of those we analyzed using relative photometry. At the beginning, we got two candidate periods, ~12 and ~24 hours. Although the RMS value is lower for the ~24-hour period, we consider that the adjustment with the lower period is closer to the shape of the lightcurve that we expect given the current 3D model of this asteroid. The results of this analysis are a period of P = 11.98 ± 0.07 h and amplitude A = 0.15±0.01 mag.

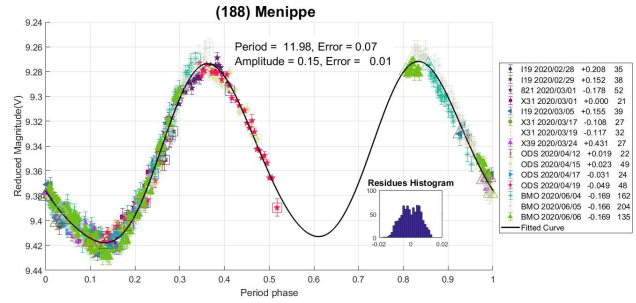

191 Kolga. We found two references to possible periods for this object: P = 13.7 ± 0.7 h, A = 0.21 ± 0.01 mag (Behrend, 2009) and P = 17.604 ± 0.001 h, A = 0.30 ± 0.02 mag (Pilcher, 2013). In our case, the analysis of the observations suggests agreement with the period published by Pilcher since the results are P = 17.59 ± 0.01 h and A = 0.50 ± 0.01 mag.

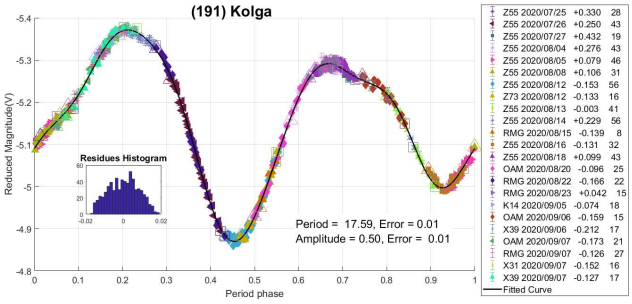

236 Honoria. This is an S-type asteroid with an estimated diameter of 77 km. There are two published periods from Behrend (2006, P = 16.8 ± 0.1 h; 2007, P = 17 h). On the other hand, Marciniak et al. (2014) found P =12.338 ± 0.002 h and (Pilcher, 2014a) reported P = 12.336 ± 0.001 h. The analysis of the GORA team data gives P = 12.34 ± 0.01 h and A = 0.10 ± 0.01 mag, making our period in agreement with those form Marciniak et al. and Pilcher.

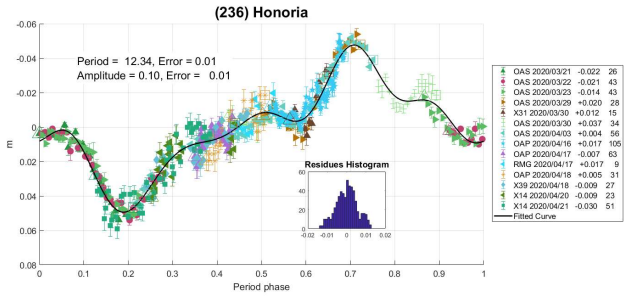

261 Prymno. This asteroid belongs to the main belt, is classified as type B within the Tholen (1984) taxonomy, and has an estimated diameter of 50 km. The last two reported periods from the literature are P = 3.9990 ± 0.0002 h with A = 0.14±0.01 mag (Behrend, 2009) and P = 8.007 ± 0.002 h with A = 0.13 ± 0.01 mag (Warner, 2009). Our data yielded P = 8.00 ± 0.01 h and A = 0.37 ± 0.02 mag, which is in accordance with that published by Warner. The difference in amplitude may be due to a change in the aspect angle.

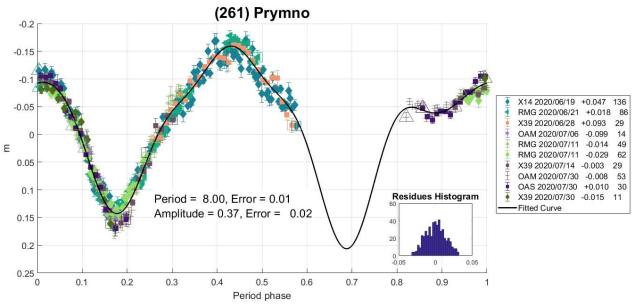

270 Anahita. This is an S-type asteroid discovered in 1887 by C.H.F Peters. The last reported periods (both sidereal) are P = 15.05906 ± 0.00005 h (Hanuš et al., 2016) and P = 15.05950 ± 0.00001 h (Ďurech et al., 2016). The analysis of our data results in a period of P = 15.07 ± 0.01 h and A = 0.32 ± 0.01 mag.

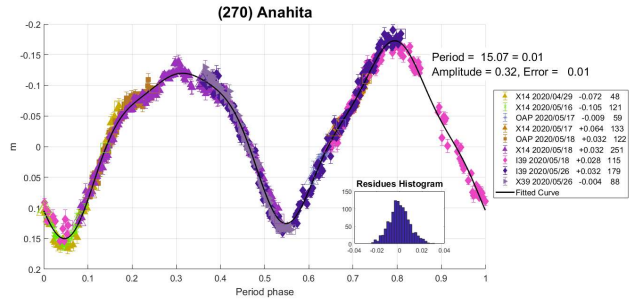

469 Argentina. This type X asteroid has three different periods published in the literature: P = 12.3 h, A = 0.12 mag (Székely et al., 2005); P = 13.122 h, A = 0.1 mag Wang et al. (2005); and P = 17.573 ± 0.003 h, A = 0.12 mag (Warner, 2007). The fitting of our lightcurves gives P = 8.79 ± 0.01 h and A = 0.11 ± 0.01 mag. In this way, we propose a new candidate period to those already published by other authors.

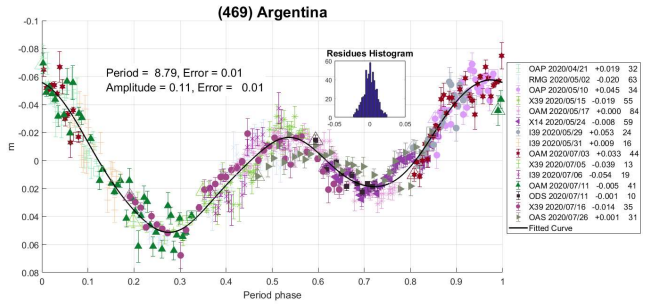

530 Turandot. The last reported period that we have found in the literature for this F-type asteroid corresponds to 19.960 ± 0.001 h with A = 0.13±0.01 mag (Pilcher, 2014b). Our period is in fairly good agreement with Pilcher and presents a small variation in the amplitude of the lightcurve, probably due to a change in the aspect angle. Our result is P = 19.94 ± 0.01 h and A = 0.17 ± 0.01 mag.

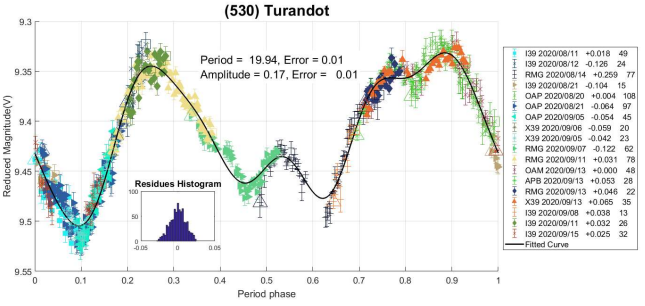

584 Semiramis. Most of the reported periods for this S-type asteroid point to 5.06 hours, for example, the last one is P = 5.0689 ± 0.0001 h with an amplitude of 0.24 ± 0.02 mag (Connour et al., 2015). Our observational data are also consistent with this value, yielding P = 5.07 ± 0.03 h and A = 0.24 ± 0.05 mag.

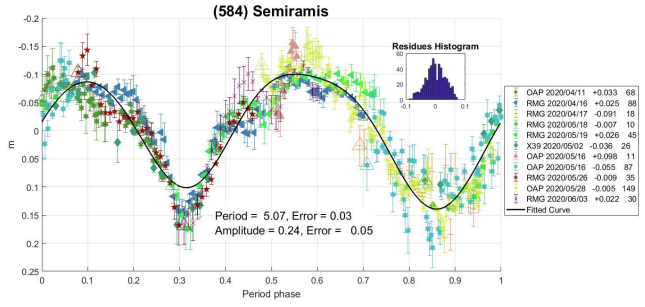

921 Jovita. This asteroid was discovered on 1919 September 4 by K. Reinmuth in Heidelberg. It has an estimated diameter of 58 km. We found two different periods in the literature: P = 23.00 ± 0.07 h with A = 0.07 ± 0.01 mag (Behrend, 2004) and P = 15.64 ± 0.02 h with A = 0.12 ± 0.02 mag (Warner, 2005). Our observations and the corresponding analysis agree with those published by Warner: P = 15.57 ± 0.01 h and A = 0.13 ± 0.01 mag.

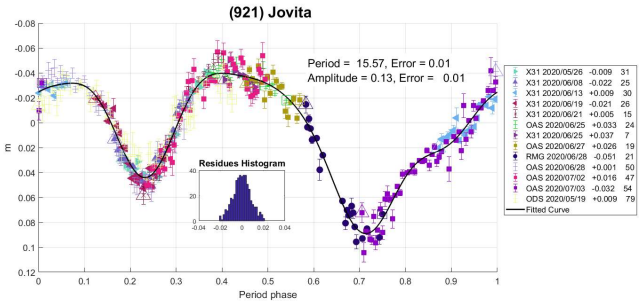

936 Kunigunde. The last two periods reported in the literature are P = 8.80 h with A = 0.25 mag (Angeli et al., 2001) and P = 8.82653 ± 0.00005 h (Hanuš et al., 2013). We obtained a result that agrees with the previous measurements: P = 8.83 ± 0.01 h, A = 0.29 ± 0.01 mag.

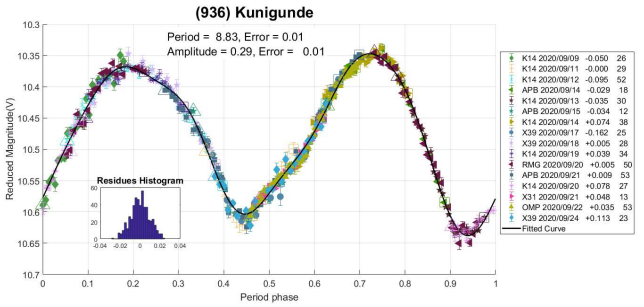

994 Othild. The last reported periods of this asteroid are 5.944 ± 0.002 h with an amplitude of 0.09 ± 0.01 mag (Behrend, 2001) and 5.9473 ± 0.0001 h with A = 0.15±0.01 mag (Behrend, 2005). The results obtained by our group are P = 5.95 ± 0.01 h with A = 0.11 ± 0.01 mag. These results are consistent with those previously published, the small difference in the amplitude of the lightcurve may be due to a change in the aspect angle.

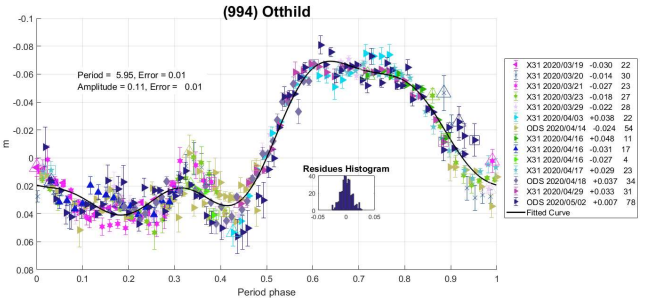

1157 Arabia. We found only one reported period in the literature, that is P = 15.225 ± 0.005 h with A = 0.37 ± 0.03 mag (Caspari, 2008). The analysis of our observations suggests a shorter period of P = 11.55 ± 0.01 h with A = 0.41 ± 0.03 mag.

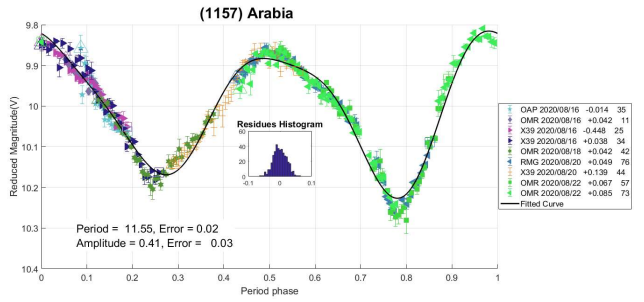

Observatory	Telescope	Camera	
Estación Astrofísica Bosque Alegre	Newtonian (1540 mm; f/4.9)	CCD	APOGEE Alta U9
Observatorio El Gato Gris	SCT (355 mm; f/10.6)	CCD	SBIG STF-8300M
Observatorio Cruz del Sur	Newtonian (200 mm; f/4.0)	CMOS	QHY-174
Observatorio Orbis Tertius	Newtonian (200 mm; f/5.0)	CCD	QHY6 Mono
Observatorio de Sencelles	SCT (254 mm; f/4.3)	CCD	SBIG ST-7XME
Observatorio Galileo Galilei	RCT ap (405 mm; f/8.0)	CCD	SBIG STF-8300M
Observatorio Antares	Newtonian (250 mm; f/5.0)	CCD	QHY9 Mono
Observatorio AstroPilar	ODK (250 mm; f/6.8)	CCD	FLI-8300M
Observatorio de Aldo Mottino	Newtonian (250 mm; f/4.7)	CCD	SBIG STF-8300M
Observatorio Astro Pulver	SCT (203 mm; f/10.3)	CMOS	QHY5 LII M
Observatorio de Ariel Stechina 1	Newtonian (254 mm; f/4.7)	CCD	SBIG STF-402
Observatorio de Ariel Stechina 2	Newtonian (305 mm; f/5.0)	CMOS	QHY 174M
Observatorio de Damián Scotta	Newtonian (300 mm; f/4.0)	CCD	SBIG ST-402 XME
Observatorio Astronómico de Moquegua	RCT APM (1000 mm; f/8)	CCD	FLI ProLine 16803
Observatorio Municipal Reconquista	Newtonian (254 mm; f/4)	CMOS	QHY 174M
Observatorio de Raúl Melia	SCT (200 mm; f/10.0)	CCD	Meade DSI Pro II
Observatorio Uraniborg	SCT (280 mm; f/6.3)	CCD	ATIK 414ex
Observatorio Mazariegos	SCT (200 mm; f/7.6)	CCD	ATIK 314L
Observatorio Nuevos Horizontes	SCT (235 mm; f/6.3)	CCD	Atik 3.14 L Plus
Observatorio Montcabrer	SCT (300 mm; f/9.2)	CCD	Moravian G4-9000
Blue Mountains Observatory	SCT Edge (355 m; f/7.0)	CCD	SBIG STF-8300M

Table I. List of observatories and equipment.

Number	Name	20yy/mm/dd	Phase	L_{PAB}	B_{PAB}	Period(h)	P.E.	Amp.	A.E.	Grp
57	Mnemosyne	07/13-09/02	11.7,17.2	258	16	26.12	0.01	0.24	0.01	MB-O
188	Menippe	02/28-06/06	*17.0,17.9	209	-8	11.98	0.07	0.15	0.01	MB-O
191	Kolga	07/25-09/08	13.7,19.9	270	11	17.59	0.01	0.50	0.01	MB-O
236	Honoria	03/21-04/21	*9.8,1.6	209	3	12.34	0.01	0.10	0.01	MB-O
261	Prymno	06/19-07/30	18.9,25.6	235	2	8.00	0.01	0.37	0.02	FLOR
270	Anahita	04/29-05/26	*9.4,6.0	236	-1	15.07	0.01	0.32	0.01	FLOR
469	Argentina	04/21-07/26	*8.7,20.4	227	-14	8.79	0.01	0.11	0.01	MB-O
530	Turandot	08/11-09/15	6.5,18.5	307	-1	19.94	0.01	0.17	0.01	MB-O
584	Semiramis	04/11-06/03	11.3,20.1	177	-12	5.07	0.03	0.24	0.05	MB-I
921	Jovita	05/19-07/03	6.2,19.7	229	11	15.57	0.01	0.13	0.01	MB-O
936	Kunigunde	09/09-09/24	*4.1,2.7	389	-3	8.83	0.01	0.29	0.01	THM
994	Otthild	03/19-05/02	*15.8,5.8	219	-11	5.95	0.01	0.11	0.01	MB-I
1157	Arabia	08/15-08/23	1.9,4.8	320	-3	11.55	0.02	0.41	0.03	MB-O
1180	Rita	07/29-09/20	2.1,14.7	304	-6	29.78	0.01	0.09	0.01	HIL
1269	Rollandia	04/03-06/14	*2.1,15.1	199	3	39.81	0.01	0.08	0.01	HIL
1594	Danjon	05/03-07/26	*10.9,30.3	242	0	116.02	0.01	0.72	0.01	MB-I
3519	Ambiorix	07/11-09/21	*9.0,27.9	305	-1	5.78	0.03	0.29	0.05	MB-I
52768	1998 OR2	05/08-05/17	36.9,33.3	236	-20	4.01	0.02	0.19	0.03	NEA

Table II. Observing circumstances and results. The phase angle is given for the first and last date. If preceded by an asterisk, the phase angle reached an extremum during the period. L_{PAB} and B_{PAB} are the approximate phase angle bisector longitude/latitude at mid-date range (see Harris et al., 1984). Grp is the asteroid family/group (Warner et al., 2009). FLOR: Flora; HIL: Hilda; MB-I/O: main-belt inner/outer; NEA: Near-Earth Asteroid; THM: Themis

1180 Rita. This P-type asteroid is a very interesting case since it has several reported periods that differ from each other: P = 9.605 ± 0.006 h, A = 0.15 ± 0.03 mag (Polishook, 2012); P = 14.902 h with A = 0.29 mag (Dahlgren et al., 1998); and P = 20.496 ± 0.005 h with A = 0.05 mag (Slyusarev et al., 2012). Our observations suggest that the period of this object is even longer: P = 29.78 ± 0.01 h with an amplitude of 0.09 ± 0.01 mag.

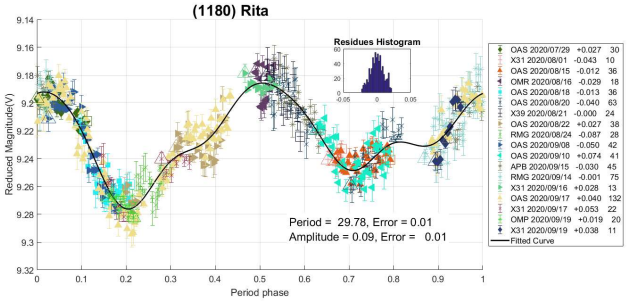

1269 Rollandia. This is a D-type asteroid with an estimated diameter of 104 km. As in the case of 188 Menippe, the analysis of the observations was made with relative photometry. Some of the previously reported periods are P = 30.98 ± 0.93 h, A = 0.02 mag (Slyusarev et al., 2012) and P = 15.32 ± 0.03 h with A = 0.13 ± 0.02 mag (Fauvaud and Fauvaud, 2013). In our case, we obtained a period similar to that found by Slyusarev: P = 39.81 ± 0.01 h with A = 0.08 ± 0.01 mag.

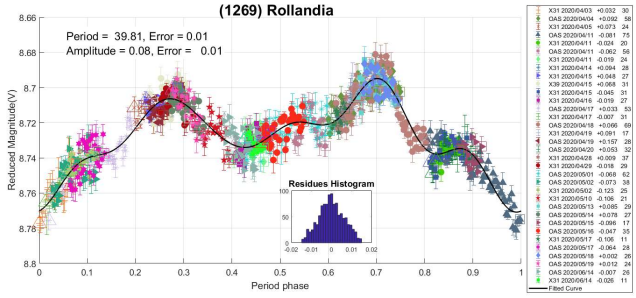

1594 Danjon. This is another object analyzed by relative photometry. Behrend (2006) reported a 12 h period for this asteroid, with an amplitude of 0.03 mag. In our case, we propose a much longer period: P = 116.02 ± 0.01 h with A = 0.72 ± 0.01 mag.

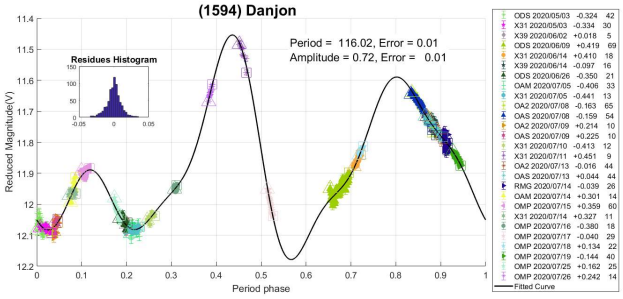

3519 Ambiorix. We found no previous reports for this object. After analyzing our observations, we propose a rotation period of P = 5.78 ± 0.03 h with an amplitude of A = 0.29 ± 0.05 mag.

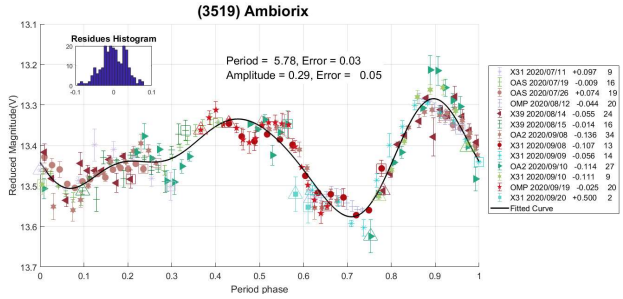

(52768) 1998 OR2. We found two different periods reported in the literature: P = 3.198 ± 0.006 h with A = 0.29 ± 0.02 mag (Betzler and Novaes, 2009) and P = 4.112 ± 0.002 h with A = 0.16 ± 0.02 mag (Koehn et al., 2014). Our results suggest a period of 4.01 ± 0.02 h with amplitude A = 0.19 ± 0.03 mag.

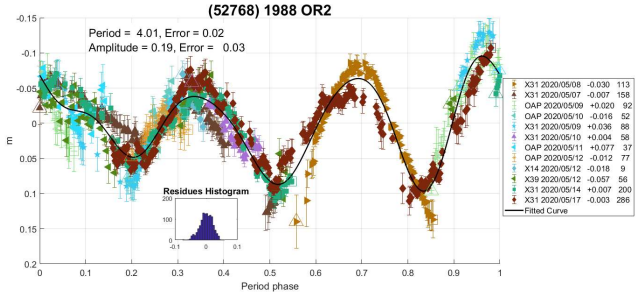

Acknowledgements

We want to thank Julio Castellano as we use his *FotoDif* program for preliminary analyses, and to Fernando Mazzone for his *Periods* program, used in final analyses.

This research has made use of the Small Bodies Data Ferret (*http://sbn.psi.edu/ferret/*), supported by the NASA Planetary System.

This research has made use of data and/or services provided by the International Astronomical Union's Minor Planet Center.

References

Angeli, C.A.; Guimarães, T.A.; Lazzaro, D.; Duffard, R.; Fernández, S.; Florczak, M.; Mothé-Diniz, T.; Carvano, J.M.; Betzler, A.S. (2001). "Rotation Periods for Small Main-Belt Asteroids from CCD Photometry." *Astron. J.* **121**, 2245-2252.

Behrend, R. (2001; 2004; 2005; 2006; 2009). Observatoire de Geneve web site. *http://obswww.unige.ch/~behrend/page_cou.html*

Betzler, A.S.; Novaes, A.B. (2009). "Photometric Observations of 1998 OR2, 1999 AQ10, and 2008 TC3." *Minor Planet Bull.* **36**, 145-147.

Caspari, P. (2008). "Minor Planet Lightcurve Analysis of 1157 Arabia and 1836 Komarov." *Minor Planet Bull.* **35**, 185-186.

Colazo, M.; Fornari, C.; Santucho, M.; Mottino, A.; Colazo, C.; Melia, R.; Vasconi, N.; Arias, D.; Pittari, C.; Suarez, N.; Pulver, E.; Ferrero, G.; Chapman, A.; Girardini, C.; Rodríguez, E.; Amilibia, G.; Anzola, M.; Tornatore, M.; Nolte, R.; Morero, S.; Oey, J. (2020a). "Asteroid Photometry and Lightcurve Analysis at Gora's Observatories."*Minor Planet Bull.* **47**, 188-191.

Colazo, L.M.; Fornari, C.; Santucho, M.; Mottino, A.; Colazo, C.; Melia, R.; Suarez, N.; Vasconi, N.; Arias, D.; Stechina, A.; Scotta, D.; García, J.; Pittari, C.; Ferrero, G. (2020b). "Asteroid Photometry and Lightcurve Analysis at GORA's Observatories - Part II." *Minor Planet Bull*. **47**, 337-339.

Connour, K.; Wright, T.; French, L.M. (2015). "Rotation Period of 584 Semiramis." *Minor Planet Bull.* **42**, 4.

Dahlgren, M.; Lahulla, J.F.; Lagerkvist, C.-I.; Lagerros, J.; Mottola, S.; Erikson, A.; Gonano-Beurer, M.; Di Martino, M. (1998). "A Study of Hilda Asteroids. V. Lightcurves of 47 Hilda Asteroids." *Icarus* **133**, 247-285.

Ditteon, R.; Hawkins, S. (2007). "Asteroid Lightcurve Analysis at the Oakley Observatory – November 2006." *Minor Planet Bull.* **34,** 59–64.

Ďurech, J.; Hanuš, J.; Oszkiewsicz, D.; Vanco, R. (2016). "Asteroid models from the Lowell photometric database." *Astron. Astrophys*. **587**, A48.

Fauvaud, S.; Fauvaud, M. (2013). "Photometry of Minor Planets. I. Rotation Periods from Lightcurve Analysis for Seven Main-Belt Asteroids." *Minor Planet Bull.* **40**, 224-229.

Hanuš, J.; Durech, J.; Broz, M.; Warner, B.D.; Pilcher, F.; Stephens, R.; Oey, J.; Bernasconi, L.; Casulli, S.; Behrend, R.; Polishook, D.; Henych, T.; Lehký, M.; Yoshida, F.; Ito, T. (2011). "A study of asteroid pole-latitude distribution based on an extended set of shape models derived by the lightcurve inversion method." *Astron. Astrophys.* **530**, A134.

Hanuš, J.; Brož, M.; Ďurech, J.; Warner, B.D.; Brinsfield, J.; Durkee, R.; Higgins, D.; Koff, R.A.; Oey, J.; Pilcher, F.; Stephens, R.; Strabla, L.P.; Ulisse, Q.; Girelli, R. (2013). "An anisotropic distribution of spin vectors in asteroid families." *Astron. Astrophys.* **559**, A134.

Hanuš, J.; Ďurech, J.; Oszkiewicz, D.A.; Behrend, R.; Carry, B.; Delbo, M.; Adam, O.; Afonina, V.; Anquetin, R.; Antonini, P.; and 159 coauthors. (2016). "New and updated convex shape models of asteroids based on optical data from a large collaboration network." *Astron. Astrophys.* **586**, A108.

Harris, A.W.; Young, J.W.; Scaltriti, F.; Zappala, V. (1984). "Lightcurves and phase relations of the asteroids 82 Alkmene and 444 Gyptis." *Icarus* **57**, 251-258.

Harris, A.W.; Young, J.W.; Dockweiler, T.; Gibson, J.; Poutanen, M.; Bowell, E. (1992). "Asteroid lightcurve observations from 1981." *Icarus* **95**, 115-147.

Koehn, B.W.; Bowell, E.L.G.; Skiff, B.A.; Sanborn, J.J.; McLelland, K.P.; Pravec, P.; Warner, B.D. (2014). "Lowell Observatory Near-Earth Asteroid Photometric Survey (NEAPS) – 2009 January through 2009 June." *Minor Planet Bull*. **41,** 286-300.

Marciniak, A.; Pilcher, F.; Santana-Ros, T.; Oszkiewicz, D.; Kankiewicz, P. (2014). "Against the bias in physics of asteroids: Photometric survey of long-period and low-amplitude asteroids." *ACM* **2014**, Poster 57.

Mazzone, F.D. (2012). *Periodos* software, version 1.0. *http://www.astrosurf.com/salvador/Programas.html*

Pilcher, F. (2013). "Rotation Period Determination for 24 Themis, 159 Aemilia, 191 Kolga, 217 Eudora, 226 Weringia, 231 Vindobona, and 538 Friederike." *Minor Planet Bull*. **40**, 85-87.

Pilcher, F. (2014a). "Lightcurves and Derived Rotation Periods for 18 Melpomene, 234 Barbara, 236 Honoria, 520 Franziska, and 525 Adelaide." *Minor Planet Bull*. **41**, 155–156.

Pilcher, F. (2014b). "Rotation Period Determinations for 24 Themis, 65 Cybele, 108 Hecuba, 530 Turandot, and 749 Malzovia." *Minor Planet Bull*. **41**, 250–252.

Polishook, D. (2012). "Lightcurves for Shape Modeling: 852 Wladilena, 1089 Tama, and 1180 Rita." *Minor Planet Bull*. **39**, 242–244.

Slyusarev, I.G.; Shevchenko, V.G.; Belskaya, I.N.; Krugly, Yu.N.; Chiorny, V.G. (2012). "CCD Photometry of Hilda Asteroids." *ACM* **2012**, #6398.

Székely, P.; Kiss, L.L.; Szabó, Gy.M.; Sárneczky, K.; Csák, B.; Váradi, M.; Mészáros, Sz. (2005). "CCD photometry of 23 minor planets." *Planet. Space Sci.* **53**, 925-936.

Tholen, D.J. (1984). "Asteroid taxonomy from cluster analysis of Photometry." Doctoral Thesis. Univ. Arizona, Tucson.

Wang, X.-B.; Zhang, X.-L.; Sheng-Hong, G. (2005). "The Distinct Light Curve Shape of the Asteroid (469)." *Earth, Moon, and Planets* **97**, 233-243.

Warner, B.D. (2005). "Lightcurve Analysis for Asteroids 242, 893, 921, 1373, 1853, 2120, 2448, 3022, 6490, 6517, 7187, 7757, and 18108." *Minor Planet Bull.* **32**, 4-7.

Warner, B.D. (2007). "Asteroid Lightcurve Analysis at the Palmer Divide Observatory, September-December 2006." *Minor Planet Bull.* **34**, 32-37.

Warner, B.D. (2009). "Asteroid Lightcurve Analysis at the Palmer Divide Observatory: 2008 December – 2009 March." *Minor Planet Bull.* **36,** 109-116.

Warner, B.D.; Harris, A.W.; Pravec, P. (2009). "The Asteroid Lightcurve Database." *Icarus* **202**, 134-146. Updated 2020 Sep. *http://www.minorplanet.info/lightcurvedatabase.html*

Warner, B.D.; Higgins, D. (2010). "Lightcurve Analysis of 188 Menippe." *Minor Planet Bull.* **37***,* 143-144.

MAIN-BELT ASTEROIDS OBSERVED FROM CS3: 2020 JULY TO SEPTEMBER

Robert D. Stephens
Center for Solar System Studies (CS3) / MoreData!
11355 Mount Johnson Ct., Rancho Cucamonga, CA 91737 USA
rstephens@foxandstephens.com

Brian D. Warner
Center for Solar System Studies (CS3) / MoreData!
Eaton, CO

(Received: 2020 October 11)

CCD photometric observations of 25 main-belt asteroids were obtained at the Center for Solar System Studies (CS3) from 2020 July to September. In addition, updated periods were found for 1582 Martir, (14923) 1994 TU3, and (23482) 1991 LV.

The Center for Solar System Studies (CS3) has seven telescopes which are normally used in program asteroid family studies. The focus is on near-Earth asteroids, but when suitable targets are not available, Jovian Trojans and Hildas are observed. When a nearly full moon is too close to the family targets being studied, targets of opportunity amongst the main-belt families were selected.

Table I lists the telescopes and CCD cameras that were used to make the observations. Images were unbinned with no filter and had master flats and darks applied. The exposures depended upon various factors including magnitude of the target, sky motion, and Moon illumination.

Telescope	Camera
0.30-m f/6.3 Schmidt-Cass	FLI Microline 1001E
0.35-m f/9.1 Schmidt-Cass	FLI Microline 1001E
0.35-m f/9.1 Schmidt-Cass	FLI Microline 1001E
0.35-m f/9.1 Schmidt-Cass	FLI Microline 1001E
0.35-m f/11 Schmidt-Cass	FLI Microline 1001E
0.40-m f/10 Schmidt-Cass	FLI Proline 1001E
0.50-m F8.1 R-C	FLI Proline 1001E

Table I: List of CS3 telescope/CCD camera combinations.

Image processing, measurement, and period analysis were done using *MPO Canopus* (Bdw Publishing), which incorporates the Fourier analysis algorithm (FALC) developed by Harris (Harris et al., 1989). The Comp Star Selector feature in *MPO Canopus* was used to limit the comparison stars to near solar color. Night-to-night calibration was done using field stars from the ATLAS catalog (Tonry et al., 2018), which has Sloan *griz* magnitudes that were derived from the GAIA and Pan-STARR catalogs and are "native" magnitudes of the catalog.

We used the ATLAS r′ (SR) magnitudes. Zero-point adjustments are mostly ≤ 0.03 mag. The occasions where larger corrections were required may have been related in part to using unfiltered observations, poor centroiding of the reference stars, and not correcting for second-order extinction terms.

The magnitudes were normalized to the comparison stars used in the earliest session and to the phase angle given in parentheses using $G = 0.15$. In other words, the data were made to seem that they were all obtained at the same time using the same comparison stars. The X-axis rotational phase ranges from –0.05 to 1.05.

The amplitude indicated in the plots (e.g. Amp. 0.23) is the amplitude of the Fourier model curve and not necessarily the adopted amplitude of the lightcurve.

For brevity, only some of the previously reported rotational periods may be referenced. A complete list is available at the asteroid lightcurve database (LCDB; Warner et al., 2009).

572 Rebekka. This inner main-belt asteroid has been studied several times in the past. We (Warner, 2007) observed it in 2007 finding a period of 5.656 h. Behrend (2009web; 2020web) reports periods of 5.6497 h and 5.650 h. Lagerkvist et al. (1998) reported a period of 5.65 h. Hanuš et al. (2013) reported a spin axis model with (λ, β) = (1°, 54°) or (158°, 39°) and a sidereal period of 5.65009 h. Our results this year are in good agreement.

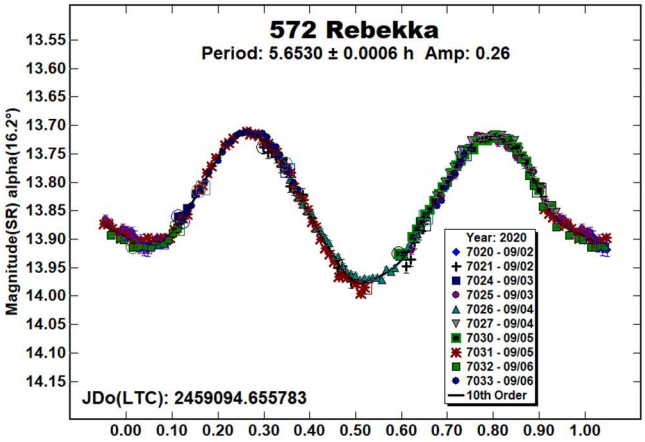

586 Thekla. This outer main-belt asteroid was a target of opportunity in the same field as 4030 Archenhold on four nights. Despite being such a low numbered asteroid, the LCDB has only three previous rotation periods: Behrend (2004web; 2007web) and Warner (2010b) each reported a period near 13.67 h, in good agreement with the results from this year.

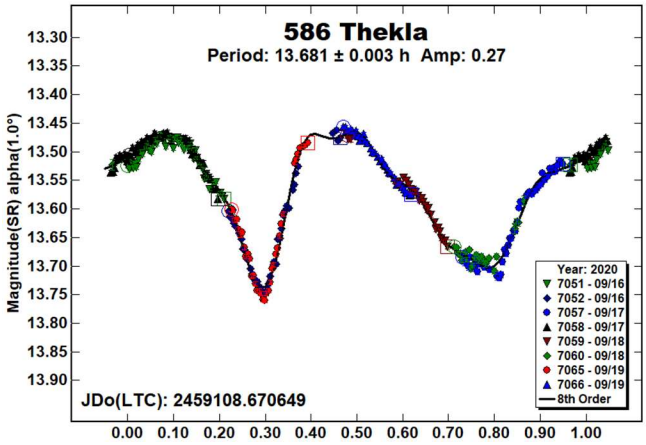

1582 Martir. We observed this outer main-belt object in 2010 May reporting a period of 9.84 h (Warner, 2010b). Recent observations from the Transiting Exoplanet Survey Satellite (TESS; McNeil et al., 2019; Pál et al., 2020) found periods near 12.37 h. Using our original data, we changed the comparison star magnitudes to SR (r′) values from the ATLAS catalog. With some minor zero-point adjustments, we could fit the data to either our original period (B) or the 12.37 h period (A) found in the TESS data. A half-period plot (C) favors the 12.37 h period, which we are adopting for this paper, but the 9.47-h solution cannot be formally excluded.

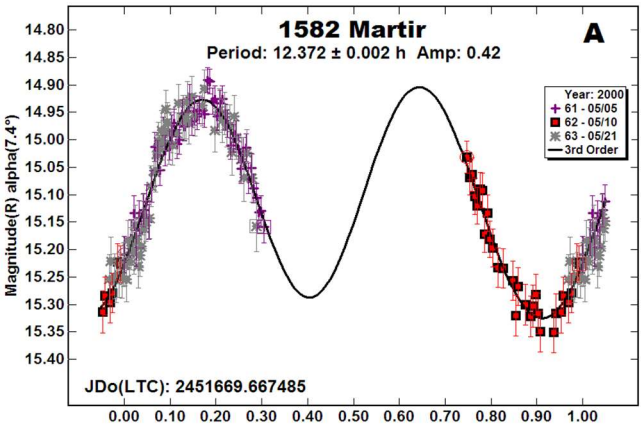

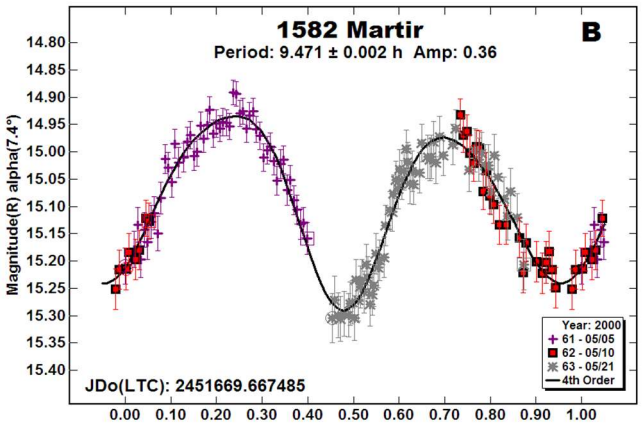

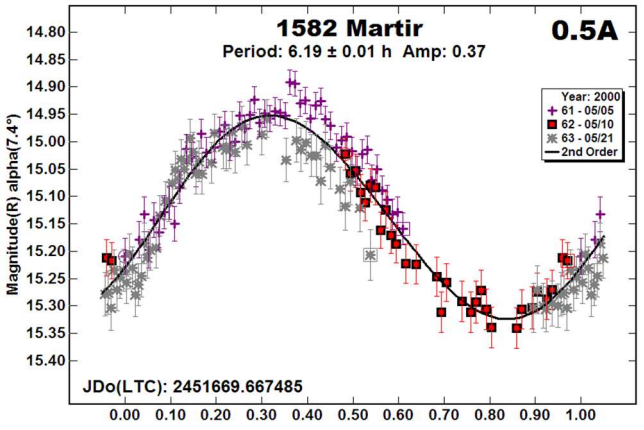

1626 Sadeya. This 16-km member of the Phocaea family/group has been observed many times in the past. Florczak et al. (1997), Behrend (2007web), Benishek (2015), and Warner (2010a; 2014a) each time finding rotational periods near 3.42 h, in good agreement with this year's result. In 2020 August, Sadeya was observed by the Photometric Survey for Asynchronous Binary Asteroids (Pravec et al. 2020web) which found it to be a binary asteroid with a P_1 = 3.42010 h and P_2 = 51.15 h.

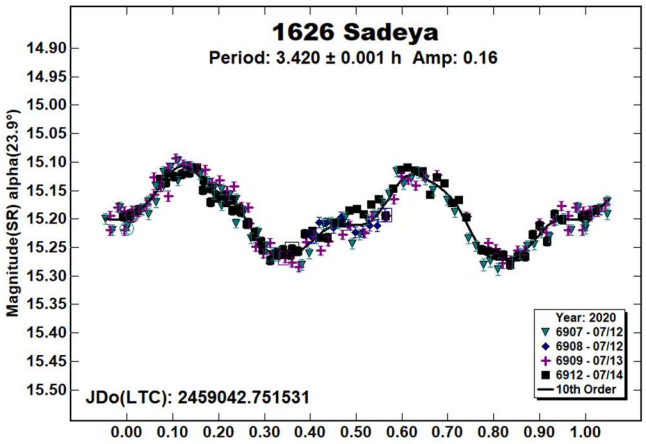

Because of the availability of dense data from Oey in the Asteroid Lightcurve Data Exchange Format database (ALCDEF, 2020), sparse data at the Asteroids - Dynamic web site (AstDyS-2, 2020), and our dense data from two apparitions, we attempted to solve for the sidereal period and pole position and create a shape model. This data was combined using *MPO LCInvert* (Bdw Publishing). This Windows-based program incorporates the algorithms developed by Kaasalainen and Torppa (2001) and Kaasalainen et al. (2001) and converted by Josef Ďurech from the original FORTRAN to C. A period search was made over a sufficiently wide range to assure finding a global minimum in χ^2 values.

The pole model showed a unique solution with J2000 ecliptic coordinates of (λ,β,P) = (152°, –9°, 3.421367 h). We note that the effects of the satellite were not removed from the data set when developing the shape/spin axis model. The full set of inversion graphics are given at the end of this paper.

2927 Alamosa. This inner main-belt object was observed by Odden et al. (2012) who found a rotational period of 4.38232 h. Our result this year is in good agreement.

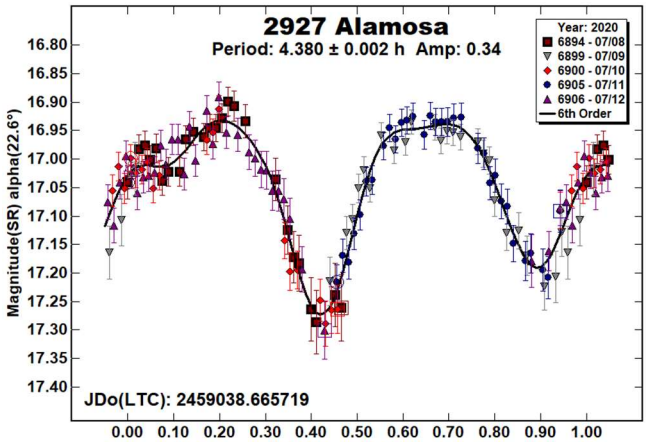

3022 Dobermann. We have worked this member of the Hungaria family/group many times in the past to develop a shape/pole model (Warner, 2005a; 2011; 2013a; 2014b; 2017) each time finding a period near 10.33 h. In addition, using data from the Transiting Exoplanet Survey Satellite (TESS), Pál et al. (2020) reported a rotational period of 10.329 h. Our results this year are in good agreement with these prior findings.

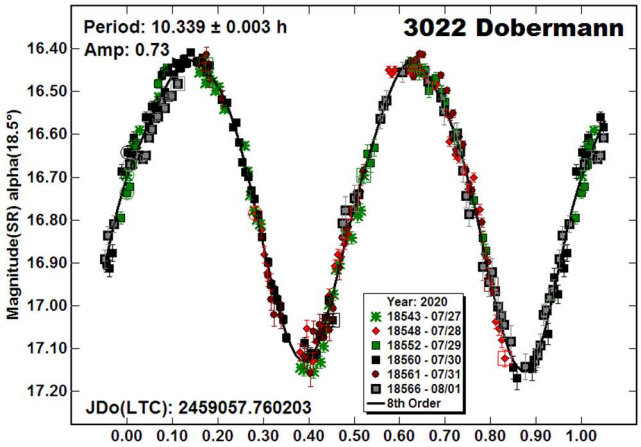

3086 Kalbaugh. We observed this member of the Hungaria family/group in the past to acquire data for a shape/pole model (Warner 2005b; 2008; 2010a; 2013b) each time finding a period of 5.18 h. Skiff et al. (2019) reports a period of 5.177 h. Using sparse data from the Lowell Observatory Database (Ďurech et al., 2016) found a sidereal period of (λ,β,*P*) = (63°,–51°,5.17907 h).

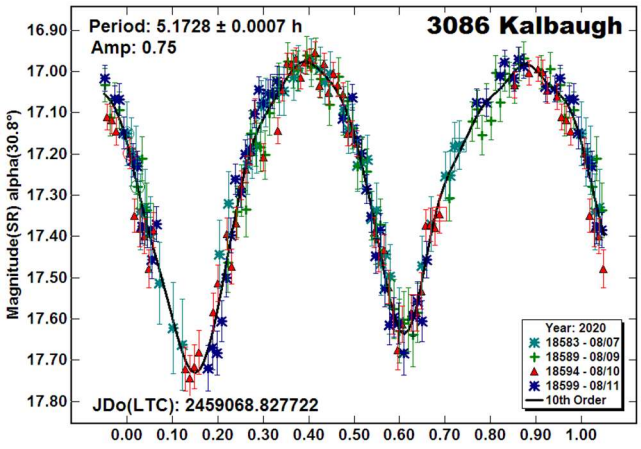

3895 Earhart. This member of the Phocaea family/group is estimated to be 11 km in size. It has been observed several times in the past (Behrend, 2009web, 3.56451 h; Behrend 2016web, 3.56445 h; Warner, 2009, 3.564 h; Aznar Macias et al., 2016, 3.556 h). Our result at this apparition is in good agreement.

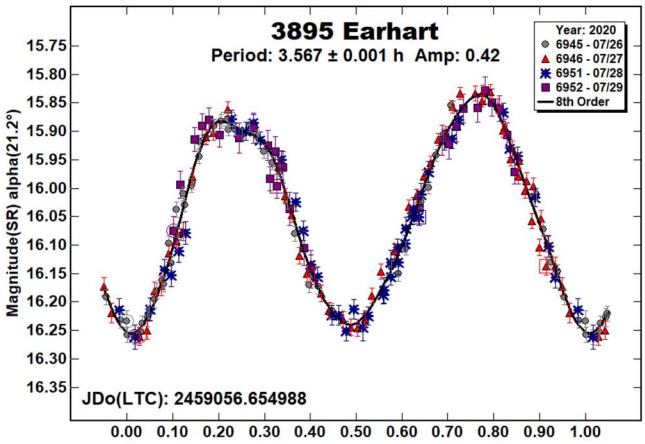

4956 Noymer. This member of the Phocaea family/group was observed in 2012 July by Waszczak et al. (2015) as part of the Palomar Transient Factory survey. They found a period of 4.366 h, which is consistent with our results this year.

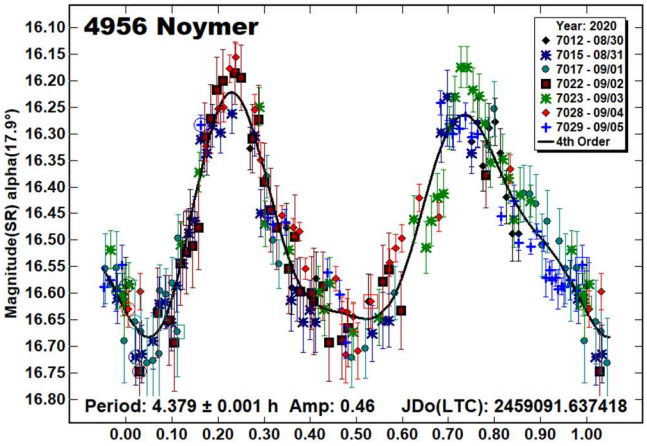

5870 Baltimore. We could not find any entries in the LCDB for this Mars-crosser, which is estimated to be 7 km in size.

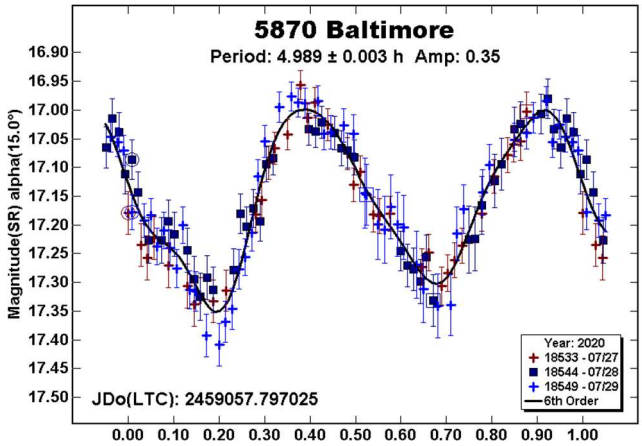

10403 Marcelgrun. Using data from the Transiting Exoplanet Survey Satellite (TESS), Pál et al. (2020) reported a rotational period of 10.3703 h for this 4-km member of the Flora family/group. This result seems to be double the period we found.

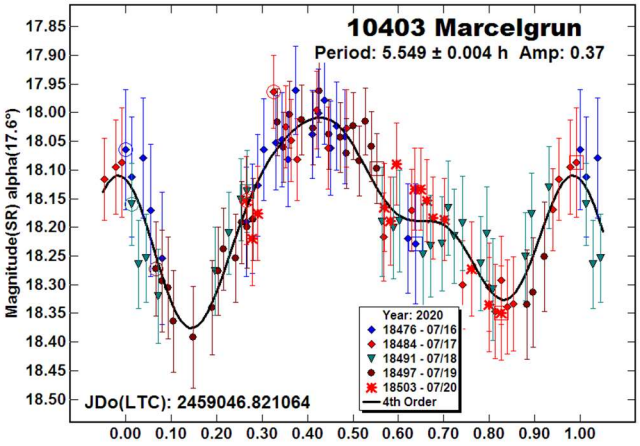

It appears this wide-field survey used only single-frequency analysis, then assumed it to be the second harmonic of the actual frequency (bimodal lightcurve; Harris, private communications). This is based on Pál et al. (2020) Eq. 1 on page 5, which implies a fit to only a single frequency, then assumed it to be the second harmonic of a bimodal curve. A single-frequency solution assumed to be 2nd-harmonic can often miss periods found with 4th-order analysis.

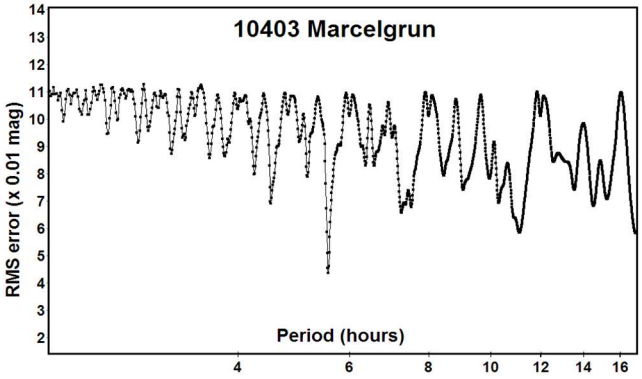

11059 Nulliusinverba. This member of the Eunomia family/group was a target of opportunity, being in the same field of 7174 Semois for two nights. There are no periods reported in the LCDB. 'Nullius in verba' is the motto of the Royal Society and is taken to mean 'take nobody's word for it'. That said, we feel this result is pretty secure.

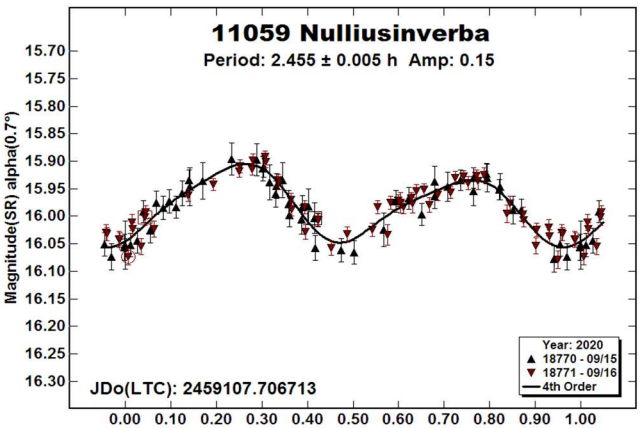

12494 Doughamilton. Using data from the Transiting Exoplanet Survey Satellite (TESS), Pál et al. (2020) reported a rotational period of 39.2603 h for this member of the Hungaria family/group. Our result is in good agreement.

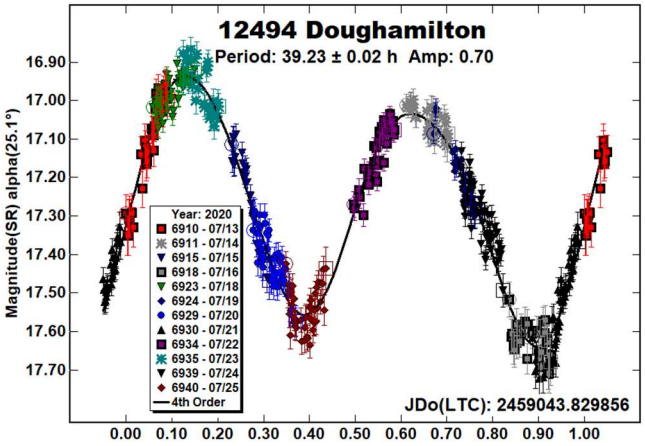

13162 Ryokkochigaku. There are no previous entries in the LCDB for this 5 km sized Vestoid. A general rule-of-thumb (Pravec et al., 2005; 2014) makes this asteroid likely to be in non-principal axis rotation (NPAR; tumbling). The fact that *MPO Canopus* found two dominant periods, neither one indicative of a satellite, adds credence to the argument for tumbling. *MPO Canopus* cannot directly analyze tumbling asteroids, so these two periods may or may not be the true periods of rotation and precession.

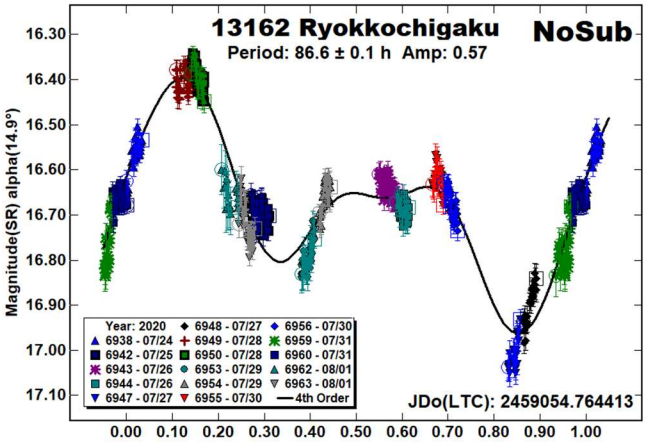

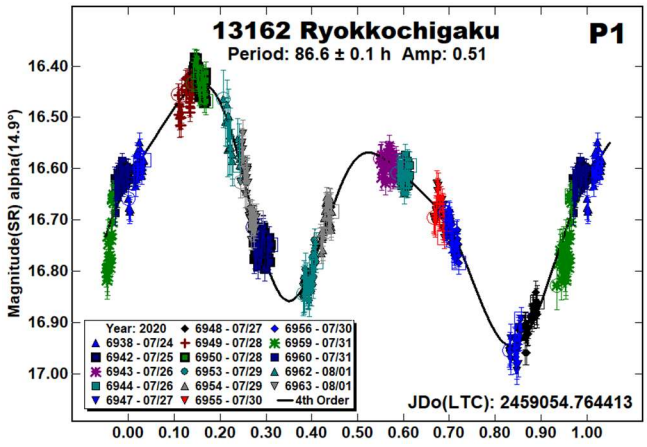

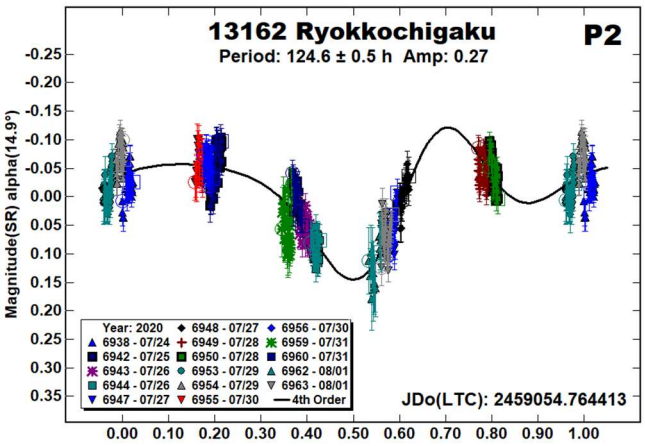

(13186) 1996 UM. This is a 3-km Hungaria that has been observed by CS3 at four previous apparitions: Warner (2013a), Warner (2014b), Warner (2016), and Stephens (2017). Each time, as in 2020, a period close to 4.30 hours was found. The amplitudes have ranged from 0.34 to 0.69 mag. The 2020 and 2012 observations were at nearly the same viewing aspect and so the amplitudes were similar, 0.69 mag in 2012 and 0.64 mag in 2020.

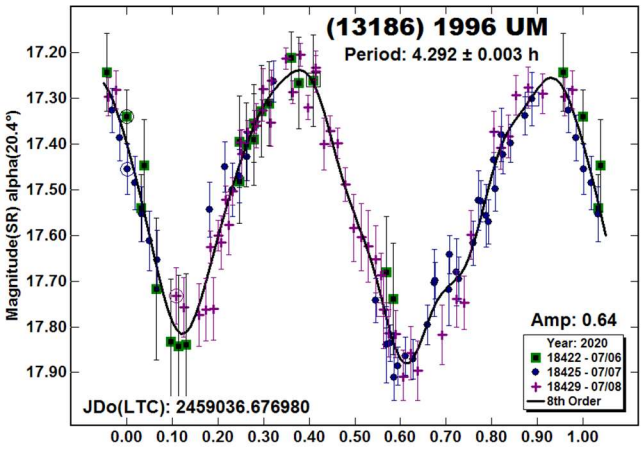

(14211) 1999 NT1. This Mars-crosser was observed three times in the past (Pray et al., 2007; Pravec et al., 2012web; 2013web), each time finding a period near 3.585 h. Our result this year is in good agreement.

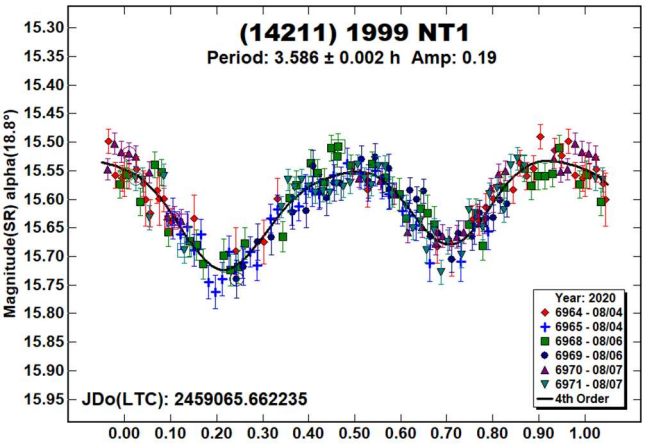

(14793) 1975 SE2. There are no previous periods in the LCDB for this 2.7 km Vestoid. It was in the field of the NEA (159402) 1999 AP10 and only observed a single night.

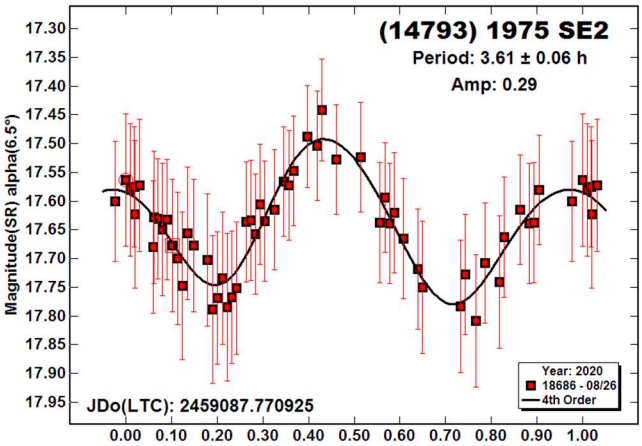

(14923) 1994 TU3. Reviewing recently published results with a period of 2.6531 h (Dose 2020) caused us to revisit our observations from 2008 which had a period of 7.300 h. We reset the comparison star magnitudes to SR values from ATLAS and redid the period search finding two solutions. These solutions are only in general agreement with the Dose results because of the sparse data. We prefer the 2.529 h period (A), which is a monomodal lightcurve. The bimodal result with a period of 5.058 h would require the Dose result to be a highly unlikely quadramodal solution.

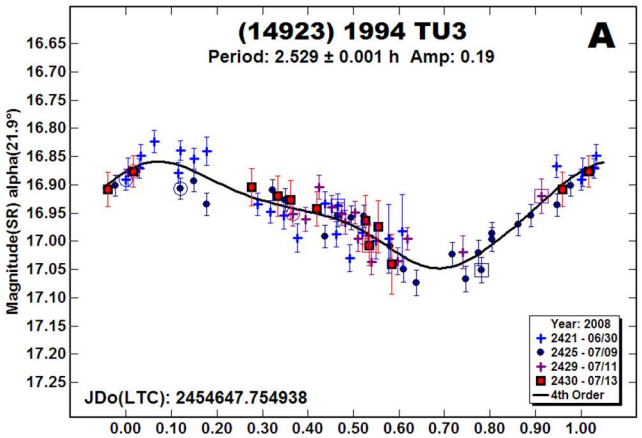

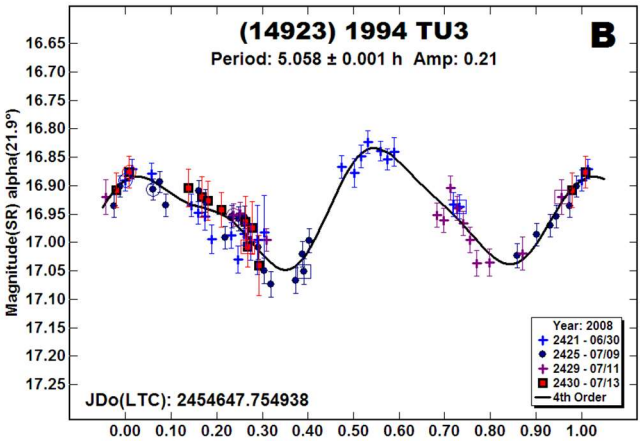

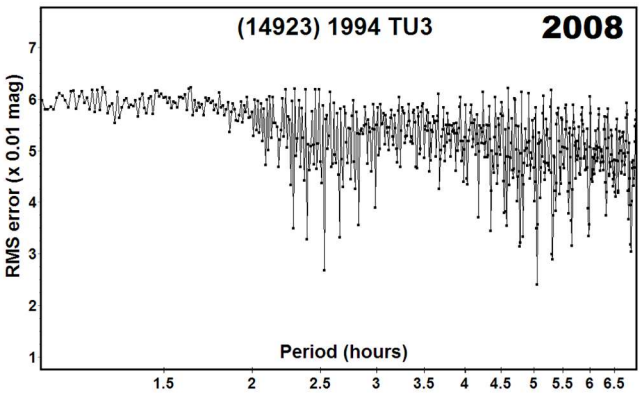

21663 Banat. Behrend (2005web) previously reported a period of 9.6 h for this outer main-belt object. Although the period spectrum for our observations this year shows many possibilities, the 15.5 h solution is the only plausible choice.

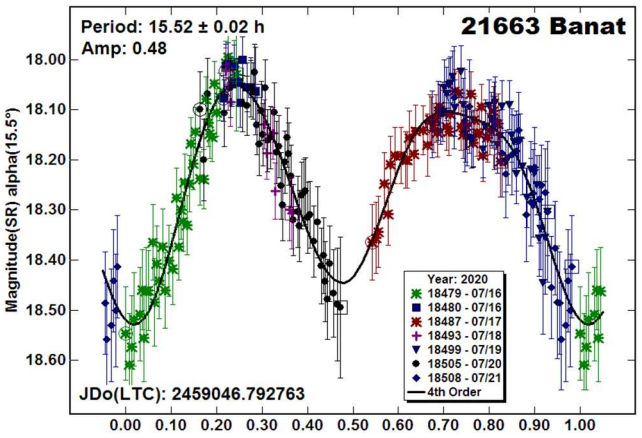

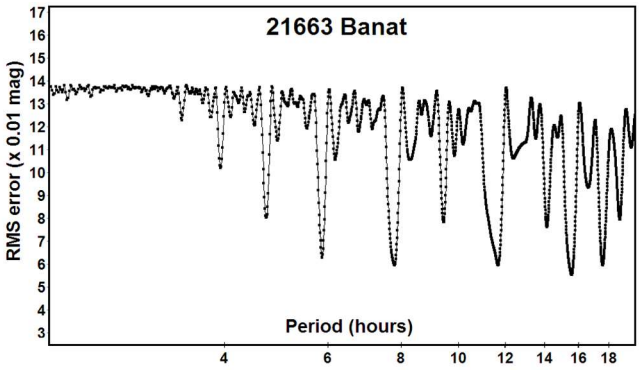

(23482) 1991 LV. We've observed this Hungaria group/family member for three apparitions: 2012 July, 2015 September, and 2020 September. After the most recent observations, we believe we have determined the true unique period.

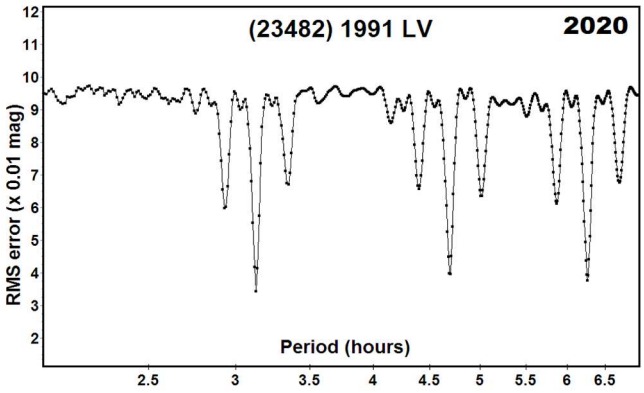

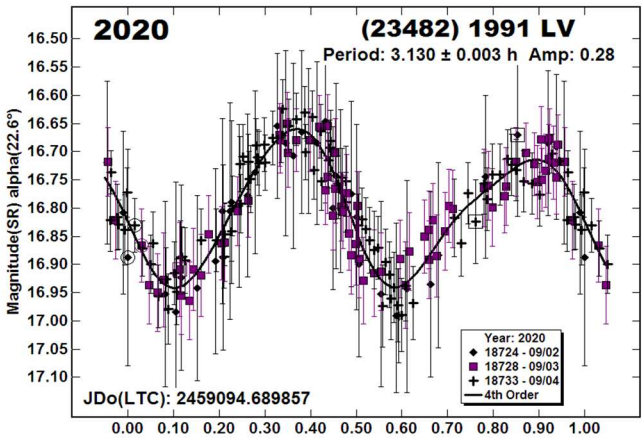

From the 2020 data, the densest set of the four apparitions, the period was uniquely-defined at 3.130 h. The two prominent solutions at longer periods produced a tri- or quadramodal lightcurve. Given the relatively low phase angle and amplitude, a bimodal solution was virtually assured (Harris et al., 2014).

The weaker "wing" at 3.357 h becomes important when looking at the results from the two previous apparitions and taking into account that the difference between 3.130 h and 3.357 h is almost exactly a one-half rotation difference over 24 hours.

The period spectrum using the 2012 data set also favors a period near 3.13 h, but not as strongly as in 2020, and the 3.35-h wing is more prominent. The slight ambiguity is likely due to the sparser dataset and the gap between the two sets of consecutive nights.

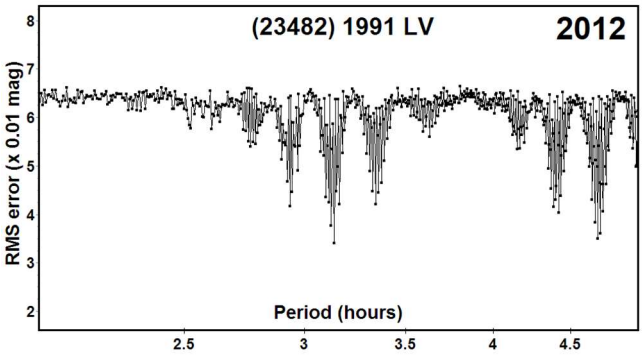

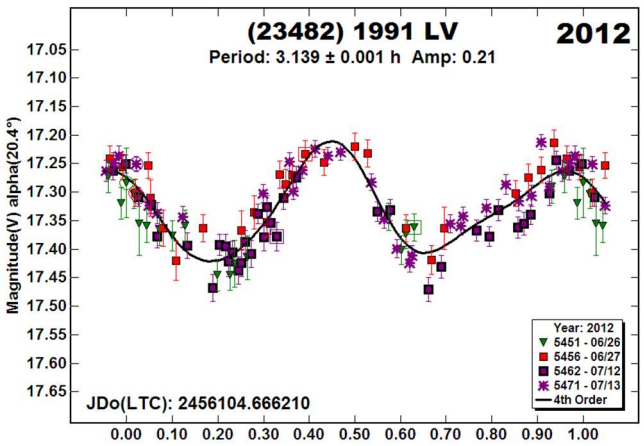

Even so, we still consider the solution of 3.139 h to be secure. Our original solution was 3.1388 h (2012). This is too precise given the dataset. The small difference between it and 3.130 h from 2020 can be attributed to the natural small differences in synodic period from one apparition and another and, again, the sparse data set.

An even sparser dataset in 2015 produced an ambiguity that led to the unfortunate adoption of a period of 3.357 h (Warner, 2016) even though the only acceptable fit of the 2012 data was 3.126 h.

We reanalyzed the 2015 data after changing the comparison star magnitudes from V in the APASS catalog (Henden et al., 2009) to Sloan r′ (SR) from the ATLAS star catalog (Tonry et al., 2018) and resetting any zero-point offsets to 0. This produced almost equally valid solutions near 3.13 and 3.35 h. The lightcurve for the latter has a shape that is more asymmetrical. Based on this, we adopted P = 3.131 h but could not formally exclude 3.356 h.

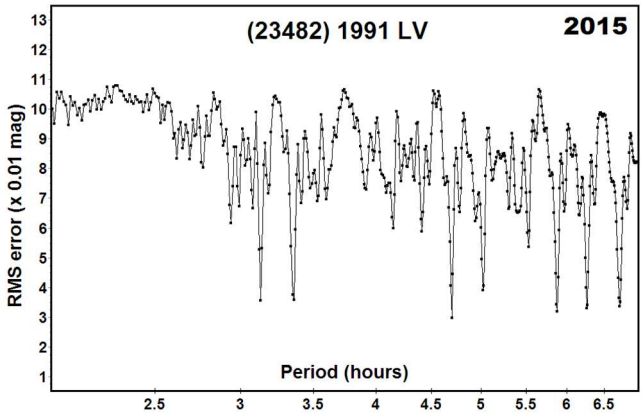

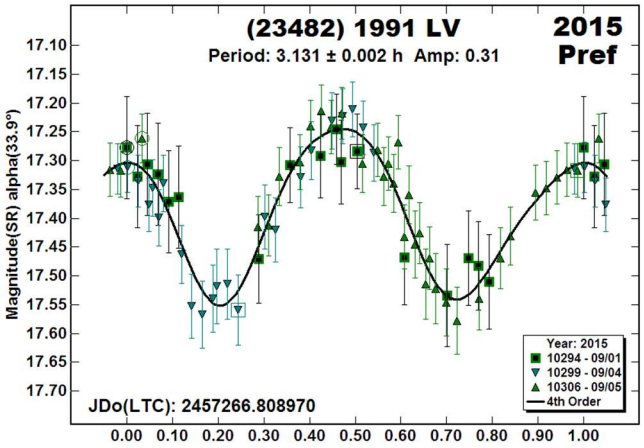

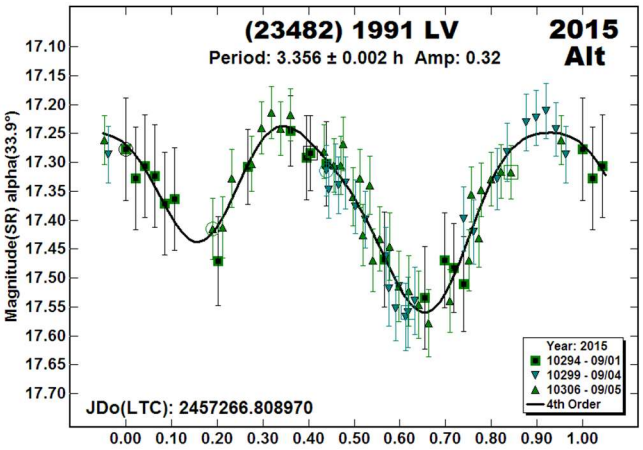

On the whole, the preponderance of evidence so strongly favors a solution of about 3.13 h that we feel safe in saying that it is the true period and that 3.35 h can be excluded.

(24177) 1999 XJ7. This member of the Flora family/group was a target of opportunity in the field of the NEA (159402) 1999 AP10. The 16.3 mag asteroid was passing over a 10.5 mag star for a good part of the last night. It was previously observed by Erasmus et al. (2020) who found a period of 3.821 h.

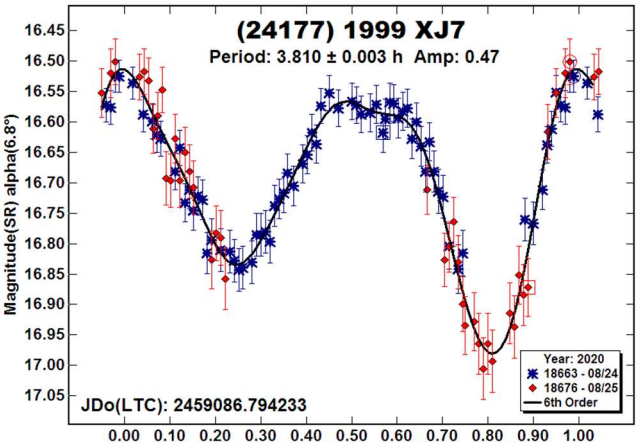

(28565) 2000 EO58. Behrend (2004web; 2020web) observed this 3-km Mars-crosser twice. Their 2004 observations report a period of 3.83 h. The scatter in the data was twice that of the 0.04 mag amplitude. They report a 11.1796 h period from their 2020 August data that shows six extrema. That reported period is a 3:1 alias of our 3.71 h period.

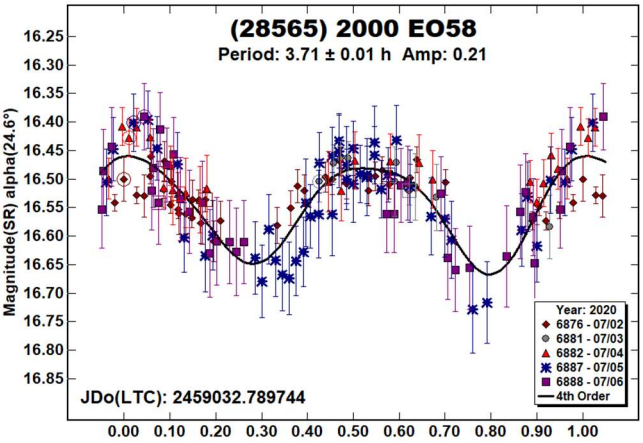

(51534) 2001 FQ132. There are no entries in the LCDB for this 2-km inner main-belt asteroid. It was a target of opportunity in the field of (159402) 1999 AP10 for two nights.

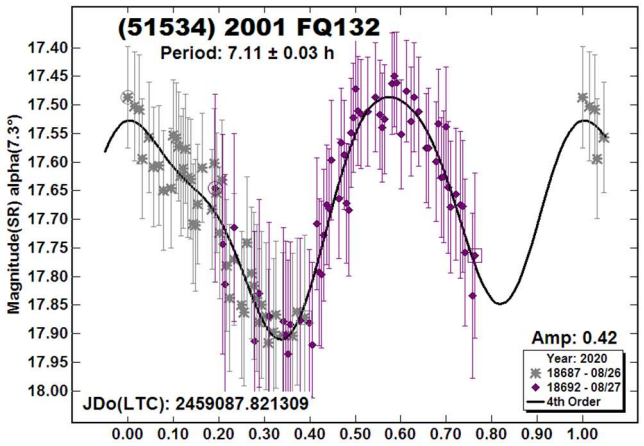

(56086) 1999 AA21. This member of the Phocaea family/group was previously observed by Pál et al. (2020) using data from the Transiting Exoplanet Survey Satellite (TESS). They reported a rotational period of 2.76957 h. Our data initially showed some variations which made us suspect the presence of a secondary period near 25 h. However, due to its low amplitude and being nearly commensurate with an Earth day, we do not have confidence that the minor deviations of a secondary period is based on a physical effect.

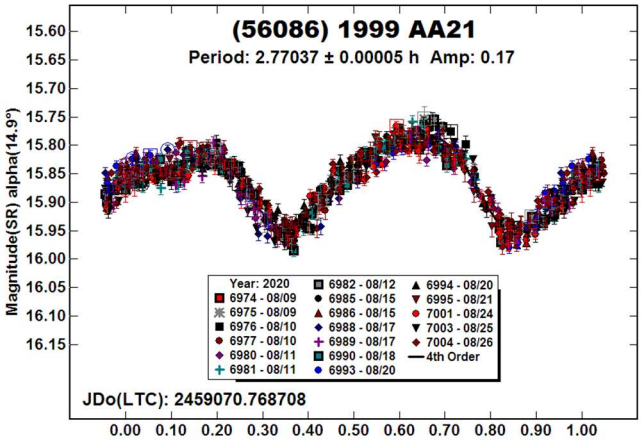

(68134) 2001 AT18. Skiff et al. (2019) observed this Mars-crosser in 2010 reporting a period of 7.104 h. Our result this year is in good agreement.

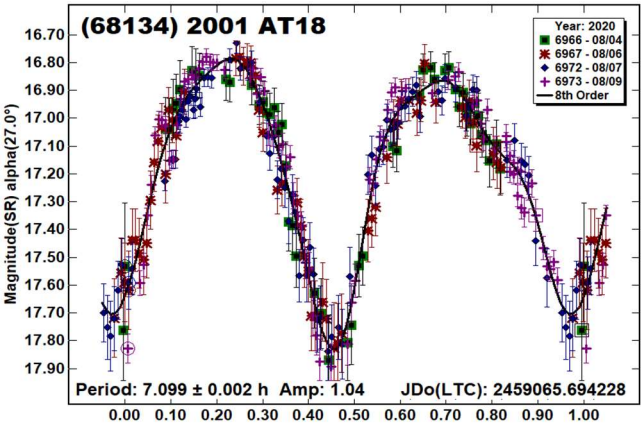

Because of the availability of dense data from Skiff in the Asteroid Lightcurve Data Exchange Format database (ALCDEF, 2020), sparse data at the Asteroids - Dynamic web site (AstDyS-2, 2020), and our dense data from two apparitions, we attempted to solve for the sidereal period and pole position and create a shape model. This data was combined using *MPO LCInvert* (Bdw Publishing).

As is often the case, the pole model showed two possible solutions 180° apart; (λ, β, *P*) = (25°, –19°, 7.107274 h) and (λ, β, *P*) = (323°, –79°, 7.107278 h). Our preferred solution is (323°, –79°) because the (25°, –19°) solution would be nearly pole-on at some point, and because of the distribution of the L_{PAB}, the lightcurve amplitude should have been significantly different between the 2010 and the 2020 apparitions. Since the observed amplitude has always been > 1.0 mag., it would require an unusually large, maybe implausible, a/b axis ratio to not have a nearly equatorial view at the two apparitions.

The full set of inversion plots is given at the end of this paper.

(96341) 1997 OX1. There are no previous lightcurve entries in the LCDB for this 2-km inner main-belt object that was a target of opportunity. There are many possible solutions for this slow amplitude, high phase angle target. We prefer the 3.019 h solution, but the 1.611 h and 4.830 h periods are possible. The 4.830 h solution cannot be ruled out because the split halves plot shows it to be asymmetrical. The position of the 1.611 h period on a frequency-diameter plot shows it to be not particularly outstanding or anomalous.

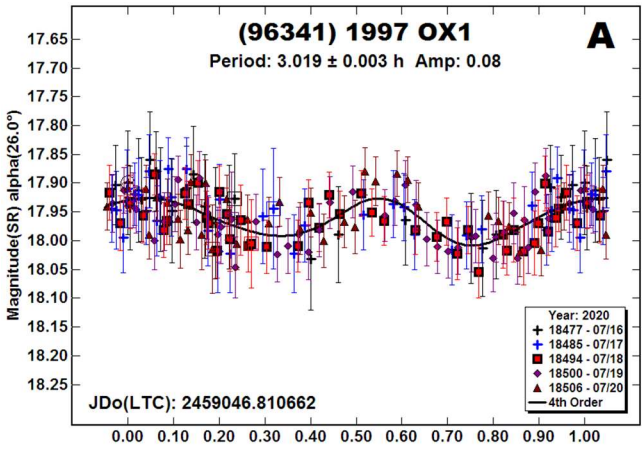

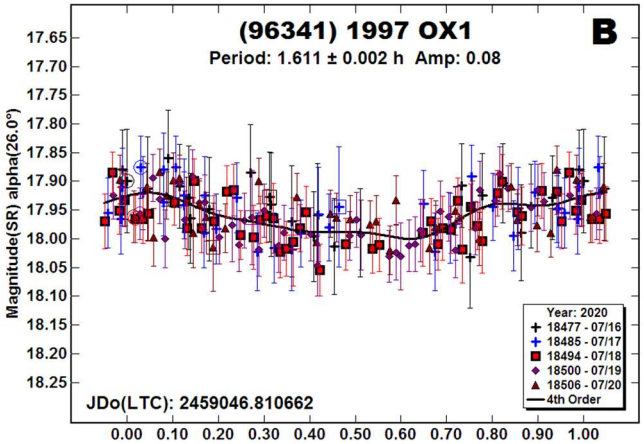

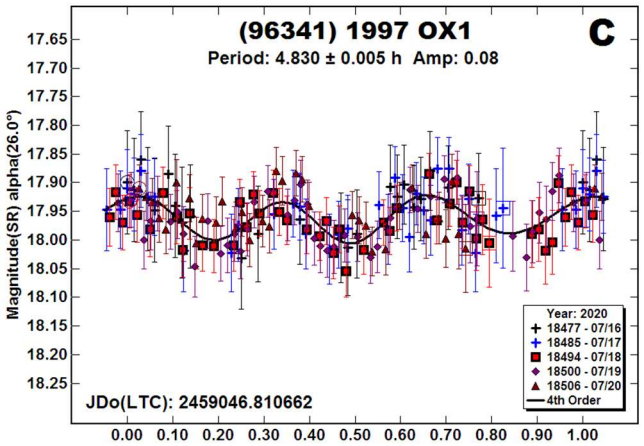

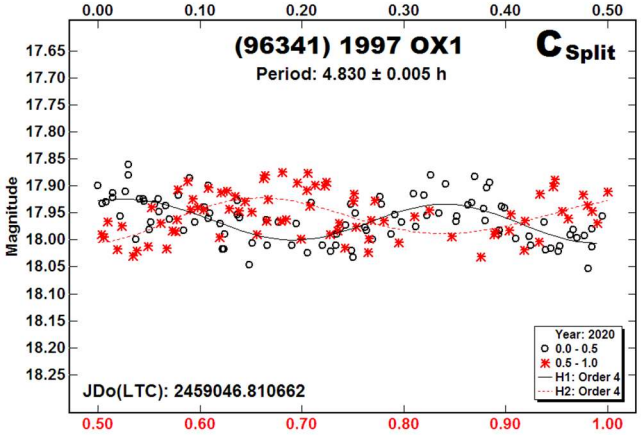

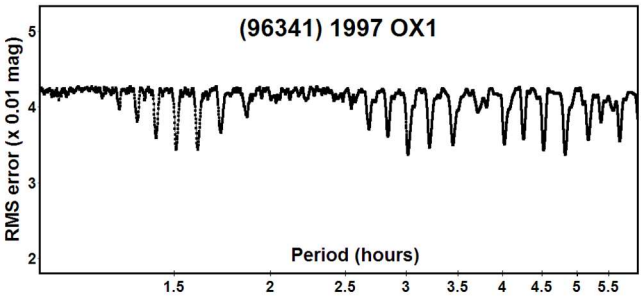

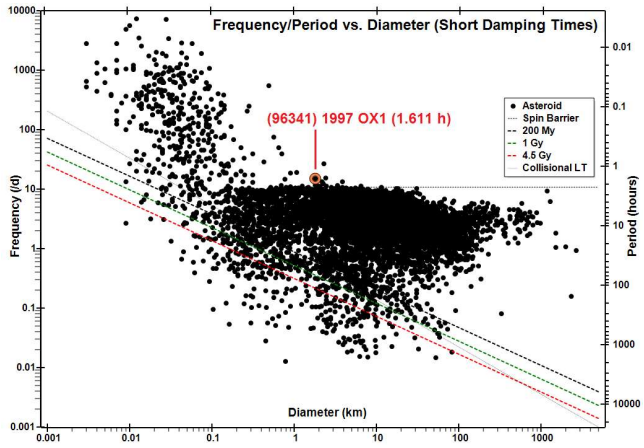

(129480) 1993 UQ8. This outer main-belt object was a target of opportunity in the field of 7174 Semois, so we only got two nights on the target. There are no previous lightcurve entries in the LCDB and, with the limited dataset, we had to estimate the period to be 27.5 h based upon a plot of the half period.

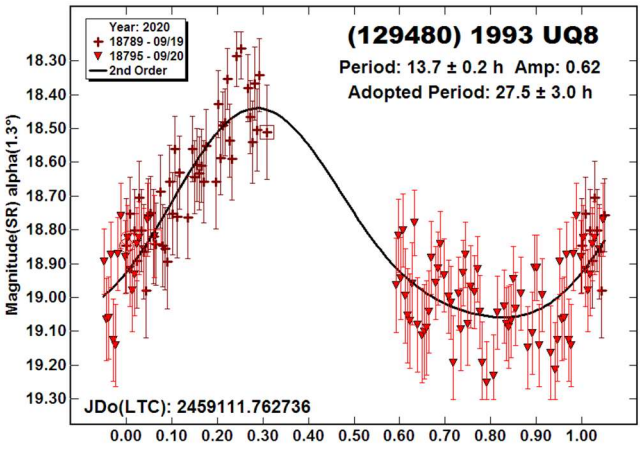

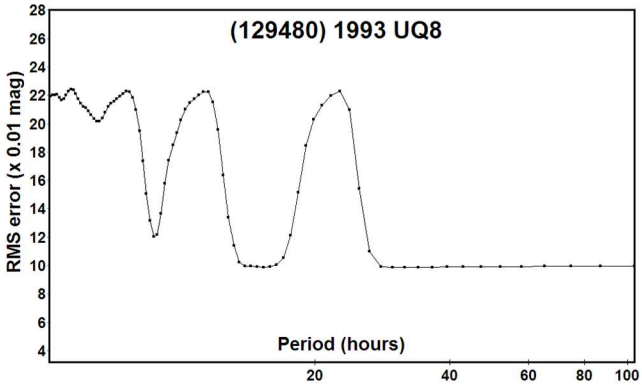

(146134) 2000 SE1. The only period found in the LCDB for this Mars-crosser was from Waszczak (2015). Their period of 21.762 h is in good agreement with this work.

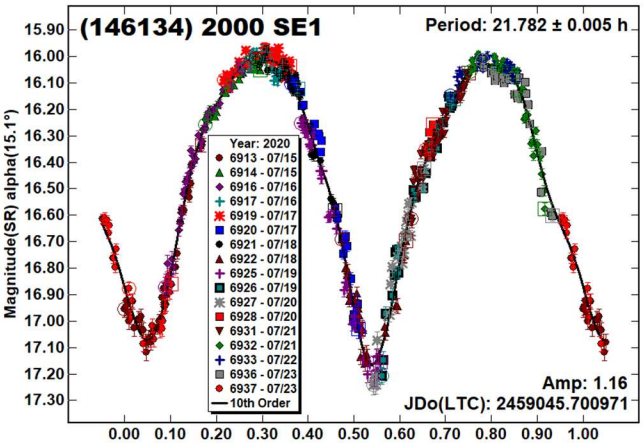

(164755) 1998 VK27. There are no entrees in the LCDB for this outer main-belt object. It was a target of opportunity in the field of the Hilda (16970) 1998 VV2.

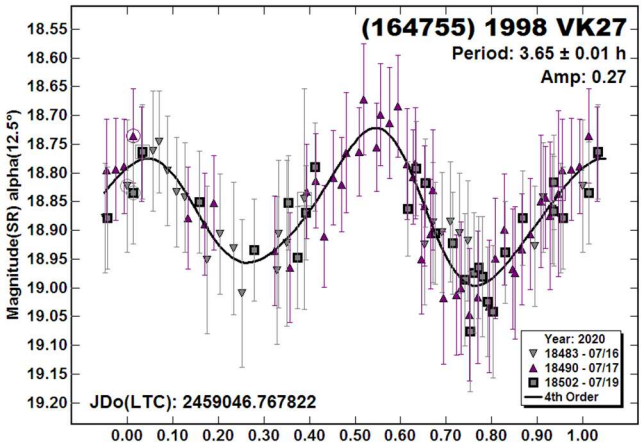

Acknowledgements

Observations at CS3 and continued support of the asteroid lightcurve database (LCDB; Warner et al., 2009) are supported by NASA grant 80NSSC18K0851. This work includes data from the Asteroid Terrestrial-impact Last Alert System (ATLAS) project. ATLAS is primarily funded to search for near earth asteroids through NASA grants NN12AR55G, 80NSSC18K0284, and 80NSSC18K1575; byproducts of the NEO search include images and catalogs from the survey area. The ATLAS science products have been made possible through the contributions of the University of Hawaii Institute for Astronomy, the Queen's University Belfast, the Space Telescope Science Institute, and the South African Astronomical Observatory. The authors gratefully acknowledge Shoemaker NEO Grants from the Planetary Society (2007, 2013). These were used to purchase some of the telescopes and CCD cameras used in this research.

Number	Name	2020 mm/dd	Phase	L_{PAB}	B_{PAB}	Period(h)	P.E.	Amp	A.E.	Grp
572	Rebekka	09/02-09/06	16.3,17.7	313	11	5.653	0.0006	0.26	0.01	MB-I
586	Thekla	09/16-09/19	1.1,2.1	351	2	13.681	0.003	0.27	0.01	MB-O
1582	Martir	2010/05/05-05/21	7.4,12.0	214	12	12.372	0.002	0.42	0.03	MB-O
1626	Sadeya	07/12-07/14	23.9,23.7	340	24	3.420	0.001	0.16	0.01	PHO
	Pole (λ, β, P)	**(152°, -9°, 3.421367 h)**	**a/b: 1.56**		**a/c: 1.19**					
2927	Alamosa	07/08-07/12	22.6,22.9	219	18	4.380	0.002	0.34	0.02	MB-I
3022	Dobermann	07/28-08/01	18.3,17.3	321	25	10.339	0.003	0.73	0.03	H
3086	Kalbaugh	08/07-08/11	30.8,30.7	26	21	5.1728	0.0007	0.75	0.03	H
3895	Earhart	07/26-07/29	21.2,21.6	261	26	3.567	0.001	0.42	0.02	PHO
4956	Noymer	08/30-09/05	18.0,19.8	312	17	4.379	0.001	0.46	0.03	PHO
5870	Baltimore	07/27-07/29	15.1,14.4	336	4	4.989	0.003	0.35	0.03	MC
10403	Marcelgrun	07/16-07/20	17.6,16.3	331	6	5.549	0.004	0.37	0.03	FLOR
11059	Nulliusinverba	09/15-09/16	0.7,0.2	354	0	2.455	0.005	0.15	0.01	EUN
12494	Doughamilton	07/13-07/25	25.1,20.0	331	-1	39.23	0.02	0.70	0.03	H
13162	Ryokkochigaku	07/24-08/01	14.9,11.4	325	7	86.6	0.1	0.5	0.1	V
						[T]124.6	0.5	0.3	0.1	
13186	1996 UM	07/06-07/08	20.4,20.7	274	32	4.292	0.003	0.64	0.04	H
14211	1999 NT1	08/04-08/07	18.8,18.8	323	22	3.586	0.002	0.19	0.02	MC
14793	1975 SE2	08/26-08/26	6.5	339	-9	3.61	0.06	0.27	0.03	V
14923	1994 TU3	2008/06/30-07/13	21.9,22.0	293	33	2.529	0.001	0.19	0.02	PHO
21663	Banat	07/16-07/21	15.5,14.0	330	5	15.52	0.02	0.48	0.04	MB-O
23482	1991 LV	09/02-09/04	22.6,22.1	359	27	3.130	0.003	0.28	0.03	H
		2015/08/30-09/05	34.1,33.5	37	16	3.358	0.002	0.31	0.03	
						[A]3.356	0.002	0.32	0.03	
		2012/06/26-07/13	18.7,18.6	300	23	3.139	0.001	0.21	0.03	
24177	1999 XJ7	08/24-08/25	6.8,6.5	339	-9	3.810	0.003	0.47	0.03	FLOR
28565	2000 EO58	07/02-07/06	*24.6,23.1	271	7	3.71	0.01	0.21	0.04	MC
51534	2001 FQ132	08/26-08/27	7.3,7.0	339	-8	7.11	0.03	0.42	0.05	MB-I
56086	1999 AA21	08/09-08/26	14.9,5.9	341	2	2.77037	0.00005	0.17	0.01	PHO
68134	2001 AT18	08/04-08/09	27.0,26.7	344	31	7.099	0.002	1.04	0.03	MC
	Pole (λ, β, P)	**(25°, -19°, 7.107274 h)**	(323°, -79°, 7.107278 h)		**a/b: 2.29**		**a/c: 1.09**			
96341	1997 OX1	07/16-07/20	*26.1,24.5	311	7	3.019	0.003	0.08	0.02	MB-I
						[A]1.611	0.002	0.08	0.02	
						[A]4.830	0.005	0.08	0.02	
129480	1993 UQ8	09/19-09/20	1.3,1.8	354	0	27.5	0.5	0.62	0.05	MB-O
146134	2000 SE1	07/15-07/23	*15.1,14.2	304	12	21.782	0.005	1.16	0.02	MC
164755	1998 VK27	07/16-07/19	12.6,11.5	317	10	3.65	0.01	0.27	0.04	MB-O

Table III. Observing circumstances and results. [A]The alternate period of an ambiguous solution. [T]Second period in a suspected tumbler. The phase angle is given for the first and last date. If preceded by an asterisk, the phase angle reached an extrema during the period. L_{PAB} and B_{PAB} are the approximate phase angle bisector longitude/latitude at mid-date range (see Harris et al., 1984). Grp is the asteroid family/group (Warner et al., 2009): EUN, Eunomia; FLOR, Flora; H, Hungaria; MC, Mars-crosser; MB-(I/O): Main belt (inner/outer); PHO, Phocaea; V,

SPIN/SHAPE MODEL FOR 1662 SADEYA

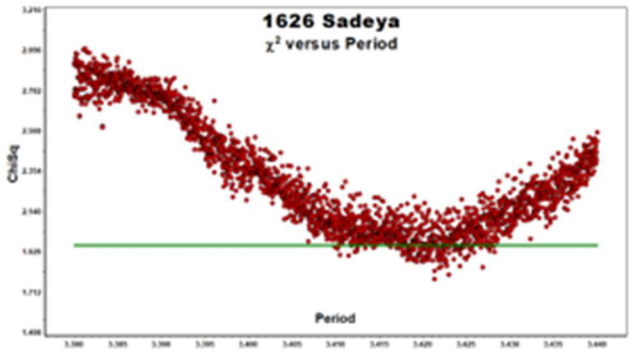

Figure 1. The initial period search results.

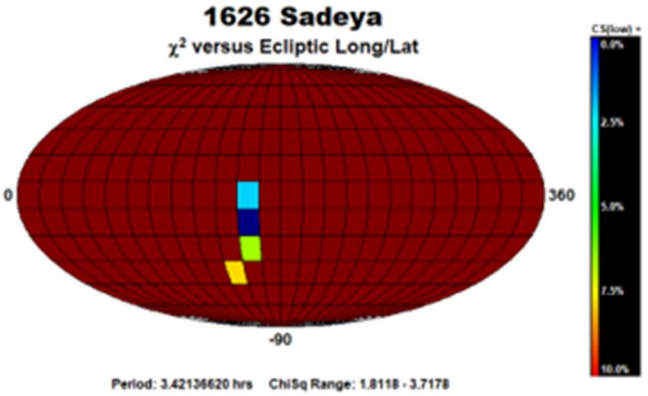

Figure 2. The pole search found two probable solutions.

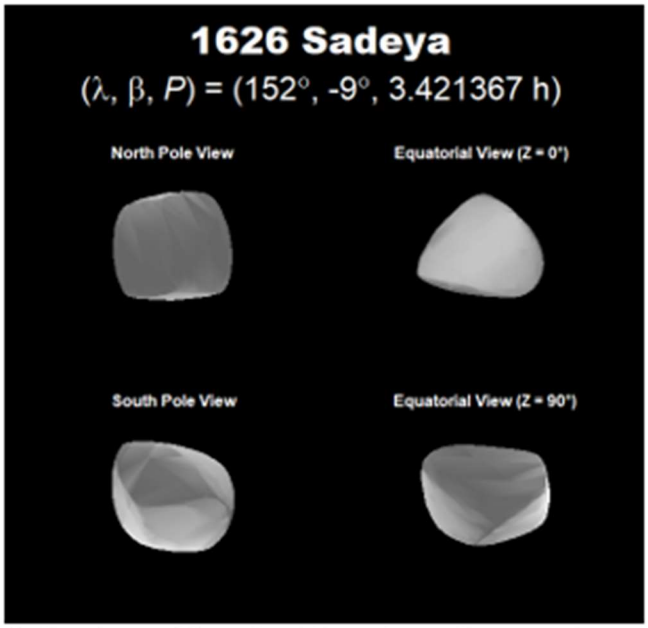

Figure 3. The shape of the asteroid based upon the secondary solution.

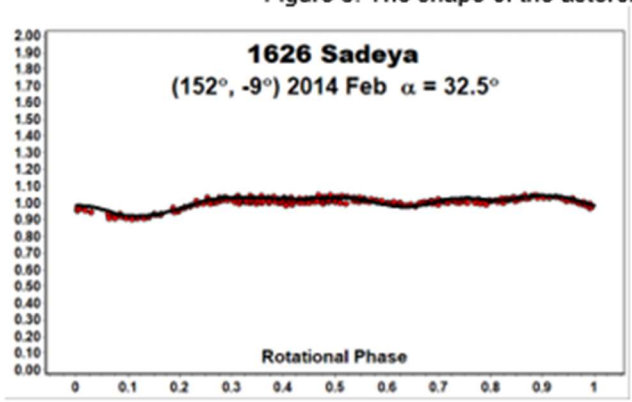

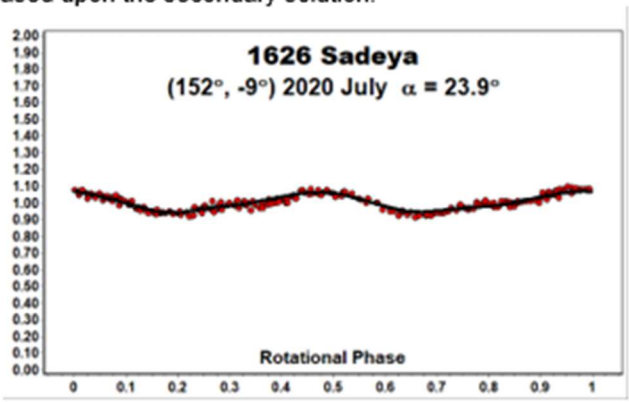

Figure 4/5. The comparison plots are against the preferred pole solution. The red dots indicate the data used for modeling while the black line is the smoothed lightcurve for generated by the shape at the time of the observations. The match is very close on both occasions, which gives confidence in the shape/spin axis model.

SPIN/SHAPE MODEL FOR (68134) 2001 AT18

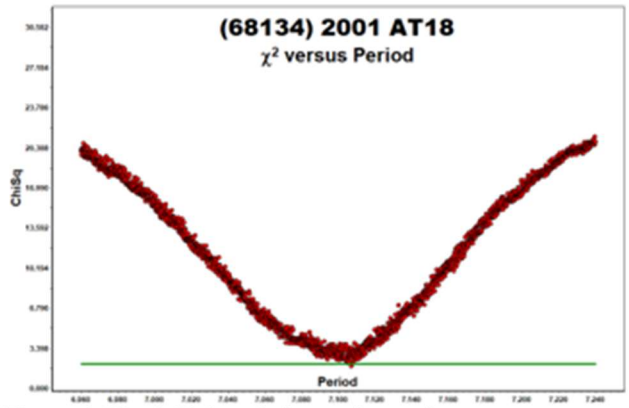

Figure 1. The initial period search results.

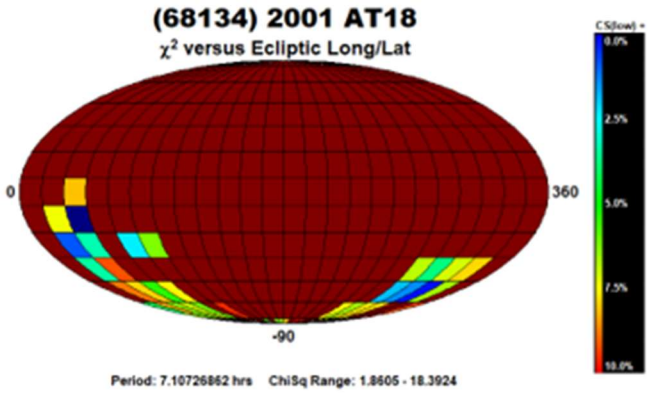

Figure 2. The pole search found two probable solutions.

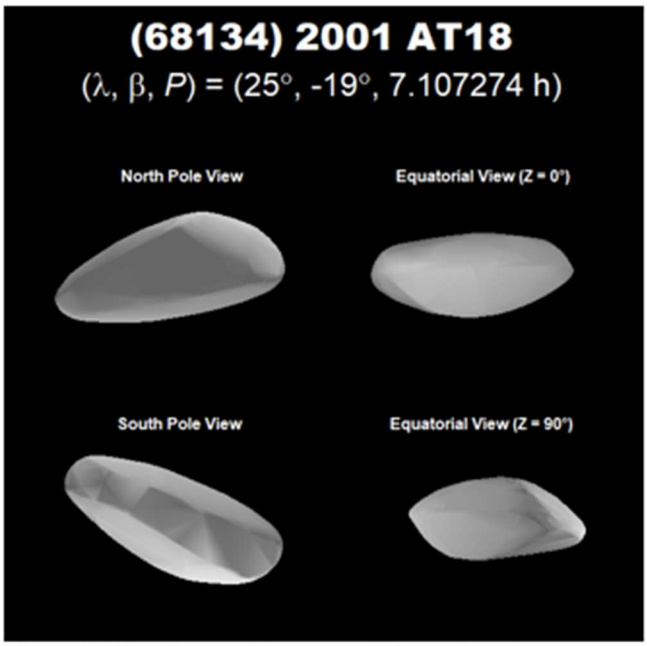

Figure 3. The shape of the asteroid based on the preferred solution.

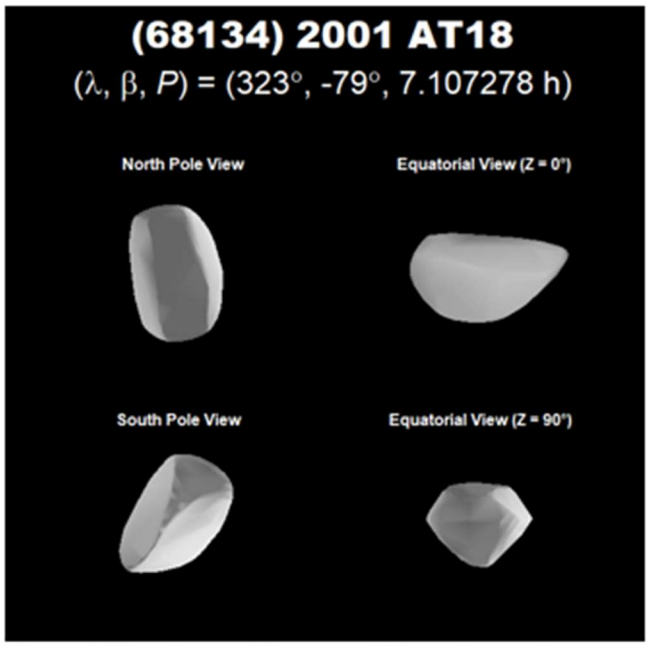

Figure 4. The shape of the asteroid based upon the secondary solution.

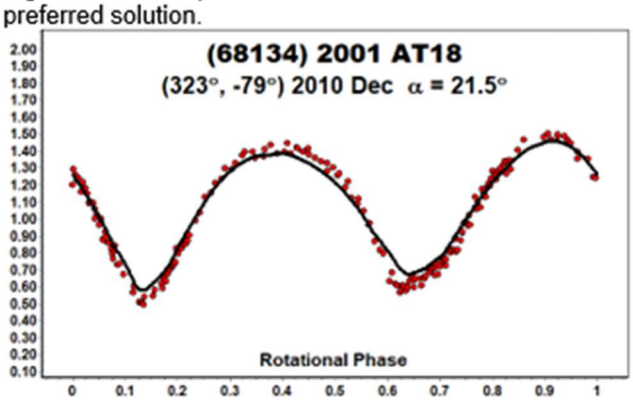

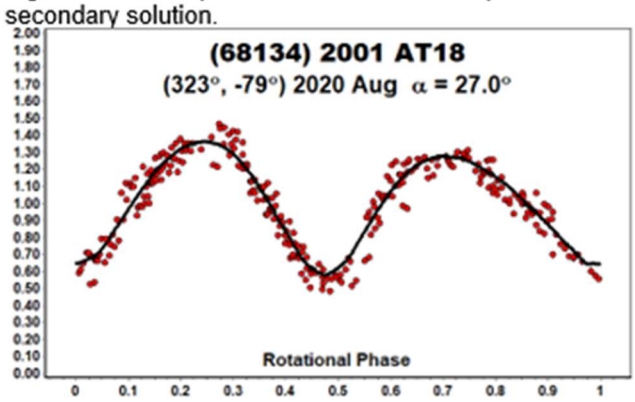

Figure 5/6. The comparison plots are against the preferred pole solution. The red dots indicate the data used for modeling while the black line is the smoothed lightcurve for generated by the shape at the time of the observations. The match is very close on both occasions, which gives confidence in the shape/spin axis model.

References

ALCDEF (2020). Asteroid Lightcurve Data Exchange Format database. *http://www.alcdef.org/*

AstDys-2 (2020). Asteroids - Dynamic web site. *https://newton.spacedys.com/astdys/*

Aznar Macias, A.; Carreno Garcerain, A.; Arce Masego, E.; Brines Rodriguez, P.; Lozano de Haro, J.; Fornas Silva, A.; Fornas Silva, G.; Mas Martinez, V.; Rodrigo Chiner, O.; Herrero Porta, D. (2016). "Twenty-one Asteroid Lightcurves at Group Observadores de Asteroides (OBAS): Late 2015 to Early 2016." *Minor Planet Bull*. **43**, 257-263.

Behrend, R., (2004web, 2005web, 2007web, 2009web, 2016web, 2020web). Observatoire de Geneve web site. *http://obswww.unige.ch/~behrend/page_cou.html*

Benishek, V. (2015). "Rotation Period Determinations for 1095 Tulipa, 1626 Sadeya, 2132 Zhukov, and 7173 Sepkoski." *Minor Planet Bull.* **42**, 75-76.

Dose, E.V. (2020). "A New Photometric Workflow and Lightcurves of Fifteen Asteroids." *Minor Planet Bull*. **47**, 324-330.

Ďurech, J.; Hanuš, J.; Oszkiewicz, D.; Vančo, R. (2016). "Asteroid models from the Lowell photometric database." *Astron. Astrophys*. **587**, A48.

Erasmus, N.; Navarro-Mesa, S.; McNeill, A.; Trilling, D.E.; Sickafoose, A.A.; Denneau, L.; Flewelling, H.; Heinze, A.; Tonry, J.L. (2020). "Investigating taxonomic diversity within asteroid families through ATLAS dual-band photometry." *Astrophys. J. Suppl. Ser.* **247**, id.13.

Florczak, M.; Dotto, E.; Barucci, M.A.; Birlan, M.; Erikson, A.; Fulchignoni, M.; Nathues, A.; Perret, L.; Thebault, P. (1997). "Rotational properties of main belt asteroids: photoelectric and CCD observations of 15 objects." *Plan. And Space Sci*. **45**, 1423-1435.

Hanuš, J.; Ďurech, J.; Brož, M.; Marciniak, A.; Warner, B.D.; Pilcher, F.; Stephens, R.; Behrend, R.; Carry, B.; and 111 coauthors. (2013). "Asteroids' physical models from combined dense and sparse photometry and scaling of the YORP effect by the observed obliquity distribution." *Astron. Astrophys.* **551**, A67.

Harris, A.W.; Young, J.W.; Scaltriti, F.; Zappala, V. (1984). "Lightcurves and phase relations of the asteroids 82 Alkmene and 444 Gyptis." *Icarus* **57**, 251-258.

Harris, A.W.; Young, J.W.; Bowell, E.; Martin, L.J.; Millis, R.L.; Poutanen, M.; Scaltriti, F.; Zappala, V.; Schober, H.J.; Debehogne, H.; Zeigler, K.W. (1989). "Photoelectric Observations of Asteroids 3, 24, 60, 261, and 863." *Icarus* **77**, 171-186.

Harris, A.W.; Pravec, P.; Galad, A.; Skiff, B.A.; Warner, B.D.; Vilagi, J.; Gajdos, S.; Carbognani, A.; Hornoch, K.; Kusnirak, P.; Cooney, W.R.; Gross, J.; Terrell, D.; Higgins, D.; Bowell, E.; Koehn, B.W. (2014). "On the maximum amplitude of harmonics on an asteroid lightcurve." *Icarus* **235**, 55-59.

Henden, A.A.; Terrell, D.; Levine, S.E.; Templeton, M.; Smith, T.C.; Welch, D.L. (2009). *http://www.aavso.org/apass*

Kaasalainen, M.; Torppa J. (2001). "Optimization Methods for Asteroid Lightcurve Inversion. I. Shape Determination." *Icarus* **153**, 24-36.

Kaasalainen, M.; Torppa, J.; Muinonen, K. (2001). "Optimization Methods for Asteroid Lightcurve Inversion. II. The Complete Inverse Problem." *Icarus* **153**, 37-51.

Lagerkvist, C.-I.; Belskaya, I.; Erikson, A.; Schevchenko, V.; Mottola, S.; Chiorny, V.; Magnusson, P.; Nathues, A.; Piironen, J. (1998). "Physical studies of asteroids. XXXIII. The spin rate of M-type asteroids." *Astron. Astrophys.* **131**, 55-62.

McNeill, A.; Mommert, M.; Trilling, D.E.; Llama, J.; Skiff, B. (2019). "Asteroid Photometry from the Transiting Exoplanet Survey Satellite: A Pilot Study." *Ap. J.* **245**, A29.

Odden, C.; French, J.; Briggs, J. (2012). "Lightcurve Analysis for Four Asteroids." *Minor Planet Bull.* **39**, 236-238.

Pál, A.; Szakáts, R.; Kiss, C.; Bódi, A.; Bognár, Z.; Kalup, C.; Kiss, L.L.; Marton, G.; Molnár, L.; Plachy, E.; Sárneczky, K.; Szabó, G.M.; Szabó, R. (2020). "Solar System Objects Observed with TESS - First Data Release: Bright Main-belt and Trojan Asteroids from the Southern Survey." *Ap. J.* **247**, A26.

Pravec, P.; Harris, A.W.; Scheirich, P.; Kušnirák, P.; Šarounová, L.; Hergenrother, C.W.; Mottola, S.; Hicks, M.D.; Masi, G.; Krugly, Yu.N.; Shevchenko, V.G.; Nolan, M.C.; Howell, E.S.; Kaasalainen, M.; Galád, A.; Brown, P.; Degraff, D.R.; Lambert, J.V.; Cooney, W.R.; Foglia, S. (2005). "Tumbling asteroids." *Icarus* **173**, 108-131.

Pravec, P.; Scheirich, P.; Ďurech, J.; Pollock, J.; Kusnirak, P.; Hornoch, K.; Galad, A.; Vokrouhlicky, D.; Harris, A.W.; Jehin, E.; Manfroid, J.; Opitom, C.; Gillon, M.; Colas, F.; Oey, J.; Vrastil, J.; Reichart, D.; Ivarsen, K.; Haislip, J.; LaCluyze, A. (2014). "The tumbling state of (99942) Apophis." *Icarus* **233**, 48-60.

Pravec, P.; Wolf, M.; Sarounova, L. (2012web, 2013web, 2020web). *http://www.asu.cas.cz/~ppravec/neo.htm*

Pray, D.P.; Kusnirak, P.; Galad, A.; Vilagi, J.; Kornos, L.; Gajdos, S.; Pikler, M.; Cervak, G.; Hsarik, M.; Oey, J.; Cooney, W.; Gross, J.; Terrell, D.; Stephens, R.D.; Higgins, D. (2007). "Lightcurve Analysis of Asteroids 2006 BQ6, 2942, 2943 3402, 3533, 6497, 6815, 7033, 12336, and 14211." *Minor Planet Bull*. **34**, 44-46.

Skiff, B.A.; McLelland, K.P.; Sanborn, J.J.; Pravec, P.; Koehn, B.W. (2019). "Lowell Observatory Near-Earth Asteroid Photometric Survey (NEAPS): Paper 4." *Minor Planet Bull*. **46**, 458-503.

Stephens, R.D. (2017). "Asteroids Observed from CS3: 2017 April - June." *Minor Planet Bull*. **44**, 321-323.

Tonry, J.L.; Denneau, L.; Flewelling, H.; Heinze, A.N.; Onken, C.A.; Smartt, S.J.; Stalder, B.; Weiland, H.J.; Wolf, C. (2018). "The ATLAS All-Sky Stellar Reference Catalog." *Astrophys. J.* **867**, A105.

Warner, B.D. (2005a). "Lightcurve analysis for asteroids 242, 893, 921, 1373, 1853, 2120, 2448 3022, 6490, 6517, 7187, 7757, and 18108." *Minor Planet Bull*. **32**, 4-7.

Warner, B.D. (2005b). "Asteroid lightcurve analysis at the Palmer Divide Observatory - Winter 2004-2005." *Minor Planet Bull*. **32**, 54-58.

Warner, B.D. (2007). "Asteroid Lightcurve Analysis at the Palmer Divide Observatory - December 2006 - March 2007." *Minor Planet Bul.* **34**, 72-77.

Warner, B.D. (2008). "Asteroid Lightcurve Analysis at the Palmer Divide Observatory: December 2007 - March 2008." *Minor Planet Bull*. **35**, 95-98.

Warner, B.D. (2009). "Asteroid Lightcurve Analysis at the Palmer Divide Observatory: 2009 March-June." *Minor Planet Bull*. **36**, 172-176.

Warner, B.D. (2010a). "Asteroid Lightcurve Analysis at the Palmer Divide Observatory: 2009 September-December." *Minor Planet Bull*. **37**, 57-64.

Warner, B.D. (2010b). "Upon Further Review: I. An Examination of Previous Lightcurve Analysis from the Palmer Divide Observatory." *Minor Planet Bull.* **37**, 127-130.

Warner, B.D. (2011). "Asteroid Lightcurve Analysis at the Palmer Divide Observatory: 2011 March - July." *Minor Planet Bull*. **38**, 190-195.

Warner, B.D. (2013a). "Asteroid Lightcurve Analysis at the Palmer Divide Observatory: 2012 June - September." *Minor Planet Bull*. **40**, 26-29.

Warner, B.D. (2013b). "Asteroid Lightcurve Analysis at the Palmer Divide Observatory: 2012 June - September." *Minor Planet Bull*. **40**, 71-80.

Warner, B.D. (2014a). "Asteroid Lightcurve Analysis at CS3-Palmer Divide Station: 2014 January-March." *Minor Planet Bull*. **41**, 144-155.

Warner, B.D. (2014b). "Asteroid Lightcurve Analysis at CS3-Palmer Divide Station: 2014 March-June." *Minor Planet Bull*. **41**, 235-241.

Warner, B.D. (2016). "Asteroid Lightcurve Analysis at CS3-Palmer Divide Station: 2015 June-September." *Minor Planet Bull*. **43**, 57-65.

Warner, B.D. (2017). "Asteroid Lightcurve Analysis at CS3-Palmer Divide Station: 2017 April thru June." *Minor Planet Bull.* **44**, 289-294.

Warner, B.D.; Harris, A.W.; Pravec, P. (2009). "The Asteroid Lightcurve Database." *Icarus* **202**, 134-146. Updated 2020 June. *http://www.minorplanet.info/lightcurvedatabase.html*

Waszczak, A.; Chang, C.-K.; Ofek, E.O.; Laher, R.; Masci, F.; Levitan, D.; Surace, J.; Cheng, Y.-C.; Ip, W.-H.; Kinoshita, D.; Helou, G.; Prince, T.A.; Kulkarni, S. (2015). "Asteroid Light Curves from the Palomar Transient Factory Survey: Rotation Periods and Phase Functions from Sparse Photometry." *Astron. J.* **150**, A75.

LIGHTCURVES OF NINETEEN ASTEROIDS

Eric V. Dose
3167 San Mateo Blvd. NE #329
Albuquerque, NM 87110
mp@ericdose.com

(Received: 2020 October 13)

Using a previously described workflow based on applying dozens of comparison stars from the ATLAS refcat catalog to each image, we have obtained and present lightcurves and synodic periods for nineteen asteroids. We also describe refinements to magnitude correction for airmass (altitude of the field of view), especially useful during periods of high extinction, for example, through atmospheric smoke resulting from recent forest fire events near the U.S. Pacific coast.

The present photometry workflow is based on that described previously (Dose, 2020b), relying on intensive application of very numerous (typically 30-150) ATLAS refcat catalog stars (Tonry et al., 2018) to each image.

Since that description, two improvements have been made to handling of atmospheric extinction, both prompted by this summer's widespread forest fires in the western United States which resulted in atmospheric smoke over the author's observing site in northern New Mexico. While prevailing upper-atmosphere winds very efficiently transported the smoke to the author's site at 1000-1500 km from the fires, extinction at the observing site changed only slowly, so that a single extinction coefficient sufficed for each night. ATLAS catalog stars were numerous enough to allow restriction of comp stars to a very narrow range of color index, so that observations continued through nights with extinction coefficients (Clear filter) up to about 0.70, where at 30º altitude only 25-30% of the light penetrates the atmosphere to reach the telescope. Exposure times were lengthened to compensate. Data from three nights with local extinction found to exceed 0.70 were rejected altogether.

In the first workflow improvement, one nightly extinction coefficient is first computed from comp stars for the night's asteroid target having the widest range in airmass; then, that extinction coefficient is applied to all targets for that night. The mixed-model regression (Gelman and Hill, 2006) on which the current workflow is based will segregate any remaining image-to-image systematic errors resulting from minor misestimation of the extinction. The advantage of starting with a good extinction estimation is not so much to get better photometric precision and accuracy, but more in clarifying the error structure so that outlier images, comp stars, and individual comp star observations can be removed properly. Nightly extinction estimation and application is not difficult and is now included in all the author's asteroid photometry.

The second workflow improvement computes an individual airmass value for each asteroid and comp star in each image, replacing the usual photometric practice of applying a center-image airmass value to all targets in that image. With extinction of 0.7, the extinction gradient near 30º above the horizon reaches 0.7 millimagnitude per arcminute of altitude; in the author's case, image corner-to-corner extinction range reached 30 millimagnitudes – much larger than ATLAS catalog magnitude uncertainties. Per-target airmasses are never worse than per-image

airmasses, and as the only disadvantage is in more computation time, the author plans to retain this improvement for future asteroid photometry.

With these two improvements, the author found it possible this summer to continue observing moderately bright targets when Clear-filter extinction reached 0.70, and to observe fainter targets (V~16-17) with normal precision when extinction reached about 0.40. In the end, by taking longer exposures and then applying the above workflow improvements, the present photometric data and lightcurves show very little effect of excess extinction from smoke. Were extinction to change more significantly during the night, especially when heavy smoke originates closer to the observing site, a proper nightly extinction value probably will not exist, and observing sessions will have to be kept shorter than the timescale of extinction change, or observations postponed to a better night.

The present workflow results in the session's raw lightcurve, that is, best estimates of asteroid magnitude on catalog basis, unreduced and without H-G adjustment. These final, catalog-basis asteroid magnitudes are imported directly into *Canopus* software (Warner, 2018) for Fourier fitting, period analysis including ruling out of aliases, and plotting. In *Canopus*, magnitudes are then adjusted for distances and for phase-angle dependence with an H-G model, using G = 0.15 for each asteroid unless otherwise specified. No nightly zero-point adjustments were needed or made to any session herein. All lightcurve data herein have been submitted to ALCDEF.

Nineteen asteroids were observed from Deep Sky West Observatory (IAU V28) in northern New Mexico. Images were acquired with a 0.35-m SCT reduced to *f*/7.7, a SBIG STXL-6303E camera without binning, cooled to -35C, and fitted with a Clear filter (Astrodon), on a PlaneWave L-500 direct-drive mount. The equipment is operated remotely via *ACP* software (DC-3 Dreams), running plan text files generated for each night by the author's python scripts (Dose, 2019 and 2020a). Most sessions cycled between 2-4 asteroids, as facilitated by the mount's rapid slews. Exposure times targeted an estimated maximum 10 millimagnitude per-observation uncertainty when possible, subject to a minimum of 90 seconds to ensure proper photometry of numerous comp stars, and limited to 900 seconds. All exposures of 120 seconds or longer, and most shorter exposures, were autoguided.

FITS images were plate-solved by *PinPoint* (DC-3 Dreams) or *TheSkyX* (Software Bisque) and calibrated using temperature-matched, median-averaged dark images and recent flat images of a flux-adjustable flat panel. Every photometric image was visually inspected; any images with poor tracking or with other light sources within 10 arcseconds of the target asteroid were excluded. Accepted photometry-ready images were submitted to the improved workflow, which applies separately measured second-order transforms from Clear filter to deliver asteroid magnitudes in Sloan r′ passband.

191 Kolga. The present synodic period determination of 17.595(7) h confirms those of 17.625 h (Warner, 2009) and 17.604 h (Pilcher, 2013) but differs from numerous other reports (Gil-Hutton and Cañada, 2003, 13.078 h; Holliday, 2001, 27.8 h; Behrend, 2009web, 27.8 h; Behrend, 2005web, 28.7 h), and it most notably differs from a web-reported period of 27.8(5) h (Behrend, 2020web) from observations reportedly made only 2-3 weeks before the data presented here. RMS error is 10 millimagnitudes.

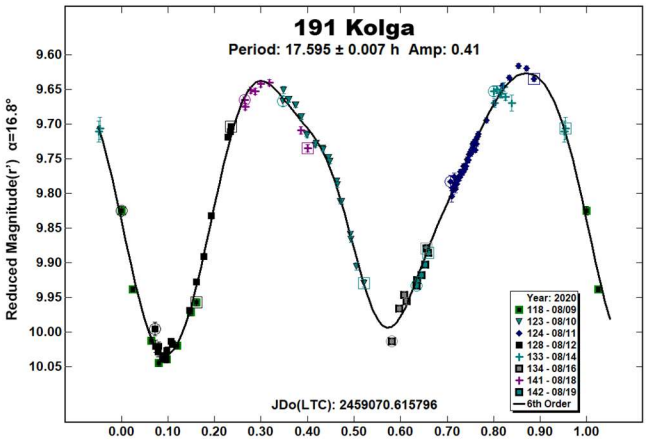

Number	Name	yyyy mm/dd	Phase	L_{PAB}	B_{PAB}	Period(h)	P.E.	Amp	A.E.	Grp
191	Kolga	2020 08/09-08/19	16.8, 18.3	270	12	17.595	0.007	0.41	0.02	MB-O
424	Gratia	2020 09/19-09/26	10.9, 8.6	18	-11	40.118	0.014	0.20	0.02	MB-O
570	Kythera	2020 09/18-09/24	10.3, 8.4	23	1	8.123	0.004	0.10	0.02	MB-O
605	Juvisia	2020 10/01-10/10	12.0, 9.8	30	18	15.851	0.003	0.18	0.01	MB-O
999	Zachia	2020 07/09-08/14	*10.1, 14.9	299	14	22.835	0.003	0.53	0.02	UKN
1108	Demeter	2020 07/12-08/05	29.2, 26.5	324	36	9.834	0.002	0.17	0.03	PHO
1306	Scythia	2020 09/30-10/13	12.7, 9.3	36	16	7.531	0.002	0.06	0.01	MB-O
1404	Ajax	2020 09/18-09/26	3.2, 4.9	342	4	29.411	0.024	0.26	0.02	TR-J
1576	Fabiola	2020 09/18-09/21	4.0, 2.9	5	0	6.889	0.002	0.26	0.01	THM
3578	Carestia	2020 10/02-10/13	17.3, 15.1	58	21	9.974	0.003	0.18	0.02	UNK
4738	Jimihendrix	2020 09/14-09/16	10.2, 9.3	10	4	5.175	0.002	0.17	0.01	EUN
5408	The	2020 09/25-10/07	12.0, 6.9	29	0	7.374	0.001	0.82	0.03	FLOR
5996	Julioangel	2020 09/18-10/03	9.5, 15.0	344	12	9.741	0.002	0.24	0.02	EUN
11220	1999 JM25	2020 09/18-10/09	7.6, 15.5	355	9	11.277	0.001	0.67	0.03	FLOR
19019	Sunflower	2020 08/07-08/12	*4.0, 4.0	318	7	3.322	0.002	0.24	0.04	MB-I
23482	1991 LV	2020 09/29-10/05	18.8, 19.3	1	25	3.139	0.001	0.33	0.03	H
23989	Farpoint	2020 08/13-09/19	*6.5, 15.5	327	8	15.244	0.003	0.47	0.06	EUN
25332	1999 KK6	2020 10/05-10/08	14.8, 14.6	10	19	2.452	0.002	0.11	0.03	H
28565	2000 EO58	2020 09/06-09/17	18.0, 23.1	327	5	2.234	0.001	0.08	0.03	MC

Table I. Observing circumstances and results. The phase angle is given for the first and last date. If preceded by an asterisk, the phase angle reached an extremum during the period. L_{PAB} and B_{PAB} are the approximate phase angle bisector longitude/latitude at mid-date range (see Harris et al., 1984). Grp is the asteroid family/group (Warner et al., 2009).

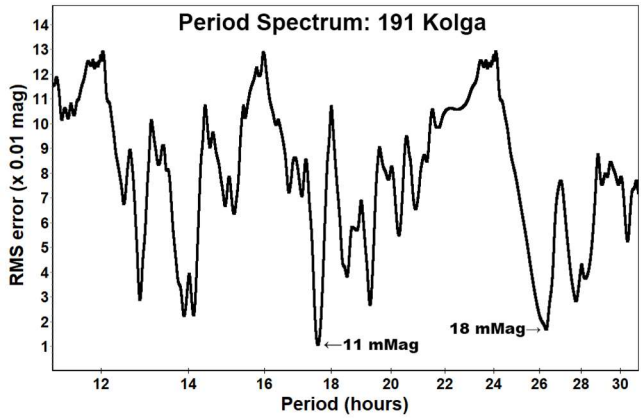

The persistence of reports of period 27.8 h for is almost certainly due to the alias (half-period per 24 hours) between 27.8 h and 17.595 h. The periodogram from present data, comprising eight sessions of observations, cannot support the 27.8 h alias; when using that candidate period, the lightcurve generated via Fourier fit is quadrimodal and not of reasonable shape. The report of 13.078 h is another alias of the present period, also of half-period per 24 h.

424 Gratia. The present synodic period of 40.118(14) h is roughly twice the two known determinations of 19.47 h (Florczak, 1997) and 20.075 h (Polakis, 2018), both assigned uncertainty codes of 3- in the LCDB (Lightcurve Data Base; Warner et al., 2009). The present data's high amplitude-to-noise and the difference in shape of the two maxima suggest that the secondary features seen at phases 0.38 and 0.86 (figure below) could be taken for a secondary minimum of a 20 h lightcurve, especially when observed at very different aspects (phase angle bisectors).

From the present observations, taken at a very different phase angle bisector from the previous ones, we propose a bimodal lightcurve of synodic period 40.118 h instead. A H-G (phase angle relation) G value of 0.0 was adopted for its superior Fourier fit to that using the standard G value of 0.15. RMS error is 6 millimagnitudes.

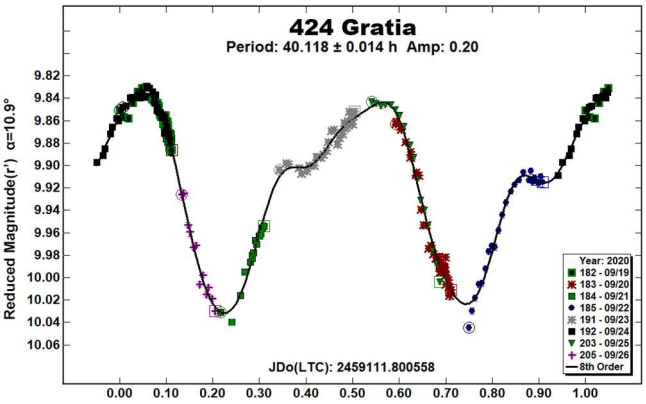

570 Kythera. This low-amplitude lightcurve yields a synodic period of 8.1230(36) h, in agreement with two previous period reports (Behrend, 2004web, 8.120 h; Aznar Macias et al., 2016, 8.074 h), but differing from previous period reports (Blanco et al., 2000, 6.919 h; Lagerkvist et al., 2001, 5.682 h; Gil-Hutton and Cañada, 2003, 6.903 h; and Chavez, 2014, 10.5 h). The proposed periods near 6.9 h differ from the present determination by one half-period per 24 h but do not appear in the present periodogram. The period of 10.5 h is based on a quite incomplete lightcurve. A G value of 0.40 markedly improved the present Fourier fit; RMS error is 8 millimagnitudes.

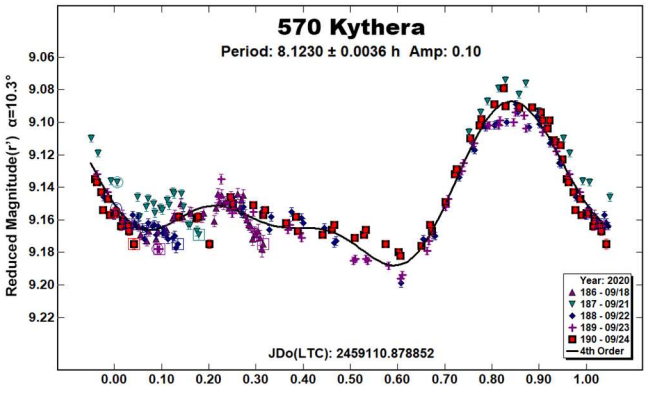

605 Juvisia. This bright outer main-belt asteroid was studied to refine its somewhat uncertain synodic period. We report a synodic period of 15.851(3) h, which agrees with three known reports, each with uncertainty code of 2 in the LCDB (Warner, 2000, 15.855 h; Menke, 2005, 15.85 h; Warner, 2011, 15.93 h). Adjusting the G (H-G) value to –0.05 from the MPC default of 0.15 markedly improved the Fourier fit. RMS error is 6 millimagnitudes.

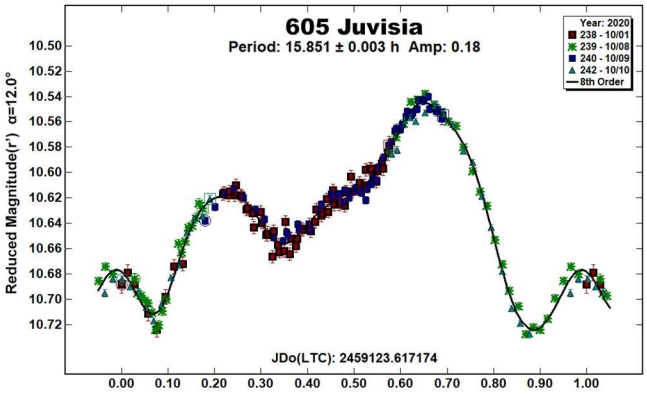

At different viewing aspect (phase angle bisector), the lightcurve has been reported to be symmetric, bimodal, and of higher amplitude (Warner, 2011). The present lightcurve shape is only loosely bimodal; the periodogram is unambiguous.

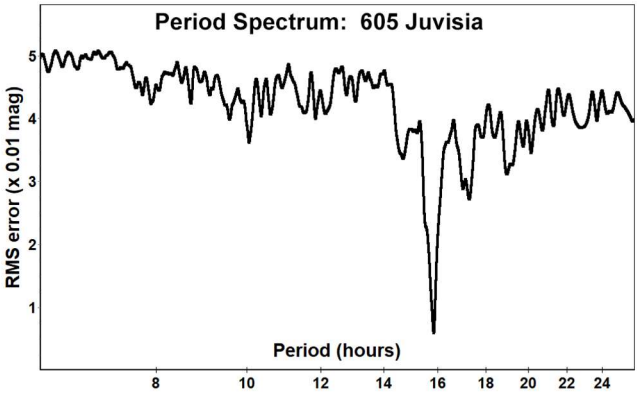

The present viewing aspect is new to this asteroid; this together with its changing lightcurve shape this suggests that asteroid shape modeling may be worthwhile. Juvisia's high orbital inclination will cause its 2022 January apparition to present another new viewing aspect as well.

999 Zachia. This well-studied asteroid of unknown group/family was observed at a new phase angle bisector to assist future shape studies. The present synodic period of 22.835(3) h agrees with all known previously reports (Warner, 2000, 22.77 h; Brines et al., 2017, 22.837; Pál et al., 2020, 22.812 h). The lightcurve is markedly bimodal and of relatively high amplitude. RMS error is 14 millimagnitudes.

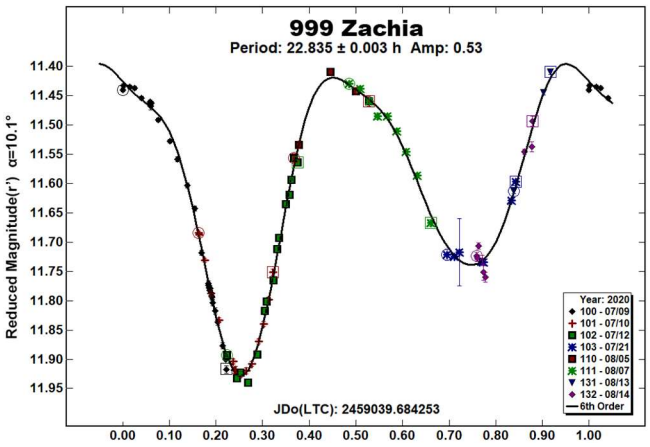

1108 Demeter. This well-studied Phocaea-family asteroid was observed to support future shape studies. The present synodic period is 9.8335(15) h, in reasonable agreement with previous reports (Behrend, 2001web, 9.701 h; Stephens, 2002, 9.70 h; Polakis and Skiff, 2016, 9.846 h; Brines et al., 2017, 9.870 h). The lightcurve is clearly bimodal and the amplitude is higher than previous reports. A G value of 0.6 optimized the Fourier fit. RMS error is 16 millimagnitudes.

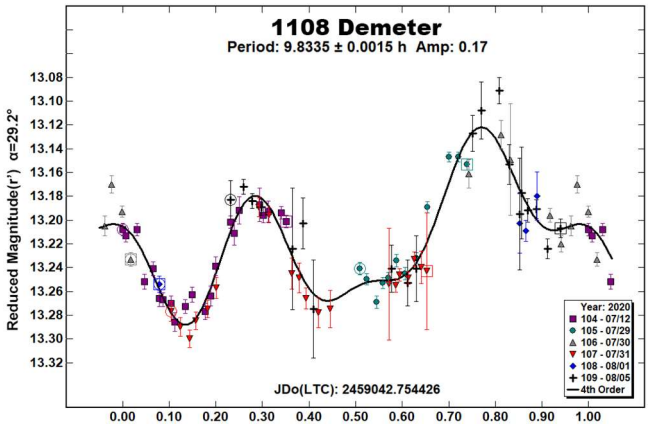

1306 Scythia. The lightcurve for this outer main-belt asteroid has been difficult to assign as monomodal or bimodal. The present observations were arranged to provide very high signal-to-noise as well as complete coverage of both monomodal and bimodal phases. The present data provide no support for a bimodal lightcurve interpretation, whether from inspection of phase plots or from periodograms or split-halves plots. The low amplitude, similar to those of other studies, allows for a monomodal lightcurve.

The proposed monomodal synodic period of 7.531(2) h matches one report (Behrend, 2008web, 7.525 h; amplitude 0.25) and is half the bimodal period in another report (Stephens, 2004, 15.05 h, amplitude 0.15). It is conceivable that the lightcurve could be bimodal at high amplitudes but effectively monomodal at viewing aspects giving low amplitudes. However, no data found in the LCDB appear to support bimodal behavior, so monomodal interpretation seems preferred. Fourier fit to the present data is improved by reducing the G value (H-G) to 0.10. RMS error is 6 millimagnitudes.

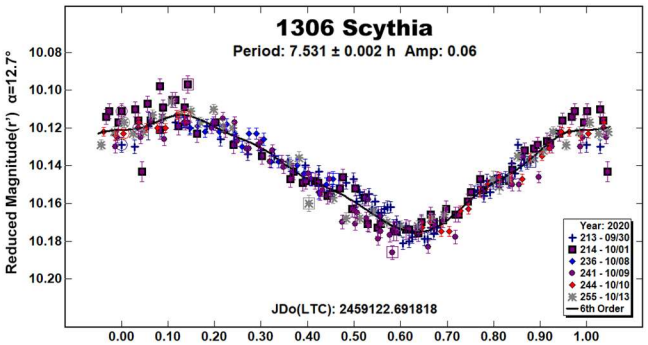

1404 Ajax. If any asteroid nomenclature contradicts history more unfortunately than does the classification of Ajax as a Trojan, the author is unaware of it. The present synodic period determination of 29.411(24) h agrees with the previous result of 29.38 h (French et al., 2011) with LCDB uncertainty code 3-, but differs from the result of 34 h (Behrend, 2009web) with uncertainty code 2- and from 28.4 h (Binzel and Sauter, 1992) with uncertainty 1. The present lightcurve is markedly bimodal. Adjusting the H-G value G to 0.35 improved the Fourier fit; RMS error is 14 millimagnitudes.

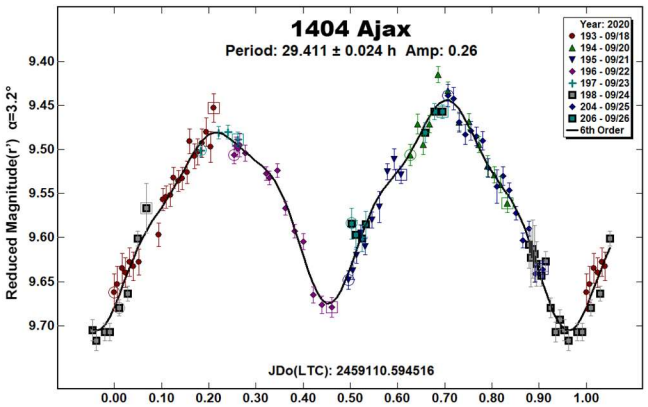

1576 Fabiola. This Themis-family asteroid was observed at a new phase angle bisector to support future shape studies. The synodic period was found to 6.889(2) h in exact agreement with that of Benishek (2018), and of very similar lightcurve shape despite the very different viewing aspect. The present result is also fairly close to an older report of 6.7 h from Lagerkvist (1978). G = 0 improved Fourier fits over the standard value of 0.15; RMS error is 12 millimagnitudes.

Night-to-night variation in the shelf feature at phase 0.6-0.7 (see figure) appears real but is difficult to explain as (a) the change is not monotonic with date of observation, and (b) the brightness decrease is not limited to one night in this one phase position, as would be likely for a binary in eclipse.

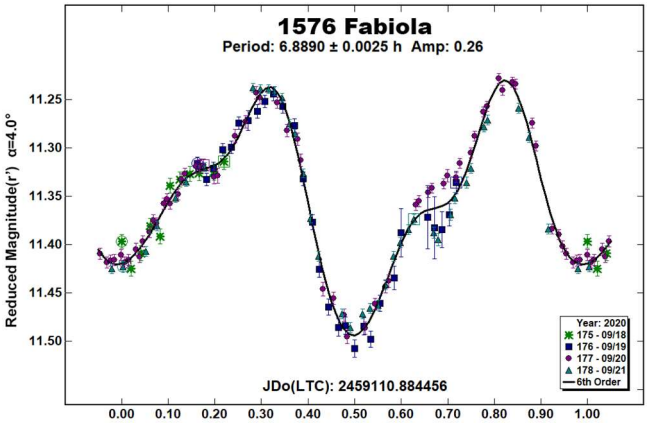

3578 Carestia. This large (diameter 59 km), very low albedo (0.02) asteroid of undetermined group was found to have a synodic period 9.974(3) h and a markedly bimodal lightcurve. This period agrees with one earlier report (Behrend, 2008web, 9.93 h) but disagrees with another (Holliday, 1997, 7.08 h) with incomplete phase coverage and substantial nightly shifts in zero-point. The present RMS error is 12 millimagnitudes.

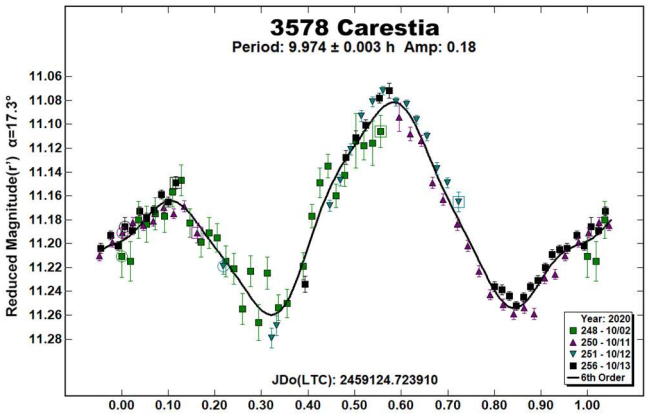

4738 Jimihendrix. This Eunomia-family asteroid was found to have a clearly bimodal lightcurve of synodic period 5.1750(25) h, in agreement with one previous survey period of 5.17729 h (Pál et al., 2020). G of 0.35 improved the Fourier fit over that of standard G of 0.15; RMS error is 9 millimagnitudes.

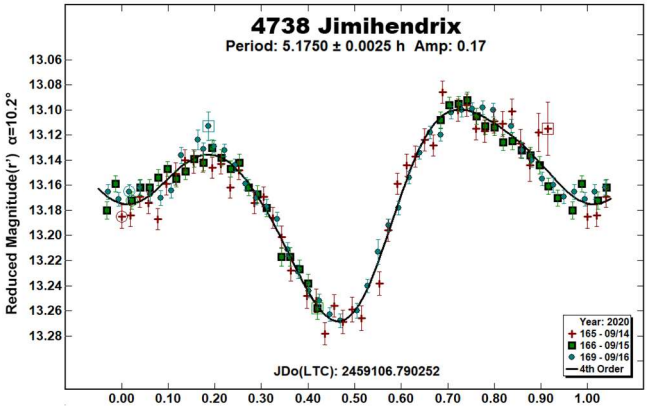

5408 The. This uniquely named Flora asteroid is confirmed to have synodic period 7.374(1) h, matching exactly the survey period previously reported (Waszczak et al., 2015, 7.374 h). The LCDB currently lists no other period reports. The slight brightness dip at phase 0.65 (see figure) appears real and is intriguing with regards to future shape modeling. A G value (H-G) of about 0.50 improved the Fourier fit over the default G of 0.15. RMS error is 41 millimagnitudes.

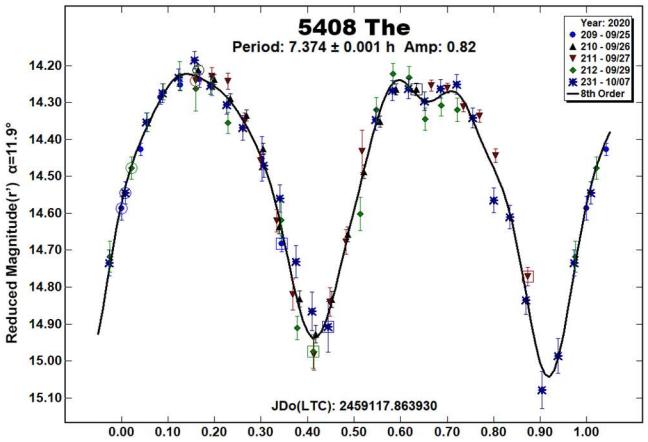

5996 Julioangel. This Eunomia-family asteroid was found to have synodic period 9.741(2) h, in agreement with the single known period report of 9.74 h (Durkee, 2018). Adjusting G value from 0.15 to 0.25 improved the Fourier fit; RMS error is 19 millimagnitudes.

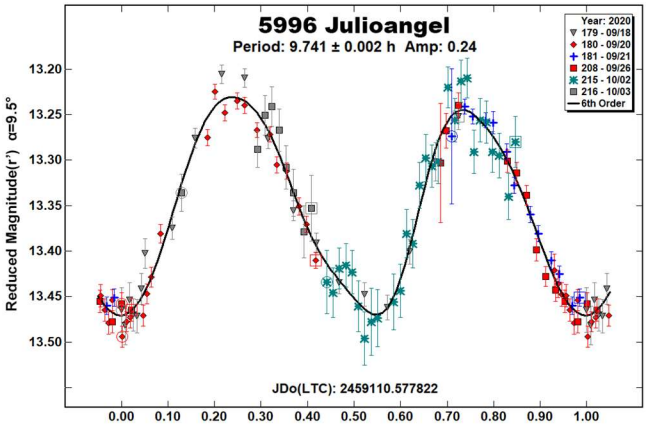

(11220) 1999 JM25. This Flora-family asteroid was found during its very favorable 2020 apparition to have synodic period of 11.277(1) h, confirming three reported periods from sparse photometry, each with LCDB-assigned uncertainty code of 2 (Waszczak et al., 2015, 11.280 h; Ďurech et al., 2018, 11.27965 h; Pál et al., 2020, 11.2733 h). A G value (H-G) of 0.20 improved the Fourier fit over G of 0.15; the present RMS error is 14 millimagnitudes. The present data suggest slightly higher amplitude at higher phase angles, as described by Zappalá et al. (1990).

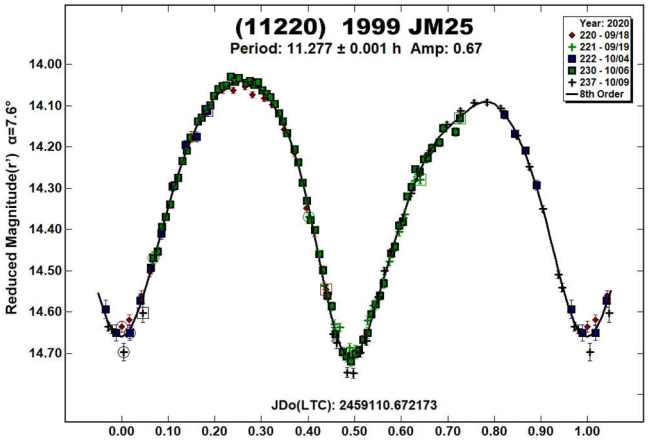

19019 Sunflower. This inner main-belt asteroid of estimated diameter 3-4 km was found to have synodic period of 3.3215(15) h, in close agreement with survey period reports of 3.320 h and 3.322 h (Waszczak et al., 2015). RMS error is 44 millimagnitudes.

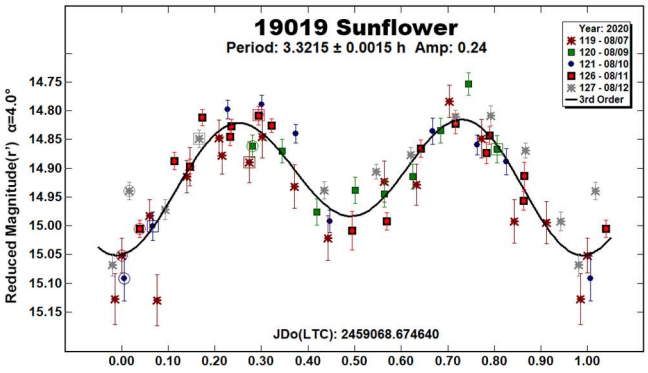

(23482) 1991 LV. This faint Hungaria was studied to rule out alises that have been problematic for this asteroid's lightcurves. We found an unambiguous synodic period of 3.1388(4) h, in agreement with 2012 observations of (Warner, 2012, 3.1388 h; Warner, 2016, 3.126 h) but not with the same author's 2015 observations (Warner, 2016, 3.357 h). RMS error is 26 millimagnitudes.

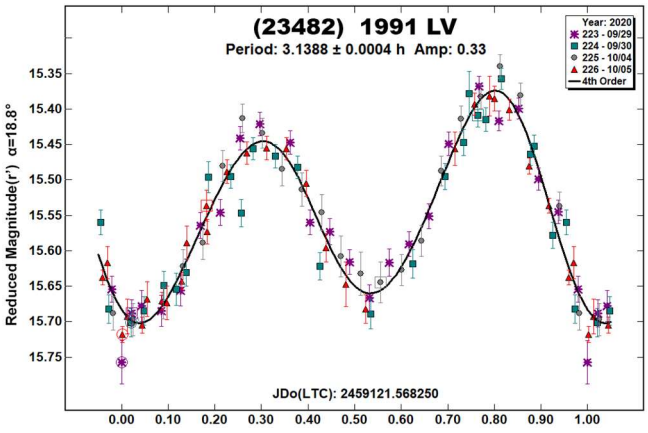

The present observations benefited from an advantageous pattern of session dates, a clearly bimodal lightcurve, and very favorable declinations permitting unusually long observations (up to 2.4 periods per session), so that the present data effectively rule out the candidate period of 3.357 h as an alias (half-period per 24 hours), as confirmed by the periodogram. No evidence of a secondary period (Warner, 2012) was seen in the present data.

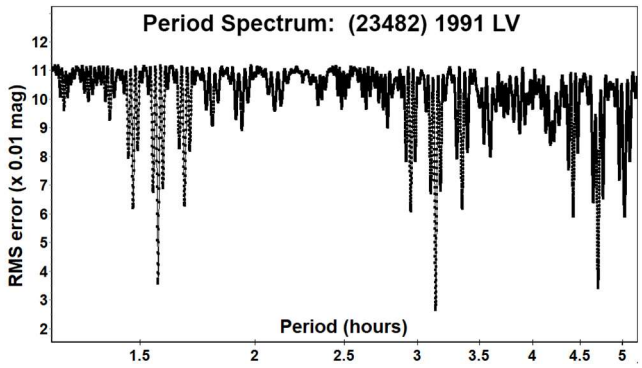

(23989) Farpoint. This Eunomia-family asteroid, named for the Kansas observatory in which the author performed his first asteroid astrometry, was discovered 1999 by Gary Hug and Graham Bell who established the observatory. The LCDB lists no previous period reports. The present synodic period of 15.244(3) appears correct despite Sloan r′ magnitudes frequently exceeding 18 as measured with a 0.35-m telescope, and despite a few sessions' occurring during the western U.S. atmospheric smoke events of August-September. RMS error is 67 millimagnitudes. This asteroid will be difficult to observe again through at least 2024.

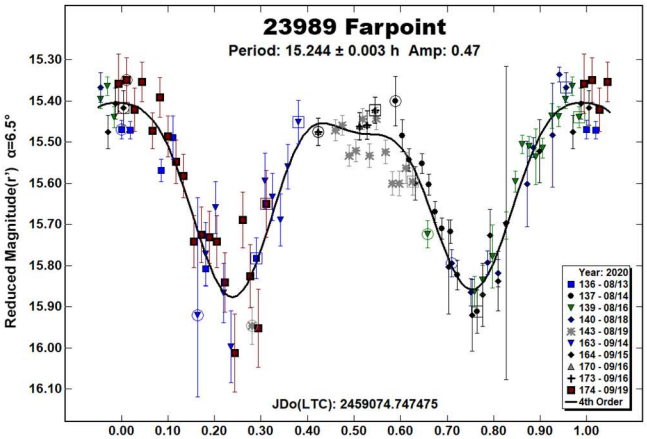

(25332) 1999 KK6. This Hungaria was observed in an effort to distinguish between a monomodal (period near 2.45 h) or bimodal (ca. 4.9 h) lightcurve. The lightcurve appears monomodal, with synodic period 2.4520(16) h, in agreement with earlier results reported as monomodal (Warner, 2008, 2.4531 h; Warner, 2013, 2.453 h; Warner, 2016, 2.4531 h). The present lightcurve is dominated by a rapid dimming of 0.09 magnitudes, 80% of the total amplitude, within 20-25 minutes (phase 0.95-0.10 in figure). RMS error is 19 millimagnitudes.

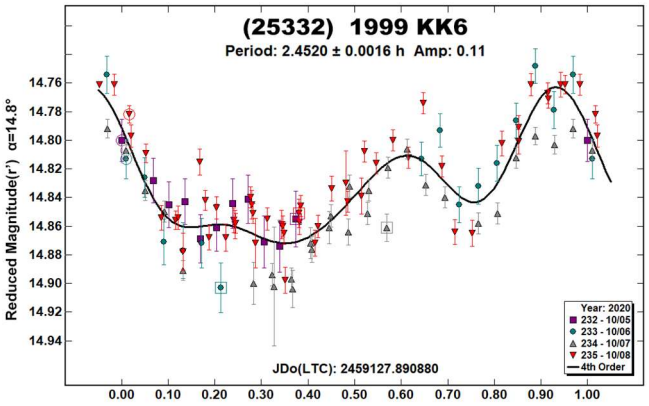

At fourth-order Fourier fitting, the monomodal period dominates; RMS error decreased very little when applying Fourier terms beyond fourth order. The low amplitude, to date always reported as 0.11 mag or less, allows for a monomodal lightcurve. Our results support a monomodal interpretation and period near 2.452 h.

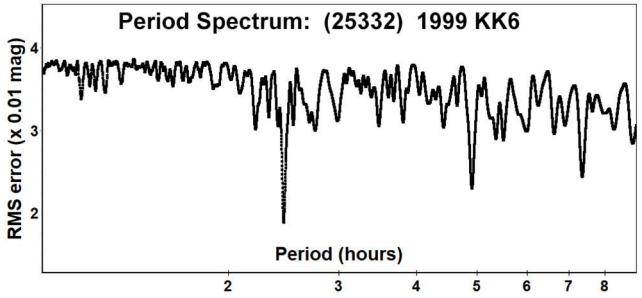

(28565) 2000 EO58. The synodic period for this small (estimated diameter 2.8-3.0 km), low-amplitude Mars-crosser remains ambiguous due to 24-hour aliasing, yielding two period estimates: 2.234 h and 2.460 h. The present observations do appear to rule out the previously reported period of 3.83 h (Behrend, 2004web) assigned a LCDB uncertainty code of 1. G value of 0.25 improved the Fourier fit over that with G assumed to be 0.15; RMS error is 19 millimagnitudes.

Given the lightcurve's low amplitude, it may not be practical to resolve this aliasing from a single geographic location; observing from at least two locations widely separated in longitude would be the best approach.

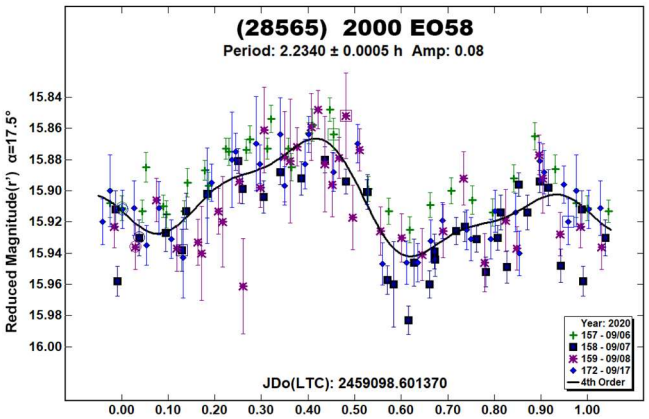

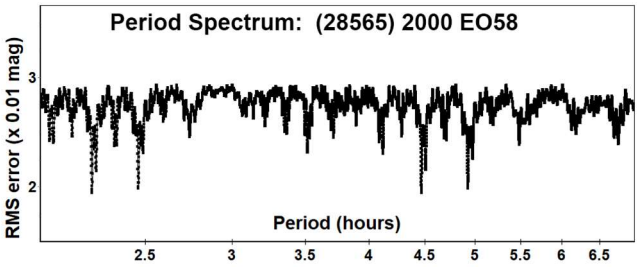

Acknowledgements

The author thanks the authors of the ATLAS paper (Tonry et al., 2018) and their very many contributors for providing without cost the ATLAS refcat2 catalog and its detailed technical descriptions.

This project's computations make extensive use of the python language interpreter and of several supporting packages (notably: pandas, ephem, matplotlib, requests, astropy, and statsmodels), all provided without cost, and without which this work would have been infeasible.

References

Aznar Macias, A.; Carreno Garcerain, A.; Arce Masego, E.; Brines Rodriguez, P.; Lozano de Haro, J.; Fornas Silva, A.; Fornas Silva, G.; Mas Martinez, V.; Rodrigo Chiner, O.; Herrero Porta, D. (2016). "Twenty-one Asteroid Lightcurves at Group Observadores de Asteroides (OBAS): Late 2015 to Early 2016." *Minor Planet Bull.* **43**, 257-263.

Behrend, R. (2001web, 2004web, 2005web, 2008web, 2009web, and 2020web). Observatoire de Geneve web site. *http://obswww.unige.ch/~behrend/page_cou.html*

Benishek, V. (2018). "Lightcurve and Rotation Period Determinations for 29 Asteroids." *Minor Planet Bull.* **45**, 82-91.

Binzel, R.P.; Sauter, L.M. (1992). "Trojan, Hilda, and Cybele asteroids: New lightcurve observations and analysis." *Icarus* **95**, 222-238.

Blanco, C.; Di Martino, M.; Riccioli, D. (2000). "New rotational periods of 18 asteroids." *Planetary and Space Science*, **48**, 271-284.

Brines, P.; Lozano, J.; Rodrigo, O.; Fornas, A.; Herrero, D.; Mas, V.; Fornas, G.; Carreño, A.; Arce, E. (2017). "Sixteen Asteroids Lightcurves at Asteroids Observers (OBAS) - MPPD: 2016 June-November." *Minor Planet Bull.* **44**, 145-149.

Chavez, C.F. (2014). "Photometric Observations of Asteroid 570 Kythera using the Virtual Telescope Project." *Minor Planet Bull.* **41**, 60.

Dose, E. (2019). Code repository "photrix", version tag 2.0.1, *https://github.com/edose/photrix*

Dose, E. (2020a). Code repository "mpc", version tag 0.1beta, *https://github.com/edose/mpc*

Dose, E. (2020b). "A New Photometric Workflow and Lightcurves of Fifteen Asteroids." *Minor Planet Bull.* **47**, 324-330.

Ďurech, J.; Hanuš, J.; Alí-Lagoa, V. (2018). "Asteroid models reconstructed from the Lowell Photometric Database and WISE data." *Astron. Astrophys.*, **617**, A57.

Durkee, R.I. (2018). "Neglected Lightcurves from the Shed of Science." *Minor Planet Bull.* **45**, 333-335.

Florczak, M.; Dotto, E.; Barucci, M.A.; Birlan, M.; Erikson, A.; Fulchignoni, M.; Nathues, A.; Perret, L.; Thebault, P. (1997). "Rotational properties of main belt asteroids: photoelectric and CCD observations of 15 objects." *Planetary and Space Science*, **45**, 1423-1435.

French, L.M.; Stephens, R.D.; Lederer, S.M.; Coley, D.R.; Rohl, D.A. (2011). "Preliminary Results from a Study of Trojan Asteroids." *Minor Planet Bull.* **38**, 116-120.

Gelman, A.; Hill, J. (2006). *Data Analysis Using Regression and Multilevel/Hierarchical Models*. Cambridge University Press, New York.

Gil-Hutton, R.; Cañada, M. (2003). "Photometry of Fourteen Main Belt Asteroids." *Rev. Mex. Astron. y Astrophys.* **39**, 69-76.

Harris, A.W.; Young, J.W.; Scaltriti, F.; Zappala, V. (1984). "Lightcurves and phase relations of the asteroids 82 Alkmene and 444 Gyptis." *Icarus* **57**, 251-258.

Holliday, B. (1997). "Photometric Observations of Minor Planet 3578 Caresia." *Minor Planet Bull.* **24**, 1.

Holliday, B. (2001). "Photometry of Asteroid 191 Kolga and 1200 Imperatrix." *Minor Planet Bull.* **28**, 13.

Lagerkvist, C.-I. (1978). "Photographic photometry of 110 main-belt asteroids." *Astron. Astrophys. Suppl. Series* **31**, 361.

Lagerkvist, C.-I.; Erikson, A.; Lahulla, F.; De Martino, M.; Nathues, A.; Dahlgren, M. (2001). "A Study of Cybele Asteroids. I. Spin Properties of Ten Asteroids." *Icarus* **149**, 190-197.

Menke, J. (2005). "Asteroid lightcurve results from Menke Observatory." *Minor Planet Bull.* **32**, 85-88.

Pál, A.; Szakáts, R.; Kiss, C.; Bódi, A.; Bognár, Z.; Kalup, C.; Kiss, L.L.; Marton, G.; Molnár, L.; Plachy, E.; Sárneczky, K.; Szabó, G.M.; Szabó, R. (2020). "Solar System Objects Observed with TESS - First Data Release: Bright Main-belt and Trojan Asteroids from the Southern Survey." *Astrophys. J. Suppl. Series* **247**, 1.

Pilcher, F. (2013). "Rotation Period Determinations for 24 Themis, 159 Aemilia 191 Kolga, 217 Eudora, 226 Weringia, 231 Vindobona, and 538 Friederike." *Minor Planet Bull.* **40**, 85-87.

Polakis, T.; Skiff, B.A. (2016). "Lightcurve Analysis for Asteroids 895 Helio and 1108 Demeter." *Minor Planet Bull.* **43**, 310.

Polakis, T. (2018). "Lightcurve Analysis for Fourteen Main-belt Minor Planets." *Minor Planet Bull.* **45**, 347-352.

Stephens, R.D. (2002). "Photometry of 866 Fatme, 894 Erda, 1108 Demeter, and 3443 Letsungdao." *Minor Planet Bull.* **29**, 2-3.

Stephens, R.D. (2004). "Photometry of 804 Hispania, 899 Jokaste, 1306 Scythia, and 2074 Shoemaker." *Minor Planet Bull.* **31**, 40-41.

Tonry, J.L.; Denneau, L.; Flewelling, H.; Heinze, A.N.; Onken, C.A.; Smartt, S.J.; Stalder, B.; Weiland, H.J.; Wolf, C. (2018). "The ATLAS All-Sky Stellar Reference Catalog." *Astrophys. J.* **867**, A105.

Warner, B. (2000). "Asteroid Photometry at the Palmer Divide Observatory." *Minor Planet Bull.* **27**, 4-6.

Warner, B.D. (2008). "Asteroid Lightcurve Analysis at the Palmer Divide Observatory: September-December 2007." *Minor Planet Bull.* **35**, 67-71.

Warner, B.D. (2009). "Asteroid Lightcurve Analysis at the Palmer Divide Observatory: 2009 March-June." *Minor Planet Bull.* **36**, 172-176.

Warner, B.D.; Harris, A.W.; Pravec, P. (2009). "The asteroid lightcurve database." *Icarus*, **202**, 134-146. Updated 2020 August. *http://www.minorplanet.info/lightcurvedatabase.html*

Warner, B.D. (2011). "Upon Further Review: IV. An Examination of Previous Lightcurve Analysis from the Palmer Divide Observatory." *Minor Planet Bull.* **38**, 52-54.

Warner, B.D. (2012). "Asteroid Lightcurve Analysis at the Palmer Divide Observatory: 2012 March-June." *Minor Planet Bull.*, **39**, 245-252.

Warner, B.D. (2013). "Rounding Up the Unusual Suspects." *Minor Planet Bull.* **40**, 36-42.

Warner, B.D. (2016). "Asteroid Lightcurve Analysis at CS3-Palmer Divide Station: 2015 December - 2016 April." *Minor Planet Bull.* **43**, 227-233.

Warner, B.D. (2018). *MPO Canopus* Software, version 10.7.12.9, BDW Publishing. *http://www.bdwpublishing.com*

Waszczak, A.; Chang, C.-K.; Ofek, E.O.; Laher, R.; Masci, F.; Levitan, D.; Surace, J.; Cheng, Y.-C.; Ip, W.-H.; Kinoshita, D.; Helou, G.; Prince, T.A.; Kulkarni, S. (2015). "Asteroid Light Curves from the Palomar Transient Factory Survey: Rotation Periods and Phase Functions from Sparse Photometry." *Astron. J.* **150**, 3.

Zappalá, V.; Cellino, A.; Barucci, A.M.; Fulchignoni, M.; Lupishko, D.F (1990), "An analysis of the amplitude-phase relationship among asteroids", *Astron. Astrophys.*, **231**, 548-560.

PHOTOMETRY OF 30 ASTEROIDS AT SOPOT ASTRONOMICAL OBSERVATORY: 2020 FEBRUARY - OCTOBER

Vladimir Benishek
Belgrade Astronomical Observatory
Volgina 7, 11060 Belgrade 38, SERBIA
vlaben@yahoo.com

(Received: 2020 Oct 15 Revised: 2020 Nov 8)

CCD photometric observations of 30 asteroids were conducted at Sopot Astronomical Observatory (SAO) from 2020 February through 2020 October. A review of the results obtained for synodic rotation periods as well as the established lightcurves is presented here.

Photometric observations of 30 asteroids were conducted at Sopot Astronomical Observatory (SAO) from 2020 February through 2020 October in order to determine the asteroids' synodic rotation periods. For this purpose, two 0.35-m *f*/6.3 Meade LX200GPS Schmidt-Cassegrain telescopes were employed. The telescopes are equipped with a SBIG ST-8 XME and a SBIG ST-10 XME CCD cameras. The exposures were unfiltered and unguided for all targets. Both cameras were operated in 2×2 binning mode, which produces image scales of 1.66 arcsec/pixel and 1.25 arcsec/pixel for ST-8 XME and ST-10 XME cameras, respectively. Prior to measurements, all images were corrected using dark and flat field frames.

Photometric reduction was conducted using *MPO Canopus* (Warner, 2018). Differential photometry with up to five comparison stars of near solar color ($0.5 \leq$ B-V ≤ 0.9) was performed using the Comparison Star Selector (CSS) utility. This helped ensure a satisfactory quality level of night-to-night zero-point calibrations and correlation of the measurements within the standard magnitude framework. Field comparison stars were calibrated using standard Cousins R magnitudes derived from the Carlsberg Meridian Catalog 15 (VizieR, 2020) Sloan r' magnitudes using the formula: R = r' - 0.22 in all cases presented in this paper. In some instances, small zero-point adjustments were necessary in order to achieve the best match between individual data sets in terms of achieving the most favorable statistical indicators of Fourier fit goodness.

For the first time, lightcurve construction and period analysis was performed using *Perfindia* custom-made software developed in the R statistical programming language (R Core Team, 2020) by the author of this paper. The essence of its algorithm is reflected in finding the most favorable solution for rotational period by minimizing the *residual standard error* of the lightcurve Fourier fit.

The lightcurve plots presented in this paper show so-called 2% error for rotational periods, i.e. an error that would cause the last data point in a combined data set by date order to be shifted by 2% (Warner, 2012) and which is represented by the following formula: $\Delta P = (0.02 * P^2) / T$, where P and T are the rotational period and the total time span of observations, respectively. Both of these quantities must be expressed in the same units.

Some of the targets presented in this paper were observed within the Photometric Survey for Asynchronous Binary Asteroids (*BinAstPhot Survey*) under the leadership of Dr Petr Pravec from Ondřejov Observatory, Czech Republic.

Table I gives the observing circumstances and results.

Observations and results

2034 Bernoulli. The photometric data obtained on four nights at SAO show an almost identical rotation period result (P = 6.249 ± 0.003 h) as found by Alkema (2013, 6.248 h) and Pal et al. (2020, 6.24919 h).

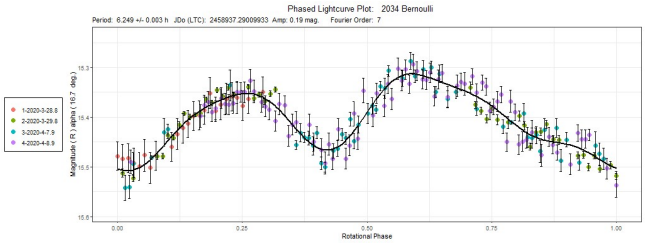

2050 Francis. This Phocaea family asteroid was followed up photometrically over a long time span of almost two months (2020 March 12 - 2020 May 09) during which a noticeable transformation of the lightcurve shape occurred, i.e. a gradual transition from a bimodal to an almost monomodal shape, indicating a change from a more equatorial view to a rather polar observing aspect. Depending on the interval of the solar phase angles in which the data were collected, three independent lightcurves were constructed. All three lightcurves show a consistent synodic rotational period (2020 Mar 12-18, 3.069 ± 0.002 h; 2020 Apr 05-09, 3.067 ± 0.003 h; 2020 May 03-09, 3.068 ± 0.002 h), which is fully consistent with a previously found period by Franco et al. (2013, 3.069 h).

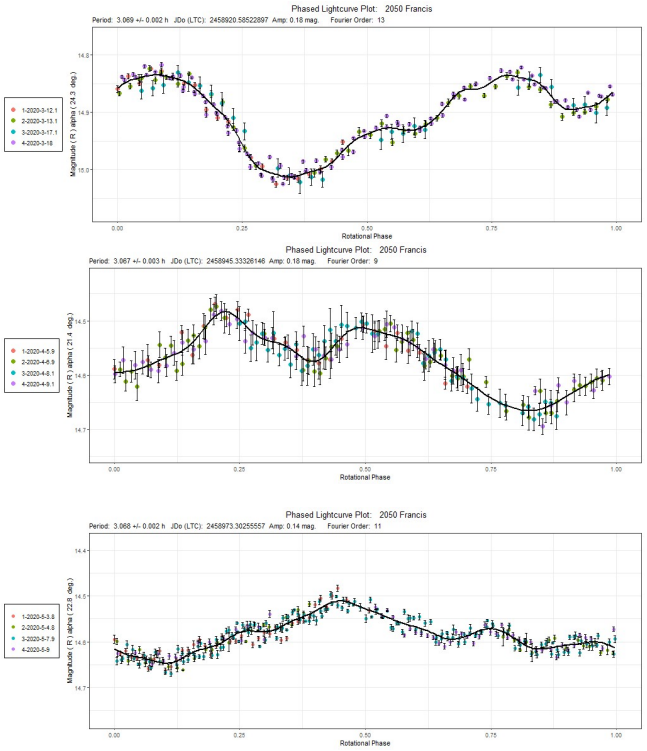

2151 Hadwiger. Several consistent synodic rotation periods were found previously, some of which are by Sada et al. (2005, 5.872 h) and Waszczak et al. (2015, 5.870 h and 5.871 h). Dense SAO photometric data taken in 2020 April yielded as a lightcurve solution a bimodal curve folded to a period of P = 5.870 ± 0.002 h.

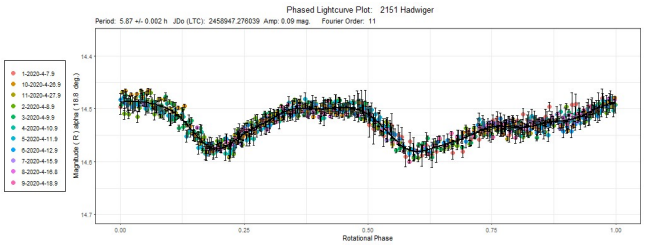

2334 Cuffey. The observations over three nights in late April and early May 2020 led to a unique bimodal solution for period of P = 5.858 ± 0.002 h, completely consistent with the two results reported by other authors: 5.858 h (Klinglesmith et al., 2013) and 5.85644 h (Pal et al., 2020).

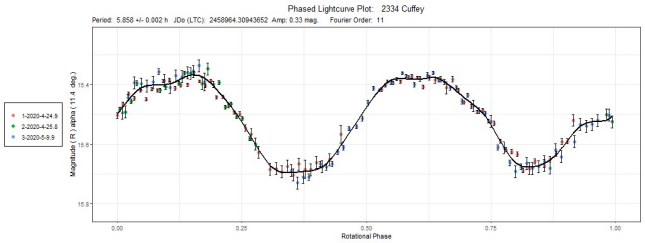

2341 Aoluta. This Flora family asteroid was found to have a rotational period of P = 3.0032 ± 0.0005 h from the SAO observations obtained on four nights between 2020 February 24 and 2020 March 12. This newly found result agrees well with the previously determined values by Sauppe et al. (2007, 3.0 h) and Behrend (2010, 2.998 h).

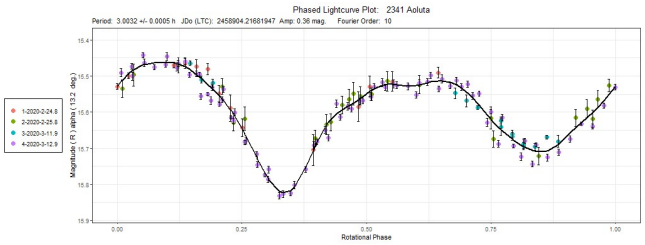

2665 Schrutka. Data obtained only over a single night in late 2020 September on this Flora family asteroid although insufficient to determine a period more accurately, still clearly indicate the value of P = 2.70 ± 0.02 h, which agrees with the previously found rotation periods by Ditteon (2010, 2.7170 h), Waszczak (2015, 2.716 h), Erasmus et al. (2020, 2.716 h) and Pal (2020, 2.71633 h) within the limits of the achieved accuracy.

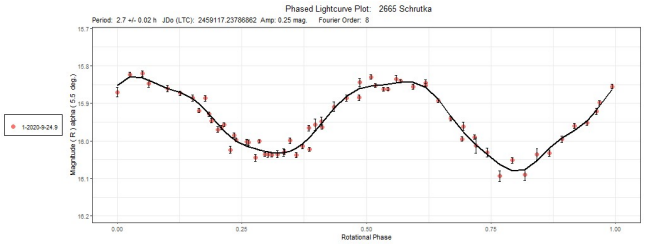

2962 Otto. A number of fairly consistent period solutions are present in the Asteroid Lightcurve Database (LCDB) (Warner et al., 2009). Some of these are by Ellsworth et al. (2002, 2.68 h) and Behrend (2007, 2.678 h; 2016, 2.67756 h; 2020, 2.67791 h). Rather densely sampled data taken on 2020 March 19 and 20 show a statistically identical result (P = 2.678 ± 0.006 h).

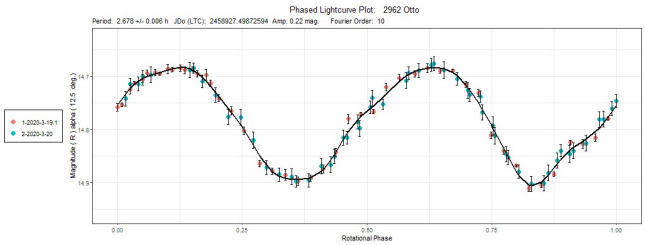

3068 Khanina. Data collected on three nights in 2020 April show a period of P = 3.560 ± 0.002 h, which is in good agreement with the result previously reported by Behrend (2010, 3.61 h).

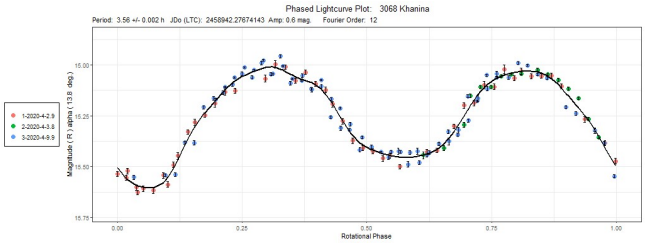

3453 Dostoevsky. Previous period results reported by Carbo et al. (2009, 3.16 h), Polishook (2009, 3.20 h), as well as by Benishek (2019, 3.16020 h) are consistent with the new rotation period result of P = 3.163 ± 0.004 h, derived from the SAO data taken on three consecutive nights in 2020 March.

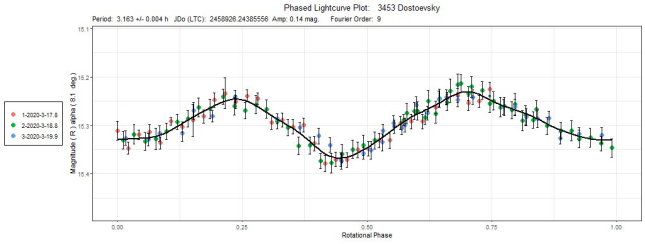

3895 Earhart. Two independent composite lightcurves were constructed from two data groups obtained in different view geometries. The first lightcurve includes data obtained in the time span 2020 May 08 - June 03. The other one is made up of data obtained on two consecutive nights in early 2020 July. Both data subsets indicate consistent unique period values of 3.5646 ± 0.0005 h and 3.57 ± 0.01 h, respectively. These values are fully in line with several previously determined periods listed in the LCDB: 3.56451 h (Behrend, 2009), 3.564 h (Warner, 2009), 3.556 h (Aznar Macias et al., 2016), 3.5645 h (Skiff, 2016).

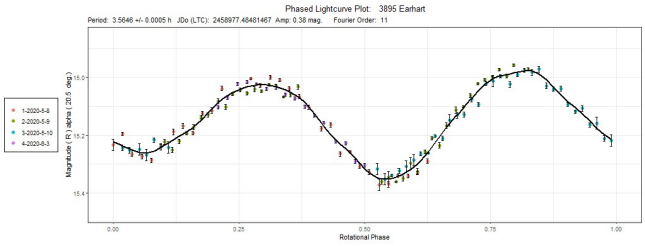

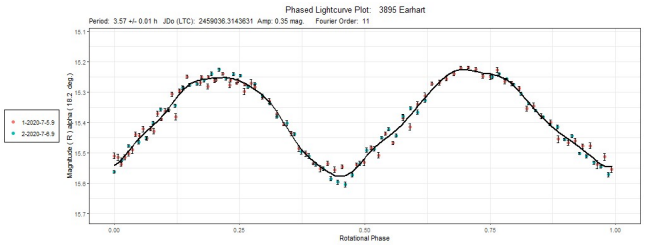

3913 Chemin. A period value of P = 3.4070 ± 0.0005 h found from the SAO data (2020 May 25 - 2020 June 13) for this *BinAstPhot Survey* target is completely consistent with previous results listed in the LCDB: 3.4077 h (Higgins and Goncalves Rui, 2007), 3.4086 (Behrend, 2009), 3.4074 h (Pravec, 2009), 3.4076 h (Chiorny et al., 2011), 3.408 h (Klinglesmith et al., 2016).

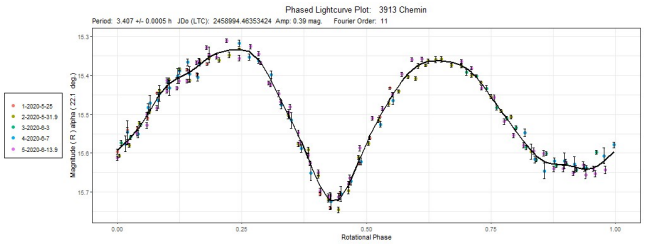

4353 Onizaki. Another *BinAstPhot Survey* target observed at SAO on five nights in late April and early May 2020. A unique bimodal solution for period of P = 4.430 ± 0.003 h was found. From the same SAO combined dataset Pravec finds 4.4296 ± 0.0002 h (Pravec, 2020) for rotation period. A quite good agreement with previously determined rotation periods is obvious in this case as well. Some of previously reported rotation period values from the LCDB are: 4.429 h (Waszczak, 2015) and 4.49 h (Behrend, 2020).

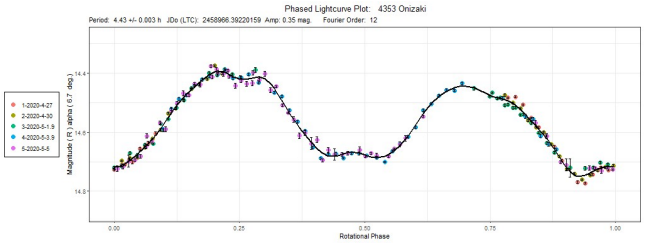

4491 Otaru. No records on previous rotation period determination reports were found. The 2020 August SAO observations unequivocally indicate a bimodal solution for a rotation period of P = 2.936 ± 0.004 h.

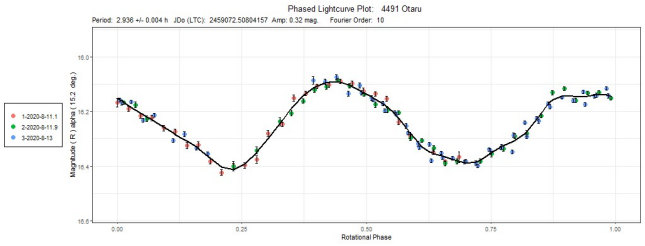

5222 Ioffe. The earliest rotation period determination for this asteroid dates back to 2006, when a value of 19.4 h was found by Warner (2006). The associated lightcurve suffers from insufficient data coverage. Waszczak et al. (2015) obtain almost half the value found by Warner, i.e. 9.739 h. The latter result is almost identical to P = 9.72 ± 0.02 h found from the dense 2020 July SAO data collected in the course of seven nights. The SAO data densely cover twice the found rotational cycle (2*P = 19.44 h), which is almost identical to the result found by Warner. The corresponding split-halves plot for the long period indicates a high degree of equality between two halves of the lightcurve, which favors the short period of 9.72 hours.

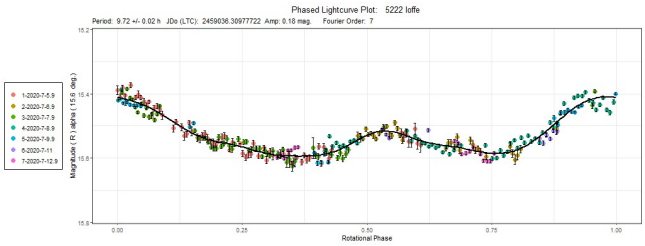

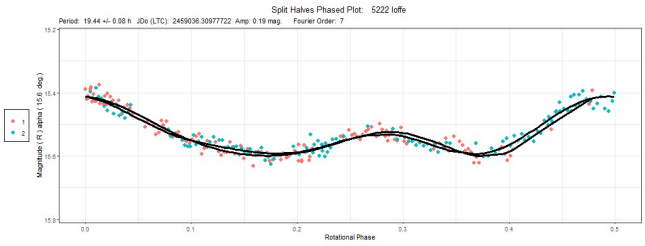

6434 Jewitt. A bimodal period solution found from the 2020 July SAO data of P = 3.237 ± 0.005 h is identical to the previous result reported by Waszczak et al. (2015, 3.237 h) and in fairly good agreement with the one found recently by Behrend (2020, 3.226 h).

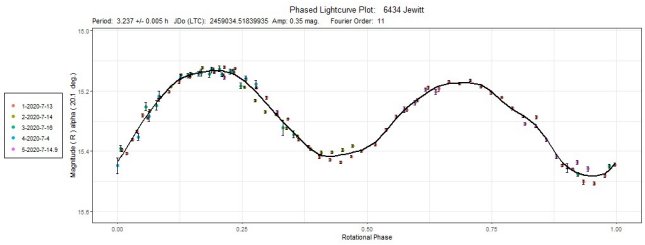

(7234) 1986 QV3. There are no records on previous rotation period determinations for this asteroid. Photometric data taken over three nights in the first half of 2020 October indicate a bimodal lightcurve solution phased to a period of P = 2.848 ± 0.003 h.

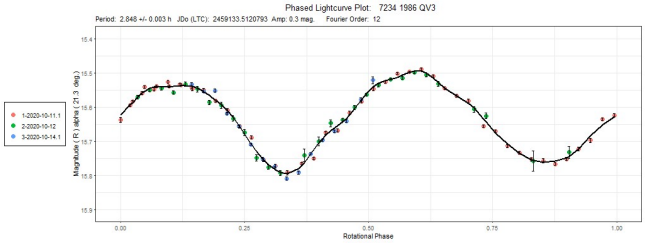

7910 Aleksola. No previous rotation period determination reports were known on this asteroid. As a *BinAstPhot* target it was observed at SAO on seven nights from 2020 May 22 through June 3. Period analysis found an unambiguous period value of P = 6.420 ± 0.003 h. From the same data Pravec derived a value of 6.4197 ± 0.0004 h.

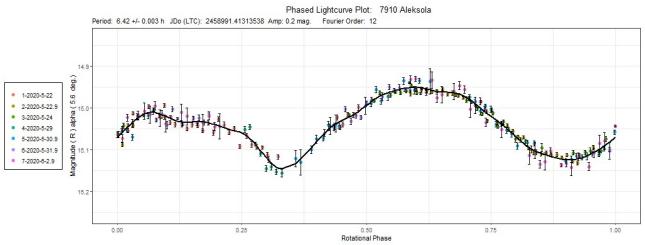

(8278) 1991 JJ. No previous rotation period determinations were known. Already the first datasets obtained indicated a slow rotation. A total of 14 datasets obtained within almost a month time span, from 2020 March 19 through 2020 April 15 covered quite evenly a large portion of a high amplitude (~1 mag.) bimodal lightcurve folded to a period of P = 75.1 ± 0.2 h as the most plausible solution that could be found from the available data.

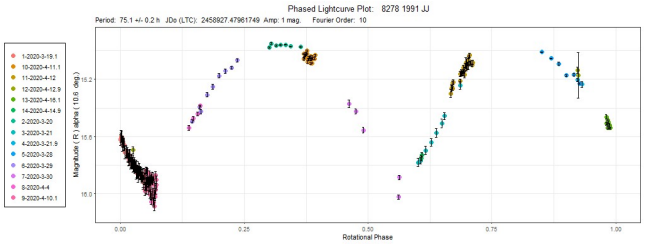

(10419) 1998 XB4. No referenced information on previous rotation period determinations were found. Data acquired over two consecutive nights in 2020 March show an unambiguous bimodal synodic rotation period of P = 7.03 ± 0.04 h.

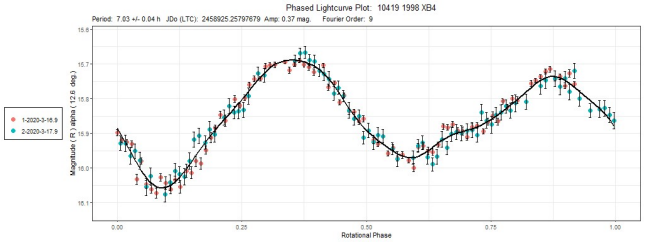

12112 Sprague. No prior rotation period determination references are known. An equivocal bimodal solution of P = 3.831 ± 0.006 h for synodic rotation period was found in period analysis which included photometric data collected over three consecutive nights in the first half of 2020 July.

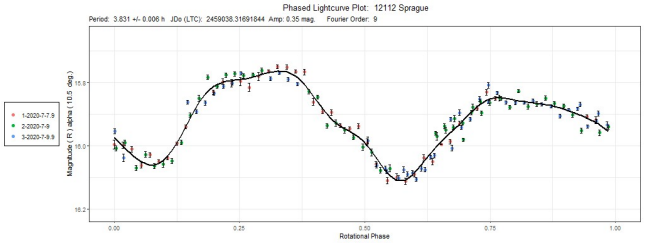

(13195) 1997 CG6. A *Binastphot Survey* target with no previously known rotation period observed at SAO in the course of four nights in 2020 February-March. Period analysis shows a bimodal solution for synodic rotation period of P = 2.9960 ± 0.0008 h. Using the same dataset Pravec (2020) found a value of 2.99598 h for period.

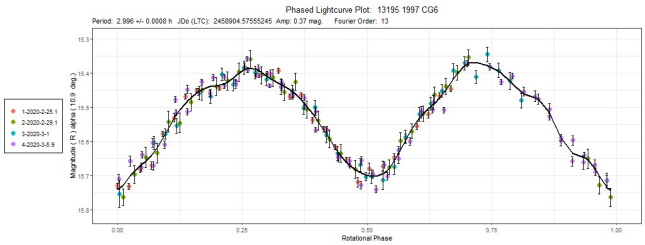

15710 Bocklin. An unambiguous bimodal solution for period of P = 7.523 ± 0.002 h was found in period analysis conducted upon the data obtained within the *Binastphot Survey* on nine nights in 2020 April-May. Pravec (2020) found a period value of 7.52248 ± 0.00009 h using the SAO data. These values are fully consistent with the recently published period result by Erasmus et al. (2020) of 7.521 h.

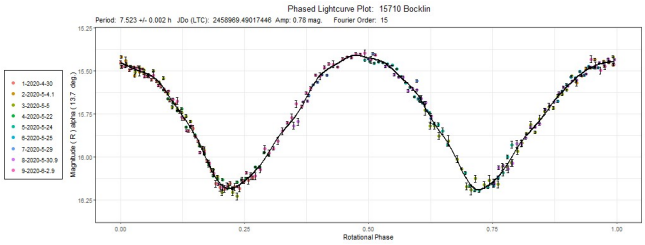

(17711) 1997 WA7. The only previous rotation period result found recently by Behrend (2020) of 3.66176 h is in good accordance with a period value of P = 3.6749 ± 0.0005 h found from the SAO observations carried out in 2020 May-June.

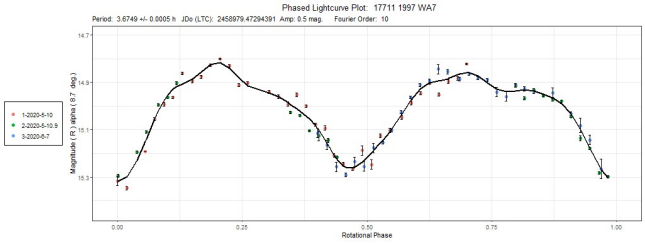

(19186) 1991 VY1. Any information on previous photometry of this Phocaea family asteroid were not found. Photometric observations of this asteroid within the *Binastphot Survey* on nine nights in 2020 August - September yielded a rotation period solution of P = 8.291 ± 0.006 h associated with a somewhat complex lightcurve. Excluding a few short datasets from the same combined SAO data, Pravec (2020) still derived almost the same result for period of 8.292 h as the most favorable one.

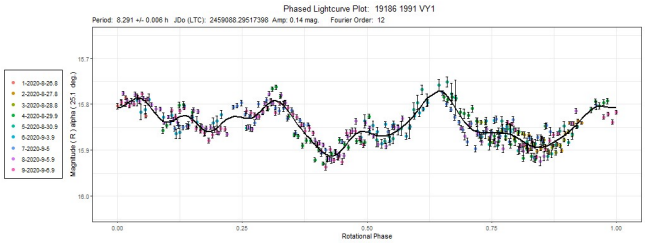

(27057) 1998 SP33. Prior reports on rotation period determinations were not known for this Mars-crossing asteroid. Period analysis performed upon the photometric data gathered on three consecutive nights in 2020 April indicate a value of P = 7.03 ± 0.02 h as the most favorable solution regardless of the slight data coverage gap in the corresponding bimodal lightcurve.

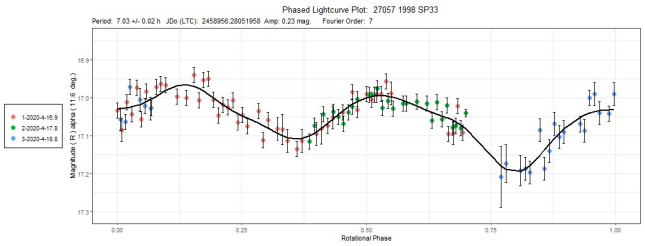

35371 Yokonozaki. A *Binastphot Survey* target with no previous references on rotation period determination. Data taken on two nights in 2020 September led to a bimodal lightcurve phased to a period of P = 2.802 ± 0.006 h as a plausible solution. From the same combined dataset Pravec (2020) independently finds a period of 2.8016 h.

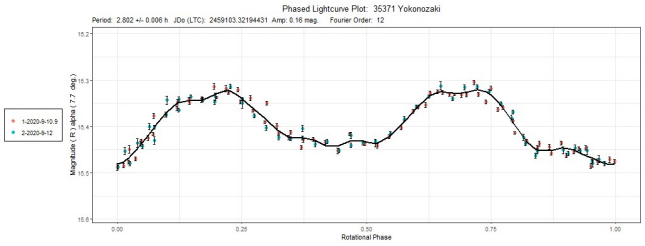

(41653) 2000 SC294. A rotation period P = 2.883 ± 0.006 h, resulting from two dense photometric datasets obtained at SAO on two consecutive nights in 2020 September significantly differs from the only previously reported period result by Waszczak et al. (2015, 2.007 h).

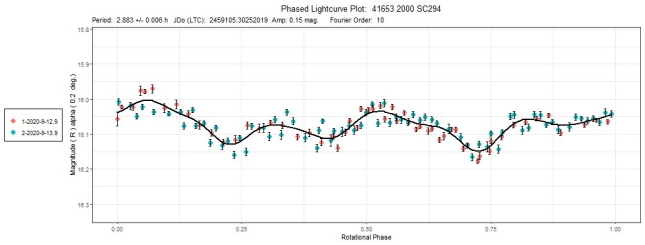

(54441) 2000 MP5. According to the LCDB this is the first rotation period determination for this Eunomia family asteroid. The observations were made on five consecutive nights in late 2020 June. Period analysis shows up several harmonically related solutions associated with the low-amplitude lightcurves. A period value of P = 3.765 ± 0.003 h is statistically the most favorable of these possible solutions. However, given the extremely low lightcurve amplitude other solutions should not be formally ruled out as possibilities.

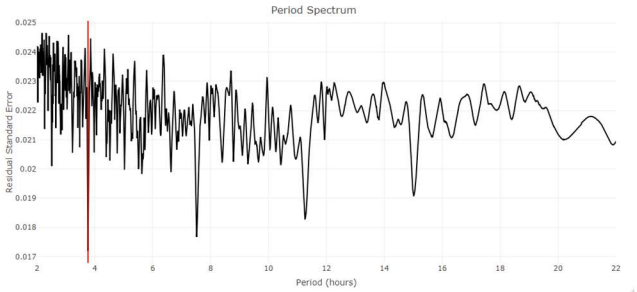

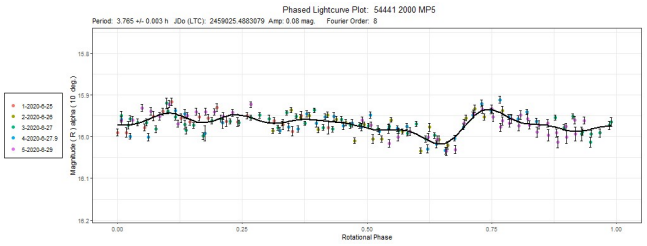

(56086) 1999 AA21. There is an excellent agreement between the only other period result recently published by Pal et al. (2020, 2.76957 h) and the value of P = 2.7699 ± 0.0006 h, determined from the four SAO datasets obtained in 2020 September.

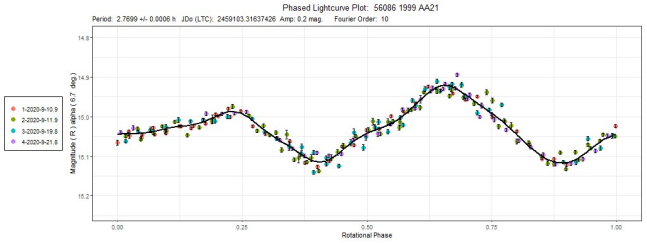

(137199) 1999 KX4. Several previous period determinations were known for this NEA. The period determined on the basis of 2020 June SAO observations of P = 2.7690 ± 0.0005 h is in full accordance with the results found by Warner (2013, 2.767 h) and Warner and Stephens (2020, 2.7697 h), and in fairly good agreement with that of Carbognani (2014, 2.797 h).

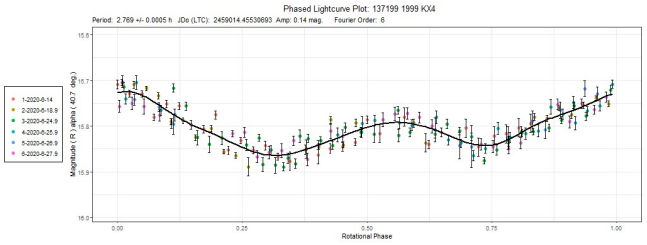

Acknowledgements

Observational work at Sopot Astronomical Observatory is supported by a 2018 Gene Shoemaker NEO Grant from The Planetary Society.

Number	Name	yy/mm/dd	Phase	L_{PAB}	B_{PAB}	Period (h)	P.E.	Amp	A.E.	Grp
2034	Bernoulli	20/03/28-20/04/08	16.7,20.5	160	6	6.249	0.003	0.19	0.02	MB-I
2050	Francis	20/03/12-20/03/18	24.3,23.5	198	34	3.069	0.002	0.18	0.02	PHO
2050	Francis	20/04/05-20/04/09	21.4,21.2	201	32	3.067	0.003	0.18	0.03	PHO
2050	Francis	20/05/03-20/05/09	22.8,23.8	204	27	3.068	0.002	0.14	0.02	PHO
2151	Hadwiger	20/04/07-20/04/27	18.8,22.5	158	12	5.870	0.002	0.09	0.02	MB-I
2334	Cuffey	20/04/21-20/05/09	11.4,18.2	197	6	5.858	0.002	0.33	0.02	FLOR
2341	Aoluta	20/02/24-20/03/13	13.2,19.8	133	5	3.0032	0.0005	0.36	0.02	FLOR
2665	Schrutka	20/09/24-20/09/25	5.5,5.6	353	6	2.70	0.02	0.25	0.02	FLOR
2962	Otto	20/03/18-20/03/20	12.5,12.7	321	-2	2.678	0.006	0.22	0.01	MB-I
3068	Khanina	20/04/02-20/04/10	13.8,17.2	172	3	3.560	0.002	0.60	0.02	FLOR
3453	Dostoevsky	20/03/17-20/03/19	8.1,9.1	162	-4	3.163	0.004	0.14	0.02	MB-I
3895	Earhart	20/05/07-20/06/03	20.5,16.5	257	32	3.5646	0.0005	0.38	0.02	PHO
3895	Earhart	20/07/05-20/07/06	18.2,18.4	259	29	3.57	0.01	0.35	0.02	PHO
3913	Chemin	20/05/24-20/06/14	*22.1,21.3	253	34	3.4070	0.0005	0.39	0.02	PHO
4353	Onizaki	20/04/26-20/05/05	6.7,4.4	225	7	4.430	0.003	0.35	0.02	MB-I
4491	Otaru	20/08/11-20/08/13	15.2,14.3	344	2	2.936	0.004	0.32	0.03	MB-I
5222	Ioffe	20/07/05-20/07/12	15.6,16.0	277	38	9.72	0.02	0.18	0.02	MB-O
6434	Jewitt	20/07/12-20/07/14	16,14.9	312	6	3.237	0.005	0.35	0.02	MB-I
7234	1986 QV3	20/10/11-20/10/14	21.3,19.8	48	-8	2.848	0.003	0.30	0.01	FLOR
7910	Aleksola	20/05/21-20/06/03	5.6,10.2	240	8	6.420	0.003	0.20	0.02	MB-I
8278	1991 JJ	20/03/18-20/04/14	*10.6,10.1	192	15	75.1	0.2	1.00	0.02	EUN
10419	1998 XB4	20/03/16-20/03/18	12.6,13.2	155	-2	7.03	0.04	0.37	0.02	MB-I
12112	Sprague	20/07/07-20/07/10	*10.5,10.5	285	23	3.831	0.006	0.35	0.02	MB-O
13195	1997 CG6	20/02/25-20/03/06	10.9,7.7	169	11	2.9960	0.0008	0.37	0.02	MB-I
15710	Bocklin	20/04/29-20/06/03	*13.7,10.0	240	9	7.523	0.002	0.12	0.02	FLOR
17711	1997 WA7	20/05/09-20/06/06	*8.7,14.2	234	14	3.6749	0.0005	0.50	0.02	EUN
19186	1991 VY1	20/08/26-20/09/07	*25.1,25.0	347	33	8.291	0.006	0.14	0.02	PHO
27057	1998 SP33	20/04/16-20/04/18	11.6,12.5	187	-3	7.03	0.02	0.23	0.03	MC
35371	Yokonozaki	20/09/10-20/09/12	7.7,6.8	-2	-1	2.802	0.006	0.16	0.02	FLOR
41653	2000 SC294	20/09/12-20/09/14	0.2,0.8	350	0	2.883	0.006	0.15	0.02	FLOR
54441	2000 MP5	20/06/24-20/06/29	10.0,10.3	272	15	3.765	0.003	0.08	0.02	EUN
56086	1999 AA21	20/09/10-20/09/21	6.7,12.9	342	8	2.7699	0.0006	0.20	0.02	PHO
137199	1999 KX4	20/06/13-20/06/27	40.7,36.9	244	18	2.7690	0.0005	0.14	0.02	NEA

Table I. Observing circumstances and results. Phase is the solar phase angle given at the start and end of the date range. If preceded by an asterisk, the phase angle reached an extrema during the period. L_{PAB} and B_{PAB} are the average phase angle bisector longitude and latitude. Grp is the asteroid family/group (Warner *et al.*, 2009): EUN = Eunomia, FLOR = Flora, MB-I/O = main-belt inner /outer, MC = Mars Crosser, NEA = near-Earth asteroid, PHO = Phocaea.

References

Alkema, M.S. (2013). "Asteroid Lightcurve Analysis at Elephant Head Observatory: 2012 November - 2013 April." *Minor Planet Bull.* **40**, 133-137.

Aznar Macias, A.; Carreno Garcerain, A.; Arce Masego, E.; Brines Rodríguez, P.; Lozano de Haro, J.; Fornas Silva, A.; Fornas Silva, G.; Mas Martínez, V.; Rodrigo Chiner, O.; Herrero Porta, D. (2016). "Twenty-one Asteroid Lightcurves at Group Observadores de Asteroides (OBAS): Late 2015 to Early 2016." *Minor Planet Bull.* **43**, 257-263.

Behrend, R. (2007, 2009, 2010, 2016, 2020). Observatoire de Geneve web site. *http://obswww.unige.ch/~behrend/page_cou.html*

Benishek, V. (2019). "Asteroid Lightcurve and Synodic Period Determinations: 2018 October - December." *Minor Planet Bull.* **46**, 208-210.

Carbo, L.; Green, D.; Kragh, K.; Krotz, J.; Meiers, A.; Patino, B.; Pligge, Z.; Shaffer, N.; Ditton, R. (2009). "Asteroid Lightcurve Analysis at the Oakley Southern Sky Observatory: 2008 October thru 2009 March." *Minor Planet Bull*. **36**, 152.

Carbognani, A. (2014). "Asteroid Lightcurves at Oavda: 2012 June - 2013 March." *Minor Planet Bull.* **41**, 4-8.

Chiorny, V.; Galad, A.; Pravec, P.; Kušnirak, P.; Hornoch, K.; Gajdoš, Š.; Kornoš, L.; Vilagi, J.; Husarik, M.; Kanuchova, Z.; Krišandova, Z.; Higgins, D.; Pray, D.P.; Durkee, R.; Dyvig, R.; Reddy, V.; Oey, J.; Marchis, F.; Stephens, R.D. (2011). "Absolute Photometry of Small Main-Belt Asteroids in 2007-2009." *Planetary and Space Science* **59**, 1482-1489.

Ditteon, R.; Kirkpatrick, E.; Doering, K. (2010). "Asteroid Lightcurve Analysis at the Oakley Southern Sky Observatory: 2009 April-May." *Minor Planet Bull.* **37**, 1-3.

Ellsworth, N.; Hughes, S.; Ditteon, R. (2002). "Photometry of Asteroids 2962 Otto and 3165 Mikawa." *Minor Planet Bull.* **29**, 68.

Erasmus, N.; Navarro-Meza, S.; McNeill, A.; Trilling, D.E.; Sickafoose, A.; Denneau, L.; Flewelling, H.; Heinze, A.; Tonry, J.L. (2020). "Investigating Taxonomic Diversity within Asteroid Families through ATLAS Dual-band Photometry." *Ap. J. Suppl. Ser*. **247**, A13.

Franco, L.; Tomassini, A.; Scardella, M. (2013). "Rotational Period of Asteroid Francis." *Minor Planet Bull.* **40**, 197.

Higgins, D.; Goncalves Rui, M.D. (2007). "Asteroid Lightcurve Analysis at Hunters Hill Observatory and Collaborating Stations - June-September 2006." *Minor Planet Bull.* **34**, 16-18.

Klinglesmith, D.A. III; Hanowell, J.; Risley, E; Janek, T.; Vargas, A.; Warren, C.A. (2013). "Etscorn Observed Asteroids: Results for Size Asteroids December 2012 - March 2013." *Minor Planet Bull.* **40**, 154-156.

Klinglesmith, D.A. III; Hendrickx, S.; Madden, K.; Montgomery, S. (2016). "Asteroid Lightcurves from Etscorn Observatory." *Minor Planet Bull.* **43**, 234-239.

Pal, A.; Szakáts, R.; Kiss, C.; Bódi, A.; Bognár, Z.; Kalup, C.; Kiss, L.L.; Marton, G.; Molnár, L.; Plachy, E.; Sárneczky, K.; Szabó, G.M.; Szabó, R. (2020). "Solar System Objects Observed with TESS – First Data Release: Bright Main-belt and Trojan Asteroids from the Southern Survey." *Ap. J. Supl. Ser*. **247**, 26-34.

Polishook, D. (2009). "Lightcurves and Spin Periods from the Wise Observatory: 2008 August-2009 March." *Minor Planet Bull.* **36**, 104-107.

Pravec, P. (2009, 2020). Photometric Survey for Asynchronous Binary Asteroids web site. *http://www.asu.cas.cz/~ppravec/newres.txt*

R Core Team (2020). R: A language and environment for statistical computing. R Foundation for Statistical Computing, Vienna, Austria. *https://www.R-project.org/*

Sada, P.V.; Canizales, E.D.; Armada, E.M. (2005). "CCD photometry of asteroids 651 Antikleia, 738 Alagasta, and 2151 Hadwiger using a remote commercial telescope." *Minor Planet Bull*. **32**, 73-75.

Sauppe, J.; Torno, S.; Lemke-Oliver, R.; Ditteon, R. (2007). "Asteroid Lightcurve Analysis at the Oakley Observatory - March/April 2007." *Minor Planet Bull.* **34**, 119-122.

Skiff, B. (2016). Submission posting on CALL web site, found at: *http://www.minorplanet.info/call.html*

VizieR (2020). *http://vizier.u-strasbg.fr/viz-bin/VizieR*

Warner, B.D. (2006). "Asteroid Lightcurve Analysis at the Palmer Divide Observatory - March-June 2006." *Minor Planet Bulletin* **33**, 85-88.

Warner, B.D. (2009). "Asteroid Lightcurve Analysis at the Palmer Divide Observatory: 2009 March - June." *Minor Planet Bull.* **36**, 172-176.

Warner, B.D. (2012). *The MPO Users Guide: A Companion Guide to the MPO Canopus/PhotoRed Reference Manuals*. BDW Publishing, Colorado Springs, CO.

Warner, B.D.; Harris, A.W.; Pravec, P. (2009). "The Asteroid Lightcurve Database." *Icarus* **202**, 134-146. Updated 2020 Aug. *http://www.minorplanet.info/lightcurvedatabase.html*

Warner, B.D. (2013). "Asteroid Lightcurve Analysis at the Palmer Divide Observatory: 2013 January - March." *Minor Planet Bull.* **40**, 137-145.

Warner, B.D. (2018). MPO Canopus software, version 10.7.11.3. *http://www.bdwpublishing.com*

Warner, B.D.; Stephens, R.D. (2020). "Near-Earth Asteroid Lightcurve Analysis at the Center for Solar System Studies: 2019 September - 2020 January." *Minor Planet Bull.* **47**, 105-120.

Waszczak, A.; Chang, C.-K.; Ofek, E.O.; Laher, R.; Masci, F.; Levitan, D.; Surace, J.; Cheng, Y.-C.; Ip, W.-H.; Kinoshita, D.; Helou, G.; Prince, T.A.; Kulkarni, S. (2015). "Asteroid Light Curves from the Palomar Transient Factory Survey: Rotation Periods and Phase Functions from Sparse Photometry." *Astron. J.* **150**, A75.

MINOR PLANETS AT UNUSUALLY FAVORABLE ELONGATIONS IN 2021

Frederick Pilcher
4438 Organ Mesa Loop
Las Cruces, NM 88011 USA
fpilcher35@gmail.com

A list is presented of minor planets which are much brighter than usual at their 2021 apparitions.

The minor planets in the lists which follow will be much brighter at their 2021 apparitions than at their average distances at maximum elongation. Many years may pass before these planets will be again as bright as in 2021. Observers are encouraged to give special attention to those which lie near the limit of their equipment.

These lists have been prepared by an examination of the maximum elongation circumstances of minor planets computed by the author for all years through 2060 with a full perturbation program written by Dr. John Reed, and to whom he expresses his thanks. Elements are from EMP 1992, except that for all planets for which new or improved elements have been published subsequently in the Minor Planet Circulars or in electronic form, the newer elements have been used. Planetary positions are from the JPL DE-200 ephemeris, courtesy of Dr. E. Myles Standish.

Any planets whose brightest magnitudes near the time of maximum elongation vary by at least 2.0 in this interval and in 2021 will be within 0.3 of the brightest occurring, or vary by at least 3.0 and in 2021 will be within 0.5 of the brightest occurring; and which are visual magnitude 14.5 or brighter, are included. For planets brighter than visual magnitude 13.5, which are within the range of a large number of observers, these standards have been relaxed somewhat to include a larger number of planets. Magnitudes have been computed from the updated magnitude parameters published in MPC28104-28116, on 1996 Nov. 25, or more recently in the Minor Planet Circulars.

Oppositions may be in right ascension or in celestial longitude. Here we use still a third representation, maximum elongation from the Sun, instead of opposition. Though unconventional, it has the advantage that many close approaches do not involve actual opposition to the Sun near the time of minimum distance and greatest brightness and are missed by an opposition-based program. Other data are also provided according to the following tabular listings: Minor planet number, date of maximum elongation from the Sun in format yyyy/mm/dd, maximum elongation in degrees, right ascension on date of maximum elongation, declination on date of maximum elongation, both in J2000 coordinates, date of brightest magnitude in format yyyy/mm/dd, brightest magnitude, date of minimum distance in format yyyy/mm/dd, and minimum distance in AU.

Users should note that when the maximum elongation is about 177° or greater, the brightest magnitude is sharply peaked due to enhanced brightening near zero phase angle. Even as near as 10 days before or after minimum magnitude the magnitude is generally about 0.4 greater. This effect takes place in greater time interval for smaller maximum elongations. There is some interest in very small minimum phase angles. For maximum elongations E near 180° at Earth distance Δ, an approximate formula for the minimum phase angle ϕ is $\phi=(180°-E)/(\Delta+1)$.

A special list of asteroids approaching the Earth more closely than 0.3 AU is provided following the list of temporal sequence of favorable elongations.

Table I. Numerical Sequence of Favorable Elongations

Planet	Max Elon D	Max E	RA	Dec	Br Mag D	Br Mag	Min Dist D	Min Dist
12	2021/07/29	162.2°	20h21m	- 1°	2021/07/29	8.7	2021/07/28	0.826
14	2021/01/24	170.1°	8h38m	+28°	2021/01/25	9.2	2021/01/30	1.336
25	2021/10/20	174.0°	1h25m	+15°	2021/10/19	10.1	2021/10/08	1.148
35	2021/03/29	176.3°	12h27m	- 7°	2021/03/29	11.2	2021/04/02	1.341
44	2021/12/10	174.5°	5h11m	+17°	2021/12/11	9.1	2021/12/14	1.134
50	2021/10/16	177.1°	1h29m	+ 6°	2021/10/16	10.6	2021/10/12	0.902
59	2021/10/10	173.2°	1h13m	+ 0°	2021/10/10	10.9	2021/10/09	1.400
60	2021/02/02	173.9°	8h54m	+11°	2021/02/01	10.0	2021/01/29	1.008
63	2021/06/03	168.9°	16h38m	-33°	2021/06/04	9.7	2021/06/06	1.101
76	2021/01/31	176.9°	8h52m	+14°	2021/01/31	11.8	2021/01/28	1.938
89	2021/08/24	169.0°	22h 1m	- 0°	2021/08/24	8.9	2021/08/26	1.106
116	2021/03/10	174.1°	11h31m	+ 9°	2021/03/10	10.7	2021/03/10	1.391
141	2021/10/14	160.0°	0h47m	+26°	2021/10/13	10.7	2021/10/11	1.132
175	2021/09/01	176.3°	22h48m	-11°	2021/09/01	11.2	2021/09/01	1.435
183	2021/08/30	163.6°	23h16m	-21°	2021/09/03	12.2	2021/09/12	1.127
188	2021/09/16	161.2°	23h 1m	+14°	2021/09/14	12.3	2021/09/09	1.377
217	2021/08/19	173.8°	21h43m	- 7°	2021/08/19	11.5	2021/08/16	0.971
227	2021/06/20	167.4°	17h51m	-35°	2021/06/19	12.3	2021/06/16	1.630
229	2021/09/15	178.2°	23h34m	- 4°	2021/09/15	13.1	2021/09/13	1.959
322	2021/11/27	178.3°	4h12m	+22°	2021/11/27	11.6	2021/11/18	1.320
330	2021/10/30	165.7°	2h38m	+ 0°	2021/10/30	14.2	2021/10/29	0.868
356	2021/01/01	165.4°	6h48m	+37°	2020/12/30	10.7	2020/12/27	1.167
359	2021/10/01	179.5°	0h29m	+ 3°	2021/10/01	11.4	2021/09/27	1.325
360	2021/11/17	161.1°	3h46m	+ 0°	2021/11/17	11.9	2021/11/17	1.529
419	2021/06/22	174.5°	18h 3m	-17°	2021/06/22	10.0	2021/06/23	0.931
448	2021/08/19	160.2°	22h23m	-31°	2021/08/19	13.9	2021/08/19	1.571
464	2021/09/09	163.4°	23h40m	-20°	2021/09/09	12.3	2021/09/10	1.253
468	2021/09/22	179.4°	23h56m	- 0°	2021/09/21	12.8	2021/09/20	1.516
477	2021/08/02	170.6°	20h58m	-26°	2021/08/02	12.1	2021/08/05	0.978
486	2021/05/13	164.7°	15h30m	- 3°	2021/05/13	12.7	2021/05/12	0.986
502	2021/02/12	168.7°	10h 9m	+23°	2021/02/12	12.6	2021/02/13	0.978
510	2021/05/15	170.9°	15h39m	-10°	2021/05/16	12.4	2021/05/23	1.277
517	2021/12/29	179.5°	6h31m	+22°	2021/12/29	12.7	2021/12/25	1.698
521	2021/11/30	172.1°	4h26m	+13°	2021/11/29	10.3	2021/11/25	1.026
571	2021/09/21	178.9°	23h53m	- 1°	2021/09/21	12.8	2021/09/26	0.874
594	2021/03/02	169.2°	11h20m	+15°	2021/03/04	14.0	2021/03/15	1.015
649	2021/10/01	174.4°	0h23m	+ 8°	2021/09/30	13.7	2021/09/24	0.861
666	2021/10/06	174.1°	0h35m	+10°	2021/10/06	12.7	2021/10/08	0.999
670	2021/10/26	171.7°	2h16m	+ 4°	2021/10/26	12.5	2021/10/22	1.306
680	2021/05/12	172.2°	15h13m	-25°	2021/05/13	12.3	2021/05/22	1.402
690	2021/11/20	175.4°	3h38m	+24°	2021/11/20	11.6	2021/11/15	1.751
755	2021/04/17	177.4°	13h44m	- 8°	2021/04/17	13.4	2021/04/19	1.750
771	2021/12/03	163.3°	4h55m	+ 5°	2021/12/04	12.7	2021/12/05	1.043
781	2021/08/06	177.8°	21h 2m	-14°	2021/08/06	13.1	2021/08/04	1.843
819	2021/07/17	173.4°	19h52m	-27°	2021/07/17	13.3	2021/07/15	0.880
846	2021/11/07	179.7°	2h50m	+16°	2021/11/07	13.4	2021/11/05	1.602
850	2021/07/28	178.2°	20h31m	-20°	2021/07/28	13.1	2021/07/24	1.712
889	2021/01/10	174.2°	7h22m	+16°	2021/01/09	13.3	2021/01/03	1.135
915	2021/12/05	169.8°	4h45m	+32°	2021/12/05	13.5	2021/12/02	0.961
938	2021/08/12	178.4°	21h31m	-16°	2021/08/12	13.9	2021/08/15	1.559
939	2021/09/24	176.9°	23h59m	+ 3°	2021/09/24	13.4	2021/09/18	0.876
942	2021/10/01	165.0°	0h51m	-10°	2021/10/01	14.5	2021/10/02	1.688
943	2021/01/02	175.6°	6h46m	+18°	2021/01/02	12.8	2021/01/04	1.488
954	2021/08/09	179.1°	21h14m	-15°	2021/08/09	13.1	2021/08/08	1.572
955	2021/06/10	157.0°	17h 6m	-45°	2021/06/12	12.9	2021/06/15	0.882
980	2021/10/01	151.8°	23h40m	+28°	2021/09/29	10.9	2021/09/27	1.259
994	2021/09/23	178.9°	0h 1m	- 0°	2021/09/23	12.6	2021/09/20	1.240
995	2021/10/21	174.2°	1h32m	+15°	2021/10/20	12.9	2021/10/15	1.267
1001	2021/12/07	179.0°	4h55m	+23°	2021/12/07	13.5	2021/12/05	1.874
1013	2021/03/01	164.0°	11h 9m	+22°	2021/02/28	12.8	2021/02/25	1.210
1026	2021/07/14	178.4°	19h36m	-23°	2021/07/14	14.5	2021/07/18	0.853
1034	2021/07/18	178.5°	19h54m	-22°	2021/07/19	12.8	2021/07/25	0.707
1123	2021/10/26	170.1°	2h16m	+ 3°	2021/10/26	13.3	2021/10/26	0.891
1132	2021/05/18	173.7°	15h36m	-25°	2021/05/19	13.0	2021/05/30	1.176
1164	2021/02/27	177.9°	10h46m	+10°	2021/02/27	14.1	2021/02/25	0.883
1247	2021/09/07	179.8°	23h 4m	- 6°	2021/09/07	13.8	2021/09/02	1.683
1284	2021/01/21	179.5°	8h14m	+20°	2021/01/21	12.9	2021/01/15	1.394
1294	2021/10/16	165.8°	1h43m	- 4°	2021/10/16	12.5	2021/10/17	1.092
1301	2021/01/15	128.7°	6h30m	-26°	2021/01/15	13.9	2021/01/15	1.253
1346	2021/11/25	155.6°	4h24m	- 3°	2021/11/24	14.1	2021/11/23	1.231
1358	2021/09/28	178.8°	0h19m	+ 0°	2021/09/28	14.4	2021/09/21	1.196
1401	2021/07/14	176.0°	19h35m	-17°	2021/07/15	13.8	2021/07/22	0.936
1450	2021/12/13	178.8°	5h24m	+24°	2021/12/13	14.1	2021/12/14	1.184
1474	2021/08/29	158.9°	22h36m	+11°	2021/09/07	13.9	2021/09/20	0.699
1479	2021/01/07	166.7°	7h25m	+35°	2021/01/07	13.9	2021/01/06	1.192
1519	2021/09/12	170.2°	23h36m	-13°	2021/09/12	14.3	2021/09/12	1.378
1545	2021/01/26	174.7°	8h39m	+23°	2021/01/26	14.0	2021/01/29	1.143
1560	2021/10/23	168.4°	1h34m	+22°	2021/10/23	13.8	2021/10/21	1.133
1625	2021/07/22	170.4°	20h12m	-29°	2021/07/21	13.9	2021/07/15	1.627
1705	2021/08/05	165.3°	20h41m	- 3°	2021/08/07	14.1	2021/08/12	0.786
1714	2021/07/26	179.2°	20h20m	-18°	2021/07/26	14.2	2021/07/21	1.227
1807	2021/10/31	177.6°	2h18m	+16°	2021/10/31	13.3	2021/10/27	0.854
1842	2021/08/27	179.8°	22h23m	-10°	2021/08/27	13.9	2021/08/18	0.967
1843	2021/06/17	179.5°	17h41m	-23°	2021/06/17	13.9	2021/06/21	1.239
1902	2021/09/04	162.1°	23h20m	-23°	2021/09/03	14.1	2021/09/01	2.137
2017	2021/06/22	169.7°	18h 2m	-13°	2021/06/23	14.3	2021/06/28	0.880
2119	2021/07/08	177.4°	19h 8m	-19°	2021/07/08	14.1	2021/07/08	0.882
2204	2021/12/22	131.2°	5h28m	-24°	2021/12/21	14.1	2021/12/20	0.705
2274	2021/04/01	178.1°	12h39m	- 6°	2021/04/01	13.5	2021/03/30	0.872
2348	2021/03/23	179.5°	12h 9m	- 1°	2021/03/23	14.4	2021/03/18	1.145
2375	2021/03/06	160.3°	11h42m	+23°	2021/03/08	14.4	2021/03/12	1.690
2431	2021/08/20	179.6°	21h57m	-12°	2021/08/20	14.1	2021/08/14	0.905
2546	2021/02/01	179.2°	9h 2m	+17°	2021/02/01	14.4	2021/02/08	1.278
2585	2021/11/26	168.5°	4h16m	+ 9°	2021/11/25	14.3	2021/11/18	0.957
2607	2021/08/19	177.4°	21h59m	-14°	2021/08/19	14.5	2021/08/20	0.829
2728	2021/08/11	175.4°	21h17m	-10°	2021/08/11	14.3	2021/08/07	1.052
2844	2021/07/20	178.9°	19h57m	-19°	2021/07/20	14.5	2021/07/17	0.838
2848	2021/09/05	179.7°	22h57m	- 6°	2021/09/05	14.5	2021/09/09	1.722
2887	2021/07/18	179.3°	19h48m	-20°	2021/07/18	14.4	2021/07/14	0.930
2892	2021/11/30	153.3°	4h 0m	+47°	2021/11/30	13.9	2021/11/29	1.612
3053	2021/08/15	173.0°	21h45m	-20°	2021/08/14	14.4	2021/08/14	0.880
3112	2021/08/13	172.0°	21h42m	-22°	2021/08/13	14.5	2021/08/11	0.902
3116	2021/08/17	168.9°	22h 4m	-23°	2021/08/18	13.8	2021/08/21	0.808
3165	2021/09/07	171.7°	23h16m	-13°	2021/09/06	14.2	2021/09/03	0.849
3178	2021/02/23	164.7°	10h 3m	- 4°	2021/02/20	13.2	2021/02/13	0.775
3277	2021/10/11	166.2°	1h26m	- 5°	2021/10/11	14.2	2021/10/10	1.325
3353	2021/05/20	173.0°	15h33m	-26°	2021/05/20	14.4	2021/05/24	0.730
3361	2021/10/29	166.9°	2h54m	+ 4°	2021/11/15	14.3	2021/11/21	0.039
3444	2021/10/28	169.6°	1h55m	+22°	2021/10/29	14.2	2021/11/02	0.960
3485	2021/07/20	178.9°	19h59m	-21°	2021/07/20	14.3	2021/07/19	1.018
3674	2021/10/02	126.2°	23h37m	+56°	2021/10/25	13.4	2021/10/25	0.655
3702	2021/08/06	172.7°	21h16m	-23°	2021/08/07	14.0	2021/08/14	1.187
3729	2021/09/19	176.5°	23h53m	- 4°	2021/09/19	14.4	2021/09/13	1.188
4082	2021/11/03	159.5°	1h58m	+34°	2021/11/02	14.4	2021/10/31	0.813
4107	2021/02/21	177.5°	10h25m	+12°	2021/02/21	13.8	2021/02/16	1.186
4155	2021/09/13	174.1°	23h35m	- 9°	2021/09/14	14.1	2021/09/17	0.865
4660	2021/11/09	166.7°	3h 8m	+29°	2021/12/07	12.4	2021/12/11	0.026
4894	2021/06/18	179.5°	17h45m	-23°	2021/06/18	14.4	2021/06/26	0.811
5064	2021/07/01	167.6°	18h34m	-10°	2021/07/01	14.2	2021/06/30	0.831
5133	2021/09/05	158.2°	23h37m	-26°	2021/09/07	14.1	2021/09/09	1.163
5189	2021/04/10	152.0°	15h 0m	+ 1°	2021/05/01	14.0	2021/05/06	0.068
5253	2021/12/08	170.9°	5h11m	+31°	2021/12/09	14.5	2021/12/16	0.705
5392	2021/12/24	145.2°	7h25m	+55°	2022/01/04	14.3	2022/01/11	0.786
5649	2021/10/05	169.0°	0h43m	+15°	2021/10/08	14.0	2021/10/17	0.663
5985	2021/07/08	179.4°	19h12m	-22°	2021/07/08	14.2	2021/07/19	0.839
6245	2021/07/10	176.8°	19h21m	-25°	2021/07/11	14.3	2021/07/18	1.043
6249	2021/10/31	173.5°	2h 4m	+19°	2021/10/31	13.3	2021/10/28	0.668
6708	2021/07/24	177.3°	20h20m	-22°	2021/07/24	14.5	2021/07/25	0.990
6914	2021/05/14	176.1°	15h21m	-22°	2021/05/14	14.4	2021/05/17	0.948
6975	2021/07/23	176.3°	20h11m	-23°	2021/07/23	14.3	2021/07/22	1.020
7430	2021/12/29	179.2°	6h36m	+23°	2021/12/29	14.1	2021/12/31	0.958
7851	2021/06/20	174.8°	17h56m	-28°	2021/06/21	14.4	2021/06/24	0.847
9601	2021/07/11	170.9°	19h33m	-30°	2021/07/11	14.0	2021/07/10	0.817
11277	2021/06/03	177.9°	16h40m	-24°	2021/06/03	14.3	2021/06/11	0.920
12008	2021/06/28	139.1°	19h45m	+13°	2021/06/19	13.6	2021/06/16	0.491
14196	2021/07/09	177.9°	19h13m	-20°	2021/07/09	14.2	2021/07/12	0.760
28913	2021/01/26	176.6°	8h34m	+22°	2021/01/26	14.4	2021/01/30	0.962
68063	2021/08/19	172.0°	21h54m	- 4°	2021/08/25	14.2	2021/09/12	0.285
143649	2021/09/22	155.6°	1h07m	+17°	2021/09/23	13.6	2021/09/23	0.099
159857	2022/01/01	132.6°	6h16m	-23°	2021/11/12	14.3	2021/11/03	0.157
163899	2021/12/01	99.1°	16h49m	+77°	2021/12/13	12.8	2021/12/17	0.036
174050	2021/02/03	178.0°	9h03m	+14°	2021/02/03	14.0	2021/02/04	0.160
231937	2021/03/15	136.5°	13h20m	-34°	2021/03/20	12.0	2021/03/21	0.014

Table II. Temporal Sequence of Favorable Elongations

Planet	Max Elon D	Max E	RA	Dec	Br Mag D	Br Mag	Min Dist D	Min Dist
356	2021/01/01	165.4°	6h48m	+37°	2020/12/30	10.7	2020/12/27	1.167
943	2021/01/02	175.6°	6h46m	+18°	2021/01/02	12.8	2021/01/04	1.488
1479	2021/01/07	166.7°	7h25m	+35°	2021/01/07	13.9	2021/01/06	1.192
889	2021/01/10	174.2°	7h22m	+16°	2021/01/09	13.3	2021/01/03	1.135
1301	2021/01/15	128.7°	6h30m	-26°	2021/01/15	13.9	2021/01/15	1.253
1284	2021/01/21	179.5°	8h14m	+20°	2021/01/21	12.9	2021/01/15	1.394
14	2021/01/24	170.1°	8h38m	+28°	2021/01/25	9.2	2021/01/30	1.336
1545	2021/01/26	174.7°	8h39m	+23°	2021/01/26	14.0	2021/01/29	1.143
28913	2021/01/26	176.6°	8h34m	+22°	2021/01/26	14.4	2021/01/30	0.962
76	2021/01/31	176.9°	8h52m	+14°	2021/01/31	11.8	2021/01/28	1.938
2546	2021/02/01	179.2°	9h 2m	+17°	2021/02/01	14.4	2021/02/08	1.278
60	2021/02/02	173.9°	8h54m	+11°	2021/02/01	10.0	2021/01/29	1.008
174050	2021/02/03	178.0°	9h03m	+14°	2021/02/03	14.0	2021/02/04	0.160
502	2021/02/12	168.7°	10h 9m	+23°	2021/02/12	12.6	2021/02/13	0.978
4107	2021/02/21	177.5°	10h25m	+12°	2021/02/21	13.8	2021/02/16	1.186
3178	2021/02/23	164.7°	10h 3m	- 4°	2021/02/20	13.2	2021/02/13	0.775
1164	2021/02/27	177.9°	10h46m	+10°	2021/02/27	14.1	2021/02/25	0.883
1013	2021/03/01	164.0°	11h 9m	+22°	2021/02/28	12.8	2021/02/25	1.210
594	2021/03/02	169.2°	11h20m	+15°	2021/03/04	14.0	2021/03/15	1.015
2375	2021/03/06	160.3°	11h42m	+23°	2021/03/08	14.4	2021/03/12	1.690

Planet	Max Elon D	Max E	RA	Dec	Br Mag D	Br Mag	Min Dist D	Min Dist
116	2021/03/10	174.1°	11h31m	+ 9°	2021/03/10	10.7	2021/03/10	1.391
231937	2021/03/15	136.5°	13h20m	-34°	2021/03/20	12.0	2021/03/21	0.014
2348	2021/03/23	179.5°	12h 9m	- 1°	2021/03/23	14.4	2021/03/18	1.145
35	2021/03/29	176.3°	12h27m	- 7°	2021/03/29	11.2	2021/04/02	1.341
2274	2021/04/01	178.1°	12h39m	- 6°	2021/04/01	13.5	2021/03/30	0.872
5189	2021/04/10	152.0°	15h 0m	+ 1°	2021/05/01	14.0	2021/05/06	0.068
755	2021/04/17	177.4°	13h44m	- 8°	2021/04/17	13.4	2021/04/19	1.750
680	2021/05/12	172.2°	15h13m	-25°	2021/05/13	12.3	2021/05/22	1.402
486	2021/05/13	164.7°	15h30m	- 3°	2021/05/13	12.7	2021/05/12	0.986
6914	2021/05/14	176.1°	15h21m	-22°	2021/05/14	14.4	2021/05/17	0.948
510	2021/05/15	170.9°	15h39m	-10°	2021/05/16	12.4	2021/05/23	1.277
1132	2021/05/18	173.7°	15h36m	-25°	2021/05/19	13.0	2021/05/30	1.176
3353	2021/05/20	173.0°	15h33m	-26°	2021/05/20	14.4	2021/05/24	0.730
63	2021/06/03	168.9°	16h38m	-33°	2021/06/04	9.7	2021/06/06	1.101
11277	2021/06/03	177.9°	16h40m	-24°	2021/06/03	14.3	2021/06/11	0.920
955	2021/06/10	157.0°	17h 6m	-45°	2021/06/12	12.9	2021/06/15	0.882
1843	2021/06/17	179.5°	17h41m	-23°	2021/06/17	13.9	2021/06/21	1.239
4894	2021/06/18	179.5°	17h45m	-23°	2021/06/18	14.4	2021/06/26	0.811
227	2021/06/20	167.4°	17h51m	-35°	2021/06/19	12.3	2021/06/16	1.630
7851	2021/06/20	174.8°	17h56m	-28°	2021/06/21	14.4	2021/06/24	0.847
419	2021/06/22	174.5°	18h 3m	-17°	2021/06/22	10.0	2021/06/23	0.931
2017	2021/06/22	169.7°	18h 2m	-13°	2021/06/23	14.3	2021/06/28	0.880
12008	2021/06/28	139.1°	19h45m	+13°	2021/06/19	13.6	2021/06/16	0.491
5064	2021/07/01	167.6°	18h34m	-10°	2021/07/01	14.2	2021/06/30	0.831
2119	2021/07/08	177.4°	19h 8m	-19°	2021/07/08	14.1	2021/07/08	0.882
5985	2021/07/08	179.4°	19h12m	-22°	2021/07/08	14.2	2021/07/19	0.839
14196	2021/07/09	177.9°	19h13m	-20°	2021/07/09	14.2	2021/07/12	0.760
6245	2021/07/10	176.8°	19h21m	-25°	2021/07/11	14.3	2021/07/18	1.043
9601	2021/07/11	170.9°	19h33m	-30°	2021/07/11	14.0	2021/07/10	0.817
1026	2021/07/14	178.4°	19h36m	-23°	2021/07/14	14.5	2021/07/18	0.853
1401	2021/07/14	176.0°	19h35m	-17°	2021/07/15	13.8	2021/07/22	0.936
819	2021/07/17	173.4°	19h52m	-27°	2021/07/17	13.3	2021/07/15	0.880
1034	2021/07/18	178.5°	19h54m	-22°	2021/07/19	12.8	2021/07/25	0.707
2887	2021/07/18	179.3°	19h48m	-20°	2021/07/18	14.4	2021/07/14	0.930
2844	2021/07/20	178.9°	19h57m	-19°	2021/07/20	14.5	2021/07/17	0.838
3485	2021/07/20	178.9°	19h59m	-21°	2021/07/20	14.3	2021/07/19	1.018
1625	2021/07/22	170.4°	20h12m	-29°	2021/07/21	13.9	2021/07/15	1.627
6975	2021/07/23	176.3°	20h11m	-23°	2021/07/23	14.3	2021/07/22	1.020
6708	2021/07/24	177.3°	20h20m	-22°	2021/07/24	14.5	2021/07/25	0.990
1714	2021/07/26	179.2°	20h20m	-18°	2021/07/26	14.2	2021/07/21	1.227
850	2021/07/28	178.2°	20h31m	-20°	2021/07/28	13.1	2021/07/24	1.712
12	2021/07/29	162.2°	20h21m	- 1°	2021/07/29	8.7	2021/07/28	0.826
477	2021/08/02	170.6°	20h58m	-26°	2021/08/02	12.1	2021/08/05	0.978
1705	2021/08/05	165.3°	20h41m	- 3°	2021/08/07	14.1	2021/08/12	0.786
781	2021/08/06	177.8°	21h 2m	-14°	2021/08/06	13.1	2021/08/04	1.843
3702	2021/08/06	172.7°	21h16m	-23°	2021/08/07	14.0	2021/08/14	1.187
954	2021/08/09	179.1°	21h14m	-15°	2021/08/09	13.1	2021/08/08	1.572
2728	2021/08/11	175.4°	21h17m	-10°	2021/08/11	14.3	2021/08/07	1.052
938	2021/08/12	178.4°	21h31m	-16°	2021/08/12	13.9	2021/08/15	1.559
3112	2021/08/13	172.0°	21h42m	-22°	2021/08/13	14.5	2021/08/11	0.902
3053	2021/08/15	173.0°	21h45m	-20°	2021/08/14	14.4	2021/08/14	0.880
3116	2021/08/17	168.9°	22h 4m	-23°	2021/08/18	13.8	2021/08/21	0.808
217	2021/08/19	173.8°	21h43m	- 7°	2021/08/19	11.5	2021/08/16	0.971
448	2021/08/19	160.2°	22h23m	-31°	2021/08/19	13.9	2021/08/19	1.571
2607	2021/08/19	177.4°	21h59m	-14°	2021/08/19	14.5	2021/08/20	0.829
68063	2021/08/19	172.0°	21h54m	- 4°	2021/08/25	14.2	2021/09/12	0.285
2431	2021/08/20	179.6°	21h57m	-12°	2021/08/20	14.1	2021/08/14	0.905
89	2021/08/24	169.0°	22h 1m	- 0°	2021/08/24	8.9	2021/08/26	1.106
1842	2021/08/27	179.8°	22h23m	-10°	2021/08/27	13.9	2021/08/18	0.967
1474	2021/08/29	158.9°	22h36m	+11°	2021/09/07	13.9	2021/09/20	0.699
183	2021/08/30	163.6°	23h16m	-21°	2021/09/03	12.2	2021/09/12	1.127
175	2021/09/01	176.3°	22h48m	-11°	2021/09/01	11.2	2021/09/01	1.435
1902	2021/09/04	162.1°	23h20m	-23°	2021/09/03	14.1	2021/09/01	2.137
2848	2021/09/05	179.7°	22h57m	- 6°	2021/09/05	14.5	2021/09/09	1.722
5133	2021/09/05	158.2°	23h37m	-26°	2021/09/07	14.1	2021/09/09	1.163
1247	2021/09/07	179.8°	23h 4m	- 6°	2021/09/07	13.8	2021/09/02	1.683
3165	2021/09/07	171.7°	23h16m	-13°	2021/09/06	14.2	2021/09/03	0.849
464	2021/09/09	163.4°	23h40m	-20°	2021/09/09	12.3	2021/09/10	1.253
1519	2021/09/12	170.2°	23h36m	-13°	2021/09/12	14.3	2021/09/12	1.378
4155	2021/09/13	174.1°	23h35m	- 9°	2021/09/14	14.1	2021/09/17	0.865
229	2021/09/15	178.2°	23h34m	- 4°	2021/09/15	13.1	2021/09/13	1.959
188	2021/09/16	161.2°	23h 1m	+14°	2021/09/14	12.3	2021/09/09	1.377
3729	2021/09/19	176.5°	23h53m	- 4°	2021/09/19	14.4	2021/09/13	1.188
571	2021/09/21	178.9°	23h53m	- 1°	2021/09/21	12.8	2021/09/26	0.874
468	2021/09/22	179.4°	23h56m	- 0°	2021/09/21	12.8	2021/09/20	1.516
143649	2021/09/22	155.6°	1h07m	+17°	2021/09/23	13.6	2021/09/23	0.099
994	2021/09/23	178.9°	0h 1m	- 0°	2021/09/23	12.6	2021/09/20	1.240
939	2021/09/24	176.9°	23h59m	+ 3°	2021/09/24	13.4	2021/09/18	0.876
1358	2021/09/28	178.8°	0h19m	+ 0°	2021/09/28	14.4	2021/09/21	1.196
359	2021/10/01	179.5°	0h29m	+ 3°	2021/10/01	11.4	2021/09/27	1.325
649	2021/10/01	174.4°	0h23m	+ 8°	2021/09/30	13.7	2021/09/24	0.861
942	2021/10/01	165.0°	0h51m	-10°	2021/10/01	14.5	2021/10/02	1.688
980	2021/10/01	151.8°	23h40m	+28°	2021/09/29	10.9	2021/09/27	1.259
3674	2021/10/02	126.2°	23h37m	+56°	2021/10/25	13.4	2021/10/25	0.655
5649	2021/10/05	169.0°	0h43m	+15°	2021/10/08	14.0	2021/10/17	0.663
666	2021/10/06	174.1°	0h35m	+10°	2021/10/06	12.7	2021/10/08	0.999
59	2021/10/10	173.2°	1h13m	+ 0°	2021/10/10	10.9	2021/10/09	1.400
3277	2021/10/11	166.2°	1h26m	- 5°	2021/10/11	14.2	2021/10/10	1.325
141	2021/10/14	160.0°	0h47m	+26°	2021/10/13	10.7	2021/10/11	1.132
50	2021/10/16	177.1°	1h29m	+ 6°	2021/10/16	10.6	2021/10/12	0.902
1294	2021/10/16	165.8°	1h43m	- 4°	2021/10/16	12.5	2021/10/17	1.092
25	2021/10/20	174.0°	1h25m	+15°	2021/10/19	10.1	2021/10/08	1.148
995	2021/10/21	174.2°	1h32m	+15°	2021/10/20	12.9	2021/10/15	1.267
1560	2021/10/23	168.4°	1h34m	+22°	2021/10/23	13.8	2021/10/21	1.133
670	2021/10/26	171.7°	2h16m	+ 4°	2021/10/26	12.5	2021/10/22	1.306
1123	2021/10/26	170.1°	2h16m	+ 3°	2021/10/26	13.3	2021/10/26	0.891
3444	2021/10/28	169.6°	1h55m	+22°	2021/10/29	14.2	2021/11/02	0.960
3361	2021/10/29	166.9°	2h54m	+ 4°	2021/11/15	14.3	2021/11/21	0.039
330	2021/10/30	165.7°	2h38m	+ 0°	2021/10/30	14.2	2021/10/29	0.868
1807	2021/10/31	177.6°	2h18m	+16°	2021/10/31	13.3	2021/10/27	0.854
6249	2021/10/31	173.5°	2h 4m	+19°	2021/10/31	13.3	2021/10/28	0.668
4082	2021/11/03	159.5°	1h58m	+34°	2021/11/02	14.4	2021/10/31	0.813
846	2021/11/07	179.7°	2h50m	+16°	2021/11/07	13.4	2021/11/05	1.602
4660	2021/11/09	166.7°	3h 8m	+29°	2021/12/07	12.4	2021/12/11	0.026
360	2021/11/17	161.1°	3h46m	+ 0°	2021/11/17	11.9	2021/11/17	1.529
690	2021/11/20	175.4°	3h38m	+24°	2021/11/20	11.6	2021/11/15	1.751
1346	2021/11/25	155.6°	4h24m	- 3°	2021/11/24	14.1	2021/11/23	1.231
2585	2021/11/26	168.5°	4h16m	+ 9°	2021/11/25	14.3	2021/11/18	0.957
322	2021/11/27	178.3°	4h12m	+22°	2021/11/27	11.6	2021/11/18	1.320
521	2021/11/30	172.1°	4h26m	+13°	2021/11/29	10.3	2021/11/25	1.026
2892	2021/11/30	153.3°	4h 0m	+47°	2021/11/30	13.9	2021/11/29	1.612
163899	2021/12/01	99.1°	16h49m	+77°	2021/12/13	12.8	2021/12/17	0.036
771	2021/12/03	163.3°	4h55m	+ 5°	2021/12/04	12.7	2021/12/05	1.043
915	2021/12/05	169.8°	4h45m	+32°	2021/12/05	13.5	2021/12/02	0.961
1001	2021/12/07	179.0°	4h55m	+23°	2021/12/07	13.5	2021/12/05	1.874
5253	2021/12/08	170.9°	5h11m	+31°	2021/12/09	14.5	2021/12/16	0.705
44	2021/12/10	174.5°	5h11m	+17°	2021/12/11	9.1	2021/12/14	1.134
1450	2021/12/13	178.8°	5h24m	+24°	2021/12/13	14.1	2021/12/14	1.184
2204	2021/12/22	131.2°	5h28m	-24°	2021/12/21	14.1	2021/12/20	0.705
5392	2021/12/24	145.2°	7h25m	+55°	2022/01/04	14.3	2022/01/11	0.786
517	2021/12/29	179.5°	6h31m	+22°	2021/12/29	12.7	2021/12/25	1.698
7430	2021/12/29	179.2°	6h36m	+23°	2021/12/29	14.1	2021/12/31	0.958
159857	2022/01/01	132.6°	6h16m	-23°	2021/11/12	14.3	2021/11/03	0.157

Table III. Numerical list of approaches closer than 0.3 AU

Planet	Max Elon D	Max E	RA	Dec	Br Mag D	Br Mag	Min Dist D	Min Dist
3361	2021/10/29	166.9°	2h54m	+ 4°	2021/11/15	14.3	2021/11/21	0.039
4660	2021/11/09	166.7°	3h 8m	+29°	2021/12/07	12.4	2021/12/11	0.026
5189	2021/04/10	152.0°	15h 0m	+ 1°	2021/05/01	14.0	2021/05/06	0.068
68063	2021/08/19	172.0°	21h54m	- 4°	2021/08/25	14.2	2021/09/12	0.285
143649	2021/09/22	155.6°	1h07m	+17°	2021/09/23	13.6	2021/09/23	0.099
159857	2022/01/01	132.6°	6h16m	-23°	2021/11/12	14.3	2021/11/03	0.157
163899	2021/12/01	99.1°	16h49m	+77°	2021/12/13	12.8	2021/12/17	0.036
174050	2021/02/03	178.0°	9h03m	+14°	2021/02/03	14.0	2021/02/04	0.160
231937	2021/03/15	136.5°	13h20m	-34°	2021/03/20	12.0	2021/03/21	0.014

USING PAN-STARRS DATA TO CALIBRATE RED LIGHTCURVE IMAGES

W. Romanishin
1933 Whispering Pines Circle, Norman OK 73072
wromanishin@ou.edu

(Received: 2020 September 22 Revised: 2020 November 8)

I investigate the utility of the Pan-STARRS photometric catalog for magnitude calibration of small telescope CCD images. With some judicious selection of stars from the Pan-STARRS catalog, I find that the Pan-STARRs data should be very useful for this purpose, due to its wide sky coverage and excellent photometry.

Asteroid lightcurves are more scientifically valuable if the magnitudes are on a standard system so that they can be compared between different observers and between measurements made at different epochs. Even if the magnitudes are not on a standard system, the consistency of magnitudes from night to night is important so that you can tie together pieces of a lightcurve without making arbitrary magnitude shifts. At many observing sites, the atmospheric conditions are not stable enough to count on night to night repeatability of atmosphere + telescope + CCD system sensitivity. Thus, a conscious effort to calibrate magnitudes in a standard system can greatly increase reliability and scientific value of your lightcurves.

Of course, the easiest and most foolproof way to calibrate magnitudes is to have stars with known magnitudes in the same CCD frame as the asteroid, or "on chip" calibration stars. To cover a large part of the sky to a depth so that there will be multiple calibration stars on any random CCD frame requires millions of stellar magnitudes. One recently released photometric catalog that may be useful for asteroid lightcurve calibration is from the Pan-STARRS project (PanSTARRS 2020). The freely available Pan-STARRS photometric and astrometric catalog has data for roughly a billion celestial objects and covers essentially the entire sky north of -30° declination.

The Pan-STARRS project is optimized for faint objects such as small NEOs and faint (mag 20-23) galaxies. Lightcurve observers with small telescopes are more interested in calibration stars in the 12-17 magnitude range. Because of the way the Pan-STARRS scans were made, "bright" stars (interpreted as those stars being brighter than the range of 14th to 15th magnitude) are not well characterized by Pan-STARRs. So, how useful is the Pan-STARRS photometry for small telescope calibration? The Pan-STARRS FAQ (PanSTARRS 2020) has a somewhat vague statement that "very conservatively" you can trust stars with *r* (red) magnitude *fainter* than 15.

I set out to make an independent check on the reliability of red Pan-STARRS photometry of stars in the 15 to 12 magnitude range. I did this by comparing Pan-STARRS *r* magnitudes of stars with *R* magnitudes from Landolt standard star fields (Clem and Landolt, 2013). I have used the *UBVR* standards measured by Landolt and collaborators for over 40 years to calibrate colors and magnitudes of objects from white dwarfs to galaxies to faint outer solar system objects. The Landolt standards catalog has been extended to include ~40,000 stars, but the stars are in small fields scattered around the sky, so are not in general useful for on chip calibrations at random sky positions.

The first step in the comparison was to account for the different red filters used by Landolt and Pan-STARRS. Landolt uses a Cousins *R* filter and Pan-STARRS uses a filter that is similar to the more readily available Sloan r filter. To make sure we keep the system apart, I will label magnitudes as R_L and r_{PS}. To find the relationship between the r_{PS} and R_L systems, I picked ~1100 Landolt standard stars from the 20 Landolt standard star fields I use most often. On my website (Romanishin, 2020) I have finding charts for these fields, with the Clem/Landolt star numbers marked. For the purposes of the comparison I picked the brightest few standard stars in each field, with typical R_L of 9 to 12, and a selection of fainter isolated standard stars (to avoid blended stars) down to the magnitude limit of the standard stars (~19 in R_L).

I then obtained r_{PS} and g_{PS} magnitudes for the same stars from the online Pan-STARRS catalog (MAST 2020). The g_{PS} filter covers roughly the wavelength range of B + V in the *UBVR* system. The color *g-r* gives a general optical color for each star. The Pan-STARRS catalog is daunting, with well over 100 columns of data. Fortunately, the website makes it easy to pick out only the data desired. For this project I downloaded a listing of six quantities for objects inside circles that encompassed the Landolt fields, setting a magnitude limit (20.5) to eliminate faint galaxies. These quantities are: raMean and decMean, to identify the stars, gMeanPSFMag and rMeanPSFMag, magnitudes for the *g* and *r* filters derived from PSF fitting, and gMeanPSFMagNpt and rMeanPSFMagNpt, the number of measurements included in each magnitude. Once I had the list of Pan-STARRS objects, I could easily match it to the corresponding Landolt star list by using the sky coordinates.

I compared R_L and r_{PS} for all stars fainter than r_{PS} =15. Figure 1 plots the difference between r_{PS} and R_L versus the $(V\text{-}R)_L$ color for these stars. Over the interval $0.2 < (V\text{-}R)_L < 0.7$ shown there is a simple linear relationship, as shown in the Figure. Redward of 0.7, the slope of the relation changes. The color range restriction is not a problem, as the color range covers virtually all solar system objects. (The solar color is $(V\text{-}R)_L = 0.35$.) This relationship allows me to use the Landolt R_L and $(V\text{-}R)_L$ data to compute a synthetic r_{PS}, which I will call r_{synL}.

$$r_{synL} = R_L + 0.20(V-R)_L + 0.12$$

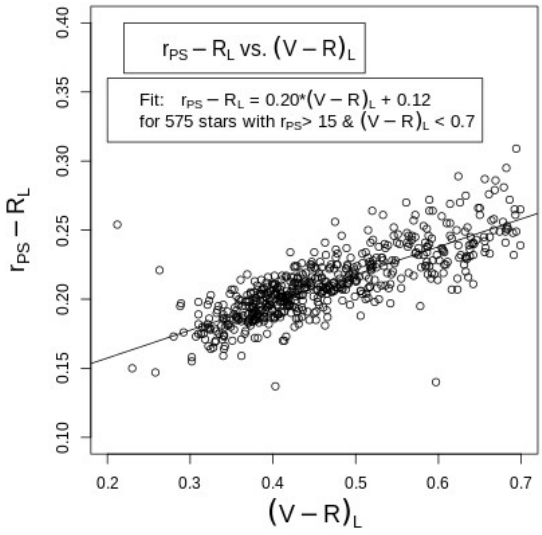

Next, I compared r_{PS} and r_{synL} for all stars in the valid color range of the r_{PS} - R_L relation, including stars brighter than 15th magnitude. I found that r_{PS} - r_{synL} is essentially zero for stars fainter than r_{PS} =13.5, but for brighter stars the differences were scattered from +0.3 to –0.3 magnitude.

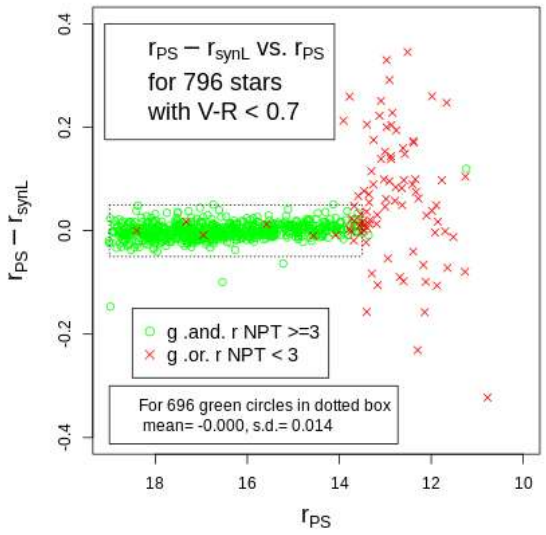

The reason for the much larger scatter of the red crosses is that the brighter stars in the Pan-STARRS catalog have magnitudes from other sources (E. Magnier, private communication). One simple way to eliminate these brighter "problem" stars is to simply require that the g and rMeanPSFMagNpt both be 3 or greater, as was done for the Figure. This is easy to do with the catalog access website, as you can "slice and dice" the objects with limits or ranges on quantities you want to download.

As for the stars fainter than r_{PS} =13.5, the magnitudes appear to be very similar to the Landolt magnitudes after adjustment for the different filters. Of the stars fainter than r_{PS} = 13.5 in the sample studied, 98% have r_{PS} values with 3 or more g and r measurements.

If you use a Pan-STARRS-like *r* filter and can find on chip stars with colors similar to those of your object, then you can find the *r* magnitude of the target directly. If you want the best magnitudes or want or need to use on chip calibration stars with color significantly different from the color of your target, say in a sparse star field where there are not many stars to choose from, you should check if your system has a color term. You can check this by observing a field with stars of a wide range of colors. I will post on my website an example of finding the color term.

If you want your asteroid magnitudes in the Landolt system, say because you are using a Cousins filter, you can also use the Pan-STARRS data to calibrate into the Landolt system using

$$R_{synPS} = r_{PS} - 0.12(g-r)_{PS} - 0.15$$

This is valid for stars with $(g\text{-}r)_{PS}$ between 0.2 and 0.9.

Of course, some fraction of the comparison stars available on your frames will be variable stars and the magnitudes from any catalog will be incorrect. The only way around this is to use as many calibration stars as possible to check for consistency and eliminate any outliers.

In summary, I suggest, if you are not already doing so, that you use a filter and calibrate so that your asteroid lightcurve magnitudes match a standard magnitude system. The best filter is probably a Sloan r. Compared to using no filter or using a V filter, observing in the red lessens atmospheric extinction and scattered light from Moon or artificial sources. Because of the change of atmospheric extinction with wavelength, observing without a filter can cause problems if the target and comparison stars are not closely matched in color. Using a red filter essentially eliminates such problems, as the extinction change with wavelength is much smaller in the red than in the bluer regions of the visible spectrum.

The Pan-STARRs photometry catalog should be an excellent source for on chip calibration stars in broadband red filters. Just use only stars fainter than r_{PS} = 13.5 that have 3 or more measurements.

Acknowledgements

No grant funds were used in this project. WR funded in part by Social Security and the Oklahoma Teachers Retirement System.

References

Clem, J.L.; Landolt, A.U. (2013). "*Faint UBVR Standard Star Fields*". *Astronomical Journal* **146**, 88.

MAST (2020). *https:/catalogs.mast.stsci.edu/panstarrs*

Pan-STARRS (2020). *https://outerspace.stsci.edu/display/PANSTARRS*

Romanishin, W. (2020). *http://www.hildaandtrojanasteroids.net*

ASTEROID-DEEPSKY APPULSES IN 2021

Brian D. Warner
Center for Solar System Studies
446 Sycamore Ave.
Eaton, CO 80615
brian@MinorPlanetObserver.com

(Received: 2020 October 10)

The following list is a *very small* subset of the results of a search for asteroid-deepsky appulses for 2021, presenting only the highlights for the year based on close approaches of brighter asteroids to brighter DSOs. For the complete set visit

http://www.minorplanet.info/ObsGuides/Appulses/DSOAppulses.htm

For any event not covered, the Minor Planet Center's web site at *https://www.minorplanetcenter.net/cgi-bin/checkmp.cgi* allows you to enter the location of a suspected asteroid or supernova and check if there are any known targets in the area.

The table gives the following data:

Date/Time	Universal Date (MM DD) and Time of closest approach
#/Name	The number and name of the asteroid
RA/Dec	The J2000 position of the asteroid
AM	The approximate visual magnitude of the asteroid
Sep/PA	The separation in arcseconds and the position angle from the DSO to the asteroid
DSO	The DSO name or catalog designation
DM	The approximate total magnitude of the DSO
DT	DSO Type: OC = Open Cluster; GC = Globular Cluster; G = Galaxy
SE/ME	The elongation in degrees from the sun and moon, respectively
MP	The phase of the moon: 0 = New, 1.0 = Full. Positive = waxing; Negative = waning

Date	UT	#	Name	RA	Dec	AM	Sep	PA	DSO	DM	DT	SE	ME	MP
01	09 19:27	130	Elektra	06:45.01	+00 15.8	11.5	158	212	Do 25	7.6	OC	156	138	-0.14
01	13 12:08	1127	Mimi	09:40.30	+14 52.8	13.9	219	233	NGC 2954	12.4	G	151	155	0.00
01	14 12:13	440	Theodora	06:05.02	+23 56.8	13.8	191	175	IC 2157	8.4	OC	157	140	0.02
01	15 12:52	313	Chaldaea	06:21.58	+02 19.3	11.5	194	212	Cr 91	6.4	OC	152	126	0.07
01	16 04:19	416	Vaticana	09:19.76	+33 47.2	12.4	85	33	NGC 2832	11.9	G	157	156	0.10
01	16 08:45	287	Nephthys	07:27.06	+13 33.6	11.2	89	204	NGC 2395	8.0	OC	170	134	0.12
01	17 03:59	1284	Latvia	08:19.43	+20 27.0	13.2	182	173	NGC 2558	12.9	G	175	136	0.17
02	08 09:52	443	Photographica	10:13.79	+06 57.9	12.6	213	209	UGC 5522	12.6	G	166	124	-0.13
02	13 17:30	412	Elisabetha	14:37.73	+02 20.9	14.0	186	341	NGC 5690	11.8	G	108	132	0.04
02	17 21:19	18	Melpomene	08:42.56	+14 15.0	9.9	218	214	NGC 2648	11.8	G	160	90	0.33
02	19 10:44	21	Lutetia	08:32.23	+22 35.7	11.7	108	14	NGC 2599	12.2	G	154	68	0.47
03	**06 20:00**	**534**	**Nassovia**	**10:47.85**	**+12 36.7**	**13.6**	**113**	**23**	**M105**	**9.3**	**G**	**171**	**108**	**-0.41**
03	08 10:58	256	Walpurga	11:48.97	-02 00.9	14.0	93	42	UGC 6780	13.0	G	169	110	-0.24
03	11 16:39	545	Messalina	10:52.03	+03 49.9	13.9	117	13	NGC 3434	12.1	G	171	166	-0.03
03	12 05:20	47	Aglaja	09:17.10	+20 04.7	13.3	40	4	NGC 2809	13.0	G	144	158	-0.01
03	14 07:01	258	Tyche	12:57.62	-12 42.3	13.1	192	34	NGC 4836	13.0	G	155	162	0.01
03	17 04:24	70	Panopaea	10:43.51	+24 56.0	12.7	60	5	NGC 3344	9.9	G	152	114	0.13
03	17 12:56	536	Merapi	13:29.37	+11 46.6	13.9	167	23	NGC 5171	12.8	G	153	149	0.15
04	08 22:36	1048	Feodosia	12:11.21	+20 10.2	13.2	47	168	NGC 4158	12.1	G	149	162	-0.09
04	14 21:16	563	Suleika	13:52.25	+02 23.0	13.0	186	15	NGC 5329	12.4	G	167	148	0.07
05	18 00:26	123	Brunhild	12:52.78	-15 26.0	13.6	159	220	NGC 4756	12.4	G	140	73	0.32
06	09 04:47	123	Brunhild	12:50.81	-14 17.9	14.0	149	327	NGC 4727	13.0	G	119	132	-0.01
06	13 20:51	814	Tauris	22:14.00	-29 25.1	13.6	5	223	NGC 7229	12.5	G	117	154	0.11
07	07 21:33	814	Tauris	22:24.00	-33 41.4	13.0	223	263	NGC 7267	12.2	G	136	115	-0.04
07	11 23:18	139	Juewa	17:17.91	-39 24.2	12.4	184	25	NGC 6318	11.8	OC	148	129	0.04
07	13 01:49	30	Urania	17:04.43	-24 49.8	11.3	237	194	NGC 6284	9.0	GC	147	111	0.10
07	16 10:32	740	Cantabia	18:41.49	-19 48.6	13.8	25	340	Pal 8	11.2	GC	166	88	0.39
07	16 23:29	352	Gisela	17:48.91	-20 20.8	13.3	74	5	NGC 6440	9.7	GC	153	69	0.45
09	03 01:11	38	Leda	18:32.06	-23 30.4	14.0	159	122	NGC 6642	8.8	GC	117	165	-0.17
09	07 07:57	191	Kolga	00:50.87	-01 53.8	12.9	84	127	NGC 271	12.0	G	153	158	0.00
09	10 10:05	419	Aurelia	18:16.39	-18 14.5	12.2	92	183	Cr 469	9.1	OC	106	61	0.15
09	10 13:02	167	Urda	00:39.85	+03 15.5	13.4	102	151	NGC 204	12.9	G	157	156	0.16
10	05 08:36	893	Leopoldina	03:41.82	-04 41.6	14.0	74	289	NGC 1417	12.1	G	135	125	-0.02
10	07 12:22	270	Anahita	06:04.99	+23 58.1	12.8	116	185	IC 2157	8.4	OC	103	118	0.02
10	08 15:24	521	Brixia	04:48.53	+10 53.9	11.6	130	170	NGC 1662	6.4	OC	122	152	0.07
11	03 03:08	626	Notburga	02:42.67	+61 32.4	12.1	40	201	NGC 1027	6.7	OC	133	119	-0.04
11	04 22:40	788	Hohensteina	01:29.00	+00 57.0	14.0	2	333	NGC 570	12.8	G	156	155	0.00
11	06 01:22	260	Huberta	02:49.35	+08 04.1	13.7	122	160	NGC 1107	12.2	G	172	161	0.02
11	08 03:28	6249	Jennifer	01:59.43	+14 00.9	13.9	27	102	NGC 774	13.0	G	167	121	0.15
11	09 08:36	665	Sabine	01:57.68	+33 10.4	14.0	113	148	NGC 750	11.9	G	159	110	0.27
11	09 14:03	980	Anacostia	23:27.54	+23 33.9	11.5	150	244	NGC 7673	12.8	G	130	74	0.29
11	10 13:20	665	Sabine	01:56.74	+33 03.3	14.0	92	329	NGC 736	12.1	G	158	94	0.40
11	11 07:39	1023	Thomana	02:49.42	+08 02.9	14.0	212	151	NGC 1107	12.2	G	170	85	0.48
12	09 02:11	625	Xenia	03:06.83	+00 49.1	13.9	137	206	NGC 1211	12.3	G	143	80	0.30
12	10 05:49	297	Caecilia	05:22.73	+33 20.5	13.9	211	173	NGC 1893	7.5	OC	169	104	0.42
12	27 16:30	626	Notburga	01:58.59	+55 30.0	12.6	115	59	NGC 744	7.9	OC	122	125	-0.43
12	29 05:50	218	Bianca	08:36.21	+00 43.1	12.9	67	6	NGC 2618	12.1	G	142	85	-0.27
12	31 20:57	635	Vundtia	09:07.58	+03 21.0	14.0	123	186	NGC 2765	12.1	G	140	114	-0.05

LIGHTCURVE PHOTOMETRY OPPORTUNITIES: 2021 JANUARY-MARCH

Brian D. Warner
Center for Solar System Studies / MoreData!
446 Sycamore Ave.
Eaton, CO 80615 USA
brian@MinorPlanetObserver.com

Alan W. Harris
MoreData!
La Cañada, CA 91011-3364 USA

Josef Ďurech
Astronomical Institute
Charles University
18000 Prague, CZECH REPUBLIC
durech@sirrah.troja.mff.cuni.cz

Lance A.M. Benner
Jet Propulsion Laboratory
Pasadena, CA 91109-8099 USA
lance.benner@jpl.nasa.gov

We present lists of asteroid photometry opportunities for objects reaching a favorable apparition and have no or poorly-defined lightcurve parameters. Additional data on these objects will help with shape and spin axis modeling using lightcurve inversion. We also include lists of objects that will or might be radar targets. Lightcurves for these objects can help constrain pole solutions and/or remove rotation period ambiguities that might come from using radar data alone.

On Better Magnitude Calibrations and H-G Data Requirements

In recent times, several catalogs with high-quality photometry have become available. A major advantage of these catalogs for lightcurve observers is the significant reduction of systematic variations for magnitude calibrations across the sky. This has led to fewer and much smaller nightly zero-point adjustments when trying to do photometric analyses.

An excellent example of taking advantage of these new resources was given by Eric Dose (2021), who developed a pipeline using the ATLAS Star Catalog (Tonry et al., 2018). Other catalogs such as Pan-STARRS, SkyMapper, and GAIA2 can be readily accessed with on-line tools to get comparison star magnitudes for a given field. This, of course, requires that an Internet connection be available at some point, either before, during, or after the initial reduction process.

The elimination, or significant reduction, of arbitrary zero-point adjustments is critical when trying to find H-G or H-G_{12} parameters. For asteroid lightcurves, even small zero-point changes can dramatically change a period solution, especially when the amplitude is low. The adjustments can also alter results when dealing with tumbling or binary asteroids.

We *strongly* suggest that all observers adopt one of the above-mentioned catalogs as their exclusive source for comparison star magnitudes as soon as possible. We also recommend that the native magnitudes of the chosen catalog be used. For example, from ATLAS or Pan-STARRS, the r′ (Sloan SR) magnitude, and not magnitudes that are the result of applying transformations that use a simple constant offset or color index dependency on two of the native magnitudes, e.g., SG/SR to Rc.

The SR magnitudes should be used when observing without (or with a Clear) filter and typical CCD cameras (e.g., FLI, SBIG, etc.) with a KAF-E chip (blue enhanced) or another chip with similar response. This is because those chips have a very good linear fit of catalog versus instrumental magnitude for the Rc and SR bands and so, if using near-solar color stars, there is no need for additional reductions such as color term correction.

Regarding H-G observations, the question of how much data is enough is often raised. The answer is, "It depends on the nature of the observing project." To that, we'd add that having just a few data points at each observing run places a much greater demand on having accurate magnitudes. If those requirements are on the order of ≤ 0.02 mag, that stretches the limits even when using the high-quality catalogs.

The H-G system is based on average light at the time of the observations, i.e., the amplitude of the lightcurve at the time must be known and, if necessary, those few data points be corrected so that they correspond to "mid-light" at the time. Since the amplitude often changes as the asteroid recedes or approaches, it's necessary to obtain enough data points during each observing run to establish or reasonably predict the mid-light magnitude.

Another reason for denser data sets is that the results from shape modeling are greatly improved by having good lightcurves from multiple phase angles within the same apparition. This is in addition to lightcurves obtained over several apparitions.

There is no set answer to the number of data points, exposure length, observing cadence that satisfies all purposes. However, it might be good to remember that you can always disregard or reject data points during analysis but you can't create them after the fact.

A good example of balancing the number of H-G data points and those needed to derive those points can be seen in the lightcurves and H-G plot (a modified version is shown here) for 86 Semele by Frederick Pilcher (2020).

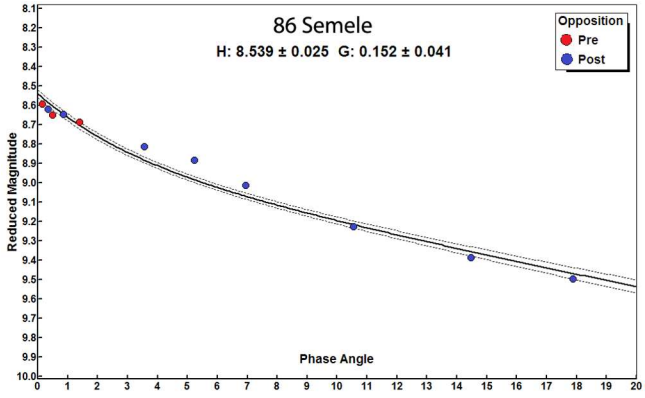

The original plot by Pilcher (2020) has been modified to make the data points easier to see and a legend replaces the explanatory text for the data points.

A final note, the H in the H-G system is, by default, Johnson V. For direct comparisons with other reported H values, it may be necessary to use a transform to go from the native magnitude used from the catalog. The web pages for the catalog used in reductions may provide or have links to the required transformation formulae.

Back to Regular Programming

We present several lists of asteroids that are prime targets for photometry during the period 2021 January-March.

In the first three sets of tables, "Dec" is the declination and "U" is the quality code of the lightcurve. See the latest asteroid lightcurve data base (LCDB from here on; Warner et al., 2009a) documentation for an explanation of the U code:

http://www.minorplanet.info/lightcurvedatabase.html

The ephemeris generator on the CALL web site allows you to create custom lists for objects reaching V ≤ 18.0 during any month in the current year and up to five years in the future, e.g., limiting the results by magnitude and declination, family, and more:

http://www.minorplanet.info/PHP/call_OppLCDBQuery.php

We refer you to past articles, e.g., Warner et al. (2009b) for more detailed discussions about the individual lists and points of advice regarding observations for objects in each list.

Once you've obtained and analyzed your data, it's important to publish your results. Papers appearing in the *Minor Planet Bulletin* are indexed in the Astrophysical Data System (ADS) and so can be referenced by others in subsequent papers. It's also important to make the data available at least on a personal website or upon request. We urge you to consider submitting your raw data to the ALCDEF database. This can be accessed for uploading and downloading data at:

http://www.alcdef.org

Containing almost 3.8 million observations for 15,000+ objects (2020 October 5), this makes the site one of the larger publicly available sources for raw asteroid time-series lightcurve data.

Now that many backyard astronomers and small colleges have access to larger telescopes, we have expanded the photometry opportunities and spin axis lists to include asteroids reaching V = 15.5 and brighter (sometimes 15.0 when the list has too many potential targets).

Lightcurve/Photometry Opportunities

Objects with U = 3– or 3 are excluded from this list since they will likely appear in the list for shape and spin axis modeling. Those asteroids rated U = 1 should be given higher priority over those rated U = 2 or 2+, but not necessarily over those with no period. On the other hand, *do not overlook asteroids with* U = 2/2+ *on the assumption that the period is sufficiently established.* Regardless, do not let the existing period influence your analysis since even highly-rated result have been proven wrong at times. Note that the lightcurve amplitude in the tables could be more or less than what's given. Use the listing only as a guide.

An entry in bold italics is a near-Earth asteroid (NEA).

Number	Name	Brightest Date	Mag	Dec	LCDB Data Period	Amp	U
6821	Ranevskaya	01 02.0	15.2	+13	2.81	0.10	2+
26520	2000 CQ75	01 04.4	15.2	+15	3.97	0.37	2
18640	1998 EF9	01 05.5	15.0	+6			
1479	Inkeri	01 07.7	14.4	+35	660.	1.30	2+
2277	Moreau	01 07.8	14.9	+23	> 12.	0.08	2-
1844	Susilva	01 08.9	15.0	+25			
8648	Salix	01 09.0	15.2	+14			
332446	***2008 AF4***	***01 09.8***	***14.3***	***+13***			
26206	1997 PJ4	01 15.2	15.4	+16			
2984	Chaucer	01 15.2	15.4	+24			
3590	Holst	01 22.8	15.0	+18	12.7635	0.20	2
13709	1998 QE13	01 25.5	15.2	+17	55.961		2
4612	Greenstein	01 28.8	15.3	+25			
2546	Libitina	02 01.9	14.3	+18	132.71	0.35	2+
174050	***2002 CC19***	***02 03.8***	***14.0***	***+17***			
87035	2000 KE2	02 04.3	15.5	+20			
1612	Hirose	02 12.8	14.8	+12	12.295	0.25	2
1724	Vladimir	02 14.0	14.8	+7	12.582	0.14-0.24	2+
5348	Kennoguchi	02 17.1	15.5	+7			
1513	Matra	02 17.1	14.8	+14	> 24.	0.1	1
13521	1991 BK	02 19.7	15.5	+21			
4107	Rufino	02 21.6	14.4	+13	15.31	0.07-0.15	2
5982	Polykletus	02 28.7	15.5	+0			
49483	1999 BP13	03 01.9	15.1	+7			
4133	Heureka	03 03.3	15.3	+1			
2288	Karolinum	03 05.0	14.4	+29	42.16	0.15-0.40	2+
2521	Heidi	03 05.4	15.1	-5	12.	0.02	1
4238	Audrey	03 07.7	15.5	+6			
2777	Shukshin	03 10.0	15.3	+10			
22295	1989 SZ9	03 16.6	15.5	+4	3.8	0.04	2
3748	Tatum	03 20.7	15.0	+6	58.21	0.54	2+
4794	Bogard	03 20.9	15.5	+1			
7685	1997 EP17	03 21.7	15.3	-3			
7637	1984 DN	03 25.1	15.5	+5			
10859	1995 GJ7	03 27.5	15.3	+0			
9967	Awanoyumi	03 29.6	15.3	+6			

Low Phase Angle Opportunities

The Low Phase Angle list includes asteroids that reach very low phase angles ($\alpha < 1°$). The "α" column is the minimum solar phase angle for the asteroid. Getting accurate, calibrated measurements (usually V band) at or very near the day of opposition can provide important information for those studying the "opposition effect." Use the on-line query form for the LCDB to get more details about a specific asteroid:

http://www.minorplanet.info/PHP/call_OppLCDBQuery.php

You will have the best chance of success working objects with low amplitude and periods that allow covering at least half a cycle every night. Objects with large amplitudes and/or long periods are much more difficult for phase angle studies since, for proper analysis, the data must be reduced to the average magnitude of the asteroid for each night. This reduction requires that you determine the period and the amplitude of the lightcurve; for long period objects that can be difficult. Refer to Harris et al. (1989) for the details of the analysis procedure.

As an aside, some use the maximum light to find the phase slope parameter (*G*). Even though the results better resemble the behavior of a spherical object of the same albedo, it can produce significantly different values for both *H* and *G* versus when using average light, which is the method used for values listed by the Minor Planet Center.

The International Astronomical Union (IAU) has adopted a new system, H-G_{12}, introduced by Muinonen et al. (2010). It will be some years before H-G_{12} becomes widely used, but not until a discontinuity flaw in the G_{12} function has be resolved. This discontinuity results in false "clusters" or "holes" in the solution density and makes it impossible to draw accurate conclusions.

We strongly encourage obtaining data as close to 0° as possible, then every 1-2° out to 7°, below which the curve tends to be non-linear due to the opposition effect. From 7° out to about 30°, observations at 3-6° intervals should be sufficient. Coverage beyond about 50° is not generally helpful since the H-G system is best defined with data from 0-30°.

It's important to emphasize that all observations should (must) be made using high-quality catalogs to set the comparison star magnitudes. These include ATLAS, Pan-STARRS, SkyMapper, and GAIA2. Catalogs such as CMC-15, APASS, or the MPOSC from *MPO Canopus* should not be used due to significant systematic errors.

Also important is that that there are sufficient data from each observing run such that their location can be found on a combined, phased lightcurve derived from two or more nights obtained *near the same phase angle.* This is so that the lightcurve amplitude isn't significantly different. If necessary, the magnitudes for the given run should be adjusted so that they correspond to mid-light of the combined lightcurve. This goes back to the H-G system being based on average, not maximum or minimum light.

For this table, the asteroid magnitudes are brighter than in others. This is because higher precision is required for this work and the asteroid may be a full magnitude or more fainter when it reaches phase angles out to 20-30°.

Num	Name	Date	α	V	Dec	Period	Amp	U
662	Newtonia	01 03.6	0.99	14.5	+20	21.095	0.42-0.51	3-
395	Delia	01 05.0	0.69	14.5	+21	19.71	0.15-0.25	2
566	Stereoskopia	01 06.7	0.93	12.7	+26	12.103	0.03-0.25	3
213	Lilaea	01 12.7	0.53	13.2	+20	12.042	0.07-0.20	3
679	Pax	01 13.1	0.29	11.8	+22	8.452	0.02-0.32	3
515	Athalia	01 14.9	0.14	14.3	+21	10.636	0.13-0.22	3
576	Emanuela	01 18.0	0.13	14.0	+21	20.404	0.06-0.13	2+
135	Hertha	01 18.6	0.86	12.0	+23	8.403	0.12-0.30	3
149	Medusa	01 20.0	0.52	12.5	+19	26.023	0.33-0.56	3
1284	Latvia	01 21.4	0.26	13.0	+20	9.55	0.10-0.23	3-
472	Roma	01 23.9	0.65	11.7	+18	9.800	0.27-0.46	3
33	Polyhymnia	01 28.0	0.65	13.3	+20	18.608	0.13-0.20	3
442	Eichsfeldia	01 28.7	0.50	12.6	+17	11.871	0.24-0.38	3
10	Hygiea	01 28.8	0.73	9.9	+16	27.630	0.09-0.33	3
317	Roxane	01 31.2	0.41	12.7	+16	8.169	0.61-0.75	3
2546	Libitina	02 01.8	0.35	14.3	+18	132.71	0.35	2+
133	Cyrene	02 02.0	0.33	12.1	+18	12.708	0.22-0.26	3
458	Hercynia	02 02.2	0.14	13.1	+17	21.806	0.10-0.48	3
1382	Gerti	02 05.1	0.73	14.5	+18	3.082	0.20-0.36	3
140	Siwa	02 06.5	0.69	12.9	+18	34.445	0.05-0.15	3
3332	Raksha	02 07.4	0.18	14.4	+15	4.806	0.25-0.36	3
431	Nephele	02 10.8	0.29	13.9	+15	13.530	0.03-0.23	3
269	Justitia	02 10.9	0.70	13.6	+12	33.128	0.14-0.25	3
633	Zelima	02 13.2	0.25	14.4	+13	11.730	0.14-0.49	3
834	Burnhamia	02 15.6	0.92	14.3	+10	13.875	0.15-0.22	3
382	Dodona	02 17.1	0.99	12.7	+09	4.113	0.39-0.42	3
1062	Ljuba	02 19.0	0.56	13.7	+13	33.8	0.17-0.18	3
1106	Cydonia	02 19.3	0.41	14.3	+10	2.679	0.10-0.28	3
77	Frigga	02 20.8	0.72	11.9	+13	9.012	0.07-0.20	3
1152	Pawona	02 23.1	0.18	13.7	+10	3.415	0.16-0.26	3
240	Vanadis	02 26.9	0.85	12.5	+11	10.64	0.08-0.34	3
545	Messalina	03 04.8	0.80	13.8	+04	7.2	0.22-0.27	3
1621	Druzhba	03 05.8	0.72	14.2	+04	99.20	0.75-0.75	3
601	Nerthus	03 10.0	0.03	14.3	+04	13.59	0.25-0.29	3
256	Walpurga	03 17.2	0.81	13.7	-01	16.664	0.25-0.58	3
2501	Lohja	03 17.4	0.71	14.0	+03	3.808	0.26-0.45	3
366	Vincentina	03 17.7	0.84	13.2	-01	12.737	0.05	3-
1458	Mineura	03 19.8	0.36	14.6	+00	36.	0.04	1
263	Dresda	03 21.2	0.37	14.4	-01	16.809	0.37-0.55	3
822	Lalage	03 24.4	0.32	14.2	-02	3.345	0.47-0.67	3
1142	Aetolia	03 24.5	0.73	14.4	+01	10.730	0.15-0.22	3-
734	Benda	03 25.2	0.11	14.3	-02	7.110	0.28-0.32	3
321	Florentina	03 26.1	0.77	14.0	+00	2.871	0.31-0.52	3

Shape/Spin Modeling Opportunities

Those doing work for modeling should contact Josef Ďurech at the email address above. If looking to add lightcurves for objects with existing models, visit the Database of Asteroid Models from Inversion Techniques (DAMIT) web site:

https://astro.troja.mff.cuni.cz/projects/damit/

Additional lightcurves could lead to the asteroid being added to or improving one in DAMIT, thus increasing the total number of asteroids with spin axis and shape models.

Included in the list below are objects that:

1. Are rated U = 3– or 3 in the LCDB.
2. Do not have reported pole in the LCDB Summary table.
3. Have at least three entries in the Details table of the LCDB where the lightcurve is rated U ≥ 2.

The caveat for condition #3 is that no check was made to see if the lightcurves are from the same apparition or if the phase angle bisector longitudes differ significantly from the upcoming apparition. The last check is often not possible because the LCDB does not list the approximate date of observations for all details records. Including that information is an on-going project.

Favorable apparitions are in bold text. NEAs are in italics.

		Brightest			LCDB Data		
Num	Name	Date	Mag	Dec	Period	Amp	U
1015	Christa	01 02.0	13.4	+18	11.23	0.12-0.20	3-
1675	Simonida	01 03.7	13.8	+36	5.289	0.16-0.65	3
1645	Waterfield	01 04.8	15.0	+22	4.861	0.18-0.20	3
395	Delia	01 05.0	14.4	+21	19.681	0.12-0.25	3
289	Nenetta	01 05.2	13.4	+13	6.902	0.18-0.20	3
1186	Turnera	01 08.1	14.5	+36	12.085	0.25-0.34	3
213	Lilaea	01 12.7	13.2	+20	12.042	0.07-0.20	3
811	Nauheima	01 13.0	14.9	+20	4.001	0.11-0.20	3
592	Bathseba	01 13.3	13.4	+9	7.747	0.22-0.32	3
504	Cora	01 15.1	14.0	+25	7.587	0.15-0.27	3
547	Praxedis	01 17.7	13.7	-5	9.105	0.04-0.12	3
109	Felicitas	01 17.8	11.4	+33	13.191	0.06-0.17	3
576	Emanuela	01 18.0	14.0	+21	20.372	0.06-0.14	3
611	Valeria	01 18.3	13.1	+1	6.977	0.08-0.28	3
1330	Spiridonia	01 18.8	14.5	+5	9.67	0.08-0.34	3
593	**Titania**	**01 19.2**	**12.1**	**+41**	**9.897**	**0.21-0.26**	**3**
273	Atropos	01 19.9	14.5	+0	23.924	0.52-0.65	3
785	Zwetana	01 20.0	12.7	+36	8.888	0.12-0.20	3
1284	**Latvia**	**01 21.4**	**13.0**	**+20**	**9.55**	**0.10-0.23**	**3-**
472	**Roma**	**01 23.9**	**11.7**	**+18**	**9.801**	**0.27-0.46**	**3**
28913	**2000 OT**	**01 26.3**	**14.5**	**+22**	**13.754**	**0.32-0.44**	**3-**
204	Kallisto	01 26.9	13.1	+7	19.489	0.09-0.26	3
1005	Arago	01 27.8	14.5	+36	8.789	0.22-0.25	3
773	Irmintraud	01 28.2	13.4	+24	6.751	0.05-0.17	3
442	Eichsfeldia	01 28.7	12.6	+17	11.871	0.24-0.38	3
1041	Asta	01 29.4	14.5	+36	7.554	0.12-0.14	3-
677	Aaltje	02 02.2	13.6	+9	16.608	0.10-0.37	3
676	Melitta	02 02.2	14.3	+12	16.743	0.04-0.20	3
1262	Sniadeckia	02 02.3	14.4	+20	17.57	0.06-0.16	3
323	Brucia	02 03.8	13.2	+39	9.463	0.15-0.36	3
1425	Tuorla	02 05.2	14.5	+0	7.75	0.17-0.40	3
1129	Neujmina	02 06.3	14.4	+6	5.084	0.06-0.20	3
3332	**Raksha**	**02 07.4**	**14.4**	**+15**	**4.806**	**0.25-0.36**	**3**
431	Nephele	02 10.8	13.9	+15	13.53	0.03-0.23	3
269	Justitia	02 11.0	13.6	+12	33.128	0.14-0.25	3
445	Edna	02 12.5	14.4	-3	19.959	0.21-0.27	3
633	Zelima	02 13.2	14.4	+13	11.73	0.14-0.49	3
3754	**Kathleen**	**02 13.9**	**14.3**	**+20**	**11.18**	**0.13-0.20**	**3-**
414	Liriope	02 15.3	14.5	+20	7.353	0.10-0.14	3-
834	Burnhamia	02 15.9	14.3	+10	13.875	0.15-0.22	3
332	Siri	02 17.7	13.8	+15	8.007	0.10-0.35	3
1062	Ljuba	02 18.9	13.7	+13	33.8	0.17-0.18	3
443	**Photographica**	**02 19.0**	**12.2**	**+8**	**19.795**	**0.24-0.34**	**3**
1106	**Cydonia**	**02 19.3**	**14.3**	**+10**	**2.679**	**0.10-0.35**	**3**
299	Thora	02 20.3	14.3	+8	272.9	0.37-0.50	3-
3178	**Yoshitsune**	**02 20.6**	**13.4**	**-5**	**7.478**	**0.52-0.53**	**3**
465	Alekto	02 22.2	13.5	+7	10.936	0.12-0.18	3
422	Berolina	02 22.2	14.1	+14	25.978	0.06-0.16	3
1567	Alikoski	02 22.8	14.2	+33	16.405	0.08-0.16	3
1152	**Pawona**	**02 23.1**	**13.7**	**+10**	**3.415**	**0.16-0.26**	**3**
888	Parysatis	02 24.7	13.1	+20	5.931	0.22-0.26	3
68348	2001 LO7	02 25.0	14.1	-1	3.331	0.08-0.30	3
240	Vanadis	02 26.8	12.5	+11	10.64	0.13-0.34	3
70	Panopaea	02 27.2	12.4	+24	15.805	0.07-0.18	3
1164	**Kobolda**	**02 27.3**	**14.1**	**+10**	**4.141**	**0.21-0.30**	**3**
1375	Alfreda	02 28.0	14.4	+17	19.14	0.17	3-
429	Lotis	02 28.8	13.9	-4	13.577	0.21-0.24	3
545	Messalina	03 04.9	13.8	+4	7.2	0.22-0.27	3
594	**Mireille**	**03 04.9**	**14.1**	**+17**	**4.966**	**0.18-0.25**	**3**
1085	Amaryllis	03 05.1	14.2	+10	18.111	0.14-0.20	3-
786	Bredichina	03 06.4	13.1	+26	29.434	0.04-0.60	3-

Num	Name	Brightest Date	Mag	Dec	LCDB Data Period	Amp	U
2375	Radek	03 08.2	14.3	+24	16.875	0.17-0.20	3
1296	Andree	03 08.6	14.2	-1	5.184	0.23-0.27	3
86	Semele	03 09.7	13.6	+10	16.634	0.13-0.18	3
374	Burgundia	03 10.4	12.5	-6	6.962	0.07-0.33	3
498	Tokio	03 15.1	13.6	+15	41.85	0.08-0.36	3
559	Nanon	03 17.0	13.1	+14	10.059	0.07-0.26	3
1305	Pongola	03 19.1	14.3	+4	8.335	0.14-0.19	3-
715	Transvaalia	03 20.7	14.4	+14	11.83	0.14-0.32	3
862	Franzia	03 24.5	14.1	-19	7.523	0.07-0.13	3
1142	Aetolia	03 24.6	14.4	+1	10.73	0.15-0.22	3-
734	Benda	03 25.1	14.3	-2	7.11	0.25-0.32	3
583	Klotilde	03 25.2	13.0	-13	9.213	0.17-0.30	3
1259	Ogyalla	03 25.2	14.3	+1	17.334	0.25-0.41	3
542	Susanna	03 25.6	14.1	+7	10.069	0.11-0.30	3
752	Sulamitis	03 28.9	13.4	+6	27.367	0.20-0.45	3

Radar-Optical Opportunities

Past radar targets:
http://echo.jpl.nasa.gov/~lance/radar.nea.periods.html

Arecibo targets:
http://www.naic.edu/~pradar
http://www.naic.edu/~pradar/ephemfuture.txt

Goldstone targets:
http://echo.jpl.nasa.gov/asteroids/goldstone_asteroid_schedule.html

These are based on *known* targets at the time the list was prepared. It is very common for newly discovered objects to move up the list and become radar targets on short notice. We recommend that you keep up with the latest discoveries the Minor Planet Center observing tools.

In particular, monitor NEAs and be flexible with your observing program. In some cases, you may have only 1-3 days when the asteroid is within reach of your equipment. Be sure to keep in touch with the radar team (through Benner's email or their Facebook or Twitter accounts) if you get data. The team may not always be observing the target but your initial results may change their plans. In all cases, your efforts are greatly appreciated.

Use the ephemerides below as a guide to your best chances for observing, but remember that photometry may be possible before and/or after the ephemerides given below. Note that *geocentric* positions are given. Use these web sites to generate updated and *topocentric* positions:

MPC: *http://www.minorplanetcenter.net/iau/MPEph/MPEph.html*
JPL: *http://ssd.jpl.nasa.gov/?horizons*

In the ephemerides below, ED and SD are, respectively, the Earth and Sun distances (AU), V is the estimated Johnson V magnitude, and α is the phase angle. SE and ME are the great circle distances (in degrees) of the Sun and Moon from the asteroid. MP is the lunar phase and GB is the galactic latitude. "PHA" indicates that the object is a "potentially hazardous asteroid", meaning that at some (long distant) time, its orbit might take it very close to Earth.

About YORP Acceleration

Many, if not all, of the targets in this section are near-Earth asteroids. These objects are particularly sensitive to YORP acceleration. YORP (Yarkovsky–O'Keefe–Radzievskii–Paddack) is the asymmetric thermal re-radiation of sunlight that can cause an asteroid's rotation period to increase or decrease. High precision lightcurves at multiple apparitions can be used to model the asteroid's *sidereal* rotation period and see if it's changing.

It usually takes four apparitions to have sufficient data to determine if the asteroid rotation rate is changing under the influence of YORP. This is why observing an asteroid that already has a well-known period remains a valuable use of telescope time. It is even more so when considering the BYORP (binary-YORP) effect among binary asteroids that has stabilized the spin so that acceleration of the primary body is not the same as if it would be if there were no satellite.

To help focus efforts in YORP detection, Table I gives a quick summary of this quarter's radar-optical targets. The family or group for the asteroid is given under the number name. Also under the name will be additional flags such as "PHA" for Potentially Hazardous Asteroid, NPAR for a tumbler, and/or "BIN" to indicate the asteroid is a binary (or multiple) system. "BIN?" means that the asteroid is a suspected but not confirmed binary. The period is in hours and, in the case of binary, for the primary. The Amp column gives the known range of lightcurve amplitudes. The App columns gives the number of different apparitions at which a lightcurve period was reported while the Last column gives the year for the last reported period. The R SNR column indicates the estimated radar SNR using the tool at:

http://www.naic.edu/~eriverav/scripts/index.php

The SNRs were calculated using the current MPCORB absolute magnitude (H), a period of 4 hours (2 hours if $D \leq 200$ m) if it's not known, and the approximate minimum Earth distance during the current quarter. These are estimates only and assume that the radars are fully functional.

If the row is in bold text, the object was found on the radar planning pages listed above. Otherwise, the planning tool at:

http://www.minorplanet.info/PHP/call_OppLCDBQuery.php

was used to find known NEAs that were V < 18.0 during the quarter.

It's rarely the case, especially for shape/spin axis modeling, that there are too many observations. Remember that the best set for modeling includes data not just from multiple apparitions but from as wide a range of phase angles during each apparition as well.

Asteroid	Period	Amp	App	Last	R SNR
2003 AF23 NEA PHA	**-**	**-**	**-**	**-**	**25 G**
2016 CO247 NEA PHA	**-**	**-**	**-**	**-**	**40**
(332446) NEA	**-**	**-**	**-**	**-**	**1000 G MAINT**
2015 NU13 NEA PHA	**-**	**-**	**-**	**-**	**220 G MAINT**
(189040) 2000 MU1 NEA	-	-	-	-	5 G
(65717) 1993 BX3 NEA	**20.46**	**0.91**	**1**	**1995**	**95 G**
(363024) 1998 OK1 NEA	**-**	**-**	**-**	**-**	**20 G**
(468727) 2919 JE87 NEA	**-**	**-**	**-**	**-**	**85 G**
2016 CL136 NEA PHA	**-**	**-**	**-**	**-**	**60 G**
(456537) 2007 BG NEA	**-**	**-**	**-**	**-**	**45 G**
(311554) 2006 BQ147 NEA	9.15	0.31	1	2015	21 G

Asteroid	Period	Amp	App	Last	R SNR
(85953) 1999 FK21 NEA	68.44	0.45 0.87	4	2018	15 G
(99942) Apophis NEA PHA	**30.56**	**0.3 1.14**	**2**	**2013**	**13 G**
(535844) 2915 BY310 NEA	**-**	**-**	**-**	**-**	**45 G**
(138127) 2000 EE14 NEA	2.586	0.2 0.26	1	2014	3 G
(462552) 2009 CB3 NEA	-	-	-	-	15 G
(351545) 1004 TE15 NEA	**-**	**-**	**-**	**-**	**20 G**
162173 Ryugu NEA	7.627	0.1 0.16	3	2020	60 G
(271480) 2004 FX31 NEA	**-**	**-**	**-**	**-**	**25 G**
(231937) 2001 FO32 NEA	**-**	**-**	**-**	**-**	**3200 G**
(514596) 2003 FG NEA	8.692	1.4	1	2003	35 G

Table I. Summary of radar-optical opportunities for the current quarter. Period and amplitude data are from the asteroid lightcurve database (LCDB; Warner et al., 2009a). SNR values are *estimates* that are affected by radar power output along with rotation period, size, and distance. They are given for relative comparisons among the objects in the list.

The "A" is for Arecibo; "G" is for Goldstone. Due to the severe damage at Arecibo in mid-2020, no SNR estimates were made for that facility. "MAINT" means that the asteroid is not scheduled because of planned maintenance. Photometric observations should still be made in case the situation at Goldstone changes.

2003 AF23 (H = 20.90, PHA)

No rotation periods are listed in the LCDB (Warner et al., 2009a). The estimated diameter is 4.4 km. The observing window is short so, with luck, the rotation period won't be too long.

DATE	RA	Dec	ED	SD	V	α	SE	ME	MP	GB
12/30	13 34.0	+32 49	0.06	0.99	17.9	85.0	91	89	+1.00	+79
01/01	12 24.6	+33 59	0.05	1.00	17.0	70.3	107	53	-0.96	+81
01/03	10 50.9	+31 39	0.05	1.01	16.2	50.5	127	18	-0.84	+63
01/05	09 16.1	+24 31	0.05	1.03	15.6	29.0	150	42	-0.65	+42
01/07	08 05.0	+15 51	0.06	1.04	15.5	13.4	166	85	-0.43	+23
01/09	07 18.4	+08 52	0.07	1.05	15.9	12.4	167	123	-0.22	+10

2016 CO247 (H = 20.50, PHA)

The estimated diameter for this NEA is 230 meters. This should be large enough so that the period won't be super-fast (P < 2 h). However, it's a good plan to assume that short exposures are required to avoid *rotational smearing* (Pravec et al., 2000). The rapid sky motion makes short exposures even more important.

DATE	RA	Dec	ED	SD	V	α	SE	ME	MP	GB
01/01	15 48.3	+29 23	0.07	0.96	18.7	108.5	68	96	-0.96	+51
01/03	14 46.6	+32 18	0.06	0.98	17.7	95.7	81	63	-0.84	+65
01/05	13 16.8	+33 02	0.05	0.99	16.7	77.6	99	33	-0.65	+82
01/07	11 35.2	+28 57	0.05	1.01	16.1	56.4	121	45	-0.43	+73
01/09	10 13.4	+21 38	0.06	1.03	15.8	37.9	140	85	-0.22	+54
01/11	09 19.3	+14 50	0.07	1.04	15.9	25.2	153	124	-0.06	+39
01/13	08 44.4	+09 49	0.08	1.06	16.2	18.2	160	157	+0.00	+30
01/15	08 21.1	+06 17	0.10	1.08	16.5	15.5	163	159	+0.04	+23
01/17	08 04.7	+03 47	0.12	1.10	16.9	15.4	163	134	+0.16	+18
01/19	07 52.8	+01 59	0.14	1.11	17.3	16.4	161	108	+0.33	+15
01/21	07 43.9	+00 40	0.16	1.13	17.6	17.8	159	84	+0.52	+12

(332446) 2008 AF4 (H = 19.65, PHA)

The only information in the LCDB is from Binzel et al. (2019), who determined this to be a type S/Sr type asteroid. The estimated diameter is 350 meters.

DATE	RA	Dec	ED	SD	V	α	SE	ME	MP	GB
01/05	14 41.3	-36 28	0.03	0.97	16.7	121.0	58	57	-0.65	+21
01/08	12 37.5	-05 28	0.03	0.99	14.5	81.6	97	29	-0.32	+57
01/11	11 18.9	+18 43	0.04	1.01	14.3	51.9	126	99	-0.06	+67
01/14	10 33.8	+29 41	0.05	1.02	14.8	37.5	141	151	+0.01	+60
01/17	10 06.0	+34 54	0.07	1.04	15.2	29.9	148	152	+0.16	+54
01/20	09 47.5	+37 42	0.09	1.06	15.7	25.5	152	115	+0.42	+50
01/23	09 34.2	+39 19	0.11	1.08	16.0	22.9	155	79	+0.70	+48
01/26	09 24.2	+40 17	0.13	1.10	16.4	21.4	156	43	+0.92	+46
01/29	09 16.5	+40 51	0.15	1.12	16.8	20.7	156	20	-1.00	+44
02/01	09 10.4	+41 08	0.17	1.14	17.1	20.7	156	48	-0.88	+43
02/04	09 05.6	+41 13	0.19	1.16	17.4	21.0	155	88	-0.58	+42
02/07	09 01.7	+41 10	0.21	1.18	17.7	21.6	154	128	-0.25	+41
02/10	08 58.8	+40 59	0.23	1.20	18.0	22.4	152	160	-0.04	+41

2015 NU13 (H = 19.50, PHA)

This NEA has an estimated diameter of 370 meters. There are no entries in the LCDB. Unfortunately, the asteroid stays close to the galactic plane and so rich star fields may hamper data reduction.

DATE	RA	Dec	ED	SD	V	α	SE	ME	MP	GB
01/15	08 14.2	-11 32	0.06	1.04	14.9	31.5	147	144	+0.04	+13
01/17	08 13.8	-03 23	0.08	1.05	15.1	22.9	155	134	+0.16	+17
01/19	08 13.4	+02 07	0.09	1.07	15.4	16.9	162	114	+0.33	+19
01/21	08 13.2	+06 00	0.11	1.09	15.6	12.6	166	91	+0.52	+21
01/23	08 13.0	+08 53	0.13	1.11	15.9	9.6	169	67	+0.70	+22
01/25	08 12.9	+11 06	0.14	1.13	16.1	7.7	171	43	+0.86	+23
01/27	08 12.9	+12 50	0.16	1.15	16.4	7.1	172	19	+0.96	+24
01/29	08 12.9	+14 14	0.18	1.16	16.7	7.4	171	14	-1.00	+24
01/31	08 13.0	+15 22	0.20	1.18	17.0	8.3	170	38	-0.94	+25
02/02	08 13.2	+16 19	0.22	1.20	17.2	9.6	168	66	-0.79	+25
02/04	08 13.4	+17 07	0.24	1.22	17.5	11.0	166	94	-0.58	+26

(189040) 2000 MU1 (H = 19.90)

Binzel et al. (2019) determined this to be a type S asteroid. The estimated diameter is 310 meters. Be wary of the large solar phase angles. These can lead to lightcurve shapes and amplitudes that defy easy period analysis.

DATE	RA	Dec	ED	SD	V	α	SE	ME	MP	GB
01/05	09 41.8	-12 03	0.20	1.12	18.3	43.9	128	38	-0.65	+30
01/08	09 58.7	-12 38	0.18	1.10	18.1	45.5	127	66	-0.32	+32
01/11	10 19.7	-13 07	0.16	1.08	17.8	47.7	126	99	-0.06	+35
01/14	10 46.4	-13 28	0.14	1.06	17.6	50.8	123	131	+0.01	+39
01/17	11 20.9	-13 30	0.12	1.05	17.4	55.3	119	155	+0.16	+44
01/20	12 05.0	-13 00	0.10	1.03	17.3	61.6	113	159	+0.42	+48
01/23	12 59.2	-11 38	0.10	1.01	17.3	70.0	105	141	+0.70	+51
01/26	14 00.4	-09 14	0.09	1.00	17.5	80.0	95	118	+0.92	+50
01/29	15 01.2	-06 09	0.09	0.98	17.9	90.1	84	92	-1.00	+44

(65717) 1993 BX3 (H = 20.80)

Mottola et al. (1995) reported a period of 20.463 h. This would suggest that a collaboration involving two or more observations at well-separated longitudes would make it easier to find the period this time around. The estimated diameter is only 200 m, so the long period makes this NEA a bit on the unusual side.

DATE	RA	Dec	ED	SD	V	α	SE	ME	MP	GB
01/01	04 10.1	-36 38	0.06	1.00	17.0	66.9	110	84	-0.96	-47
01/11	05 49.4	-41 14	0.05	1.00	16.5	64.6	113	115	-0.06	-29
01/21	07 55.2	-37 00	0.05	1.01	16.2	54.8	123	93	+0.52	-5
01/31	09 26.8	-25 18	0.06	1.03	16.2	41.3	137	43	-0.94	+18
02/10	10 15.4	-13 52	0.07	1.05	16.4	28.1	150	131	-0.04	+34
02/20	10 39.7	-05 13	0.09	1.08	16.6	16.0	162	99	+0.52	+45
03/02	10 52.4	+00 47	0.12	1.11	16.9	5.8	173	35	-0.90	+51
03/12	10 59.8	+04 42	0.15	1.15	17.5	6.2	173	169	-0.02	+55
03/22	11 05.9	+07 01	0.20	1.19	18.4	13.8	163	69	+0.54	+58
04/01	11 12.7	+08 05	0.25	1.23	19.2	20.4	155	70	-0.85	+60

(363024) 1998 OK1 (H = 19.32, PHA)

Mainzer et al. (2016) used WISE observations to find a diameter of 560 meters and albedo of 0.099 when using H = 19.4. This is darker than many NEAs. The LCDB shows 70 NEAs with $p_V \leq 0.10$. On the other hand, there are 3429 objects in the LCDB with $0.18 \leq p_V \leq 0.25$.

DATE	RA	Dec	ED	SD	V	α	SE	ME	MP	GB
01/20	23 32.4	+19 43	0.08	0.95	17.9	111.9	64	31	+0.42	-39
01/23	00 11.7	+38 20	0.07	0.97	17.1	96.5	79	49	+0.70	-24
01/26	01 10.4	+54 18	0.08	0.99	16.7	81.5	94	62	+0.92	-8
01/29	02 33.6	+64 19	0.10	1.01	16.7	69.9	105	74	-1.00	+4
02/01	04 09.6	+68 24	0.11	1.03	16.9	61.6	113	92	-0.88	+12
02/04	05 31.2	+68 38	0.14	1.06	17.1	55.9	118	114	-0.58	+18
02/07	06 28.1	+67 12	0.16	1.08	17.4	51.7	121	134	-0.25	+23
02/10	07 06.0	+65 17	0.18	1.10	17.6	48.7	123	137	-0.04	+26
02/13	07 32.1	+63 20	0.21	1.12	17.9	46.4	125	119	+0.02	+29

(468727) 2010 JE87 (H = 20.70, PHA)

Mainzer et al. (2016) reported D = 0.308 ± 0.016 km, p_V = 0.108 ± 0.027 when using H = 20.60. There is no rotation period given in the LCDB. This one is decidedly for Northern observers.

DATE	RA	Dec	ED	SD	V	α	SE	ME	MP	GB
01/28	16 23.1	+54 52	0.04	0.99	16.9	86.1	91	88	+0.99	+43
01/29	15 48.2	+62 49	0.05	0.99	16.9	78.1	99	76	-1.00	+44
01/30	15 02.5	+68 42	0.05	1.00	16.9	71.6	105	69	-0.98	+44
01/31	14 05.5	+72 36	0.06	1.01	17.0	66.5	110	66	-0.94	+43
02/01	13 01.4	+74 42	0.07	1.01	17.1	62.4	114	68	-0.88	+42
02/02	11 59.2	+75 23	0.07	1.02	17.2	59.3	117	74	-0.79	+41
02/03	11 06.6	+75 07	0.08	1.03	17.4	56.7	119	82	-0.69	+40
02/04	10 25.6	+74 20	0.09	1.03	17.5	54.7	121	92	-0.58	+39
02/05	09 54.7	+73 19	0.10	1.04	17.7	53.1	122	102	-0.47	+38
02/06	09 31.3	+72 14	0.10	1.05	17.8	51.8	123	112	-0.36	+38
02/07	09 13.5	+71 09	0.11	1.05	17.9	50.7	124	121	-0.25	+37

2016 CL136 (H = 21.40, PHA)

Masiero et al. (2016) used WISE data to find a diameter of 0.123 ± 0.057 km and albedo of 0.316 ± 0.3599. Some 3-4 color photometry and H-G observations might narrow down the taxonomic class and so, within limits, narrow the range of albedos.

DATE	RA	Dec	ED	SD	V	α	SE	ME	MP	GB
01/30	14 59.0	+24 17	0.05	0.99	17.6	82.1	95	70	-0.98	+61
01/31	14 12.7	+28 22	0.04	1.00	16.9	70.7	107	49	-0.94	+72
02/01	13 08.8	+32 03	0.04	1.01	16.3	56.3	122	32	-0.88	+84
02/02	11 50.4	+33 37	0.04	1.01	15.7	39.8	139	34	-0.79	+75
02/03	10 32.6	+32 06	0.04	1.02	15.4	24.0	155	55	-0.69	+60
02/04	09 30.0	+28 34	0.04	1.03	15.3	12.5	167	80	-0.58	+46
02/05	08 45.0	+24 40	0.05	1.03	15.5	10.5	169	102	-0.47	+35
02/06	08 13.4	+21 14	0.06	1.04	16.1	15.5	164	123	-0.36	+27
02/07	07 50.8	+18 26	0.06	1.05	16.5	20.8	158	142	-0.25	+21
02/08	07 34.2	+16 12	0.07	1.05	17.0	25.2	153	158	-0.16	+17
02/09	07 21.7	+14 24	0.08	1.06	17.4	28.8	149	169	-0.09	+13
02/10	07 12.0	+12 58	0.09	1.06	17.7	31.7	145	163	-0.04	+10

(456537) 2007 BG (H = 19.50)

The diameter for this NEA is given by Mainzer et al. (2016) to be 0.308 ± 0.108 km; they list an albedo of 0.242 ± 0.186 based on using H = 19.5. The size should make it less likely that the asteroid is super-fast rotator. The geometry of the approach has the asteroid getting out of the galactic plane just as the solar elongation is decreasing below 90°.

DATE	RA	Dec	ED	SD	V	α	SE	ME	MP	GB
01/25	10 46.6	-51 10	0.18	1.04	18.2	66.7	104	103	+0.86	+7
01/28	10 39.7	-52 58	0.17	1.04	18.0	66.8	104	84	+0.99	+5
01/31	10 30.3	-54 56	0.15	1.03	17.8	67.1	105	68	-0.94	+3
02/03	10 17.3	-57 07	0.14	1.03	17.6	67.8	105	64	-0.69	+0
02/06	09 58.8	-59 32	0.12	1.02	17.4	69.0	104	74	-0.36	-4
02/09	09 31.5	-62 08	0.11	1.02	17.2	70.8	103	88	-0.09	-8
02/12	08 49.7	-64 43	0.10	1.01	17.0	73.7	101	97	+0.00	-13
02/15	07 45.3	-66 38	0.08	1.00	16.8	78.1	97	95	+0.11	-20
02/18	06 14.3	-66 18	0.07	0.99	16.8	84.4	91	88	+0.34	-28
02/21	04 35.5	-61 25	0.06	0.98	16.8	93.4	83	84	+0.62	-40

(311554) 2006 BQ147 (H = 18.70)

Stephens (2015) reported a period of 9.15 h for this 540-meter NEA. The lightcurve amplitude was 0.31 mag at a solar phase angle of 48°. Considering that alone, the amplitude of the lightcurve this apparition could be even larger. However, the phase angle bisector longitude, λ_{PAB}, will be nearly 100° different. This could mean an entirely different view of the asteroid, e.g., pole-on instead of equatorial.

Since the λ_{PAB} will change dramatically during the apparition, shape/spin axis modeling would benefit greatly by getting 2-4 separate lightcurves over the entire interval of the ephemeris and so reveal any changes in the lightcurve shape and/or amplitude.

DATE	RA	Dec	ED	SD	V	α	SE	ME	MP	GB
01/28	12 23.4	-17 17	0.26	1.12	18.0	52.8	115	75	+0.99	+45
01/31	12 31.6	-15 32	0.23	1.11	17.7	52.1	117	38	-0.94	+47
02/03	12 41.0	-13 13	0.21	1.10	17.4	51.4	119	14	-0.69	+50
02/06	12 52.2	-10 05	0.18	1.09	17.1	50.7	121	48	-0.36	+53
02/09	13 05.9	-05 46	0.16	1.08	16.7	50.2	123	88	-0.09	+57
02/12	13 23.4	+00 13	0.13	1.07	16.3	50.4	124	127	+0.00	+62
02/15	13 46.8	+08 35	0.11	1.05	16.0	52.1	123	158	+0.11	+67
02/18	14 19.7	+19 52	0.10	1.04	15.8	56.6	119	148	+0.34	+69
02/21	15 07.8	+33 28	0.09	1.02	15.8	65.0	110	118	+0.62	+60
02/24	16 17.6	+46 18	0.09	1.01	16.2	76.1	99	95	+0.87	+45
02/27	17 47.3	+54 27	0.10	0.99	16.8	86.8	87	89	+1.00	+31
03/02	19 16.0	+57 00	0.12	0.97	17.4	95.5	78	93	-0.90	+19
03/05	20 24.1	+56 09	0.14	0.95	18.0	102.0	70	94	-0.62	+11

(85953) 1999 FK21 (H = 18.10)

Several rotation periods are reported in the LCDB. Skiff (2011) found a period of 28.1 h. Warner (2018), however, found a period of 68.44 h with lightcurve amplitude of 0.87 mag based on observations in 2018 April. The data could not be fit to a period near 28 h. Pravec et al. (2019) reported a period of 27.88 h using data form 2014 and a period of 28.08 using data from 28.08.

This calls for a coordinated campaign of observers at well-separated longitudes. Using one of the high-quality catalogs for comp star magnitudes will be important in this case.

DATE	RA	Dec	ED	SD	V	α	SE	ME	MP	GB
02/18	04 21.8	-43 00	0.14	0.99	16.9	86.9	85	60	+0.34	-45
02/20	04 54.7	-35 40	0.15	1.00	16.7	79.8	92	57	+0.52	-38
02/22	05 19.6	-28 39	0.16	1.02	16.7	73.7	98	54	+0.71	-32
02/24	05 38.7	-22 20	0.17	1.04	16.7	68.6	102	56	+0.87	-25
02/26	05 53.8	-16 51	0.18	1.05	16.8	64.7	106	65	+0.98	-20
02/28	06 06.1	-12 10	0.20	1.07	16.9	61.6	108	82	-0.99	-15
03/02	06 16.3	-08 12	0.22	1.08	17.1	59.3	110	103	-0.90	-12
03/04	06 24.9	-04 50	0.24	1.10	17.3	57.6	111	125	-0.73	-8
03/06	06 32.4	-01 58	0.26	1.11	17.4	56.3	111	146	-0.51	-5
03/08	06 39.1	+00 29	0.28	1.12	17.6	55.3	111	155	-0.29	-3
03/10	06 45.0	+02 35	0.30	1.14	17.8	54.6	111	144	-0.12	+0
03/12	06 50.5	+04 25	0.32	1.15	17.9	54.0	111	124	-0.02	+2
03/14	06 55.5	+06 00	0.34	1.16	18.1	53.7	110	102	+0.01	+4

99942 Apophis (H = 18.90, PHA)

This approximately 400-m NEA will be the subject of many campaigns during this year's approach in order to characterize it in as much detail as possible and refine its orbit. All this is in anticipation of the extremely close flyby in 2029 April. There are three reported periods in the LCDB, all near 30.55 h: Behrend (2005), Oey (2014), and Pravec et al. (2014).

The asteroid will be available for several weeks. Given the long period, a coordinated campaign of observers is recommended.

DATE	RA	Dec	ED	SD	V	α	SE	ME	MP	GB
01/01	11 40.3	-14 00	0.24	1.05	18.3	68.0	99	61	-0.96	+45
01/11	11 44.1	-16 18	0.22	1.07	17.9	61.9	107	79	-0.06	+44
01/21	11 41.9	-18 14	0.19	1.08	17.5	54.9	116	144	+0.52	+42
01/31	11 31.0	-19 25	0.17	1.09	16.9	46.4	127	34	-0.94	+40
02/10	11 07.8	-19 13	0.14	1.10	16.3	35.9	139	119	-0.04	+37
02/20	10 30.7	-16 31	0.12	1.10	15.7	24.9	152	101	+0.52	+35
03/02	09 45.0	-10 41	0.11	1.10	15.4	21.9	156	52	-0.90	+31
03/12	09 02.1	-02 49	0.11	1.09	15.8	33.4	143	151	-0.02	+27
03/22	08 31.2	+04 49	0.12	1.07	16.3	48.3	126	36	+0.54	+24
04/01	08 13.1	+10 59	0.14	1.06	16.9	61.5	112	113	-0.85	+23
04/11	08 04.1	+15 48	0.15	1.04	17.4	73.0	99	110	-0.01	+23

(535844) 2015 BY310 (H = 21.70, PHA)

Pravec et al. (2019) reported a period of 0.0926702 h (5.56 min) for this 140-m NEA. Based on Pravec et al. (2000), exposures should be no more than about 60 sec to avoid *rotational smearing*. This is when a single exposure covers too much a full rotation and so details about the shape and amplitude are reduced or even lost.

The observing window is fairly short and hampered by close proximity to a nearly full moon and low galactic longitudes. The larger the telescope, the better the chances for success in this case.

DATE	RA	Dec	ED	SD	V	α	SE	ME	MP	GB
02/20	07 39.5	+21 55	0.09	1.06	17.9	35.4	142	49	+0.52	+20
02/22	07 30.8	+19 55	0.08	1.05	17.8	39.2	138	24	+0.71	+17
02/24	07 21.1	+17 26	0.07	1.04	17.7	43.3	134	9	+0.87	+14
02/26	07 09.8	+14 21	0.06	1.03	17.6	48.0	129	35	+0.98	+11
02/28	06 56.7	+10 27	0.06	1.02	17.5	53.3	124	66	-0.99	+6
03/02	06 41.1	+05 31	0.05	1.02	17.4	59.5	118	98	-0.90	+0
03/04	06 22.1	-00 42	0.05	1.01	17.3	66.9	111	127	-0.73	-7
03/06	05 58.6	-08 25	0.04	1.00	17.4	75.6	102	145	-0.51	-15
03/08	05 29.4	-17 32	0.04	0.99	17.6	85.5	92	133	-0.29	-26

(138127) 2000 EE14 (H = 17.01)

Warner (2014) found a period of 2.586 h. Vaduvescu et al. (2017) found a similar period of 2.5904 h. The period and size of 1.2 km make this a good candidate for being a binary asteroid.

Don't give up it too soon. It's not uncommon for observations over a few consecutive nights to show no signs of a satellite (deviations in the main lightcurve) only to be followed by a period of several days that reveals mutual events (occultations/eclipses) due to the satellite.

DATE	RA	Dec	ED	SD	V	α	SE	ME	MP	GB
01/21	15 49.7	-36 13	0.37	0.85	18.1	98.9	59	144	+0.52	+14
01/31	15 54.3	-29 19	0.32	0.92	17.6	92.5	69	84	-0.94	+19
02/10	16 06.3	-19 34	0.26	0.97	17.1	86.9	78	56	-0.04	+24
02/20	16 24.7	-04 30	0.21	1.00	16.4	81.7	86	164	+0.52	+30
03/02	16 51.5	+18 40	0.17	1.01	15.9	77.9	92	58	-0.90	+35
03/12	17 34.6	+46 23	0.17	1.01	16.0	78.8	91	90	-0.02	+32
03/22	18 59.4	+67 20	0.21	1.00	16.5	83.7	84	87	+0.54	+24
04/01	21 50.7	+75 53	0.26	0.97	17.2	89.5	75	108	-0.85	+17

(462550) 2009 CB3 (H = 19.51)

No rotation periods were found in the LCDB. The estimated diameter is 370 m, so it's unlikely, but not impossible, that the rotation period is less than 2 h. The large phase angles may lead to unusually-shaped lightcurves.

DATE	RA	Dec	ED	SD	V	α	SE	ME	MP	GB
03/05	03 56.4	+26 08	0.08	0.98	17.4	97.4	78	173	-0.62	-21
03/06	04 39.7	+30 42	0.08	0.99	17.2	87.8	87	171	-0.51	-11
03/07	05 19.4	+33 49	0.09	1.00	17.1	79.8	95	168	-0.39	-2
03/08	05 54.1	+35 45	0.10	1.02	17.1	73.2	101	163	-0.29	+5
03/09	06 23.4	+36 51	0.11	1.03	17.2	67.9	106	157	-0.20	+11
03/10	06 47.7	+37 24	0.13	1.04	17.3	63.7	110	149	-0.12	+15
03/11	07 07.9	+37 36	0.14	1.05	17.5	60.4	113	141	-0.06	+19
03/12	07 24.7	+37 37	0.15	1.07	17.6	57.6	115	132	-0.02	+22
03/13	07 38.8	+37 30	0.17	1.08	17.8	55.4	117	123	+0.00	+25
03/14	07 50.7	+37 19	0.18	1.09	17.9	53.6	118	113	+0.01	+27
03/15	08 00.9	+37 05	0.19	1.10	18.1	52.1	119	103	+0.03	+29

(351545) 2005 TE15 (H = 19.70)

Based on the LCDB, the rotation period for this NEA is unknown. The estimated diameter is 340 m.

DATE	RA	Dec	ED	SD	V	α	SE	ME	MP	GB
02/25	12 16.9	+58 53	0.19	1.11	18.0	45.8	127	53	+0.93	+58
02/27	12 14.2	+60 43	0.17	1.10	17.9	47.7	125	50	+1.00	+56
03/01	12 10.2	+62 45	0.16	1.09	17.8	49.9	123	60	-0.96	+54
03/03	12 04.6	+65 00	0.15	1.08	17.7	52.4	121	77	-0.82	+51
03/05	11 56.4	+67 30	0.14	1.06	17.6	55.4	118	97	-0.62	+49
03/07	11 44.1	+70 18	0.13	1.05	17.5	58.8	115	114	-0.39	+46
03/09	11 24.4	+73 25	0.12	1.04	17.4	62.7	111	123	-0.20	+42
03/11	10 49.4	+76 50	0.11	1.03	17.3	67.4	107	121	-0.06	+38
03/13	09 38.9	+80 11	0.10	1.02	17.3	72.9	102	108	+0.00	+33
03/15	07 15.5	+81 55	0.09	1.01	17.3	79.4	96	90	+0.03	+28
03/17	04 35.4	+79 19	0.08	1.00	17.3	87.1	88	70	+0.12	+21

162173 Ryugu (H = 19.22, PHA)

Ryugu has an equatorial diameter of about 1 km. Its pole-to-pole diameter is about 870 m (Watanabe et al., 2019). The Hayabusa2 spacecraft launched by Japan reached the asteroid on 2018 June. The close-up images showed the shape to be a "spinning top", i.e., mostly spherical but with an equatorial bulge that is believed to be caused by material trying to escape from the asteroid due to centrifugal force but, after failing to do so, settles down near the equator.

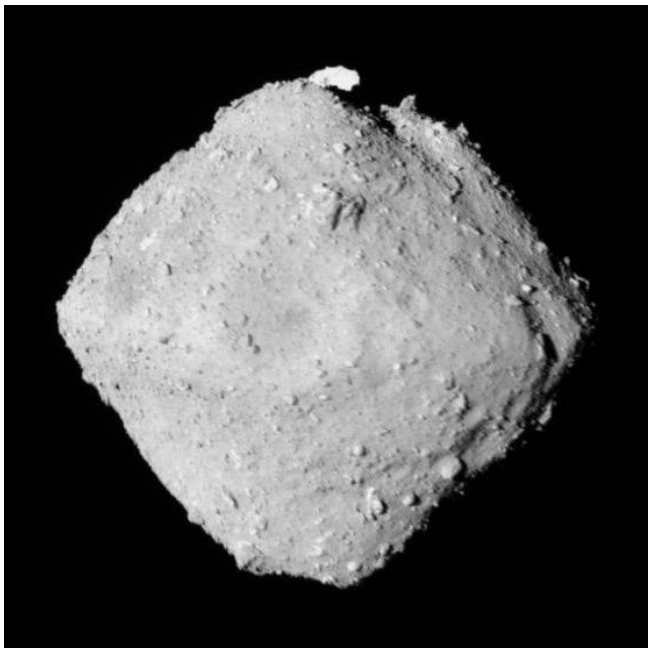

Credit: JAXA Hayabusa2.

After obtaining surface samples, the spacecraft started its return journey to Earth in 2019 November. As of this writing (2020 October), the spacecraft should complete its homeward trip sometime in 2020 December.

There are several reports of a period of about 7.63 h in the LCDB, e.g., Abe (2008) and Müller et al. (2011), which are from Earth-based observations. Most accurate is that from Watanabe et al. (2019), who used space craft observations to find a period of 7.63262 h. On the other hand, Warner and Stephens (2021) found a period of 7.404 h and could not make the data fit the slightly longer period nor explain the significant difference.

DATE	RA	Dec	ED	SD	V	α	SE	ME	MP	GB
02/10	09 14.7	-70 28	0.10	1.00	17.0	79.1	95	85	-0.04	-15
02/20	09 54.3	-64 28	0.11	1.02	17.0	69.4	104	106	+0.52	-8
03/02	10 16.2	-57 52	0.12	1.05	16.9	59.4	114	65	-0.90	-1
03/12	10 30.4	-50 26	0.13	1.08	16.9	49.4	125	115	-0.02	+6
03/22	10 42.2	-42 14	0.15	1.11	16.9	40.1	134	90	+0.54	+15
04/01	10 54.3	-33 58	0.17	1.14	17.0	33.3	141	64	-0.85	+23
04/11	11 07.3	-26 27	0.20	1.17	17.3	30.3	144	145	-0.01	+31

(271480) 2004 FX31 (H = 17.52)

Mainzer et al. (2016) found D = 0.709 ± 0.223 km and p_V = 0.352 ± 0.222 when using H = 17.5. The albedo seems high for an NEA. Reducing it by one-half sigma, to about 0.2, would make the value more typical and the estimated diameter would then be about 930 m. Here is another case where 3-4 color photometry and finding the H-G parameters *might* help get a better idea of the taxonomic class and, based on averages for a given taxonomic class, refine the adopted albedo value.

DATE	RA	Dec	ED	SD	V	α	SE	ME	MP	GB
03/20	17 47.8	+37 14	0.13	1.01	15.9	80.8	92	119	+0.35	+28
03/22	17 24.2	+41 00	0.14	1.02	15.9	75.0	97	112	+0.54	+33
03/24	17 02.7	+43 50	0.15	1.04	16.0	70.2	101	99	+0.73	+38
03/26	16 43.3	+45 56	0.17	1.05	16.1	66.2	105	84	+0.90	+41
03/28	16 25.8	+47 29	0.18	1.07	16.2	62.9	108	71	+0.99	+44
03/30	16 10.0	+48 38	0.20	1.08	16.4	60.1	110	64	-0.98	+46
04/01	15 55.7	+49 28	0.22	1.10	16.5	57.7	112	68	-0.85	+48
04/03	15 42.8	+50 02	0.23	1.11	16.6	55.6	113	79	-0.66	+50
04/05	15 31.1	+50 25	0.25	1.13	16.8	53.8	114	93	-0.43	+52
04/07	15 20.5	+50 38	0.27	1.14	16.9	52.3	115	107	-0.24	+53
04/09	15 10.8	+50 44	0.29	1.16	17.0	50.9	116	117	-0.09	+55

(231937) 2001 FO32 (H = 17.70, PHA)

Binzel et al. (2019) found this to be a type S/Sr asteroid. Using a default albedo of 0.2 for the S complex, the estimated diameter is 860 m. There is no rotation period listed in the LCDB.

Note that the ephemeris is split into two blocks. The first covers March while the second reaches into May, after the asteroid comes out of conjunction with the Sun.

DATE	RA	Dec	ED	SD	V	α	SE	ME	MP	GB
03/01	12 58.2	-31 35	0.42	1.30	17.8	35.9	130	36	-0.96	+31
03/06	13 02.4	-32 19	0.31	1.23	17.1	36.3	133	52	-0.51	+30
03/11	13 08.6	-33 13	0.21	1.16	16.2	37.0	136	109	-0.06	+30
03/16	13 23.3	-34 51	0.11	1.08	14.7	39.4	136	151	+0.06	+28
03/21	16 40.6	-41 30	0.02	1.00	11.7	73.8	105	160	+0.44	+3
03/26	00 19.5	+27 11	0.09	0.92	21.2	152.6	25	126	+0.90	-35

04/30	01 18.7	+20 51	0.95	0.31	18.3	92.2	18	125	-0.88	-42
05/05	01 44.4	+17 30	1.12	0.30	17.5	61.8	15	62	-0.38	-44
05/10	02 15.4	+14 35	1.26	0.36	17.5	39.0	13	8	-0.03	-44
05/15	02 46.0	+12 19	1.38	0.44	17.9	27.9	12	47	+0.09	-42
05/20	03 13.9	+10 33	1.48	0.54	18.3	23.6	12	103	+0.52	-39

(514596) 2003 FG (H = 19.60)

Pravec et al. (2005) reported the rotation period to be 8.692 h with no obvious signs of tumbling. Given the size and rotation period, this 360-m NEA would be a good candidate for tumbling (Pravec et al., 2005; 2014). Accurately-calibrated data will be necessary to confirm whether or not the asteroid might be in a low-level of tumbling.

The period being nearly being commensurate with an Earth day suggests forming a collaboration of observers well-separated in longitude.

DATE	RA	Dec	ED	SD	V	α	SE	ME	MP	GB
03/20	14 41.6	-16 02	0.23	1.18	18.3	35.7	136	151	+0.35	+39
03/22	14 46.7	-18 15	0.20	1.15	18.0	36.5	136	129	+0.54	+37
03/24	14 53.4	-21 12	0.18	1.13	17.6	37.8	136	106	+0.73	+33
03/26	15 02.8	-25 14	0.15	1.11	17.2	40.2	134	83	+0.90	+29
03/28	15 17.3	-31 00	0.12	1.08	16.9	44.2	131	60	+0.99	+22
03/30	15 42.9	-39 37	0.10	1.06	16.5	51.5	124	42	-0.98	+12
04/01	16 39.4	-52 14	0.08	1.03	16.4	64.3	112	36	-0.85	-4
04/03	19 17.2	-64 35	0.07	1.00	16.7	84.6	92	43	-0.66	-27

References

Abe, M.; Kawakami, K.; Hasegawa, S.; Kuroda, D.; Yoshikawa, M.; Kasuga, T.; Kitazato, K.; Sarugaku, Y.; Kinoshita, D.; Miyasaka, S.; Urakawa, S.; Okumura, S.; Takagi, Y.; Takato, N.; Fujiyoshi, T.; Terada, H.; Wada, T.; Ita, Y.; Vilas, F.; Weissman, R.P. (2008). "Ground-based Observational Campaign for Asteroid 162173 1999 JU3." *Lunar & Planetary Sci. XXXIX*. **No. 1391**, p. 1594.

Behrend, R. (2005). Observatoire de Geneve web site. *http://obswww.unige.ch/~behrend/page_cou.html*

Binzel, R.P.; DeMeo, F.E.; Turtelboom, E.V.; Bus, S.J.; Tokunaga, A.; Burbine, T.H.; Lantz, C.; Polishook, D.; Carry, B.; Morbidelli, A.; Birlan, M.; Vernazza, P.; Burt, B.J.; Moskovitz, N.; Slivan, S.M.; Thomas, C.A.; Rivkin, A.S.; Hicks, M.D.; Dunn, T.; Reddy, V.; Sanchez, J.A.; Granvik, M.; Kohout, T. (2019). "Compositional distributions and evolutionary processes for the near-Earth object population: Results from the MIT-Hawaii Near-Earth Object Spectroscopic Survey (MITHNEOS)." *Icarus* **324**, 41-76.

Dose, E. (2021). "A New Photometric Workflow and Lightcurves of Fifteen Asteroids." *Minor Planet Bull*. **47**, 324-330.

Harris, A.W.; Young, J.W.; Contreiras, L.; Dockweiler, T.; Belkora, L.; Salo, H.; Harris, W.D.; Bowell, E.; Poutanen, M.; Binzel, R.P.; Tholen, D.J.; Wang, S. (1989). "Phase relations of high albedo asteroids: The unusual opposition brightening of 44 Nysa and 64 Angelina." *Icarus* **81**, 365-374.

Mainzer, A.K.; Bauer, J.M.; Cutri, R.M.; Grav, T.; Kramer, E.A.; Masiero, J.R.; Nugent, C.R.; Sonnett, S.M.; Stevenson, R.A.; Wright, E.L. (2016). "NEOWISE Diameters and Albedos V1.0." NASA Planetary Data System.

Masiero, J.R.; Redwing, E.; Mainzer, A.K.; Bauer, J.M.; Cutri, R.M.; Grav, T.; Kramer, E.; Nugent, C.R.; Sonnett, S.; Wright, E.L. (2018). "Small and Nearby NEOs Observed by NEOWISE During the First Three Years of Survey: Physical Properties." *Astron. J.* **156**, A60.

Mottola, S.; De Angelis, G.; Di Martino, M.; Erikson, A.; Hahn, G.; Neukum, G. (1995). "The near-earth objects follow-up program: First results." *Icarus* **117**, 62-70.

Muinonen, K.; Belskaya, I.N.; Cellino, A.; Delbò, M.; Levasseur-Regourd, A.-C.; Penttilä, A.; Tedesco, E.F. (2010). "A three-parameter magnitude phase function for asteroids." *Icarus* **209**, 542-555.

Müller, T.G.; Ďurech, J.; Hasegawa, S.; Abe, M.; Kawakami, K.; Kasuga, T.; Kinoshita, D.; Kuroda, D.; Urakawa, S.; Okumura, S.; Sarugaku, Y.; Miyasaka, S.; Takagi, Y.; Weissman, P.R.; Choi, Y.-J.; Larson, S.; Yanagisawa, K.; Nagayama, S. (2011). "Thermo-physical properties of 162173 (1999 JU3), a potential flyby and rendezvous target for interplanetary missions." *Astron. Astrophys*. **525**, A145.

Oey, J. (2014). "Lightcurve Analysis of Asteroids from Blue Mountains Observatory in 2013." *Minor Planet Bull*. **41**, 276-281.

Pilcher, F. (2020). "Lightcurves and Rotation Periods of 83 Beatrix, 86 Semele, 118 Peitho, 153 Hilda, 527 Euryanthe, and 549 Jessonda." *Minor Planet Bull*. **47**, 192-195.

Pravec, P.; Hergenrother, C.; Whiteley, R.; Sarounova, L.; Kusnirak, P.; Wolf, M. (2000). "Fast Rotating Asteroids 1999 TY2, 1999 SF10, and 1998 WB2." *Icarus* **147**, 477-486.

Pravec, P.; Harris, A.W.; Scheirich, P.; Kušnirák, P.; Šarounová, L.; Hergenrother, C.W.; Mottola, S.; Hicks, M.D.; Masi, G.; Krugly, Yu.N.; Shevchenko, V.G.; Nolan, M.C.; Howell, E.S.; Kaasalainen, M.; Galád, A.; Brown, P.; Degraff, D.R.; Lambert, J.V.; Cooney, W.R.; Foglia, S. (2005). "Tumbling asteroids." *Icarus* **173**, 108-131.

Pravec, P.; Scheirich, P.; Durech, J.; Pollock, J.; Kusnirak, P.; Hornoch, K.; Galad, A.; Vokrouhlicky, D.; Harris, A.W.; Jehin, E.; Manfroid, J.; Opitom, C.; Gillon, M.; Colas, F.; Oey, J.; Vrastil, J.; Reichart, D.; Ivarsen, K.; Haislip, J.; LaCluyze, A. (2014). "The tumbling state of (99942) Apophis." *Icarus* **233**, 48-60.

Pravec, P.; Wolf, M.; Sarounova, L. (2019). *http://www.asu.cas.cz/~ppravec/neo.htm*

Skiff, B.A. (2011). Posting on CALL web site. *http://www.minorplanet.info/call.html*

Stephens, R.D. (2015). "Asteroids Observed from CS3: 2015 January – March." *Minor Planet Bull*. **42**, 200-203.

Tonry, J.L.; Denneau, L.; Flewelling, H.; Heinze, A.N.; Onken, C.A.; Smartt, S.J.; Stalder, B.; Weiland, H.J.; Wolf, C. (2018). "The ATLAS All-Sky Stellar Reference Catalog." *Astrophys. J.* **867**, A105.

Vaduvescu, O.; Macias, A.A.; Tudor, V.; Predatu, M.; Galád, A.; Gajdoš, Š.; Világi, J.; Stevance, H.F.; Errmann, R.; Unda-Sanzana, E.; Char, F.; Peixinho, N.; Popescu, M.; Sonka, A.; Cornea, R.; Suciu, O.; Toma, R.; Santos-Sanz, P.; Sota, A.; Licandro, J.; Serra-Ricart, M.; Morate, D.; Mocnik, T.; Diaz Alfaro, M.; Lopez-Martinez, F.; McCormac, J.; Humphries, N. (2017). "The EURONEAR Lightcurve Survey of Near Earth Asteroids." *Earth, Moon, and Planets* **120**, 41-100.

Warner, B.D. (2014). "Near-Earth Asteroid Lightcurve Analysis at CS3-Palmer Divide Station: 2014 January-March." *Minor Planet Bull*. **41**, 157-168.

Warner, B.D. (2018). "Near-Earth Asteroid Lightcurve Analysis at CS3-Palmer Divide Station: 2018 April-June." *Minor Planet Bull*. **45**, 366-379.

Warner, B.D.; Stephens, R.D. (2021). "On Confirmed and Suspected Binary Asteroids Observed at the Center for Solar System Studies." *Minor Planet Bull.* **48**, 40-49.

Warner, B.D.; Harris, A.W.; Pravec, P. (2009a). "The asteroid lightcurve database." *Icarus* **202**, 134-146.

Warner, B.D.; Harris, A.W.; Pravec, P.; Durech, J.; Benner, L.A.M. (2009b). "Lightcurve Photometry Opportunities: 2009 October-December." *Minor Planet Bulletin* **36**, 188-190.

Watanabe, S.; Hirabayashi, M.; Hirata, N.; and 85 co-authors (2019). "Hayabusa2 arrives at the carbonaceous asteroid 162173 Ruygu – A spinning top rubble pile." *Science* **364**, 268-272

IN THIS ISSUE

This list gives those asteroids in this issue for which physical observations (excluding astrometric only) were made. This includes lightcurves, color index, and H-G determinations, etc. In some cases, no specific results are reported due to a lack of or poor-quality data. The page number is for the first page of the paper mentioning the asteroid. EP is the "go to page" value in the electronic version.

Number	Name	EP	Page	Number	Name	EP	Page	Number	Name	EP	Page
19764	2000 NF5	30	30	65936	1998 FJ69	7	7	498066	2007 RM133	8	8
21663	Banat	56	56	68134	2001 AT18	56	56		2003 BK47	30	30
23482	1991 LV	56	56	85275	1994 LY	11	11		2005 QS10	30	30
23482	1991 LV	69	69	87684	2000 SY2	30	30		2006 HB	30	30
23989	Farpoint	69	69	96341	1997 OX1	56	56		2006 NL	30	30
24177	1999 XJ7	56	56	129480	1993 UQ8	56	56		2006 UD63	30	30
25332	1999 KK6	69	69	136900	1998 HL49	30	30		2007 VX137	30	30
27057	1998 SP33	77	77	137108	1999 AN10	30	30		2014 LW21	30	30
28565	2000 EO58	56	56	137199	1999 KX4	77	77		2016 NV38	30	30
28565	2000 EO58	69	69	145656	4788 P-L	30	30		2016 PN	30	30
35371	Yokonozaki	77	77	146134	2000 SE1	56	56		2018 CB	26	26
41653	2000 SC294	77	77	162173	Ryugu	30	30		2018 GE3	26	26
51534	2001 FQ132	56	56	164755	1998 VK27	56	56		2018 LM4	30	30
52768	1998 OR2	50	50	285990	2001 SK9	30	30		2020 KK7	26	26
53435	1999 VM40	30	30	380128	1997 WB21	30	30		2020 PL2	20	20
54441	2000 MP5	77	77	411165	2010 DF1	30	30		2020 SN	30	30
56086	1999 AA21	56	56	450648	2006 UC63	30	30		2020 SW	26	26
56086	1999 AA21	77	77	480936	2003 QH5	30	30				

THE MINOR PLANET BULLETIN (ISSN 1052-8091) is the quarterly journal of the Minor Planets Section of the Association of Lunar and Planetary Observers (ALPO, http://www.alpo-astronomy.org). Current and most recent issues of the *MPB* are available on line, free of charge from:

http://www.minorplanet.info/MPB

The Minor Planets Section is directed by its Coordinator, Prof. Frederick Pilcher, 4438 Organ Mesa Loop, Las Cruces, NM 88011 USA (fpilcher35@gmail.com). Dr. Alan W. Harris (MoreData! Inc.; harrisaw@colorado.edu), and Dr. Petr Pravec (Ondrejov Observatory; ppravec@asu.cas.cz) serve as Scientific Advisors. The Asteroid Photometry Coordinator is Brian D. Warner (Center for Solar System Studies), Palmer Divide Observatory, 446 Sycamore Ave., Eaton, CO 80615 USA (brian@MinorPlanetObserver.com).

The Minor Planet Bulletin is edited by Professor Richard P. Binzel, MIT 54-410, 77 Massachusetts Ave, Cambridge, MA 02139 USA (rpb@mit.edu). Brian D. Warner (address above) is Associate Editor, and Dr. David Polishook, Department of Earth and Planetary Sciences, Weizmann Institute of Science (david.polishook@weizmann.ac.il) is Assistant Editor. The *MPB* is produced by Dr. Pedro A. Valdés Sada (psada2@ix.netcom.com). The MPB is distributed by Dr. Melissa Hayes-Gehrke. Direct all subscriptions, contributions, address changes, etc. to:

Dr. Melissa Hayes-Gehrke
UMD Astronomy Department
1113 PSC Bldg 415
College Park, MD 20742 USA
(mhayesge@umd.edu)

Effective with Volume 38, the *Minor Planet Bulletin* is a limited print journal, where print subscriptions are available only to libraries and major institutions for long-term archival purposes. In addition to the free electronic download of the *MPB* noted above, electronic retrieval of all *Minor Planet Bulletin* articles (back to Volume 1, Issue Number 1) is available through the Astrophysical Data System:

http://www.adsabs.harvard.edu/

Authors should submit their manuscripts by electronic mail (rpb@mit.edu). Author instructions and a Microsoft Word template document are available at the web page given above. All materials must arrive by the deadline for each issue. Visual photometry observations, positional observations, any type of observation not covered above, and general information requests should be sent to the Coordinator.

* * * * *

The deadline for the next issue (48-2) is January 15, 2021. The deadline for issue 48-3 is April 15, 2021.